FORWARD GENETICS TO UNRAVEL NOVEL GENES AND THEIR FUNCTIONS IN TOMATO FRUIT DEVELOPMENT

By

Satya Swathi Nadakuduti

A DISSERTATION

Submitted to
Michigan State University
in partial fulfillment of the requirements
for the degree of

Plant Breeding, Genetics and Biotechnology - Horticulture - Doctor of Philosophy

2014

ABSTRACT

FORWARD GENETICS TO UNRAVEL NOVEL GENES AND THEIR FUNCTIONS IN TOMATO FRUIT DEVELOPMENT

By

Satya Swathi Nadakuduti

Tomato (*Solanum lycopersicum*) is a member of the large and phenotypically diverse Solanaceae family that includes several other agriculturally valuable crops such as potato, eggplant, pepper, petunia and tobacco. Along with its role as an important vegetable crop, tomato also serves as an excellent model system for studying fleshy fruit development. This dissertation focuses on the characterization of four tomato mutants: *sticky peel* (*pe*), *uniform gray-green* (*ug*), *peach* (*p*), and *easy peel* (*ep*) that each display altered phenotypes associated with fruit development. The main research objectives were (1) to evaluate the phenotypes of these mutants (2) position each locus on the tomato genetic map and isolate the mutant genes by positional cloning and (3) functionally characterize the genes to determine their role in tomato fruit development.

Fruit of the *pe* mutant have sticky and glossy fruit surface and are cutin deficient with an altered wax profile. In addition, several phenotypes attributed to altered epidermal cell function are apparent in *pe*, including altered leaf cuticle composition, leading to increased transpiration, a lower trichome density and reduced anthocyanin accumulation. Genetic mapping revealed that *pe* encodes a new allele of *CUTIN DEFICIENT 2* (*CD2*), a member of the Class IV homeodomain-leucine zipper transcription factor (TF) family that was previously only associated with a fruit-specific cuticle deficiency. The Arabidopsis *anthocyaninless 2* mutant encodes a homolog of *CD2* and additional characterization of this mutant revealed that it also exhibits a mildly cutin deficient phenotype, thus revealing a regulatory link between cuticle and flavonoid

biosynthesis. This study identified a null allele of *CD2* and further extended the role of *CD2* to multiple pathways operating within the epidermis that have evolved as adaptations to stress thus revealing its role as a master regulator of epidermal cell function.

In tomato, a latitudinal gradient of chloroplast development exists, which leads to the formation of a green shoulder at the peduncle end of the fruit that positively impacts the nutrient content of ripe fruit. Fruit of the *ug* mutant lack the green shoulder surrounding the calyx. Positional cloning revealed that *UG* encodes *TKN4*, a class I Knotted1-like homeobox (KNOX) TF. *KNOX* genes typically influence plant morphology through maintenance of meristem activity. However, this research identified a previously undefined role for these TFs in the establishment of chloroplast gradients in tomato fruit through regulating the expression of the *GOLDEN 2-LIKE* TF, *SlGLK2*, and it's distant homolog *ARABIDOPSIS PSEUDORESPONSE REGULATOR-LIKE* (*SlAPRR2-LIKE*). This study has identified an atypical role for *KNOX* in regulating fleshy fruit development and defined functional interactions between well-studied, yet previously disparate, TFs that influence fruit chloroplast development.

Fruit of the *p* mutant are dull, covered by dense trichomes with altered epidermal cell structure and cuticular composition. Fruit of the *ep* mutant can be peeled easily with limited damage to the underlying pericarp cells. Inter-specific crosses of *p* and *ep* mutants with *S. pimpinellifolium* were performed to generate F_2 mapping populations that were screened with genetic markers to assign the mutant loci to chromosomes 2 and 8, respectively, although the mapping is still in progress. The aim of this research is to ultimately isolate these mutant loci by positional cloning and perform functional analysis of each gene. Together, the work presented in this dissertation expands the current knowledge base on the molecular factors that influence fruit development.

This work is dedicated to my loving husband, Raghu for all his support to follow my dream.

ACKNOWLEDGEMENTS

My life as a graduate student for the past five years at Michigan State University has been the most challenging and at the same time, most rewarding. I have to step back in time to thank people who are responsible to change the scope of my education and thereby my life by inspiring me to pursue higher education, my father and my brother. When I went to pursue my Master's in Hannover, Germany, Dr. Hartmut Stützel, my mentor, has greatly solidified my passion for science and research, which naturally led me to PhD. I feel very lucky in life to marry an amazing person, which also gave me an opportunity to come to MSU to fulfill my dream.

First, I am extremely thankful to Dr. Cornelius Barry who accepted me as his graduate student and gave me an opportunity to get premiere education and be part of a great research community, here at MSU. I have the privilege of being one of his first students and have learnt a lot from him. Along with working in science, improving writing skills, the most important thing that I learned is time management, which he emphasized right from the beginning. Preparing a task list has now integrated into my everyday life. He has been a great mentor and provided tremendous support at every stage of my research along with helping me immensely with my dissertation. He always prioritized his students, which always kept me motivated at work.

In addition to Corny, I would like to render my sincere thanks to members of my guidance committee, Dr. John Ohlrogge, Dr. Rob Last and Dr. Robin Buell for readily accepting to be on my committee. Collaboration with John has been a great boost to my work. John has given me great moral support and strength. Few minutes of our conversation have always provided me much comfort and encouragement. Rob and Robin, I believe, contribute to all graduate students by offering amazing courses that form a strong base for every student. My first year of taking their courses has made a great impression on me. I greatly appreciate their time to

discuss my research updates as well as their valuable suggestions regarding my current research and future options.

All the past and present Barry lab members have helped me along the way and created a friendly environment in the lab. My special thanks to Bill, Chelsy and Matt for their contributions to *TKN4* and *easy peel* projects and Charity, for helping me in green house especially during my pregnancy. Dr. Eliana Gonzales-Vigil has been a great friend and advisor. I also thank Krystle, Julia, Dr. Qian Ma who always lent a helping hand. My hearty thanks to Dr. Dylan Kosma and Dr. Mike Pollard for introducing me to the cuticle world and educating me further. I would also like to thank John's other lab members who were always helpful and friendly.

More broadly, I would like to thank the Plant Breeding, Genetics, and Biotechnology program and the Department of Horticulture. I thank all the members of joint lab for devoting their time to listen to my research updates and for their helpful comments. I would also like to thank the friendly staff in this department for their help. My thanks to all the friends I have made in the university who contributed one way or the other during my time at MSU.

I feel extremely blessed to have a very closely knit family and would like to express great love to all. Especially, my husband, Raghu who did everything he possibly could, to make my dream of studying at MSU come true. My one year old son, Pranav brought so much joy and fulfillment in our lives and brought the family even closer. Two amazing ladies in my life, my mom and my mother-in-law, took great care of our baby and us during the past one year, without whom I couldn't have reached this stage.

Finally I would like to thank all the women in science, who are my constant inspiration.

TABLE OF CONTENTS

LIST OF TABLES

LIST OF FIGURES

CHAPTER I

Tomato (*Solanum lycopersicum*), a model crop species for studying fruit development

Tomato genetics and genomics-based resources

Tomato (*Solanum lycopersicum*) is a member of the large and phenotypically diverse Solanaceae family that includes several other agriculturally valuable crops such as potato, eggplant, pepper, petunia and tobacco. Tomato and its wild relatives originated in South America (Ecuador, Peru and Chile) and is believed to have been domesticated in Central America (Rick, 1991; Peralta and Spooner, 2007). The genetic basis of domestication and artificial selection evaluated by comparative transcriptomics of cultivated tomato and its wild relatives revealed only very few changes at both the sequence and transcriptome level associated with this event (Bai and Lindhout, 2007; Paran and van der Knaap, 2007; Chakrabarti et al., 2013; Koenig et al., 2013; Bergougnoux, 2014). Tomato is a fleshy fruit bearing species and an important commodity for both the fresh market and processing industries. In the United States, the production was 12.5 million tons in 2011 with a gross production value of $11.7 billion. With worldwide production reaching almost 162 million tons in 2012, tomato is the seventh most important crop species after maize, rice, wheat, potatoes, soybeans and cassava (FAOSTAT, http://faostat3.fao.org) (Bergougnoux, 2014). Along with its role as an important crop, tomato also serves as an excellent model system for studying a range of biological processes, including fleshy fruit development and ripening, plant specialized metabolism, plant pathogen and pest interactions, wound signaling etc., Due to its importance as a model crop species numerous resources have been developed for tomato and its close relatives to facilitate research and crop improvement (Kimura and Sinha, 2008; Menda et al., 2013).

The C.M Rick Tomato Genetics Resource Center (TGRC) in University of California, Davis maintains seed stocks of germplasm resources including cultivars, wild relatives, monogenic mutants, and miscellaneous genetic stocks of tomato (http://tgrc.ucdavis.edu/). Wild

relatives constitute a reservoir of genetic and phenotypic diversity and yield viable crosses with cultivated tomato species. Thousands of spontaneous monogenic mutants were catalogued and are publicly available. A comprehensive mutant library was also developed in the background of the inbred variety M82 derived from EMS (ethyl methane sulfonate) and fast-neutron mutagenesis which contains several thousand mutants accessible at "The Genes That Make Tomatoes" (http://zamir.sgn.cornell.edu/mutants) (Menda et al., 2004). Recombinant inbred line populations (Paterson et al., 1991; Goldman et al., 1995; Ashrafi et al., 2009) as well as introgression line populations developed from wild relatives in *S. lycopersicum* backgrounds (Eshed and Zamir, 1995; Monforte and Tanksley, 2000) have greatly facilitated the quantitative trait loci (QTL) based studies. Micro-Tom, a cultivar with small stature and short generation time has been adopted as a model system for tomato functional genomics and accelerated transformation protocols and several genomic resources have been developed, including EMS mutants and TILLING populations (Meissner et al., 1997; Emmanuel and Levy, 2002; Matsukura et al., 2008).

The first "classical" linkage map of tomato, created with morphological and physiological markers on all 12 linkage groups was developed (Butler, 1968) and was later expanded (Rick, 1975). This facilitated the mapping of isozymes, which led to the first isozyme linkage map (Tanksley and Rick, 1980). Subsequently, high-density molecular linkage maps were constructed by mapping restriction fragment length polymorphism (RFLP) and amplified fragment length polymorphism (AFLP) markers to the tomato genome (Paterson et al., 1988; Tanksley et al., 1992; Haanstra et al., 1999). Several RFLP markers were converted into PCR-based Cleaved Amplified Polymorphic Sequence markers (Frary et al., 2005). For construction of physical maps, Yeast artificial chromosome (YAC) libraries (Martin et al., 1992) and bacterial

artificial chromosome libraries (BACs) (Budiman et al., 2000) were constructed from tomato which were successfully used for several positional cloning experiments. Tomato expressed sequence tag (EST) clones and microarrays are available through (http://ted.bti.cornell.edu/). Furthermore, with the advent of high throughput genotyping platforms, high density single nucleotide polymorphisms (SNPs) arrays and high density genetic maps are now available (Hamilton et al., 2012; Sim et al., 2012). A high quality reference genome sequence of the 'Heinz 1706' cultivar is now available (The Tomato Genome Consortium, 2012) and re-sequencing efforts for 150 tomato genomes including landraces, wild species as well as modern varieties is ongoing and will further aid in understanding the basis of adaptation, evolution and address the intra- and inter-specific relationships (http://www.tomatogenome.net/). Repositories for tomato information include The SOL Genomics Network (http://solgenomics.net/), Solanaceae Genomics Resource (http://solanaceae.plantbiology.msu.edu), the Tomato Functional Genomics Database (http://ted.bti.cornell.edu/) and a comprehensive list of other genomic databases available for tomato is given in (Ronning, 2013).

Tomato fruit anatomy

Botanically, tomato fruit is a berry, which develops from a fertilized ovary and contains seeds within a fleshy pericarp. Tomato fruit pericarp is formed from the outer ovary wall, which forms the bulk of the fruit. The pericarp surrounds the placenta and locules. In immature green fruit, the placental tissue is firm and fills the locules but by the mature green stage, locular tissue becomes jelly like and contains seeds. The pericarp consists of an outer exocarp constituting the fruit skin, parenchymatous mesocarp with vasculature and an inner endocarp. Basic anatomy of the tomato fruit is shown in Figure 1.1. The pericarp wall may also be divided into outer walls called septa, which separate the adjacent locules and the inner wall known as columella. The

number of locules is dependent on the number of carpels present in the gynoecium and can range from two to many (Lippman and Tanksley, 2001; Munos et al., 2011). The exocarp consists of the single cell epidermal layer that is covered by an extracellular cuticle and 3-5 layers of hypodermal collenchyma cells. The mesocarp constitutes the largest portion of the pericarp and consists of several layers of large vacuolated parenchyma cells and the vascular tissue. Collenchyma and parenchyma are the main metabolic factories of fruit pericarp as they regulate energy metabolism in the fruit. Collenchyma cells are a source of energy as they contain large number of chloroplasts and parenchyma cells are energy sinks as they accumulate starch granules (Matas et al., 2011). Endocarp limits the pericarp and consists of a single layer of inner epidermal cells. There is also a cuticle covering the surface of inner epidermis that faces the locular cavity. Unlike the cuticle covering the outer epidermis, the cuticle covering the inner epidermis does not undergo thickening during fruit development (Matas et al., 2011). Using laser capture micro-dissection (Matas et al., 2011) collected five principal tissues of tomato pericarp: outer and inner epidermal layers, collenchyma, parenchyma, and vascular tissues at their maximal growth phase and characterized the cell-specific transcriptome by pyrosequencing. This precise method of sample collection facilitated the interrogation of the cell-specific transcriptome profiles in developing fruit, revealing preferential expression of classes of genes in particular cell types. For example, all the starch synthesis-related transcripts were enriched in all fruit tissues except inner epidermis, suggesting that there could be photosynthetic capacity in all tissues. However, transcript abundance of genes specifically related to photosynthesis, photorespiration and photosystems are enriched in collenchyma cells, present just beneath the outer epidermis but not in interior layers including parenchyma cells suggesting that photosynthesis might be restricted to outer collenchyma (Matas et al., 2011).

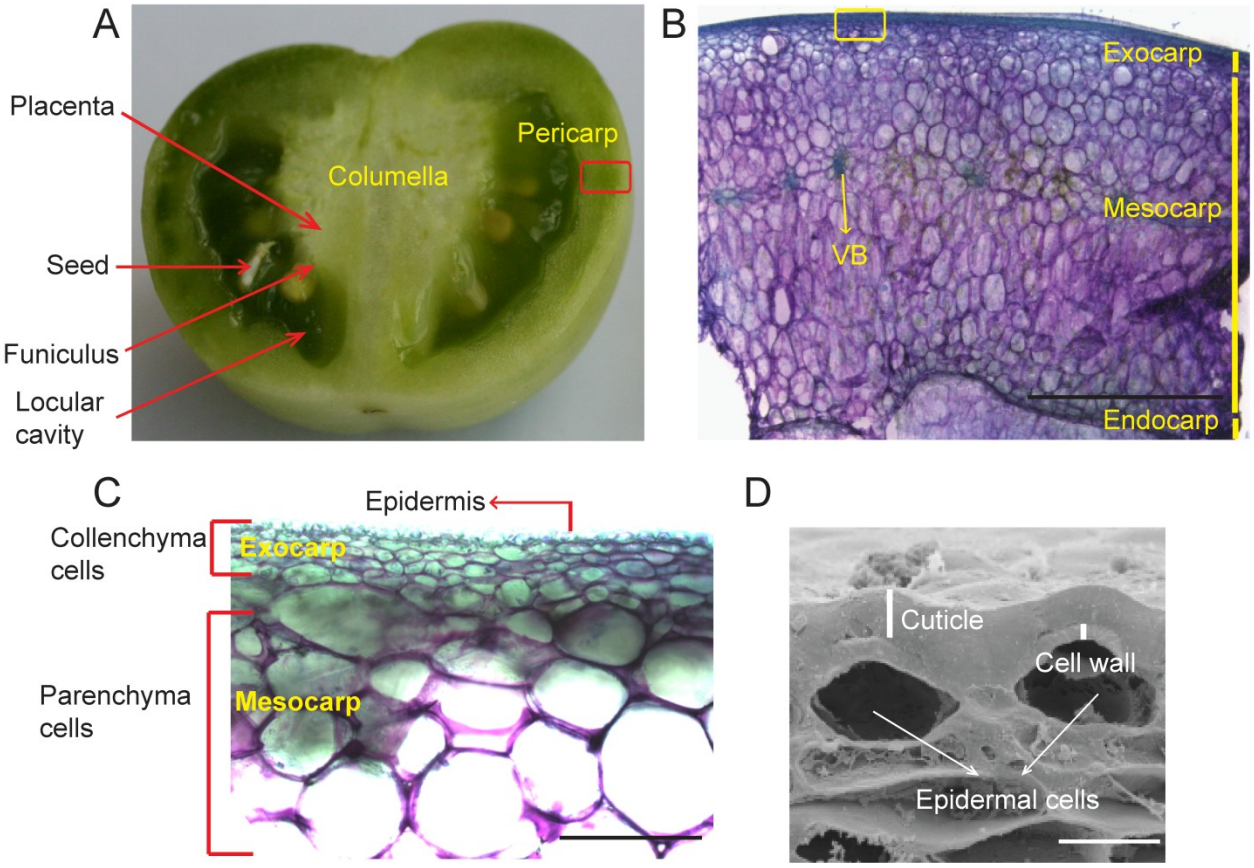

Figure 1.1. Tomato fruit anatomy A) Cross section of mature green (MG) tomato fruit. The red box across the pericarp represents the section shown in B) Free hand section of MG tomato fruit stained with toluidine blue showing different layers of fruit pericarp along with vascular bundles (VB). The yellow box represents exocarp region, which is further expanded in C) The Exocarp and mesocarp regions are shown specifying their cell types. D) Scanning electron micrograph showing outer epidermis of the tomato fruit with thick fruit cuticle. (Scale bar for B = 2mm; C = 100µm and D = 20µm).

Transcripts associated with cuticle metabolism were specific to the outer epidermis, although some were also expressed in the inner epidermis.

Genetic regulation of tomato fruit development

Fruits are essential component of human diet and are specialized organs unique to plants. Tomato fruit development can be divided into four stages from floral initiation to fruit ripening. Phase I is a 2-3 week period where floral initiation and production of mature flower occurs. It is during this phase that the identity, number as well as shape of floral organs are determined. This phase requires the coordinated spatial and temporal expression of transcription factors, including MADS-box genes, originally characterized in Arabidopsis and *Antirrhinum majus* that specify floral organ identity and gave rise to the ABC model of floral identity (Bowman et al., 1989; Schwarz-Sommer et al., 1990; Coen and Meyerowitz, 1991; Gustafson-Brown et al., 1994; Ferrandiz et al., 2000; Pelaz et al., 2000; Pinyopich et al., 2003; Bowman et al., 2012). Phase II is an active cell division period in the ovary beginning at anthesis and continues for the first 7-10 days after successful fertilization. This phase is characterized by the interplay of hormonal signals, primarily involving auxin and gibberellins that promote the expression of genes involved in cell division and expansion (Kibler and Bangerth, 1982; Gillaspy et al., 1993; de Jong et al., 2009; Seymour et al., 2013). Phase III is a period of 6-7 weeks (end of cell division until a week before onset of ripening) where fruit growth occurs through cell expansion. This phase results in a remarkable increase in the size of the fleshy fruit. Phase IV is the ripening phase that initiates after growth has stopped and the seed has matured. This phase involves rapid chemical and structural changes that determine fruit aroma, color, texture, and biochemical composition (e.g., acids and sugars) but not fruit size and shape and is accompanied by rapid changes in transcriptional reprogramming (Gillaspy et al., 1993; Alba et al., 2005). Interestingly, many of

the regulators of fruit ripening are shared with genes involved in fruit development and dehiscence in Arabidopsis, suggesting evolutionary conserved mechanisms regulate these processes. MADS box family transcription factors (TFs) serve as central regulators of fruit development and ripening, not only in Arabidopsis and tomato but also in several other fruit species (Boss et al., 2002; Tadiello et al., 2009; Klee and Giovannoni, 2011; Seymour et al., 2011; Handa et al., 2012). *SHATTERPROOF* (*SHP*) *SHP1, 2* in Arabidopsis specify valve margin formation and dehiscence for controlled seed dispersal (Ferrandiz et al., 2000; Liljegren et al., 2000) and its tomato ortholog, *TAGL1* (*AGAMOUS-LIKE1*) is involved in fleshy fruit expansion and ripening (Vrebalov et al., 2009). Similarly, *APETALA2* in Arabidopsis affects silique development by negatively regulating replum formation and valve margin lignification (Ripoll et al., 2011), and its tomato ortholog, *SlAP2a* is a negative regulator of fruit ripening (Karlova et al., 2011; Chung et al., 2012). *RIPENING INHIBITOR* is a master regulator of ripening (Vrebalov et al., 2002), and is a member of the *SEPALLATA* sub-family of MADS-box genes that are involved in growth and development of floral organs including sepals (Pelaz et al., 2000; Zahn et al., 2005). *FRUITFULL* (*FUL*) in Arabidopsis plays a role in silique development by promoting cell expansion in valves causing elongation of the silique (Gu et al., 1998). Tomato contains two close homologs of *FUL*, *FUL1* and *FUL2*, which are functionally redundant and down regulation of both impairs color development in the fruit and affects fruit ripening processes (Bemer et al., 2012; Shima et al., 2013). Thus, members of this family of TFs share functional similarities.

When an ovary develops into a fruit, the ovary wall becomes the pericarp. The fruit pericarp is derived from cells within interna1 layer L3 in the shoot apical meristem (SAM). The number of cells that make up L3 determine the size of the floral meristem and carpel number,

which in turn governs the size of the pericarp. This is demonstrated from studies with inter-specific chimeras between *S. lycopersicum* and *S. peruvianum* genotypes differing in the number of carpels per flower and also chimeras generated by grafting using periclinal chimeras differing in their genetic makeup in meristem cell layers. Thereby, as pericarp forms the bulk of the fruit, L3 can directly determine the eventual sink size and strength of the developing fruit whereas L1 and L2 contribute to the outer and inner epidermal cell layers (Szymkowiak and Sussex, 1992; Huala and Sussex, 1993).

Forward genetics-based approaches provide insight into genes involved in fruit development and ripening

Many insights into the molecular basis of fruit development and ripening have been achieved through the characterization of monogenic mutants and exploitation of natural variation coupled with QTL analysis. Complex traits such as yield, shape and nutritional quality are quantitative traits influenced by multiple genes. Two of the early fruit-related QTLs identified were related to yield. The *fruit weight 2.2* locus was identified as a key factor in the evolution of fruit size during tomato domestication and the *brix 9-2-5* QTL, which influences sugar content was localized to an invertase gene (Frary et al., 2000; Fridman et al., 2000). Subsequently, multiple studies have mapped and identified QTLs for various fruit characteristics in several segregating populations derived from inter-specific crosses, including those associated with fruit size, shape, weight, soluble solid content, pH, color, and fruit firmness (Grandillo et al., 2013).

Insight into fleshy fruit development and ripening has also been achieved through the characterization and identification of loci encoded by numerous monogenic mutants of tomato that possess altered fruit phenotypes. These studies have identified master regulators of ripening encoded by the *ripening inhibitor* and *Colorless non-ripening* loci (Robinson and Tomes, 1968; Vrebalov et al., 2002; Manning et al., 2006), loci involved in ethylene response (Lanahan et al.,

1994; Wilkinson et al., 1995; Barry et al., 2005; Barry and Giovannoni, 2006), carotenoid and flavonoid biosynthesis (Mustilli et al., 1999; Ronen et al., 2000; Isaacson et al., 2002; Liu et al., 2004; Adato et al., 2009), cuticle biosynthesis (Isaacson et al., 2009; Nadakuduti et al., 2012; Yeats et al., 2012) and chloroplast development (Barry et al., 2012; Powell et al., 2012).

Fruit chloroplast development and its role in influencing fruit quality

Fleshy fruits are generally defined as a sink tissue, although fruit photosynthesis can contribute up to 20% of the total fruit photosynthate (Hetherington et al., 1998). Chloroplast development and the carbohydrate status of unripe fruits impact the composition and quality of ripe fruit (Hobson and Bedford, 1989; Powell et al., 2012; Sagar et al., 2013). Despite its importance in defining ripe fruit quality, the genetic mechanisms that control fruit chloroplast development are not completely understood. However, emerging evidence suggests that plastid development is differentially regulated in fruit and leaf tissues of tomato and in fruit, is controlled by three transcription factors (TFs), (Powell et al., 2012; Pan et al., 2013; Sagar et al., 2013; Nguyen et al., 2014) a tomato *GOLDEN 2-LIKE* homolog designated, *SlGLK2*, a tomato homolog of *ARABIDOPSIS PSEUDO RESPONSE REGULATOR 2-LIKE* (*SlAPRR2-LIKE*), and *AUXIN RESPONSE FACTOR 4* (*SlARF4*). Fruit chloroplast development is positively influenced through the action of *SlGLK2* and *SlAPRR2-LIKE*, whereas auxin, acting through *SlARF4*, negatively impacts this process (Powell et al., 2012; Pan et al., 2013; Sagar et al., 2013).

Fruits of *SlARF4 / DR12* -antisense lines are dark green when immature due to increase in chloroplast number and enhanced chloroplast development. In addition, *ARF4 / DR12* -antisense fruits display an unusual pattern of cell division in the pericarp, where cells continue to divide throughout development, unlike in wild type where this process ceases 7-10 days after fertilization. Fruits are blotchy when ripe and display increased firmness and density, enhanced

sugar content and prolonged shelf-life with reduced water loss at the ripe stage (Jones et al., 2002; Sagar et al., 2013; Sagar et al., 2013).

The *uniform ripening* (*u*) locus regulates the formation of an amorphous dark green shoulder that surrounds the calyx end of tomato fruit. *u* mutants have lower chlorophyll levels in green fruit which translates to reduced carotenoid and sugar contents in ripe fruits. *U* encodes *SlGLK2* that belongs to GARP family of Myb TFs (Powell et al., 2012). GLK TFs regulate chloroplast differentiation through promotion of nuclear-encoded photosynthesis-related gene expression (Fitter et al., 2002; Yasumura et al., 2005; Waters et al., 2008; Waters et al., 2009). In C3 plants, pairs of GLKs often act redundantly to regulate chloroplast development, whereas in C4 plants, including maize, each GLK has a specific role in bundle sheath and mesophyll cells that is largely determined by their differential expression (Langdale and Kidner, 1994; Rossini et al., 2001; Waters et al., 2008; Waters et al., 2009; Wang et al., 2013). In tomato, *SlGLK2* determines both chlorophyll accumulation as well as distribution within developing fruit. Breeders have selected for the *u* locus to achieve uniform ripening in fruits, which results in lower chlorophyll content and thereby less efficient in photosynthesis and compromised carotenoid and carbohydrate levels in the ripe fruit (Powell et al., 2012). Tomato possesses two *GLK*s, *SlGLK1* and *SlGLK2* that are functionally equivalent, however differential expression of these genes ensures that *SlGLK2* functions in fruits while *SlGLK1* functions primarily in leaf tissue (Nguyen et al., 2014). In addition, the expression of *SlGLK2* is elevated in the stem end of tomato fruit and promotes the gradient of chloroplast development that leads to the formation of the green-shoulder that surrounds that calyx of the fruit. The chloroplast gradient and ripening gradients were further investigated by RNA-seq analysis of three sections made along the vertical axis of the fruit. Together with the expected chlorophyll biosynthetic genes whose

expression is enriched in the stem end, additional genes, including the *KNOX* transcription factors, *TKN2* and *TKN4* were also up-regulated in this region, suggesting that they may play a role in either fruit chloroplast development and / or the formation of gene expression gradients in tomato fruit (Nguyen et al., 2014).

The tomato fruit cuticle: structure and function

The cuticle is considered one of the most important adaptation strategies for the colonization of plants to terrestrial environments owing to its ability to retain water and protect against ultra-violet radiation (Kolattukudy, 1980; Edwards, 1993; Kolattukudy, 2001). In addition the cuticle withstands biotic stresses, such as insect and pathogen infestations, and plays a major role in plant morphogenesis by preventing cell-cell adhesion and providing structural support by withstanding turgor pressure from the underlying cells (Kolattukudy, 1980; Sieber et al., 2000; Riederer and Schreiber, 2001; Wellesen et al., 2001; Nawrath, 2006; Pollard et al., 2008; Yeats and Rose, 2013).

In tomato, the exocarp, also referred to as the fruit skin is the outermost layer of the fruit pericarp comprised of the cuticle, outer epidermis and 3-5 layers of sub-dermal collenchyma cells (Bargel and Neinhuis, 2005). The mechanical performance of the exocarp, mainly attributed to the cuticle, has physiological and economic significance due to its impermeable cuticle covering that helps to minimize water loss, pathogen infection, reduce the incidence of cracking and provide color and gloss to the fruit surface (Chu and Thompson, 1972; Emmons and Scott, 1997; Emmons and Scott, 1998; Matas et al., 2004; Dominguez et al., 2011). The cuticle is synthesized by the epidermal cells and is deposited at the surface of these cells and is associated with a network of embedded polysaccharides that extend from their cell walls. The cuticle is heterogeneous and is comprised of a cutin matrix together with intra- and epicuticular waxes.

Cutin is a polymer formed by inter-esterification of hydroxy fatty acids with small amounts of glycerol, phenylpropanoids and dicarboxylic acids (Kolattukudy, 2001). The intra-cuticular waxes are embedded in the cutin framework while the epi-cuticular waxes are present on the surface. The cuticle can be demarcated as a 'cuticle layer' that is close to the epidermis consisting of cutin and polysaccharides and an overlying 'cuticle proper' consisting of primarily cutin and waxes at the air-fruit interface (Walton, 1990; Heredia, 2003). Arabidopsis has served as the primary model to decipher several steps in cutin and wax biosynthesis, but with the exception of its flower cutin, Arabidopsis has an atypical cutin composition compared to other species (Bonaventure et al., 2004; Franke et al., 2005; Li-Beisson et al., 2009). Tomato fruit possesses a thick prominent astomatous cuticle which is primarily made of a typical cutin monomer 10, 16-dihydroxyhexadecanoic acid that comprises greater than 80% of the cutin by weight (Vogg et al., 2004; Kosma et al., 2010) and more recently, tomato has become increasingly utilized to study aspects of cuticle biosynthesis and function.

The 10, 16-diOH fatty acid-based cutin of tomato

Tomato cutin is dominated by a C16 family of mostly ω-hydroxy fatty acids with mid chain hydroxyl groups or epoxy group and dicarboxylic acids making up to 85% of the total cutin. However, similarly modified C18 fatty acids are also detected in tomato cutin, which together with *cis* and *trans*-coumaric acids make up the remainder of the cutin (Isaacson et al., 2009; Kosma et al., 2010; Nadakuduti et al., 2012). The fatty acids constituting typical tomato fruit cutin monomers are listed in Figure 1.2. The pathway leading to formation of C16 type of cutin is fairly well understood through recent advancements made using both Arabidopsis and tomato. *De novo* fatty acid synthesis occurs exclusively inside the chloroplasts of epidermal cells, which supplies acyl chains for polymer assembly (Ohlrogge and Jaworski, 1997). Further

modifications to the acyl chains occur outside the chloroplasts in the endoplasmic reticulum. In Arabidopsis, hydroxylation of C16 fatty acid at the terminal position to yield ω-hydroxy C16 fatty acids is carried out by CYP86A4 (Li-Beisson et al., 2009), a tomato homolog of this enzyme, designated *SlCYP86A69*, was recently identified by cloning the *cutin deficient 3* (*cd3*) mutant. Mutants at the *slcyp86a69* locus display reduced cuticle thickness with altered cutin composition (Shi et al., 2013). Further hydroxylation in the mid chain position to produce the major monomer, 10, 16-dihydroxy C16 fatty acid is carried out by CYP77A6, a mid-chain hydroxylase (Li-Beisson et al., 2009). A transcriptome study of tomato fruit pericarp identified two *CYP77A* genes that are highly expressed in the outer epidermis, suggesting that they may be candidates for mid-chain hydroxylases (Matas et al., 2011). The steps involving the formation of dicarboxylic acid and epoxy acids are currently unclear.

Once the modified fatty acids are produced, these cutin fatty acyl precursors are linked to glycerol by glycerol-3-phosphate acyltransferases (GPATs). For cutin biosynthesis the unique bi-functional acyl transferases, GPAT4 and GPAT6 are required. These enzymes act as acyltransferases to esterify acyl groups, predominantly to the *sn*-2 position of glycerol 3 phosphate and also possess phosphatase activity that yields *sn*-2 monoacylglycerol (2-MAG). It was predicted that 2-MAG could be a potential cutin precursor that is exported outside of the epidermal cells for external cutin assembly (Li et al., 2007; Yang et al., 2010). The ATP binding cassette (ABC) transporter *ABCG12* is implicated in the transport of cutin monomers (Pighin et al., 2004; Bird et al., 2007). Although cutin is a polymer, the steps required for its assembly, including the mechanism of inter-esterification of hydroxy fatty acids and glycerol, the site of polymerization, and the molecules that are exported from epidermal cells to their exterior surfaces remained unresolved (Pollard et al., 2008; Beisson et al., 2012). Recently, identification

of *CD1* by map based cloning of tomato *cutin deficient 1* mutant provided answers to some of these questions. *CD1* encodes a member of the glycine–aspartic acid–serine-leucine motif lipase/hydrolase (GDSL) super family of enzymes. Immunolocalization of CD1 in fruit demonstrated that it is exclusively localized within the cuticle, outside of the epidermal cells while *CD1* transcripts preferentially accumulate within epidermal cells. The detection of the MAG species 2-mono (10, 16-dihydroxyhexadecanoyl) glycerol in the wax fraction of *cd1* fruit, further strengthened the existing hypothesis that 2-MAG could be a precursor for cutin synthesis that is exported outside the epidermal cell and this mechanism is probably disrupted in *cd1*. Purified recombinant CD1 protein catalyzed acyltransferase reactions *in vitro*, resulting in formation of up to seven 10, 16-dihydroxyhexadecanoyl monomers whereas, site-directed mutagenesis of the conserved catalytic serine to alanine eliminated this activity. Together, these results indicate that CD1 is a cutin synthase which catalyzes cutin polymerization outside the cell using a 2-MAG species as acyl donor and the growing polymer chain as an acyl acceptor (Yeats et al., 2012). Although *cd1* is a null mutant (Yeats et al., 2012), fruit are not completely cutin deficient, indicating the presence of other cutin synthases or functionally similar proteins that are yet to be identified (Isaacson et al., 2009). Solution state NMR analysis using *in-vitro* synthesized CD1 protein indicated that it catalyzes primarily the formation of linear cutin oligomers, thus the question of branching and cross-linking in the cutin polymer remains unresolved (Yeats et al., 2014). The identified steps in the cutin biosynthetic pathway pertaining to tomato cutin are presented in Figure1.3.

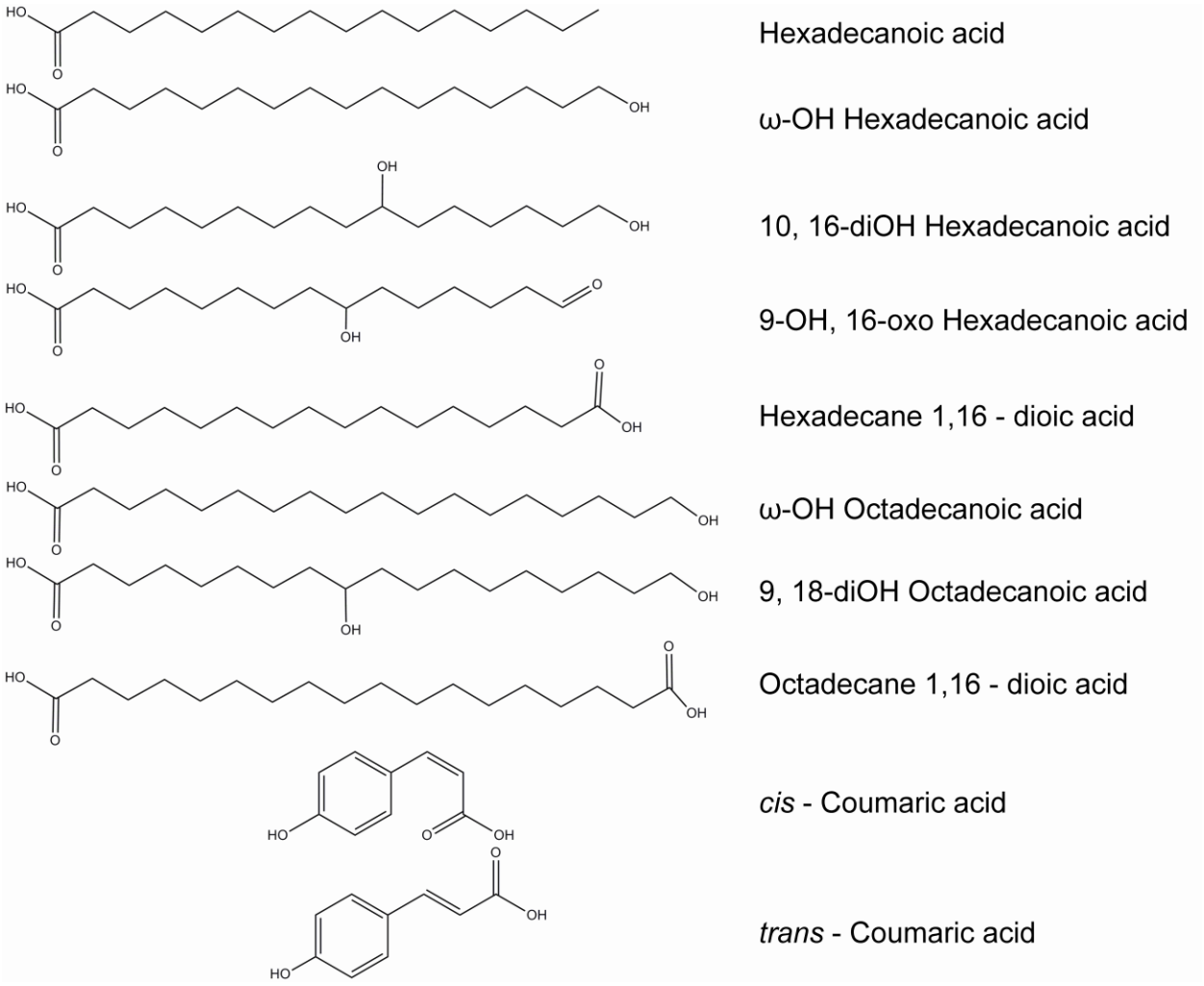

Figure 1.2. The structures of typical cutin monomers found in tomato fruit cutin. The free fatty acid form is given for each monomer, although *in vivo*, these monomers may also be present as acyl-CoAs or glycerolipids. The structures of tomato fruit cutin monomers reported in (Nadakuduti et al., 2012) are presented here.

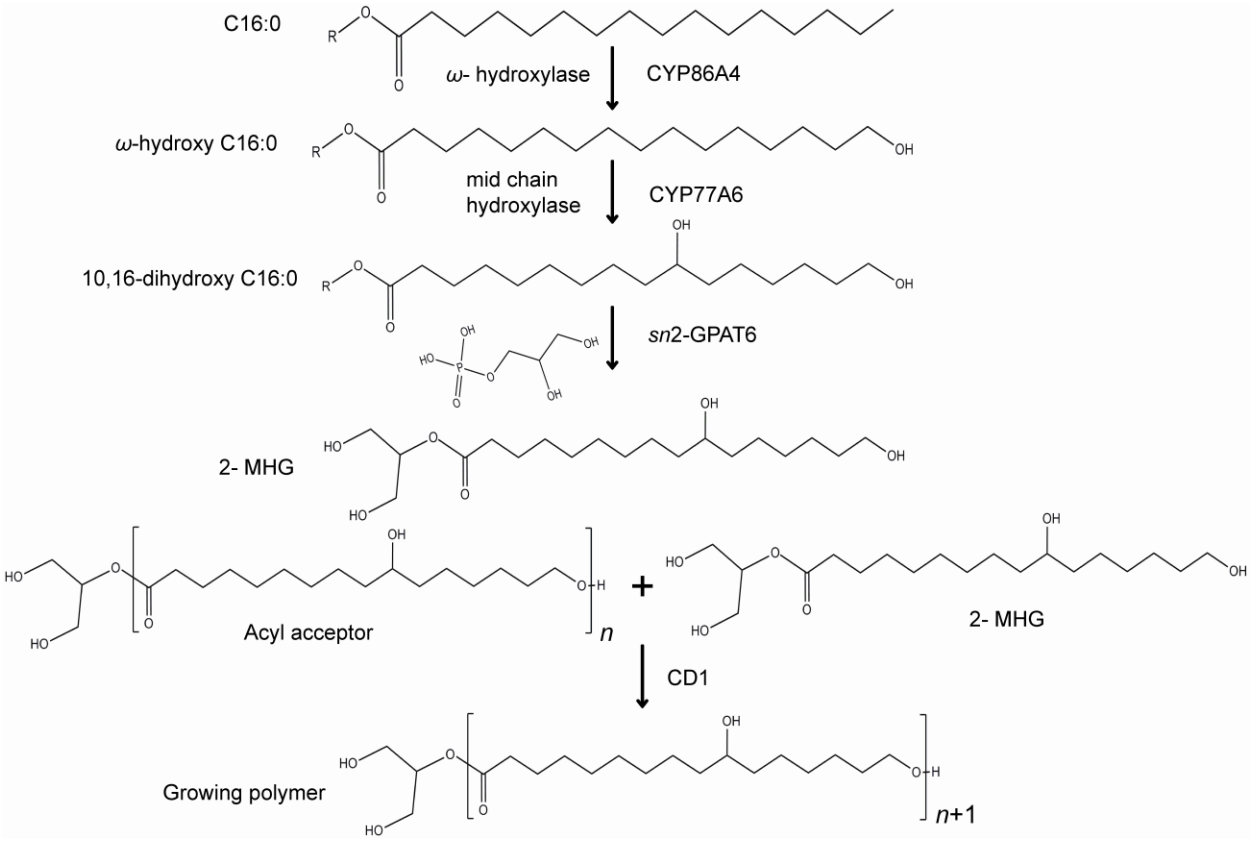

Figure 1.3. Biosynthesis of C16 family of fatty acyl monomers. The free fatty acids formed in the chloroplast undergo modifications in the endoplasmic reticulum to produce cutin monomers. The terminal and mid-chain hydroxylation reactions are carried out by CYP450s. A plant-specific bi-functional GPAT6 enzyme esterifies 10, 16-dihydroxyhexadecanoyl group, to *sn*-2 position of glycerol 3-phosphate yielding 2-mono (10, 16-dihydroxyhexadecanoyl) glycerol (2-MHG), an initial intermediate precursor for cutin polymer assembly is the form in which it is exported outside the epidermal cell. CD1 catalyzes the polymerization of these monomers by transferring the hydroxyacyl group from 2-MHG to the growing polymer external to epidermal cell. *In-vivo*, substrates may be acyl-CoAs (R = CoA), free fatty acids (R = H) or glycerolipids. The sequential order of these reactions is inferred but not experimentally determined (Li-Beisson et al., 2009; Beisson and Ohlrogge, 2012; Yeats and Rose, 2013).

Composition and functions of tomato cuticular waxes

Cuticular wax is a complex mixture of a series of very-long-chain (VLC) aliphatic lipids, triterpenoids, and minor compounds, such as sterols and flavonoids (Kunst and Samuels, 2003). Forward and reverse genetics approaches as well as epidermal transcriptome analysis in Arabidopsis have led to molecular characterization of enzymes catalyzing major steps in wax biosynthesis and export, contributing to our understanding of the importance of waxes in plants (McNevin et al., 1993; Suh et al., 2005; Kunst and Samuels, 2009; Bernard and Joubes, 2013; Lee and Suh, 2013). Cuticular waxes are involved in regulating water relations in plants by forming a waterproof barrier. In plants, transpirational water loss is mainly regulated by stomates and to a certain extent by cuticular wax. As tomato fruit lacks stomata, cuticular wax becomes crucial for water regulation (Vogg et al., 2004). Tomato fruit wax consists of very long chain fatty acids (C20-C32), straight chain (C23-C33) and branched alkanes (C30-C32), alkenes (C33), alcohols (C20-32), triterpenoids, sterols and *cis*, *trans*-coumarates, although it is dominated in abundance by very long chain alkanes and triterpenoids (Bauer et al., 2004; Kosma et al., 2010; Nadakuduti et al., 2012). Although many components of tomato wax are known, up to 15 percent of the total wax composition remains unknown (Nadakuduti et al., 2012). A representative from each wax class is provided in Figure 1.4. The function of cuticular waxes in tomato fruit was demonstrated by analyzing mutants with altered cuticle properties. Fruits of the *lecer6* mutant lack a *β*-ketoacyl-CoA synthase, a component of the VLC fatty acid elongase complex (Leide et al., 2007). The *lecer6* mutant fruit show reduced *n*-alkanes in the fruit wax, which directly correlates with their water loss. In the 'Delayed Fruit Deterioration' (DFD) cultivar of tomato,

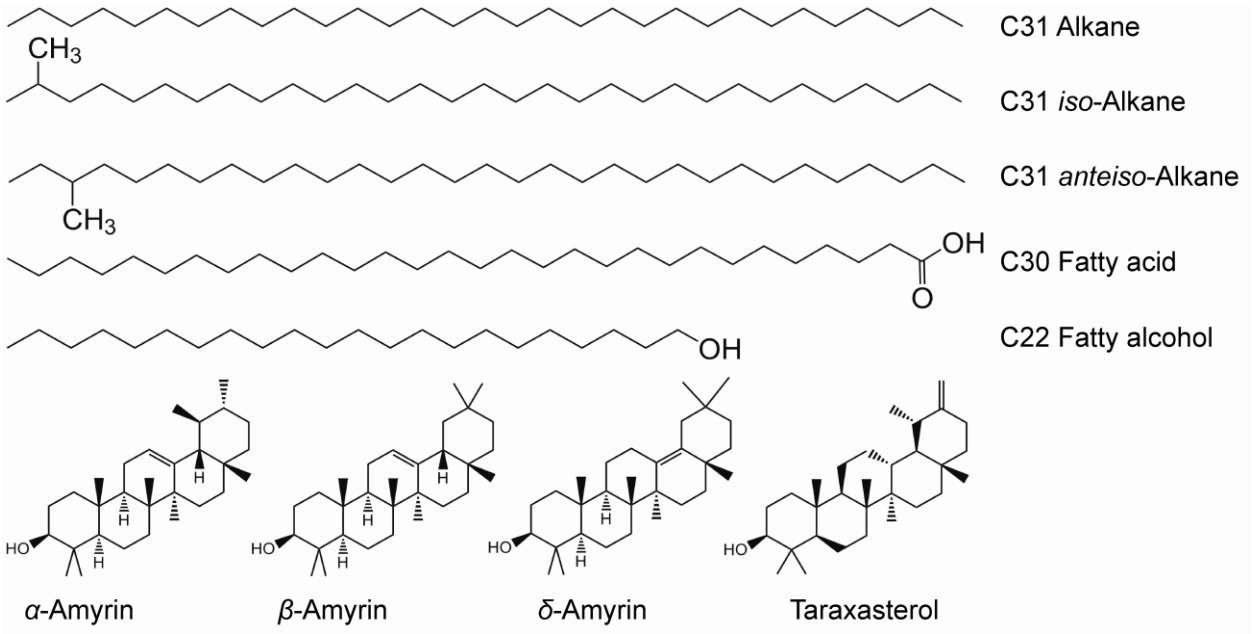

Figure 1.4. Tomato cuticular wax components. The structure of a representative compound belonging to each class of tomato fruit cuticular wax is provided.

fruits undergo normal ripening, but remain firm with no loss of integrity for remarkably long periods after they ripen (Saladie et al., 2007). Characterization of this cultivar revealed that, although polysaccharide components of the cell wall are critical for fruit texture, alterations in cuticle architecture is also an integral component of the fruit ripening process. The total amount of wax was higher in DFD than was observed in wild type with a 5-fold increase in *n*-alkadienes observed but no increase in *n*-alkanes. There was also a doubling of the total cutin in ripe fruits of the DFD compared to wild type. These studies show the importance of fruit cuticular waxes in mediating water relations in tomato fruit.

Regulators of cuticle biosynthesis

The regulation of cuticle synthesis is complex as it is influenced by various factors, including several biotic and abiotic stresses (Aharoni et al., 2004; Chassot et al., 2007; Kosma et al., 2009; Seo et al., 2009; Kosma et al., 2010; Seo and Park, 2010; Bourdenx et al., 2011). The epidermal cells are highly specialized and serve as the site of synthesis for cutin precursors and wax biosynthesis and their proximity to the adjacent environment influences the expression of epidermal cell-specific transcription factors and thereby metabolic activity of these cells (Javelle et al., 2011). Regulatory genes involved in cuticle biosynthesis have been identified in both Arabidopsis and tomato. WAX INDUCER1/SHINE1 (WIN1 / SHN1), SHN2 and SHN3 form a small, distinct group of proteins belonging to the APETALA2/ethylene-responsive factor transcription factor family (Aharoni et al., 2004; Broun et al., 2004; Kannangara et al., 2007; Shi et al., 2011). Over-expression of *WIN1*/*SHN1* in Arabidopsis increases epicuticular wax biosynthesis, which led to a characteristic shiny leaf phenotype and plants that display increased drought tolerance (Kannangara et al., 2007). However, the phenotypes associated with *WIN1*/*SHN1* over-expression were not restricted to wax accumulation as an increase in cutin was

also observed together with altered epidermal cell structure, altered trichome number and branching and an atypical stomatal index (Aharoni et al., 2004; Broun et al., 2004; Kannangara et al., 2007). Recently, *SlSHN3* of tomato has been characterized through over-expression and RNAi lines (Shi et al., 2013). Silencing of *SlSHN3* resulted in reduced cutin and wax content of tomato fruit cuticles due to down regulation of an array of cutin metabolism genes. For example, the CYP450 family members *SlCYP77A1*, *SlCYP86A68* and *SlCYP86A69*, Arabidopsis homologs of which were previously shown to catalyze fatty acid hydroxylation (Li-Beisson et al., 2009), were down-regulated. Concomitant with altered cuticle composition, *SlSHN3* RNAi lines displayed increased water loss and decreased resistance to fungal infection. However, the impact of *SlSHN3* silencing may extend beyond cuticle biosynthesis as genes related to epidermal patterning were also down-regulated compared to untransformed lines (Shi et al., 2013).

In tomato, characterization of the *cd2* mutant led to identification of *CUTIN DEFICIENT 2,* a homeodomain-leucine zipper IV transcription factor (HD-ZIP IV) involved in cuticle biosynthesis in fruits (Isaacson et al., 2009). HD-ZIP IV TFs are master regulators of epidermal cell function (Ingram et al., 1999; Kubo et al., 1999; Nakamura et al., 2006; Javelle et al., 2010; Javelle et al., 2011). Fruits of the *cd2* mutant are severely cutin deficient and also have an altered wax profile. Characterization of the *sticky peel* (*pe*) mutant which carries a second mutant allele at the *cd2* locus indicates that *CD2* is a master regulator of epidermal cell function in tomato, with functions that extend beyond fruit cuticle biosynthesis. For example, leaves of the *pe* mutant are also cutin deficient and possess increased water permeability. In addition, characterization of *pe* revealed that *CD2* also influences several additional epidermal cell-related phenotypes,

including trichome differentiation, anthocyanin accumulation (Nadakuduti et al., 2012) together with altered sugar and glycoalkaloid profiles in fruit (Kimbara et al., 2012).

CD2 and SlSHN3 represent tomato TFs that have pleiotropic affects on epidermal cell function, including cuticle biosynthesis. Other MYB TFs that regulate cuticle biosynthesis have been identified in Arabidopsis including, MYB106, MYB16 (Oshima et al., 2013) along with MYB30 and MYB96 that are biotic and abiotic stress responsive (Raffaele et al., 2008; Seo et al., 2009). WXP1, an AP2-domain TF that regulates wax biosynthesis and confers drought tolerance has been identified in *Medicago sativa* (Zhang et al., 2005). Homologs of all the TFs identified in other species are yet to be characterized in tomato. The transcriptional network that regulates cuticle biosynthesis has yet to be clearly established through investigation of the downstream targets for each TF to reveal their function in plant development and epidermal cell function. Although several advances have been made in cuticle biology, aspects such as the structure of the cutin polymer, intra and extra cellular transport mechanisms of cutin monomers and waxes, enzymes for the synthesis of dicarboxylic acids, epoxy acids, and alkanes together with the complete polymerization of cutin, the order of the reactions and substrates specificities of the enzymes remain to be determined (Pollard et al., 2008; Beisson et al., 2012; Yeats and Rose, 2013).

REFERENCES

REFERENCES

Adato A, Mandel T, Mintz-Oron S, Venger I, Levy D, Yativ M, Dominguez E, Wang Z, De Vos RC, Jetter R, Schreiber L, Heredia A, Rogachev I, Aharoni A (2009) Fruit-surface flavonoid accumulation in tomato is controlled by a SlMYB12-regulated transcriptional network. PLoS Genet. **5:** e1000777

Aharoni A, Dixit S, Jetter R, Thoenes E, van Arkel G, Pereira A (2004) The SHINE clade of AP2 domain transcription factors activates wax biosynthesis, alters cuticle properties, and confers drought tolerance when overexpressed in Arabidopsis. Plant Cell **16:** 2463-2480

Alba R, Payton P, Fei ZJ, McQuinn R, Debbie P, Martin GB, Tanksley SD, Giovannoni JJ (2005) Transcriptome and selected metabolite analyses reveal multiple points of ethylene control during tomato fruit development. Plant Cell **17:** 2954-2965

Ashrafi H, Kinkade M, Foolad MR (2009) A new genetic linkage map of tomato based on a *Solanum lycopersicum* x *S. pimpinellifolium* RIL population displaying locations of candidate pathogen response genes. Genome **52:** 935-956

Bai Y, Lindhout P (2007) Domestication and breeding of tomatoes: what have we gained and what can we gain in the future? Ann. Bot. **100:** 1085-1094

Bargel H, Neinhuis C (2005) Tomato (*Lycopersicon esculentum* Mill.) fruit growth and ripening as related to the biomechanical properties of fruit skin and isolated cuticle. J. Exp. Bot. **56:** 1049-1060

Barry CS, Aldridge GM, Herzog G, Ma Q, McQuinn RP, Hirschberg J, Giovannoni JJ (2012) Altered chloroplast development and delayed fruit ripening caused by mutations in a zinc metalloprotease at the *lutescent2* locus of tomato. Plant Physiol. **159:** 1086-1098

Barry CS, Giovannoni JJ (2006) Ripening in the tomato *Green-ripe* mutant is inhibited by ectopic expression of a protein that disrupts ethylene signaling. Proc. Natl. Acad. Sci. USA **103:** 7923-7928

Barry CS, McQuinn RP, Thompson AJ, Seymour GB, Grierson D, Giovannoni JJ (2005) Ethylene insensitivity conferred by the *Green-ripe* and *Never-ripe 2* ripening mutants of tomato. Plant Physiol. **138:** 267-275

Bauer S, Schulte E, Thier HP (2004) Composition of the surface wax from tomatoes - II. Quantification of the components at the ripe red stage and during ripening. Eur. Food Res. Technol. **219:** 487-491

Beisson F, Li-Beisson Y, Pollard M (2012) Solving the puzzles of cutin and suberin polymer biosynthesis. Curr. Opin. Plant Biol. **15:** 329-337

Beisson F, Ohlrogge J (2012) Plants: knitting a polyester skin. Nat. Chem. Biol. **8:** 603-604

Bemer M, Karlova R, Ballester AR, Tikunov YM, Bovy AG, Wolters-Arts M, Rossetto PdB, Angenent GC, de Maagd RA (2012) The tomato FRUITFULL homologs TDR4/FUL1 and MBP7/FUL2 regulate ethylene-independent aspects of fruit ripening. Plant Cell **24:** 4437-4451

Bergougnoux V (2014) The history of tomato: from domestication to biopharming. Biotechnol. Adv. **32:** 170-189

Bernard A, Joubes J (2013) Arabidopsis cuticular waxes: advances in synthesis, export and regulation. Prog. Lipid Res. **52:** 110-129

Bird D, Beisson F, Brigham A, Shin J, Greer S, Jetter R, Kunst L, Wu XW, Yephremov A, Samuels L (2007) Characterization of Arabidopsis ABCG11/WBC11, an ATP binding cassette (ABC) transporter that is required for cuticular lipid secretion. Plant J. **52:** 485-498

Bonaventure G, Beisson F, Ohlrogge J, Pollard M (2004) Analysis of the aliphatic monomer composition of polyesters associated with Arabidopsis epidermis: occurrence of octadeca-*cis*-6, *cis*-9-diene-1,18-dioate as the major component. Plant J. **40:** 920-930

Boss PK, Sensi E, Hua C, Davies C, Thomas MR (2002) Cloning and characterisation of grapevine (*Vitis vinifera L.*) MADS-box genes expressed during inflorescence and berry development. Plant Sci. **162:** 887-895

Bourdenx B, Bernard A, Domergue F, Pascal S, Leger A, Roby D, Pervent M, Vile D, Haslam RP, Napier JA, Lessire R, Joubes J (2011) Overexpression of Arabidopsis *ECERIFERUM1* promotes wax very-long-chain alkane biosynthesis and influences plant response to biotic and abiotic stresses. Plant Physiol. **156:** 29-45

Bowman JL, Smyth DR, Meyerowitz EM (1989) Genes directing flower development in Arabidopsis. Plant Cell **1:** 37-52

Bowman JL, Smyth DR, Meyerowitz EM (2012) The ABC model of flower development: then and now. Development **139:** 4095-4098

Broun P, Poindexter P, Osborne E, Jiang CZ, Riechmann JL (2004) WIN1, a transcriptional activator of epidermal wax accumulation in Arabidopsis. Proc. Natl. Acad. Sci. USA **101:** 4706-4711

Budiman MA, Mao L, Wood TC, Wing RA (2000) A deep-coverage tomato BAC library and prospects toward development of an STC framework for genome sequencing. Genome Res **10:** 129-136

Butler L (1968) Linkage summary. Rep. Tomato Genet. Coop. **18:** 4-6

Chakrabarti M, Zhang N, Sauvage C, Munos S, Blanca J, Canizares J, Diez MJ, Schneider R, Mazourek M, McClead J, Causse M, van der Knaap E (2013) A cytochrome P450 regulates a domestication trait in cultivated tomato. Proc. Natl. Acad. Sci. USA **110:** 17125–17130

Chassot C, Nawrath C, Metraux JP (2007) Cuticular defects lead to full immunity to a major plant pathogen. Plant J. **49:** 972-980

Chu MCY, Thompson AE (1972) Comparative anatomy of pericarps of four tomato mutants. J. Am. Soc. Hort. Sci. **97:** 478-481

Chung MY, Vrebalov J, Alba R, Lee J, McQuinn R, Chung JD, Klein P, Giovannoni J (2012) A tomato (*Solanum lycopersicum*) *APETALA2/ERF* gene, *SlAP2a*, is a negative regulator of fruit ripening. Plant J **64:** 936-947

Coen ES, Meyerowitz EM (1991) The war of the whorls: genetic interactions controlling flower development. Nature **353:** 31-37

de Jong M, Mariani C, Vriezen WH (2009) The role of auxin and gibberellin in tomato fruit set. J. Exp. Bot. **60:** 1523-1532

Dominguez E, Cuartero J, Heredia A (2011) An overview on plant cuticle biomechanics. Plant Sci. **181:** 77-84

Edwards D (1993) Cells and tissues in the vegetative sporophytes of early land plants. New Phytol. **125:** 225-247

Emmanuel E, Levy AA (2002) Tomato mutants as tools for functional genomics. Curr. Opin. Plant Biol. **5:** 112-117

Emmons CLW, Scott JW (1997) Environmental and physiological effects on cuticle cracking in tomato. J. Am. Soc. Hortic. Sci. **122:** 797-801

Emmons CLW, Scott JW (1998) Ultrastructural and anatomical factors associated with resistance to cuticle cracking in tomato (*Lycopersicon esculentum Mill.*). Int. J. Plant Sci. **159:** 14-22

Eshed Y, Zamir D (1995) An introgression line population of *Lycopersicon pennellii* in the cultivated tomato enables the identification and fine mapping of yield-associated QTL. Genetics **141:** 1147-1162

Ferrandiz C, Liljegren SJ, Yanofsky MF (2000) Negative regulation of the *SHATTERPROOF* genes by FRUITFULL during Arabidopsis fruit development. Science **289:** 436-438

Fitter DW, Martin DJ, Copley MJ, Scotland RW, Langdale JA (2002) *GLK* gene pairs regulate chloroplast development in diverse plant species. Plant J. **31:** 713-727

Franke R, Briesen I, Wojciechowski T, Faust A, Yephremov A, Nawrath C, Schreiber L (2005) Apoplastic polyesters in Arabidopsis surface tissues - a typical suberin and a particular cutin. Phytochemistry **66:** 2643-2658

Frary A, Nesbitt TC, Grandillo S, Knaap E, Cong B, Liu J, Meller J, Elber R, Alpert KB, Tanksley SD (2000) *fw2.2*: a quantitative trait locus key to the evolution of tomato fruit size. Science **289:** 85-88

Frary A, Xu Y, Liu J, Mitchell S, Tedeschi E, Tanksley S (2005) Development of a set of PCR-based anchor markers encompassing the tomato genome and evaluation of their usefulness for genetics and breeding experiments. Theor. Appl. Genet. **111:** 291-312

Fridman E, Pleban T, Zamir D (2000) A recombination hotspot delimits a wild-species quantitative trait locus for tomato sugar content to 484 bp within an invertase gene. Proc. Natl. Acad. Sci. USA **97:** 4718-4723

Gillaspy G, Bendavid H, Gruissem W (1993) Fruits-a developmental perspective. Plant Cell **5:** 1439-1451

Goldman IL, Paran I, Zamir D (1995) Quantitative trait locus analysis of a recombinant inbred line population derived from a *Lycopersicon esculentum* x *Lycopersicon cheesmanii* cross. Theor. Appl. Genet. **90:** 925-932

Grandillo S, Termolino P, van der Knaap E (2013) Molecular mapping of complex traits in tomato. *In* BE Liedl, JA Labate, JR Stommel, A Slade, C Kole, eds, Genetics, genomics, and breeding of tomato. Science, pp 150-227

Gu Q, Ferrandiz C, Yanofsky MF, Martienssen R (1998) The *FRUITFULL* MADS-box gene mediates cell differentiation during Arabidopsis fruit development. Development **125:** 1509-1517

Gustafson-Brown C, Savidge B, Yanofsky MF (1994) Regulation of the Arabidopsis floral homeotic gene *APETALA1*. Cell **76:** 131-143

Haanstra JPW, Wye C, Verbakel H, Meijer-Dekens F, van den Berg P, Odinot P, van Heusden AW, Tanksley S, Lindhout P, Peleman J (1999) An integrated high density RFLP-AFLP map of tomato based on two *Lycopersicon esculentum* x *L. pennellii* F_2 populations. Theor. Appl. Genet. **99:** 254-271

Hamilton JP, Sim SC, Stoffel K, Van Deynze A, Buell CR, Francis DM (2012) Single nucleotide polymorphism discovery in cultivated tomato via sequencing by synthesis. Plant Genome **5:** 17-29

Handa AK, Tiznado-Hernandez ME, Mattoo AK (2012) Fruit development and ripening: a molecular perspective, section E: Biotechnology for improvement of yield and quality traits. *In* A Altman, PM Hasegawa, eds, Plant biotechnology and agriculture: prospects for the 21st century. Elsevier Inc., pp 405-424

Heredia A (2003) Biophysical and biochemical characteristics of cutin, a plant barrier biopolymer. Biochim. Biophys. Acta **1620:** 1-7

Hetherington SE, Smillie RM, Davies WJ (1998) Photosynthetic activities of vegetative and fruiting tissues of tomato. J. Exp. Bot. **49:** 1173-1181

Hobson G, Bedford L (1989) The composition of cherry tomatoes and its relation to consumer acceptability. J Hortic Sci **64:** 321 - 329

Huala E, Sussex IM (1993) Determination and cell interactions in reproductive meristems. Plant Cell **5:** 1157-1165

Ingram GC, Magnard JL, Vergne P, Dumas C, Rogowsky PM (1999) *ZmOCL1*, an *HDGL2* family homeobox gene, is expressed in the outer cell layer throughout maize development. Plant Mol. Biol. **40:** 343-354

Isaacson T, Kosma DK, Matas AJ, Buda GJ, He YH, Yu BW, Pravitasari A, Batteas JD, Stark RE, Jenks MA, Rose JKC (2009) Cutin deficiency in the tomato fruit cuticle consistently affects resistance to microbial infection and biomechanical properties, but not transpirational water loss. Plant J. **60:** 363-377

Isaacson T, Ronen G, Zamir D, Hirschberg J (2002) Cloning of *tangerine* from tomato reveals a carotenoid isomerase essential for the production of beta-carotene and xanthophylls in plants. Plant Cell **14:** 333-342

Javelle M, Klein-Cosson C, Vernoud V, Boltz V, Maher C, Timmermans M, Depege-Fargeix N, Rogowsky PM (2011) Genome-wide characterization of the HD-ZIP IV transcription factor family in maize: preferential expression in the epidermis. Plant Physiol. **157:** 790-803

Javelle M, Vernoud V, Depege-Fargeix N, Arnould C, Oursel D, Domergue F, Sarda X, Rogowsky PM (2010) Overexpression of the epidermis-specific homeodomain-leucine zipper IV transcription factor OUTER CELL LAYER1 in maize identifies target genes involved in lipid metabolism and cuticle biosynthesis. Plant Physiol. **154:** 273-286

Jones B, Frasse P, Olmos E, Zegzouti H, Li ZG, Latche A, Pech JC, Bouzayen M (2002) Down-regulation of DR12, an auxin-response-factor homolog, in the tomato results in a pleiotropic phenotype including dark green and blotchy ripening fruit. Plant J. **32:** 603-613

Kannangara R, Branigan C, Liu Y, Penfield T, Rao V, Mouille G, Hofte H, Pauly M, Riechmann JL, Broun P (2007) The transcription factor WIN1/SHN1 regulates cutin biosynthesis in *Arabidopsis thaliana*. Plant Cell **19:** 1278-1294

Karlova R, Rosin FM, Busscher-Lange J, Parapunova V, Do PT, Fernie AR, Fraser PD, Baxter C, Angenent GC, de Maagd RA (2011) Transcriptome and metabolite profiling show that APETALA2a is a major regulator of tomato fruit ripening. Plant Cell **23:** 923-941

Kibler SB, Bangerth F (1982) Relationship between cell number, cell size and fruit size of seeded fruits of tomato (*Lycopersicon esculentum* Mill.), and those induced parthenocarpically by the application of plant growth regulators. Plant Growth Regul. **1:** 143-154

Kimbara J, Yoshida M, Ito H, Hosoi K, Kusano M, Kobayashi M, Ariizumi T, Asamizu E, Ezura H (2012) A novel class of sticky peel and light green mutations causes cuticle deficiency in leaves and fruits of tomato (*Solanum lycopersicum*). Planta **236:** 1559-1570

Kimura S, Sinha N (2008) Tomato (*Solanum lycopersicum*): A model fruit-bearing crop. Cold Spring Harbor Protocols **2008:** pdb.emo105

Klee HJ, Giovannoni JJ (2011) Genetics and control of tomato fruit ripening and quality attributes. Annu. Rev. Genet. **45:** 41-59

Koenig D, Jimenez-Gomez JM, Kimura S, Fulop D, Chitwood DH, Headland LR, Kumar R, Covington MF, Devisetty UK, Tat AV, Tohge T, Bolger A, Schneeberger K, Ossowski S, Lanz C, Xiong GY, Taylor-Teeples M, Brady SM, Pauly M, Weigel D, Usadel B, Fernie AR, Peng J, Sinha NR, Maloof JN (2013) Comparative transcriptomics reveals patterns of selection in domesticated and wild tomato. Proc. Natl. Acad. Sci. USA **110:** E2655-E2662

Kolattukudy PE (1980) Bio-polyester membranes of plants - cutin and suberin. Science **208:** 990-1000

Kolattukudy PE (2001) Polyesters in higher plants. *In* Advances in Biochemical Engineering Biotechnology. Biopolyesters, pp 1-49

Kosma DK, Bourdenx B, Bernard A, Parsons EP, Lu S, Joubes J, Jenks MA (2009) The impact of water deficiency on leaf cuticle lipids of Arabidopsis. Plant Physiol. **151:** 1918-1929

Kosma DK, Nemacheck JA, Jenks MA, Williams CE (2010) Changes in properties of wheat leaf cuticle during interactions with Hessian fly. Plant J. **63:** 31-43

Kosma DK, Parsons EP, Isaacson T, Lü S, Rose JKC, Jenks MA (2010) Fruit cuticle lipid composition during development in tomato ripening mutants. Physiol. Plant. **139:** 107-117

Kubo H, Peeters A, Aarts M, Pereira A, Koornneef M (1999) *ANTHOCYANINLESS2*, a homeobox gene affecting anthocyanin distribution and root development in Arabidopsis. Plant Cell **11:** 1217 - 1226

Kunst L, Samuels AL (2003) Biosynthesis and secretion of plant cuticular wax. Prog. Lipid Res. **42:** 51-80

Kunst L, Samuels L (2009) Plant cuticles shine: advances in wax biosynthesis and export. Curr. Opin. Plant Biol. **12:** 721-727

Lanahan MB, Yen HC, Giovannoni JJ, Klee HJ (1994) The *Never ripe* mutation blocks ethylene perception in tomato. Plant Cell **6:** 521-530

Langdale JA, Kidner CA (1994) Bundle-sheath defective, a mutation that disrupts cellular differentiation in maize leaves. Development **120:** 673-681

Lee SB, Suh MC (2013) Recent advances in cuticular wax biosynthesis and its regulation in Arabidopsis. Mol. Plant. **6:** 246-249

Leide J, Hildebrandt U, Reussing K, Riederer M, Vogg G (2007) The developmental pattern of tomato fruit wax accumulation and its impact on cuticular transpiration barrier properties: Effects of a deficiency in a *β*-ketoacyl-coenzyme A synthase (LeCER6). Plant Physiol. **144:** 1667-1679

Li-Beisson Y, Pollard M, Sauveplane V, Pinot F, Ohlrogge J, Beisson F (2009) Nanoridges that characterize the surface morphology of flowers require the synthesis of cutin polyester. Proc. Natl. Acad. Sci. USA **106:** 22008-22013

Li YH, Beisson F, Koo AJK, Molina I, Pollard M, Ohlrogge J (2007) Identification of acyltransferases required for cutin biosynthesis and production of cutin with suberin-like monomers. Proc. Natl. Acad. Sci. USA **104:** 18339-18344

Liljegren SJ, Ditta GS, Eshed Y, Savidge B, Bowman JL, Yanofsky MF (2000) *SHATTERPROOF* MADS-box genes control seed dispersal in Arabidopsis. Nature **404:** 766-770

Lippman Z, Tanksley SD (2001) Dissecting the genetic pathway to extreme fruit size in tomato using a cross between the small-fruited wild species *Lycopersicon pimpinellifolium* and *L.esculentum* var. giant heirloom. Genetics **158:** 413-422

Liu YS, Roof S, Ye ZB, Barry C, van Tuinen A, Vrebalov J, Bowler C, Giovannoni J (2004) Manipulation of light signal transduction as a means of modifying fruit nutritional quality in tomato. Proc. Natl. Acad. Sci. USA **101:** 9897-9902

Manning K, Tor M, Poole M, Hong Y, Thompson AJ, King GJ, Giovannoni JJ, Seymour GB (2006) A naturally occurring epigenetic mutation in a gene encoding an SBP-box transcription factor inhibits tomato fruit ripening. Nat. Genet. **38:** 948-952

Martin GB, Ganal MW, Tanksley SD (1992) Construction of a yeast artificial chromosome library of tomato and identification of cloned segments linked to two disease resistance loci. Mol. Gen. Genet. **233:** 25-32

Matas AJ, Cobb ED, Bartsch JA, Paolillo DJ, Niklas KJ (2004) Biomechanics and anatomy of *Lycopersicon esculentum* fruit peels and enzyme-treated samples. Am. J. Bot. **91:** 352-360

Matas AJ, Yeats TH, Buda GJ, Zheng Y, Chatterjee S, Tohge T, Ponnala L, Adato A, Aharoni A, Stark R, Fernie AR, Fei ZJ, Giovannoni JJ, Rose JKC (2011) Tissue- and cell-type specific transcriptome profiling of expanding tomato fruit provides insights into metabolic and regulatory specialization and cuticle formation. Plant Cell **23:** 3893-3910

Matsukura C, Aoki K, Fukuda N, Mizoguchi T, Asamizu E, Saito T, Shibata D, Ezura H (2008) Comprehensive resources for tomato functional genomics based on the miniature model tomato Micro-Tom. Curr. Genomics **9:** 436-443

McNevin JP, Woodward W, Hannoufa A, Feldmann KA, Lemieux B (1993) Isolation and characterization of *eceriferum* (*cer*) mutants induced by T-DNA insertions in *Arabidopsis thaliana*. Genome **36:** 610-618

Meissner R, Jacobson Y, Melamed S, Levyatuv S, Shalev G, Ashri A, Elkind Y, Levy A (1997) A new model system for tomato genetics. Plant J. **12:** 1465-1472

Menda N, Semel Y, Peled D, Eshed Y, Zamir D (2004) In silico screening of a saturated mutation library of tomato. Plant J. **38:** 861-872

Menda N, Strickler SR, Mueller LA (2013) Advances in tomato research in the post-genome era. Plant Biotechnol. **30:** 243-256

Monforte AJ, Tanksley SD (2000) Development of a set of near isogenic and backcross recombinant inbred lines containing most of the *Lycopersicon hirsutum* genome in a *L. esculentum* genetic background: a tool for gene mapping and gene discovery. Genome **43:** 803-813

Munos S, Ranc N, Botton E, Berard A, Rolland S, Duffe P, Carretero Y, Le Paslier MC, Delalande C, Bouzayen M, Brunel D, Causse M (2011) Increase in tomato locule number is controlled by two single-nucleotide polymorphisms located near *WUSCHEL*. Plant Physiol. **156:** 2244-2254

Mustilli AC, Fenzi F, Ciliento R, Alfano F, Bowler C (1999) Phenotype of the tomato *high pigment-2* mutant is caused by a mutation in the tomato homolog of DEETIOLATED1. Plant Cell **11:** 145-157

Nadakuduti SS, Pollard M, Kosma DK, Allen C, Ohlrogge JB, Barry CS (2012) Pleiotropic phenotypes of the *sticky peel* mutant provide new insight into the role of *CUTIN DEFICIENT2* in epidermal cell function in tomato. Plant Physiol. **159:** 945-960

Nakamura M, Katsumata H, Abe M, Yabe N, Komeda Y, Yamamoto KT, Takahashi T (2006) Characterization of the class IV homeodomain-leucine zipper gene family in Arabidopsis. Plant Physiol. **141:** 1363-1375

Nawrath C (2006) Unraveling the complex network of cuticular structure and function. Curr. Opin. Plant Biol. **9:** 281-287

Nguyen CV, Vrebalov JT, Gapper NE, Zheng Y, Zhong S, Fei Z, Giovannoni JJ (2014) Tomato *GOLDEN2-LIKE* transcription factors reveal molecular gradients that function during fruit development and ripening. Plant Cell **26:** 585-601

Ohlrogge JB, Jaworski JG (1997) Regulation of fatty acid synthesis. Annu. Rev. Plant Physiol. Plant Mol. Biol. **48:** 109-136

Oshima Y, Shikata M, Koyama T, Ohtsubo N, Mitsuda N, Ohme-Takagi M (2013) MIXTA-like transcription factors and WAX INDUCER1/SHINE1 coordinately regulate cuticle development in Arabidopsis and *Torenia fournieri*. Plant Cell **25:** 1609-1624

Pan Y, Bradley G, Pyke K, Ball G, Lu CG, Fray R, Marshall A, Jayasuta S, Baxter C, van Wijk R, Boyden L, Cade R, Chapman NH, Fraser PD, Hodgman C, Seymour GB (2013) Network inference analysis identifies an *APRR2-Like* gene linked to pigment accumulation in tomato and pepper fruits. Plant Physiol. **161:** 1476-1485

Paran I, van der Knaap E (2007) Genetic and molecular regulation of fruit and plant domestication traits in tomato and pepper. J. Exp. Bot. **58:** 3841-3852

Paterson AH, Damon S, Hewitt JD, Zamir D, Rabinowitch HD, Lincoln SE, Lander ES, Tanksley SD (1991) Mendelian factors underlying quantitative traits in tomato: comparison across species, generations, and environments. Genetics **127:** 181-197

Paterson AH, Lander ES, Hewitt JD, Peterson S, Lincoln SE, Tanksley SD (1988) Resolution of quantitative traits into Mendelian factors by using a complete linkage map of restriction fragment length polymorphisms. Nature **335:** 721-726

Pelaz S, Ditta GS, Baumann E, Wisman E, Yanofsky MF (2000) B and C floral organ identity functions require *SEPALLATA* MADS-box genes. Nature **405:** 200-203

Peralta IE, Spooner DM (2007) History, origin and early cultivation of tomato (Solanaceae). *In* Genetic Improvement of Solanaceous Crops. Volume 2: Tomato. Science, Enfield, NH, pp 1-24

Pighin JA, Zheng H, Balakshin LJ, Goodman IP, Western TL, Jetter R, Kunst L, Samuels AL (2004) Plant cuticular lipid export requires an ABC transporter. Science **306:** 702-704

Pinyopich A, Ditta GS, Savidge B, Liljegren SJ, Baumann E, Wisman E, Yanofsky MF (2003) Assessing the redundancy of MADS-box genes during carpel and ovule development. Nature **424:** 85-88

Pollard M, Beisson F, Li YH, Ohlrogge JB (2008) Building lipid barriers: biosynthesis of cutin and suberin. Trends Plant Sci. **13:** 236-246

Powell ALT, Nguyen CV, Hill T, Cheng KL, Figueroa-Balderas R, Aktas H, Ashrafi H, Pons C, Fernandez-Munoz R, Vicente A, Lopez-Baltazar J, Barry CS, Liu YS, Chetelat R, Granell A, Van Deynze A, Giovannoni JJ, Bennett AB (2012) *Uniform ripening* encodes a *Golden 2-like* transcription factor regulating tomato fruit chloroplast development. Science **336:** 1711-1715

Raffaele S, Vailleau F, Leger A, Joubes J, Miersch O, Huard C, Blee E, Mongrand S, Domergue F, Roby D (2008) A MYB transcription factor regulates very-long-chain fatty

acid biosynthesis for activation of the hypersensitive cell death response in Arabidopsis. Plant Cell **20:** 752-767

Rick CM (1975) The tomato. *In* Handbook of Genetics, Ed King RC Vol 2. Plenum Press, New York, NY, USA, pp 247–280

Rick CM (1991) Tomato. Longman Scientific and Technical, Essex, England.

Riederer M, Schreiber L (2001) Protecting against water loss: analysis of the barrier properties of plant cuticles. J. Exp. Bot. **52:** 2023-2032

Ripoll JJ, Roeder AH, Ditta GS, Yanofsky MF (2011) A novel role for the floral homeotic gene *APETALA2* during Arabidopsis fruit development. Development **138:** 5167-5176

Robinson RW, Tomes ML (1968) Ripening inhibitor: a gene with multiple effects on ripening. Rep. Tomato Genet. Coop. **18:** 36-37

Ronen G, Carmel-Goren L, Zamir D, Hirschberg J (2000) An alternative pathway to beta-carotene formation in plant chromoplasts discovered by map-based cloning of *beta* and *old-gold* color mutations in tomato. Proc. Natl. Acad. Sci. USA **97:** 11102-11107

Ronning CM (2013) Role of bioinformatics as a tool in tomato research *In* JL In BE Liedl, JR Stommel, A Slade, C Kole, ed, Genetics, genomics, and breeding of tomato. Science, pp 428-454

Rossini L, Cribb L, Martin DJ, Langdale JA (2001) The maize *Golden2* gene defines a novel class of transcriptional regulators in plants. Plant Cell **13:** 1231-1244

Sagar M, Chervin C, Mila I, Hao Y, Roustan J, Benichou M, Gibon Y, Biais B, Maury P, Latche A, Pech JC, Bouzayen M, Zouine M (2013a) Sl-ARF4, an auxin response factor involved in the control of sugar metabolism during tomato fruit development. Plant Physiol. **161:** 1362-1374

Sagar M, Chervin C, Roustant JP, Bouzayen M, Zouine M (2013b) Under-expression of the auxin response factor Sl-ARF4 improves postharvest behavior of tomato fruits. Plant signaling & behavior **8:** 10,e25647

Saladie M, Matas AJ, Isaacson T, Jenks MA, Goodwin SM, Niklas KJ, Ren XL, Labavitch JM, Shackel KA, Fernie AR, Lytovchenko A, O'Neill MA, Watkins CB, Rose JKC (2007) A reevaluation of the key factors that influence tomato fruit softening and integrity. Plant Physiol. **144:** 1012-1028

Schwarz-Sommer Z, Huijser P, Nacken W, Saedler H, Sommer H (1990) Genetic control of flower development by homeotic genes in *Antirrhinum majus*. Science **250:** 931-936

Seo PJ, Park CM (2010) MYB96-mediated abscisic acid signals induce pathogen resistance response by promoting salicylic acid biosynthesis in Arabidopsis. New Phytol. **186:** 471-483

Seo PJ, Xiang F, Qiao M, Park JY, Lee YN, Kim SG, Lee YH, Park WJ, Park CM (2009) The MYB96 transcription factor mediates abscisic acid signaling during drought stress response in Arabidopsis. Plant Physiol. **151:** 275-289

Seymour GB, Ostergaard L, Chapman NH, Knapp S, Martin C (2013) Fruit development and ripening. Annu. Rev. Plant Biol. **64:** 219-241

Seymour GB, Ryder CD, Cevik V, Hammond JP, Popovich A, King GJ, Vrebalov J, Giovannoni JJ, Manning K (2011) A *SEPALLATA* gene is involved in the development and ripening of strawberry (*Fragaria x ananassa* Duch.) fruit, a non-climacteric tissue. J. Exp. Bot. **62:** 1179-1188

Shi JX, Adato A, Alkan N, He YH, Lashbrooke J, Matas AJ, Meir S, Malitsky S, Isaacson T, Prusky D, Leshkowitz D, Schreiber L, Granell AR, Widemann E, Grausem B, Pinot F, Rose JKC, Rogachev I, Rothan C, Aharoni A (2013) The tomato SlSHINE3 transcription factor regulates fruit cuticle formation and epidermal patterning. New Phytol. **197:** 468-480

Shi JX, Malitsky S, De Oliveira S, Branigan C, Franke RB, Schreiber L, Aharoni A (2011) SHINE transcription factors act redundantly to pattern the archetypal surface of Arabidopsis flower organs. PLoS Genet. **7:** e1001388

Shima Y, Kitagawa M, Fujisawa M, Nakano T, Kato H, Kimbara J, Kasumi T, Ito Y (2013) Tomato FRUITFULL homologues act in fruit ripening via forming MADS-box transcription factor complexes with RIN. Plant Mol. Biol. **82:** 427-438

Sieber P, Schorderet M, Ryser U, Buchala A, Kolattukudy P, Metraux J-P, Nawrath C (2000) Transgenic Arabidopsis plants expressing a fungal cutinase show alterations in the structure and properties of the cuticle and postgenital organ fusions. Plant Cell **12:** 721-737

Sim SC, Durstewitz G, Plieske J, Wieseke R, Ganal MW, Van Deynze A, Hamilton JP, Buell CR, Causse M, Wijeratne S, Francis DM (2012) Development of a large SNP genotyping array and generation of high-density genetic maps in tomato. Plos One **7:** e40563

Suh MC, Samuels AL, Jetter R, Kunst L, Pollard M, Ohlrogge J, Beisson F (2005) Cuticular lipid composition, surface structure, and gene expression in Arabidopsis stem epidermis. Plant Physiol. **139:** 1649-1665

Szymkowiak EJ, Sussex IM (1992) The internal meristem layer (L3) determines floral meristem size and carpel number in tomato periclinal chimeras. Plant Cell **4:** 1089-1100

Tadiello A, Pavanello A, Zanin D, Caporali E, Colombo L, Rotino GL, Trainotti L, Casadoro G (2009) A *PLENA*-like gene of peach is involved in carpel formation and subsequent transformation into a fleshy fruit. J. Exp. Bot. **60:** 651-661

Tanksley SD, Ganal MW, Prince JP, de Vicente MC, Bonierbale MW, Broun P, Fulton TM, Giovannoni JJ, Grandillo S, Martin GB, et al. (1992) High density molecular linkage maps of the tomato and potato genomes. Genetics **132:** 1141-1160

Tanksley SD, Rick CM (1980) Isozymic gene linkage map of the tomato: applications in genetics and breeding. Theor. Appl. Genet. **58:** 161-170

The Tomato Genome Consortium (2012) The tomato genome sequence provides insights into fleshy fruit evolution. Nature **485:** 635-641

Vogg G, Fischer S, Leide J, Emmanuel E, Jetter R, Levy AA, Riederer M (2004) Tomato fruit cuticular waxes and their effects on transpiration barrier properties: functional characterization of a mutant deficient in a very-long-chain fatty acid *β*-ketoacyl-CoA synthase. J. Exp. Bot. **55:** 1401-1410

Vrebalov J, Pan IL, Arroyo AJM, McQuinn R, Chung M, Poole M, Rose JKC, Seymour G, Grandillo S, Giovannoni J, Irish VF (2009) Fleshy fruit expansion and ripening are regulated by the tomato *SHATTERPROOF* gene *TAGL1*. Plant Cell **21:** 3041-3062

Vrebalov J, Ruezinsky D, Padmanabhan V, White R, Medrano D, Drake R, Schuch W, Giovannoni J (2002) A MADS-box gene necessary for fruit ripening at the tomato *ripening-inhibitor* (*rin*) locus. Science **296:** 343-346

Walton T (1990) Waxes, cutin and suberin. *In* Methods in plant biochemistry, Ed Harwood, J.L. and Bowyer, J.R. Vol 4. Academic Press, London, pp 105–158

Wang P, Fouracre J, Kelly S, Karki S, Gowik U, Aubry S, Shaw M, Westhoff P, Slamet-Loedin I, Quick WP, Hibberd J, Langdale J (2013) Evolution of *GOLDEN2-LIKE* gene function in C3 and C4 plants. Planta **237:** 481-495

Waters MT, Moylan EC, Langdale JA (2008) GLK transcription factors regulate chloroplast development in a cell-autonomous manner. Plant J. **56:** 432-444

Waters MT, Wang P, Korkaric M, Capper RG, Saunders NJ, Langdale JA (2009) GLK transcription factors coordinate expression of the photosynthetic apparatus in Arabidopsis. Plant Cell **21:** 1109-1128

Wellesen K, Durst F, Pinot F, Benveniste I, Nettesheim K, Wisman E, Steiner-Lange S, Saedler H, Yephremov A (2001) Functional analysis of the *LACERATA* gene of Arabidopsis provides evidence for different roles of fatty acid omega-hydroxylation in development. Proc. Natl. Acad. Sci. USA **98:** 9694-9699

Wilkinson JQ, Lanahan MB, Yen HC, Giovannoni JJ, Klee HJ (1995) An ethylene-inducible component of signal transduction encoded by *Never-ripe*. Science **270:** 1807-1809

Yang WL, Pollard M, Li-Beisson Y, Beisson F, Feig M, Ohlrogge J (2010) A distinct type of glycerol-3-phosphate acyltransferase with *sn*-2 preference and phosphatase activity producing 2-monoacylglycerol. Proc. Natl. Acad. Sci. USA **107:** 12040-12045

Yasumura Y, Moylan EC, Langdale JA (2005) A conserved transcription factor mediates nuclear control of organelle biogenesis in anciently diverged land plants. Plant Cell **17:** 1894-1907

Yeats TH, Martin LBB, Viart HMF, Isaacson T, He Y, Zhao L, Matas AJ, Buda GJ, Domozych DS, Clausen MH, Rose JKC (2012) The identification of cutin synthase: formation of the plant polyester cutin. Nat. Chem. Biol. **8:** 609-611

Yeats TH, Rose JKC (2013) The formation and function of plant cuticles. Plant Physiol. **163:** 5-20

Zahn LM, Kong H, Leebens-Mack JH, Kim S, Soltis PS, Landherr LL, Soltis DE, Depamphilis CW, Ma H (2005) The evolution of the *SEPALLATA* subfamily of MADS-box genes: a preangiosperm origin with multiple duplications throughout angiosperm history. Genetics **169:** 2209-2223

Zhang JY, Broeckling CD, Blancaflor EB, Sledge MK, Sumner LW, Wang ZY (2005) Overexpression of *WXP1*, a putative *Medicago truncatula* AP2 domain-containing transcription factor gene, increases cuticular wax accumulation and enhances drought tolerance in transgenic alfalfa (*Medicago sativa*). Plant J. **42:** 689-707

CHAPTER II

Pleiotropic phenotypes of the *sticky peel* (*pe*) mutant provide new insight into the role of CUTIN DEFICIENT2 in epidermal cell function in tomato

Satya Swathi Nadakuduti[1], Mike Pollard[2], Dylan K. Kosma[2], Charles Allen Jr.[1], John B. Ohlrogge[2] and Cornelius S. Barry[1*]

Plant Physiology (2012): 159(3): 945-60

Abstract

Plant epidermal cells have evolved specialist functions associated with adaptation to stress. These include the synthesis and deposition of specialized metabolites such as waxes and cutin together with flavonoids and anthocyanins, which have important roles in providing a barrier to water loss and protection against UV radiation, respectively. Characterization of the *sticky peel* (*pe*) mutant of tomato revealed several phenotypes indicative of a defect in epidermal cell function, including reduced anthocyanin accumulation, a lower density of glandular trichomes and an associated reduction in trichome derived terpenes. In addition, *pe* mutant fruit are glossy and peels have increased elasticity due to a severe reduction in cutin biosynthesis and altered wax deposition. Leaves of the *pe* mutant are also cutin deficient and the epicuticular waxes contain a lower proportion of long chain alkanes. Direct measurements of transpiration, together with chlorophyll leaching assays, indicate increased cuticular permeability of *pe* leaves. Genetic mapping revealed that the *pe* locus represents a new allele of *CUTIN DEFICIENT 2* (*CD2*), a member of the Class IV Homeodomain-Leucine Zipper gene family, previously only associated with cutin deficiency in tomato fruit. *CD2* is preferentially expressed in epidermal cells of tomato stems and is a homolog of Arabidopsis *ANTHOCYANINLESS 2* (*ANL2*). Analysis of cuticle composition in leaves of *anl2* revealed that cutin accumulates to approximately 60 percent of the levels observed in wild-type Arabidopsis. Together, these data provide new insight into the role of *CD2* and *ANL2* in regulating diverse metabolic pathways and in particular, those associated with epidermal cells.

Introduction

Plants are continually exposed to environmental changes that impact their fitness and survival. Changes in light intensity, light quality, temperature and water availability occur on a daily basis and insect pests and pathogens pose a constant threat. Consequently, plants have evolved a suite of physical and chemical adaptations and defenses against abiotic and biotic stresses that have facilitated their colonization of diverse environments. The surface properties of plants are crucial to their successful adaptation to stress. The epidermal cell layer and associated structural appendages such as trichomes, together with the cuticle form the primary physical and chemical barriers that protect plants against multiple stresses (Glover, 2000; Sieber et al., 2000; Schilmiller et al., 2008; Javelle et al., 2011). Furthermore, the surface properties of plants are dynamic and can change in response to stress, therefore influencing the physiology of the plant (Lu et al., 1996; Ingram et al., 2000; Abe et al., 2003; Ingram, 2008; Kosma et al., 2009; Wang et al., 2011).

The metabolism of epidermal cells is programmed for the synthesis of lipids that form the cuticle, a heterogeneous lipid-based barrier comprised of cutin, intra and epicuticular waxes and polysaccharides that covers the aerial surfaces of all terrestrial plants. In addition to serving as the principal barrier to water loss (Kolattukudy, 1980; Riederer and Schreiber, 2001; Pollard et al., 2008) the cuticle provides structural support, possesses anti-adhesive properties that limit pathogen infection, resists insect feeding and oviposition, and has reflective properties that reduce heat load and limit the effect of UV-radiation (Bargel et al., 2006). Furthermore, the chemical properties of the cuticle are dynamic with both cuticle deposition and wax composition altering in response to water stress and abscisic acid (ABA) (Kosma et al., 2009; Wang et al., 2011). The epidermal and sub-epidermal cells are also sites of phenylpropanoid biosynthesis, and

in particular the synthesis and accumulation of flavonoids and anthocyanins (Martin and Gerats, 1993; Hichri et al., 2011; Matas et al., 2011). Anthocyanins protect plants through their UV radiation absorbing properties and their synthesis is influenced by stress and can vary with light intensity and wavelength (Beggs et al., 1987; Li et al., 1993; Christie et al., 1994; Landry et al., 1995; Fuglevand et al., 1996; Steyn et al., 2002). Together, these studies highlight the importance of the epidermal cell layer in the synthesis of compounds important for stress adaptation in plants that likely contributed to colonization of the terrestrial environment by early land plants (Edwards et al., 1996; Cooper-Driver, 2001).

Many enzymes, transporters and regulatory factors required for the biosynthesis and deposition of cuticular lipids have been identified and characterized in Arabidopsis (Li et al., 2007; Panikashvili et al., 2007; Samuels et al., 2008; Panikashvili et al., 2009; Li-Beisson et al., 2010; Li et al., 2010; McFarlane et al., 2010; Seo et al., 2011; Wu et al., 2011). Tomato fruit also serve as a powerful system for investigating the physical properties and biosynthesis of the cuticle fostered in large part by the abundance of cuticular lipid deposited during fleshy fruit development, its astomatous nature and relevance in fruit cracking and postharvest storage (Emmons and Scott, 1997; Emmons and Scott, 1998; Matas et al., 2004; Bargel and Neinhuis, 2005). Genomics- and proteomics-based approaches have identified genes and proteins preferentially expressed in the fruit peel, and perturbation of several genes through mutagenesis has revealed altered fruit cuticle phenotypes (Vogg et al., 2004; Hovav et al., 2007; Mintz-Oron et al., 2008; Isaacson et al., 2009; Yeats et al., 2010; Matas et al., 2011).

Fruit of the *sticky peel* (*pe*) mutant of tomato have a “rubbery” surface texture rather than the typical smooth surface associated with wild-type fruit rendering fruits “sticky” to the touch (Butler, 1952). In addition, *pe* fruits have a highly glossy fruit surface, a phenotype recently

associated with cutin deficiency (Isaacson et al., 2009). In this study, a combination of microscopy and chemical analysis revealed that *pe* fruit are cutin deficient and have an altered wax profile. In addition, several phenotypes attributed to altered epidermal cell function are apparent in *pe*, including cutin deficiency and altered wax deposition in leaves, together with increased cuticular permeability, lower trichome density and reduced anthocyanin accumulation. Genetic mapping indicated that *pe* encodes a new allele of *CUTIN DEFICIENT 2* (*CD2*), which encodes a member of the Class IV Homeodomain-leucine zipper (HD-ZIP IV) family, and was previously only associated with a fruit-specific reduction in cuticle biosynthesis (Isaacson et al., 2009). In addition, we show that mutation in a *CD2* homolog at the *anthocyaninless 2* (*anl2*) locus of Arabidopsis also causes a cutin deficient phenotype in rosette leaves. Together, these data identify additional roles for *CD2* and *ANL2*, defining a regulatory link between cuticle and flavonoid biosynthesis, two pathways that operate within epidermal cells that are critical for plant responses to stress.

Results

Introgression of the *pe* allele into the Ailsa Craig genetic background

At the initiation of this research, the genetic background of the *pe* mutant was unknown. Therefore, we initiated a backcross strategy to introgress the *pe* mutation into the Ailsa Craig (AC) genetic background, a cultivar previously selected for introgression of varied morphological mutants of tomato (Darby et al., 1978). The mutant and wild-type plants used in the following experiments were derived from a BC_2F_2 population that we estimate contains approximately 93.75% of the AC genetic background. Therefore, the influence of the genetic background on the data presented is likely to be minimal.

Altered morphology and trichome chemistry of the *pe* mutant

In addition to the previously documented sticky peel phenotype of *pe* fruit (Butler, 1952), the *pe* mutant exhibits a short stature with pale green leaves and stems (Figure 2.1A). Five week-old wild-type Ailsa Craig (AC) plants had an average dry weight of 6.45 g whereas the dry weight of *pe* plants was 3.86 g. Glandular trichomes are epidermal cell appendages that are prevalent on the surface of tomato plants and synthesize a suite of specialized metabolites known, or hypothesized to play a role in plant defense responses against pests and pathogens (Schilmiller et al., 2008). Type VI glandular trichomes are the most abundant glandular trichomes on the tomato leaf surface (Kang et al., 2010) and these are reduced greater than three-fold in *pe* (Figure 2.1B-D). The type VI glandular trichomes of cultivated tomato synthesize a mixture of mono- and sesqui-terpenes of which β-phellandrene predominates (Schilmiller et al., 2009). The volatile terpene levels in leaf dips of AC and *pe* were compared (Figure 2.2).

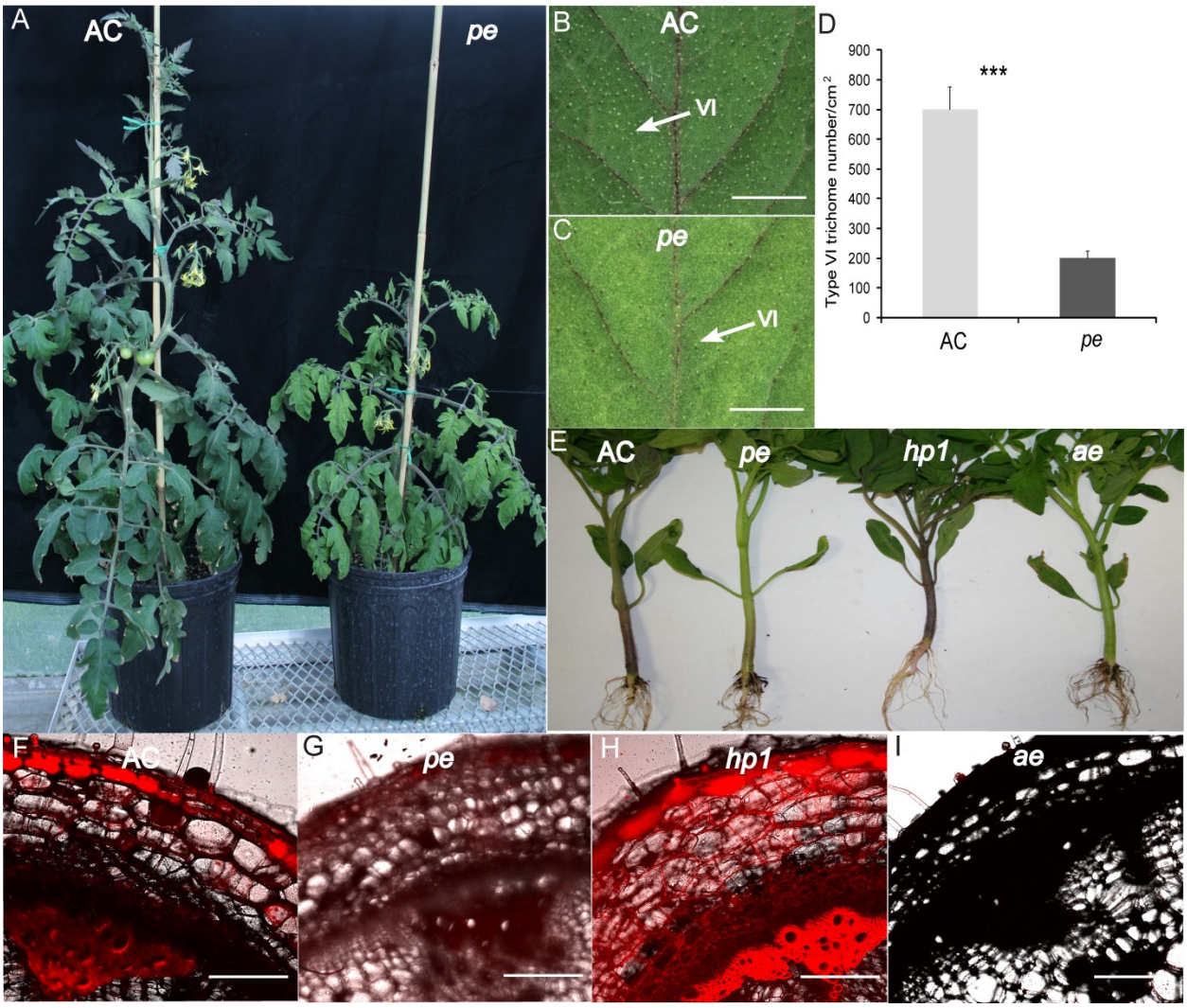

Figure 2.1. Phenotypic variation between AC and *pe*. A) Whole plant phenotype of AC and *pe.* B & C) Light micrographs of trichomes on leaves of AC and *pe.* Type VI glandular trichomes are indicated by arrow heads, scale bar = 2 mm. D) Density of glandular type VI trichomes on the adaxial leaf surface of AC and *pe*. Data are presented as the mean of $n=8$ ± SE on adaxial side of AC and *pe* leaves. Asterisks denote significant differences (***, $p < 0.001$) as determined by Student's *t tests*. E) Comparison of anthocyanin accumulation in the stems of AC and *pe*. Stems of the *high pigment 1* (*hp1*) and *entirely anthocyaninless* (*ae*) mutants are shown for comparison. F – I) Autofluorescence of anthocyanins in AC, *pe*, *hp1* and *ae* visualized by confocal laser scanning microscopy (Scale bar = 200 µm).

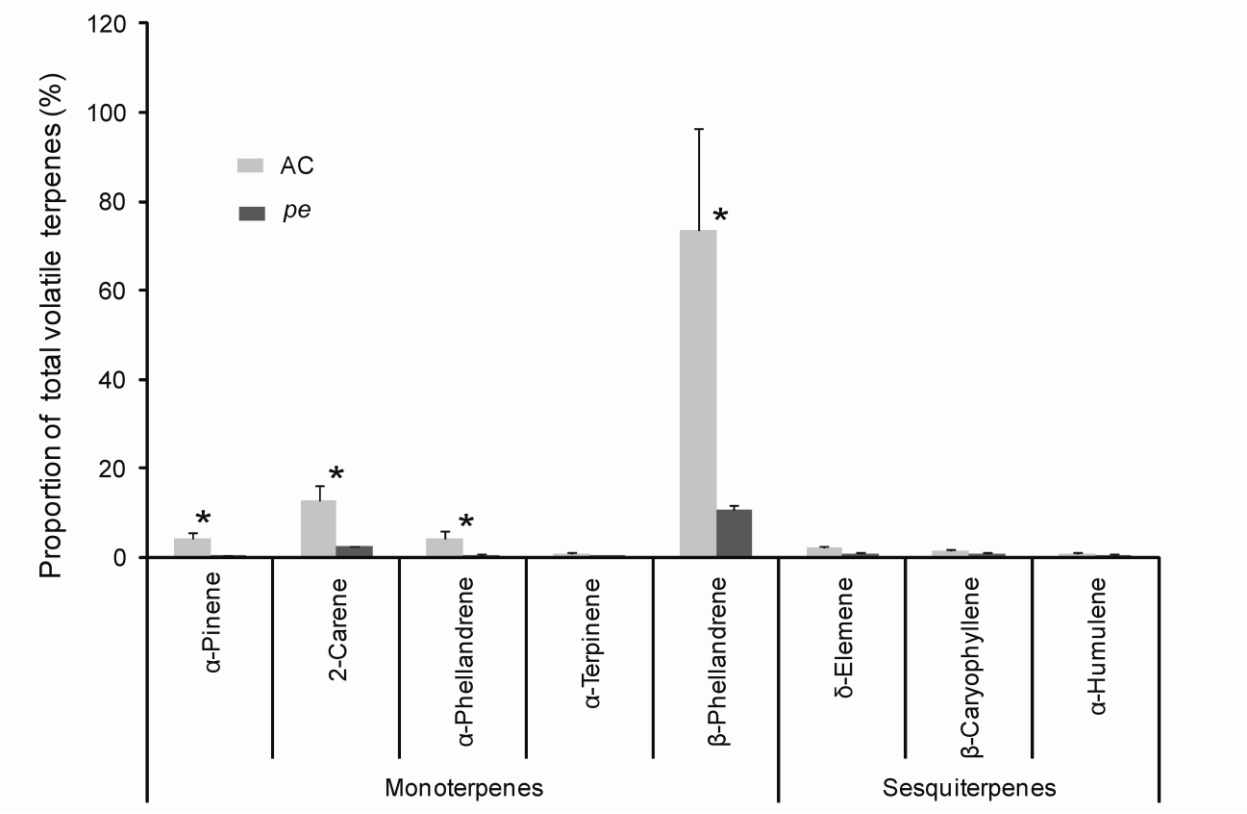

Figure 2.2. Comparison of relative monoterpene and sesquiterpene levels in AC and *pe* trichomes as determined by leaf dip analysis. Proportions of individual volatile terpenes are expressed as percentage relative to the abundance in wild type (AC) n=3 ±SE. Asterisks denote significant differences (*, $p< 0.05$) as determined by Student's *t tests*.

Consistent with the reduced abundance of type VI glandular trichomes on the surface of *pe* leaves, volatile terpene levels are also significantly reduced to approximately 16 percent of that observed in wild-type.

Reduced anthocyanin accumulation in *pe*

To investigate the pale phenotype of *pe* in more detail, chlorophyll and anthocyanin levels were determined in fully expanded and meristematic leaves. Chlorophyll levels in AC and *pe* are not significantly altered but anthocyanin content is reduced by approximately 85% in *pe* (Table 2.1). The anthocyanins represent an endpoint of the phenylpropanoid pathway and are known to accumulate in epidermal and sub-epidermal cell layers (Martin and Gerats, 1993; Hichri et al., 2011). The distribution of anthocyanins within the stems of AC and *pe* was compared by confocal laser scanning microscopy and stems of the *high-pigment 1* and *entirely anthocyaninless* (*ae*) mutants were included as positive and negative controls, respectively (Figure 2.1E-I). Images reveal two main patterns of anthocyanin distribution in AC, with accumulation observed in the epidermal and sub-epidermal cells and also surrounding the vasculature (Figure 2.1F). In contrast anthocyanin accumulation is greatly reduced in stems of *pe* (Figure 2.1G).

Table 2.1 Anthocyanin and chlorophyll content of AC and *pe* leaves

	Mature leaves		Meristematic leaves	
	AC	*pe*	AC	*pe*
Anthocyanin content (AU 535 nm g^{-1} FW)	12.4 ± 2.1***	1.9 ± 0.6	13.1 ± 1.0***	5.4 ± 0.63
Chlorophyll content (µg ml^{-1})	54.8 ± 2.0	53.3 ± 3.1	67.3 ± 0.6	66.4 ± 0.8

Data represents the mean of *n*=5 ± SE. Asterisks denote significant differences between genotypes of the same developmental stage (***, p< 0.001) as determined by Student's *t tests.*

Lignin content is not altered in *pe*

Like anthocyanins, lignin also represents an endpoint of the phenylpropanoid pathway (Vogt, 2010). Reduced lignin synthesis in plants is associated with stunted growth, mediated by increased salicylic acid levels (Brown et al., 2001; Li et al., 2010; Gallego-Giraldo et al., 2011). To investigate whether the semi-dwarf phenotype of *pe* is related to reduced accumulation of lignin, the total lignin content in leaves and stems of AC and *pe* was analyzed. The total percent acetyl bromide soluble lignin (% ABSL) as well as individual lignin monomers of AC and *pe* leaves showed no significant differences between the two genotypes (Table 2.2).

Table 2.2. Lignin composition of leaves and stems in AC and *pe* (µg mg^{-1} AIR)

	Total %ABSL	G	S	H
Leaves AC	2.50 ± 0.16	5.95 ± 0.45	2.20 ± 0.53	0.06 ± 0.01
Leaves *pe*	2.19 ± 0.23	4.50 ± 0.54	1.75 ± 0.31	0.04 ± 0.01
Stems AC	3.07 ± 0.26	14.57 ± 0.43	2.98 ± 0.24	0.09 ± 0.02
Stems *pe*	3.06 ± 0.21	14.62 ± 0.45	4.24 ± 0.39	0.09 ± 0.02

AIR, Alcohol Insoluble Residue; ABSL, Acetyl Bromide Soluble Lignin. G, S, and H refer to guaiacyl, syringyl and p hydroxyphenyl lignin monomers, respectively. Data are shown as means ± SE (n = 5). No significant differences exist between AC and pe as determined by Student's t tests.

The *pe* fruit cuticle has altered physical and chemical properties

Fruits of the *pe* mutant are highly glossy and are sticky to the touch when compared to wild type (Figure 2.3A and B) (Butler, 1952). In addition, we observed that ripe *pe* fruits are generally crack resistant. The average Young's elastic modulus (Y) is approximately two-fold greater than wild type, indicating increased stiffness of the *pe* fruit peel (Figure 2.3C). Glossiness and increased stiffness in tomato fruit peels is associated with cutin deficiency (Isaacson et al., 2009). Scanning electron microscopy (SEM) images of *pe* fruit indicated reduced cuticle deposition compared to AC fruit (Figure 2.3D-G).

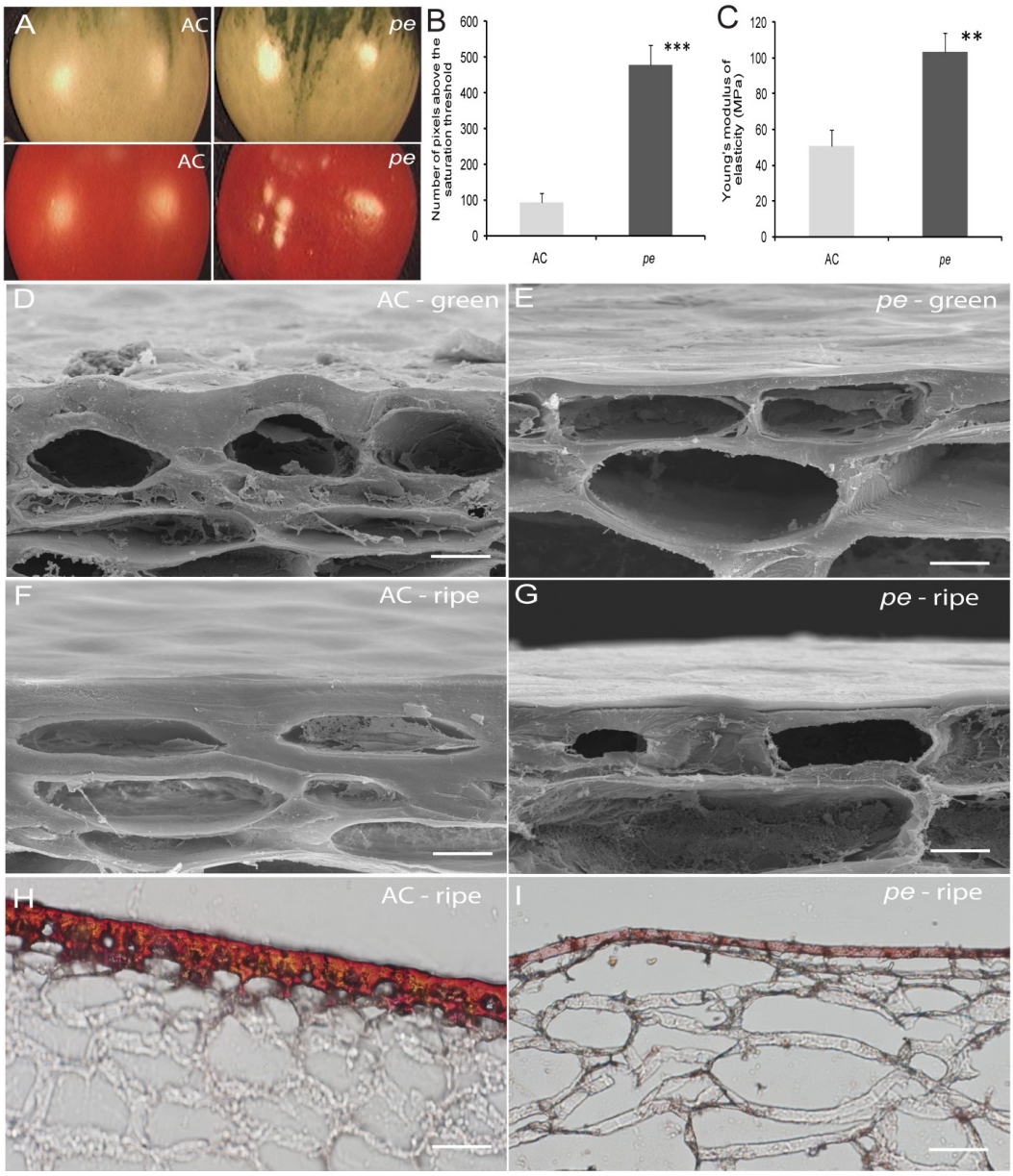

Figure 2.3. Fruit phenotypes of *pe*. A) Increased glossiness in *pe* fruits compared to AC. B) Quantitative analysis of glossiness in ripe fruits of AC and *pe*. The values of number of pixels above the saturation threshold represent the mean values (n=5) ±SE. C) Average Young's modulus of elasticity (n=5) ±SE. Asterisks denote significant differences (**, $p < 0.01$; ***, $p < 0.001$) as determined by Student's *t tests*. D – G) Scanning electron micrographs of AC and *pe* fruits at the green and ripe stages of development. Note reduced cuticle deposition in the *pe* mutant (Scale bar = 20 µm). H & I) Light-micrographs of cuticular lipid distribution in ripe fruits using Sudan IV staining. Scale bar = 50 µm.

Staining of cryosections of the fruit peel of AC and *pe* with the lipid reactive stain, Sudan IV confirmed reduced cuticle lipid deposition in the *pe* mutant (Figure 2.3H-I). The chemical composition of *pe* fruit cuticles is significantly altered compared to that of AC fruits. The cutin monomer load (mass/area) in ripe *pe* fruits is approximately 2% of that in AC and 6.5% of AC levels in green fruits (Table 2.3). Furthermore, the large reduction in cutin monomer content is observed for all hexadecanoic acid-derived cutin monomers, together with *cis*- and *trans*-coumaric acid, products of the phenylpropanoid pathway. The notable exception to the general reduction of cutin monomers in *pe* is the abundance of the hexadecanoic acid itself, which has slightly increased abundance in mutant fruit, particularly at the green stage of development. Altered glossiness of plant surfaces is often associated with changes in wax composition (Chen et al., 2003; Aharoni et al., 2004; Bourdenx et al., 2011). The total wax load is not significantly different between AC and *pe* fruits at either the green or ripe stages of development (Table 2.4). However, the cutin monomer to wax ratio, signifying relative proportion of wax within the cutin matrix, falls dramatically from approximately 75:1 (1086.5 : 14.42 μg cm^{-2}) in ripe fruits of AC to 1.6:1 (26.1 : 15.7 μg cm^{-2}) in *pe* (Table 2.3 and Table 2.4). Also, the composition of individual wax components is significantly altered. For example, alkanes constitute approximately 40% of the total wax load in AC fruits but between 55 – 62% in *pe* fruits due largely to increases in C31 - C33 alkanes at both the green and ripe stages of fruit development (Figure 2.3, Tables 2.4 and 2.5).

Table 2.3. Cutin monomer composition in fruit cuticles of AC and *pe* in µg cm^{-2} (%)

	Green fruit		Ripe fruit	
Cutin monomer	AC	*pe*	AC	*pe*
cis - Coumarate	4.8±1.1(1.6)	ND	6.9±0.8(0.6)	ND
trans - Coumarate	11.3 ± 2.5(3.6)***	0.6±0.1(2.9)	27.6±3.4(2.5)***	0.5±0.1(2.0)
Hexadecanoic acid	0.7±0.1(0.2)	1.82±0.6(9.0)*	1.3±0.2(0.1)	1.4±0.7(5.4)
Hexadecane 1,16 - dioic acid	6.2± 1.0(2.0)	ND	12.7±1.7(1.2)***	0.4±0.1(1.7)
C16:1 Hexadecenoic acid	1.6±0.1(0.5)	ND	9.3±1.3(0.9)***	0.2±0.05(0.8)
16-OH Hexadecanoic acid	4.7±1.1(1.5)***	0.32±0.05(1.6)	22.6±3.9(2.1)***	0.4±0.1(1.6)
9-OH, 16-oxo Hexadecanoic acid	3.9±0.4(1.3)	ND	25.2±5.0(2.3)***	0.4±0.1(1.5)
Octadecane 1,16 - dioic acid	2.1±0.2(0.7)	ND	3.8±0.6(0.4)	ND
8-OH Hexadecane 1,16 - dioic acid	2.5±0.4(0.8)	ND	18.3±4.3(1.7)***	0.6±0.1(2.1)
18-OH Octadecanoic acid	2.3±0.6(0.7)	ND	7.8±1.2(0.7)***	0.3±0.1(1.2)
10, 16-diOH Hexadecanoic acid	176.4±6.0(57.1)***	3.1±1.4(15.5)	827.2±18.5(76.1)***	6.8±0.9(26.0)
9, 18-diOH Octadecanoic acid	2.2±0.6(0.7)	ND	12.6±1.9(1.2)***	0.1±0.05(0.4)
Unidentified	90.0±19.3(29.2)	14.4±1.2(71.0)	111.2±20.5(10.2)	14.9±4.4(57.1)
Total	308.8±20.5***	20.2±1.2	1086.5±22.1***	26.1±5.9

Data represents the mean of n=5 ± SE. ND, not detected. Asterisks denote significant differences between genotypes of the same developmental stage (*, $p < 0.05$; ***, $p < 0.001$) as determined by Student's *t tests*.

Table 2.4.Total wax load in fruits of AC and *pe* at green and ripe stages in µg cm^{-2}

	Total load	Hydrocarbons	Alcohols	Fatty acids	Triterpenoids/ Sterols/ Coumarate	Unidentified
AC green fruit	19.72±1.24	6.86 ± 0.81	1.46 ± 0.06***	0.38 ± 0.05	9.25 ± 0.70***	1.77 ± 0.54
pe green fruit	16.03 ± 2.31	9.81 ± 0.84*	0.53 ± 0.02	0.46 ± 0.07	1.32 ± 0.12	3.91 ± 1.91
AC ripe fruit	14.42 ± 0.91	5.61 ± 0.84	0.96 ± 0.06**	0.74 ± 0.10	4.98 ± 0.21***	2.13 ± 0.25
pe ripe fruit	15.71 ± 1.82	8.86 ± 0.94**	0.64 ± 0.03	1.19 ± 0.13**	2.07 ± 0.17	2.94 ± 0.43

Hydrocarbons in the table include alkanes, iso-alkanes, anteiso alkanes and alkenes. Data are shown as means ± SE (n = 5). Asterisks denote significant differences between genotypes of the same developmental stage (*, $p < 0.05$; **, $p < 0.01$; ***, $p < 0.001$) as determined by Student's *t tests*.

Table 2.5. Fruit wax composition of AC and *pe* in µg cm^{-2} x 10^2

Wax class	C chain length/compound	Green fruit		Ripe fruit	
		AC	*pe*	AC	*pe*
Alkanes	C23:0	4.6 ± 0.3	3.5 ± 0.4	2.1 ± 0.2	3.2 ± 0.7
	C25:0	1.2 ± 0.3	2.1 ± 1.2	1.3 ± 0.6	1.2 ± 0.2
	C26:0	2.3 ± 0.5	1.1 ± 0.4	8.2 ± 1.6	5.6 ± 0.6
	C27:0	11.4 ± 4.7	34.7 ± 7.2*	6.2 ± 1.5	13.0 ± 5.3*
	C28:0	3.7 ± 0.5	3.1 ± 0.8	3.3 ± 0.5	7.5 ± 0.7**
	C29:0	87.3 ± 4.3***	39.1 ± 5.3	61.9 ± 3.7	55.1 ± 4.3
	C30:0	56.4 ± 4.7	52.5 ± 5.8	39.8 ± 3.4	58.9 ± 5.6**
	C31:0	374.6 ± 69.1	508.0 ± 57.4*	276.7 ± 23.4	415.4 ±42.3**
	C32:0	45.4 ± 8.7	101.1 ± 10.7**	31.2 ± 4.0	98.6 ± 6.9***
	C33:0	28.1 ± 6.5	118.1 ± 17.1**	44.1 ± 4.6	83.0 ± 13.5*
Iso alkanes	C29:0	9.1 ± 0.3	8.3 ± 1.1	9.8 ± 0.5	10.5 ± 1.3
	C30:0	0.8 ± 0.3	1.1 ± 0.6	1.4 ± 0.2	2.4 ± 0.7
	C31:0	31.8 ± 2.5	58.4± 4.5***	20.2 ± 2.0	75.9 ± 6.7***
	C32:0	8.8 ± 1.3	17.4 ± 1.4**	5.6 ± 0.6	23.9 ± 3.0***
	C33:0	13.7 ± 1.2	21.1 ± 1.8**	11.7 ± 1.1	21.5 ± 2.6**
Anteiso alkanes	C31:0	1.8 ± 0.2	2.8 ± 1.8	1.0 ± 0.3	1.5 ± 0.3
	C32:0	2.8 ± 0.5	7.3 ± 0.7***	1.9 ± 0.4	7.3 ± 0.9***
Alkenes	C33:2	2.6 ± 0.8**	1.1 ± 0.5	31.8 ± 8.7**	1.6 ± 0.6
	C35:2	ND	ND	3.3 ± 0.4	ND
Alkanols	C20:0	10.0 ± 3.1	5.2 ± 2.5	2.7 ± 0.8	1.1 ± 0.2
	C22:0	1.6 ± 0.3	4.2 ± 1.2	1.5 ± 0.3	3.2 ± 0.3*
	C23:0	3.3 ± 0.9	4.8 ± 0.7	4.4 ± 0.3	7.2 ± 1.2
	C24:0	1.2 ± 0.3	1.1 ± 0.3	2.9 ± 0.8	1.3 ± 0.6
	C25:0	0.4 ± 0.2	ND	4.3 ± 0.8	ND
	C26:0	1.8 ± 0.5	3.0 ± 0.3	1.7 ± 0.1	9.6 ± 1.7***
	C27:0	3.0 ± 0.3	1.5 ± 0.6	1.7 ± 0.3	3.5 ± 0.5*
	C28:0	15.1 ± 1.0	12.2 ± 1.8	15.0 ± 0.9	17.1 ± 2.7
	C29:0	9.4 ± 1.7	1.2 ± 0.3	5.2 ± 1.1**	1.5 ± 0.2
	C30:0	27.7 ± 3.0	3.4 ± 1.1	13.2 ± 0.6***	2.2 ± 0.5
	C32:0	59.9 ± 3.2	11.4 ± 3.4	22.0 ± 3.6***	3.1 ± 0.6
Alkenols	C22:2	1.3 ± 0.2	1.4 ± 0.4	4.1 ± 1.0	1.7 ± 0.3
	C24:2	11.4 ± 1.7**	2.2 ± 0.8	5.3 ± 0.8	8.5 ± 1.9
	C26:2	0.6 ± 0.2	1.0 ± 0.4	12.0 ± 0.5	3.6 ± 0.5
Fatty acids	C16:0	10.8 ± 0.9	15.2 ± 2.1	38.0 ± 1.6	76.4 ± 8.0**
	C18:0	8.0 ± 1.0	8.4 ± 0.5	9.6 ± 0.1	15.9 ± 2.0
	C 20:0	12.1 ± 5.5	4.9 ± 1.1	7.8 ± 0.4	6.7 ± 1.5
	C22:0	1.1 ± 0.1	2.1 ± 1.9	1.2 ± 0.1	3.7 ± 0.9*
	C24:0	3.2 ± 0.9	5.9 ± 3.4	14.8 ± 0.8	11.2 ± 1.0
	C25:0	0.4 ± 0.2	5.2 ± 0.4	1.1 ± 0.2	2.6 ± 1.8
	C26:0	2.7 ± 0.2	4.8 ± 2.3	1.6 ± 0.1	3.3 ± 0.9
Triterpenoids/	trans - Coumarate	21.3 ± 5.8*	2.7 ± 0.5	3.0 ± 0.6	3.4± 0.7
Sterols/Coumarate	psi Taraxasterol	32.9 ± 2.3***	5.3 ± 1.7	15.3 ± 0.7***	4.3 ± 0.5
	Taraxasterol	47.9 ± 3.0***	10.0 ± 1.6	25.1 ± 2.3*	11.3 ± 0.6
	delta amyrin	387.6 ± 27.2***	48.1 ± 4.9	211.1 ± 9.5***	66.0 ± 4.1
	ß amyrin	182.7 ± 18.7***	27.8 ± 3.7	105.0 ± 5.3**	81.4 ± 3.8
	α amyrin	201.3 ± 14.7***	23.3 ± 2.4	112.3 ± 4.3***	31.7 ± 1.8
	Cycloartenol	3.6 ± 1.0	1.4 ± 0.4	1.0 ± 0.2	2.2 ± 0.7
	Lupeol	8.6 ± 0.9***	1.9 ± 0.3	4.1 ± 0.3	2.6 ± 0.7
	Multiflorenol	40.0 ± 2.7*	12.0 ± 8.0	21.0 ± 1.0***	4.8 ± 1.2

Data are shown as means ± SE (n = 5). Asterisks denote significant differences between genotypes of the same developmental stage (*, $p < 0.05$; **, $p < 0.01$; ***, $p < 0.001$) as determined by Student's *t tests*.

Fatty acids constitute a relatively minor component of the total wax load ranging from 2 - 5% in both AC and *pe* and there are no significant differences at the green stage, although ripe fruits of the mutant have a significantly higher fatty acid content due mainly to a two-fold increase in hexadecanoic acid. In contrast to the general increase in the levels of long chain alkanes and fatty acids in the epicuticular wax of *pe*, the fatty alcohols (alkanols and alkenols) together with coumarates, sterols and triterpenoids show a general reduction in *pe* compared to AC. In particular, the amyrins, which accumulate to similar levels as the alkanes in wild-type fruit, are reduced by approximately 86% in green fruit of *pe* (Figure 2.4, Tables 2.4 and 2.5). Alkanes are well known to constitute much of the epicuticular wax, whereas triterpenoids are almost exclusively intracuticular waxes (Vogg et al., 2004). Thus the reduction in triterpenoids but not alkanes with the loss of cutin is consistent with the differential localization of these waxes.

Altered surface chemistry and increased water conductance in *pe* leaves

To investigate whether the altered surface chemistry observed in *pe* is restricted to fruit or is a more general phenotype of the mutant, the cutin and wax composition of the leaves of AC and *pe* were compared. As was observed in fruit, the major monomer identified in tomato leaf cutin is also 9(10),16-dihydroxyhexadecanoic acid constituting between 20 – 25% of the total cutin monomer load (Figure 2.5). Additional monomers identified include several fatty acids and the phenylpropanoids *cis*- and *trans*-coumaric acid together with caffeic acid. The overall cutin monomer load in leaves of *pe* is 54% of that in AC, with an approximately five-fold reduction in 9(10),16-dihydroxyhexadecanoic acid and significant reductions in additional monomers (Figure 2.5A).

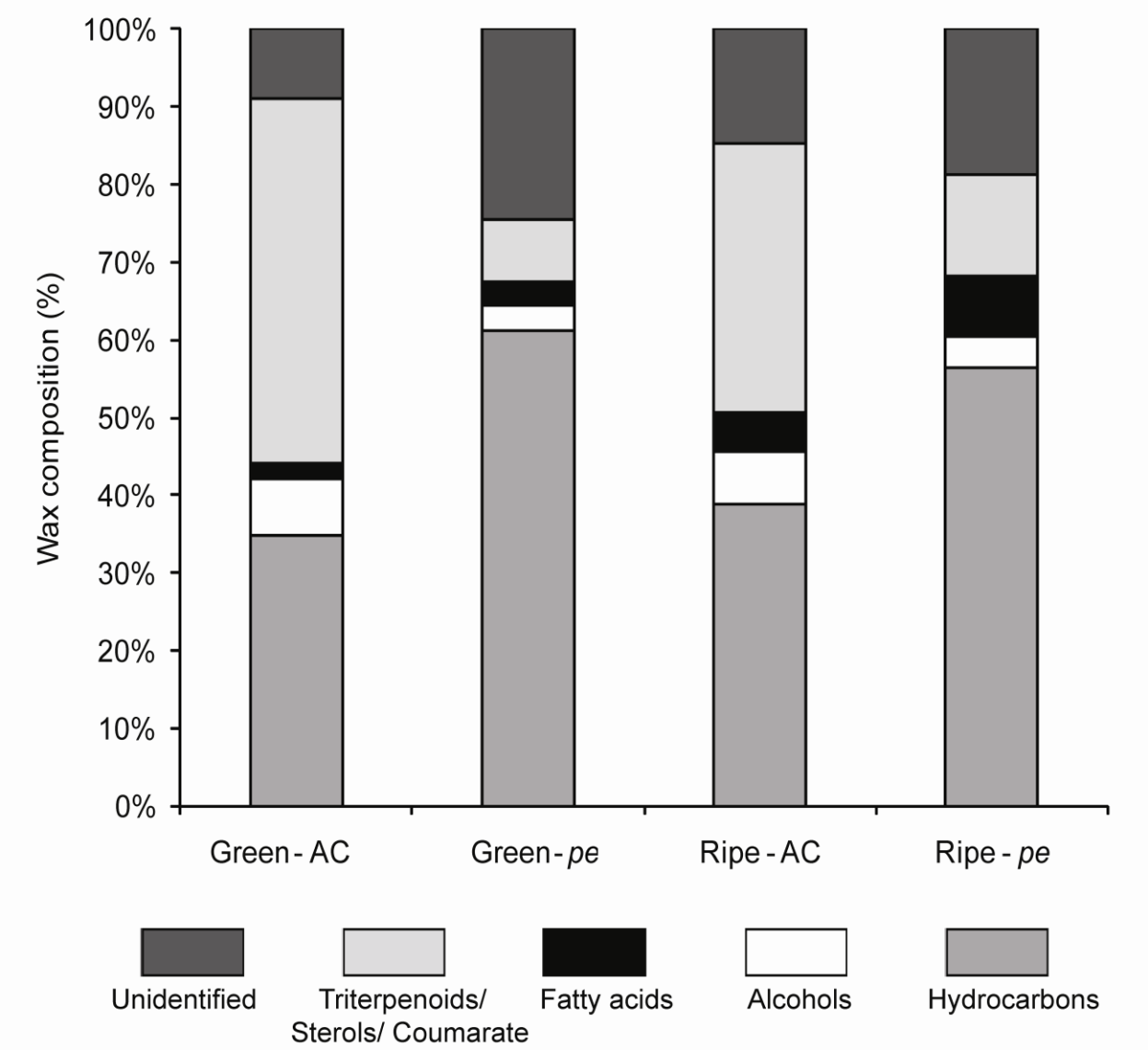

Figure 2.4. Relative fruit wax composition in AC and *pe*. Fruit wax content of green and ripe stage fruits were analyzed by GC. The wax components were grouped under five classes; i) Hydrocarbons, consisting of alkanes, branched alkanes and alkenes ii) Alcohols, iii) Fatty acids iv) Triterpenoids, sterols and coumarates and v) Unidentified compounds. The relative percentage of each class comprising the total wax load is shown.

Tomato leaf cuticular wax components identified in this study comprise *n*-alkanes, iso-alkanes, anteiso alkanes, petacyclic triterpenoids, sterol derivatives and fatty acids. Among these, alkanes and branched alkanes constituted the major fraction (up to 90%) of all the identified wax composition in wild-type leaves. The total leaf wax load is reduced by 30% in the mutant. This is mainly attributed to significant reduction in alkanes. Interestingly all the straight chain alkanes in the *pe* mutant were reduced by approximately 50% compared to wild-type, whereas branched-chain alkanes are essentially unaltered (Figure 2.5B). As both wax and cutin loads decrease in leaf, unlike in fruit (Table 2.3 and Table 2.4), the cutin monomer to wax ratio changes only fractionally in the *pe* mutant, from 2.3 (5.85 : 2.53 μg cm^{-2}) to 1.8 (3.20 : 1.80 μg cm^{-2}) (Figure 2.5). This clearly shows a differential regulation of straight chain and branched hydrocarbons in fruit and leaf cuticular wax, suggesting they may be independently regulated.

Cuticular waxes play a pivotal role in limiting water loss in plants. The levels of alkanes within cuticular waxes are often positively correlated with increased resistance to cuticular water loss and an increase in cuticular wax abundance, particularly alkanes can occur during water stress (Grncarevic and Radler, 1967; Kosma et al., 2009; Bourdenx et al., 2011; Seo et al., 2011). Furthermore, altered cutin composition may disrupt the intermolecular packing of waxes within the cutin matrix, although this relationship remains unclear (Pollard et al., 2008; Schreiber, 2010; Buschhaus and Jetter, 2011). Given the reduction in alkane and cutin monomer content in the leaves of the *pe* mutant, the rate of leaf water loss from mutant leaves was determined. The *pe* mutant does not have an obviously wilty phenotype however leaf water conductance in intact *pe* leaves was approximately 3-fold higher than in AC (Figure 2.6A). Similarly, an increase in the

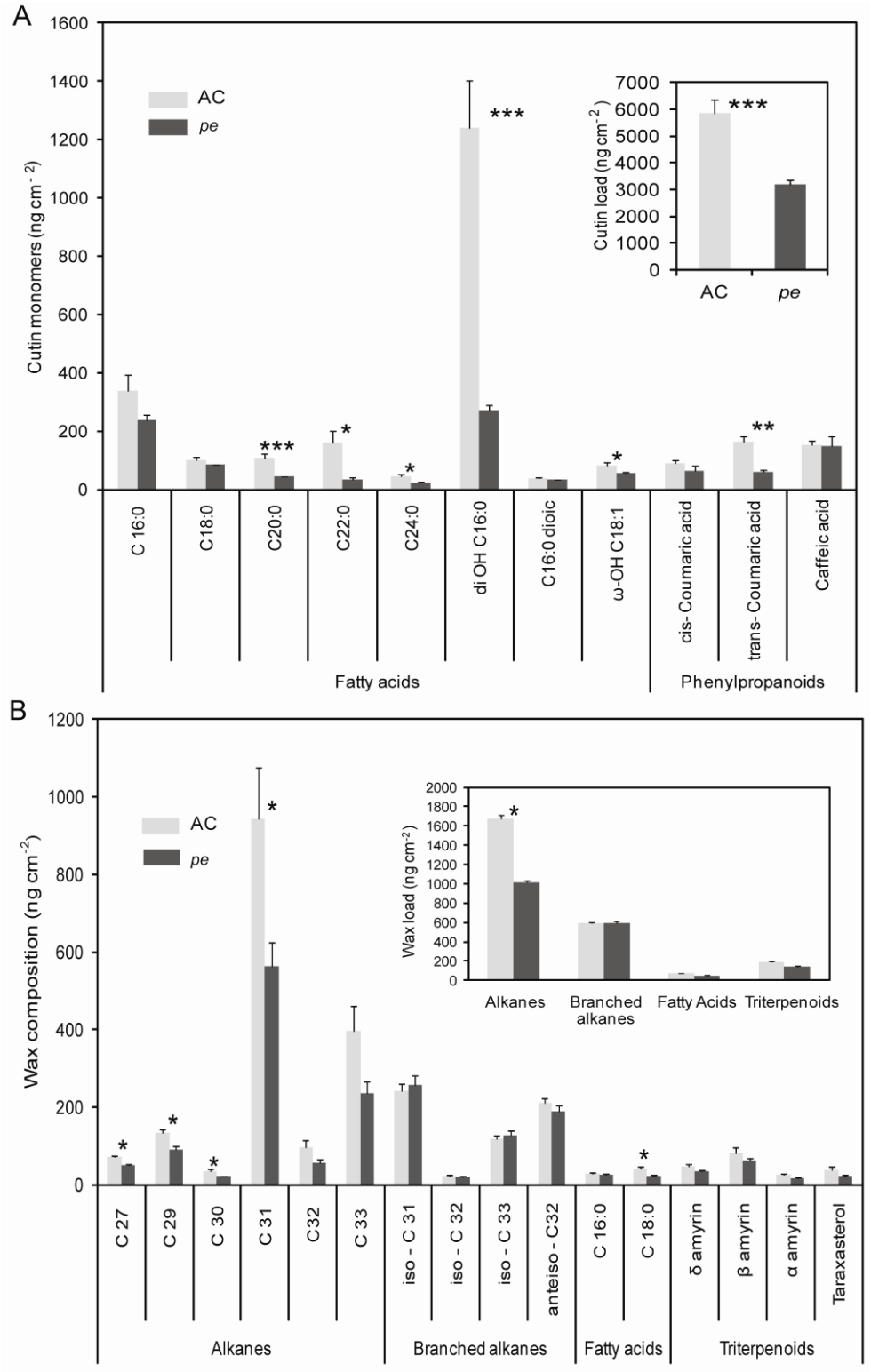

Figure 2.5. Leaf cutin and wax profiles of AC and *pe*.

Figure 2.5 (cont'd)

A) Leaf cutin components were grouped into i) fatty acids and ii) phenylpropanoids. B) Leaf wax constituents were grouped into four classes i) Alkanes, ii) Branched chain alkanes, iii) Fatty acids, and iv) Triterpenoids. Inset graphs indicate total cutin and wax loads in AC and *pe*. Values represent mean values (n=5) ±SE. Asterisks denote significant differences (*, $p < 0.05$; **, $p < 0.01$; ***, $p < 0.001$) as determined by Student's *t tests*.

rate of chlorophyll leaching was observed in *pe* leaves (Figure 2.6B), a phenomena previously shown to be associated with cuticle permeability (Kosma et al., 2009). Previous research indicated that defects in cutin biosynthesis can lead to alterations in stomatal structure including impaired development of cuticular ledges that lie between adjacent guard cells (Li et al., 2007). Scanning electron micrographs of the leaf surface did not reveal any structural differences in the stomata of the *pe* mutant (Figure 2.6C). Furthermore, the average stomatal density on the abaxial leaf surface in wild type leaves (30 in 0.55 mm^2) is higher than in *pe* leaves (21 in 0.55 mm^2) (Figure 2.6D). Together, these data suggest that enhanced rate of water loss from the leaves of *pe* mutant is due to cuticular water loss and not to altered stomatal structure or density.

Root suberin and wax composition are not dramatically altered in *pe*

The altered cutin and wax composition observed in the leaves and fruits of *pe* suggested the possibility of a general perturbation in synthesis of fatty acid derived polymers. This was investigated by determining the suberin and wax content in roots of *pe*. The aliphatic components that account for nearly 90% of the total suberin, together with the aromatic components are not significantly altered in *pe* (Figure 2.7A). In addition, the overall root wax load is largely unaltered in *pe* although small increases in abundance of β-C22:0 mono-acyl-glycerol, C29:2 sterol, and C18:0 and C22:0 primary alcohols are observed (Figure 2.7B).

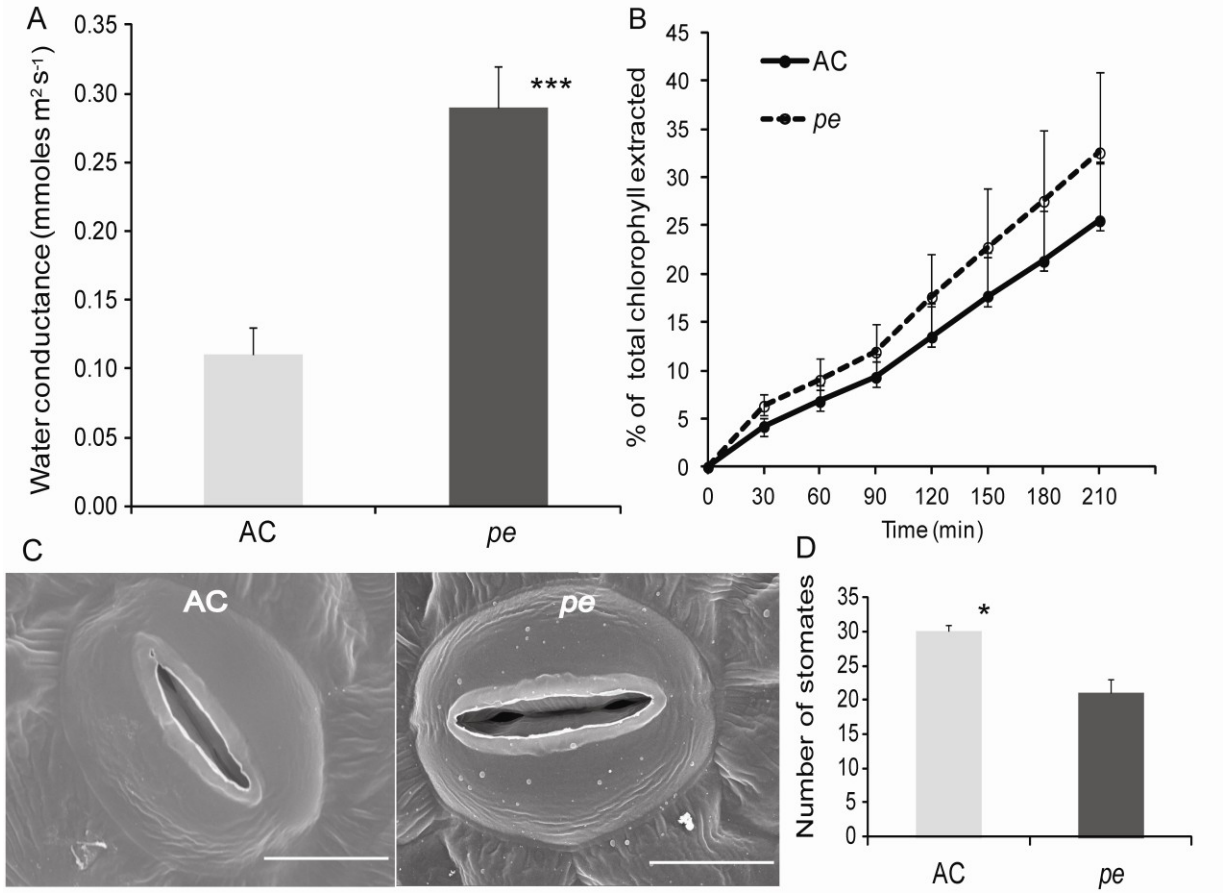

Figure 2.6. Increased cuticular permeability in *pe*. A) Leaf water conductance in AC and *pe* (*n*=5) ±SE. B) Chlorophyll leaching expressed as percent of total leaf chlorophyll extracted after 24 hours (*n*= 5) ±SE. C) Scanning electron micrographs of representative stomata on the abaxial leaf surface of AC and *pe* (Scale bar = 5 µm). D) Stomatal density on abaxial leaf surface area of 0.55mm^2 (*n*= 10 ±SE). Asterisks denote significant differences (*, $p < 0.05$; ***, $p < 0.001$) as determined by Student's *t tests*.

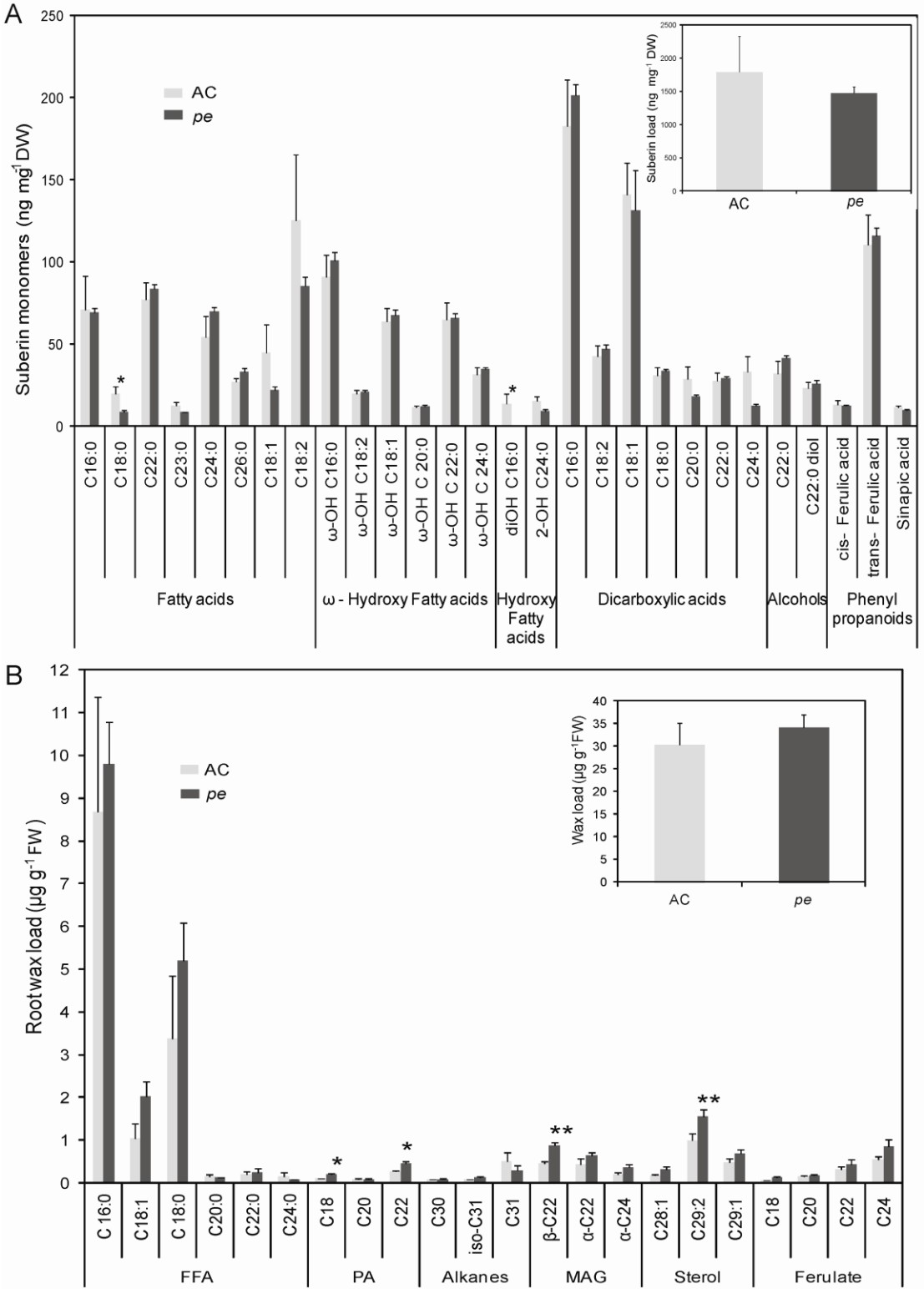

Figure 2.7. Suberin and root wax composition in AC and *pe*.

Figure 2.7 (cont'd)

A) Suberin monomer content in roots of AC and *pe* as analyzed by gas chromatography. Absolute amounts of suberin monomers are shown as mean values ($n=5$) in ng mg^{-1} dry weight. The graph inset indicates the total suberin load. B) Root wax profile in AC and *pe*. Root waxes were divided into 6 classes: FFA- free fatty acids; PA- primary alcohols; alkanes; MAG - mono acyl glycerols; sterols and ferulates (For ferulates, alkyl chain length indicated). Absolute amounts of individual components are shown as mean values ($n=5$) in µg mg^{-1} fresh weight. The graph inset indicates the total root wax load. Error bars in A & B represent standard error of the mean. Asterisks denote significant differences (*, $p < 0.05$; **, $p < 0.01$) as determined by Student's *t tests*.

Mapping of the *pe* locus and candidate gene identification

The *pe* locus was provisionally mapped to chromosome 1 of the classical genetic map of tomato (Mutschler et al., 1987). An F_2 mapping population segregating for the *pe* mutant allele was generated through crosses between *S. lycopersicum* (*pe/pe*) (LA2467*)* and *S. pimpinellifolium* (*PE/PE*) (LA1589). The mutant plants were pale green in color and this phenotype co-segregated with the cutin deficient, sticky and glossy fruit phenotype in the F_2 population. The F_2 population was genotyped with chromosome 1 molecular markers, revealing that the *pe* locus is located within a 424 kb interval between C2_At4g00090 and cTOA-13-J3 (Figure 2.8A). This mapping interval contains the *CUTIN DEFICIENT 2* (*CD2*) gene, which encodes a HD-ZIP IV protein, with homology to *ANL2* of Arabidopsis (Kubo et al., 1999; Isaacson et al., 2009). A single G > A substitution causes the conversion of a conserved glycine to arginine at position 736 of the protein at the *cd2* locus which results in a glossy and cutin deficient fruit phenotype with a total cutin load of approximately 10% of wild type fruits (Isaacson et al., 2009). The similarity in phenotype and map position of *pe* and *cd2* suggested that *pe* may be allelic to *cd2*. To investigate this hypothesis, the *CD2* gene was cloned and sequenced from the *pe* mutant revealing the insertion of a G nucleotide following nucleotide 2045. This insertion causes a frame shift mutation resulting in the incorporation of four spurious amino acids followed by a premature stop codon that truncates the predicted protein by 160 amino acids in *pe* (Figure 2.8A). To confirm that a mutation in the *CD2* gene is responsible for the *pe* mutant phenotype, VIGS experiments were performed using two constructs targeting separate regions of the *CD2* gene. *CD2* silenced lines showed a 20-30% reduction in height compared with TRV2-empty vector control lines and leaves showed sectors of pale coloration characteristic of the *pe* mutant (Figure 2.8B-D).

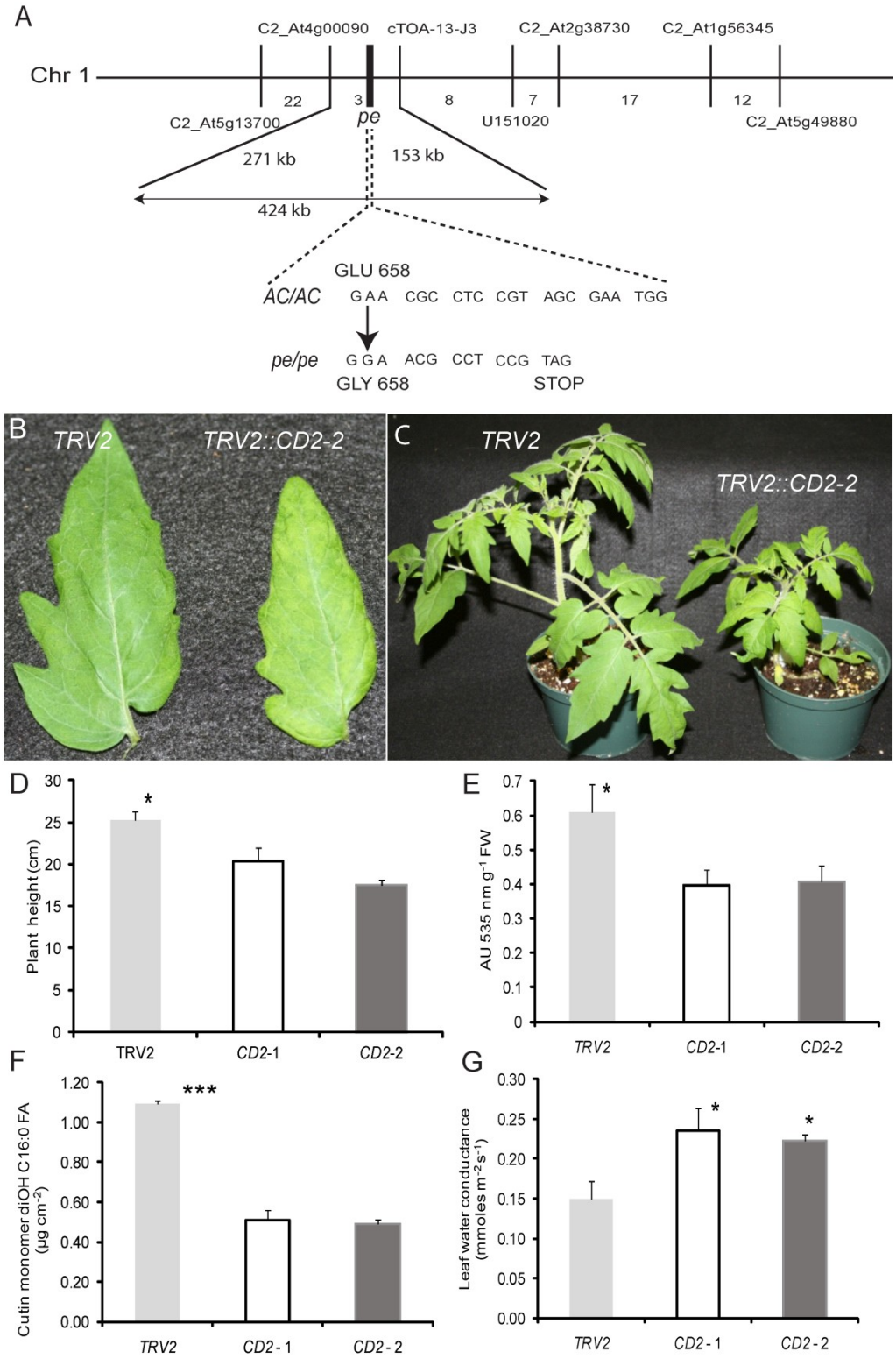

Figure 2.8. Characterization of the *pe* locus and silencing of *CD2*.

Figure 2.8 (cont'd)

A) Genetic map of the *pe* locus. Genetic markers and the number of recombinant individuals between adjacent markers from a total of 114 F_2 plants are shown. The approximate physical distance between the flanking markers and the *pe* locus is indicated. Sequence analysis of the *CD2* gene from AC and *pe* revealed a single G nucleotide insertion following nucleotide 2045 leading to a frame shift mutation. B – G) Silencing of *CD2* recreates the *pe* mutant phenotype. B) Pale leaf phenotype in a *CD2-2* VIGS line. C) Short stature of a *CD2*-2 VIGS line D) Plant height of *CD2* VIGS lines. E) Anthocyanin content of *CD2* VIGS lines. F) The major leaf cutin monomer 9(10), 16-dihydroxyhexadecanoic acid is reduced in *CD2* silenced lines. G) *CD2* silencing impairs leaf cuticle barrier properties and increases water conductivity. All values D – G represent mean values (n=5) ±SE. *TRV2* empty vector control lines were used for all comparisons. Asterisks denote significant differences (*, $p < 0.05$; ***, $p < 0.001$) as determined by Student's *t tests*.

Anthocyanin levels were reduced in the *CD2* silenced lines by approximately 30-35% (Figure 2.8E). The major leaf cutin monomer 9(10), 16-dihydroxyhexadecanoic acid was reduced by 50% in the silenced lines and there was a concomitant increase in the leaf water conductance (Figure 2.8F and G). Together, these data indicate that the *pe* mutant phenotype is caused by a mutation in *CD2*.

Mutation at the *anthocyaninless 2* locus leads to cutin deficiency

Phylogenetic analysis indicated that CD2 is closely related to a number of HD-ZIP IV proteins including several that impact epidermal cell development and cuticle biosynthesis (Nakamura et al., 2006; Javelle et al., 2010; Javelle et al., 2011) (Figure 2.9A). *HD-ZIP IV* genes are typically expressed in epidermal cells and expression analysis indicated that *CD2* transcripts are enriched in stem peels, which are comprised of a mixture of epidermal and sub-epidermal cells, compared to the levels observed in whole stem and stem core with the peel removed (Figure 2.9B).

ANL2 is the closest Arabidopsis homolog to *CD2* (Figure 2.9A) and is also preferentially expressed in epidermal cells (http://efp.ucr.edu/cgi-bin/absolute.cgi). Furthermore, both *pe* and *anl2* mutants have reduced anthocyanin accumulation (Kubo et al., 1999) (Figure 2.1). These similarities led us to hypothesize that *anl2* mutants would also be cutin deficient. This was confirmed in rosette leaves of *anl2,* which exhibit approximately a 40% reduction in cutin monomer load together with a 25% reduction in the alkane load of the cuticular waxes compared to Col-0 (Figure 2.10).

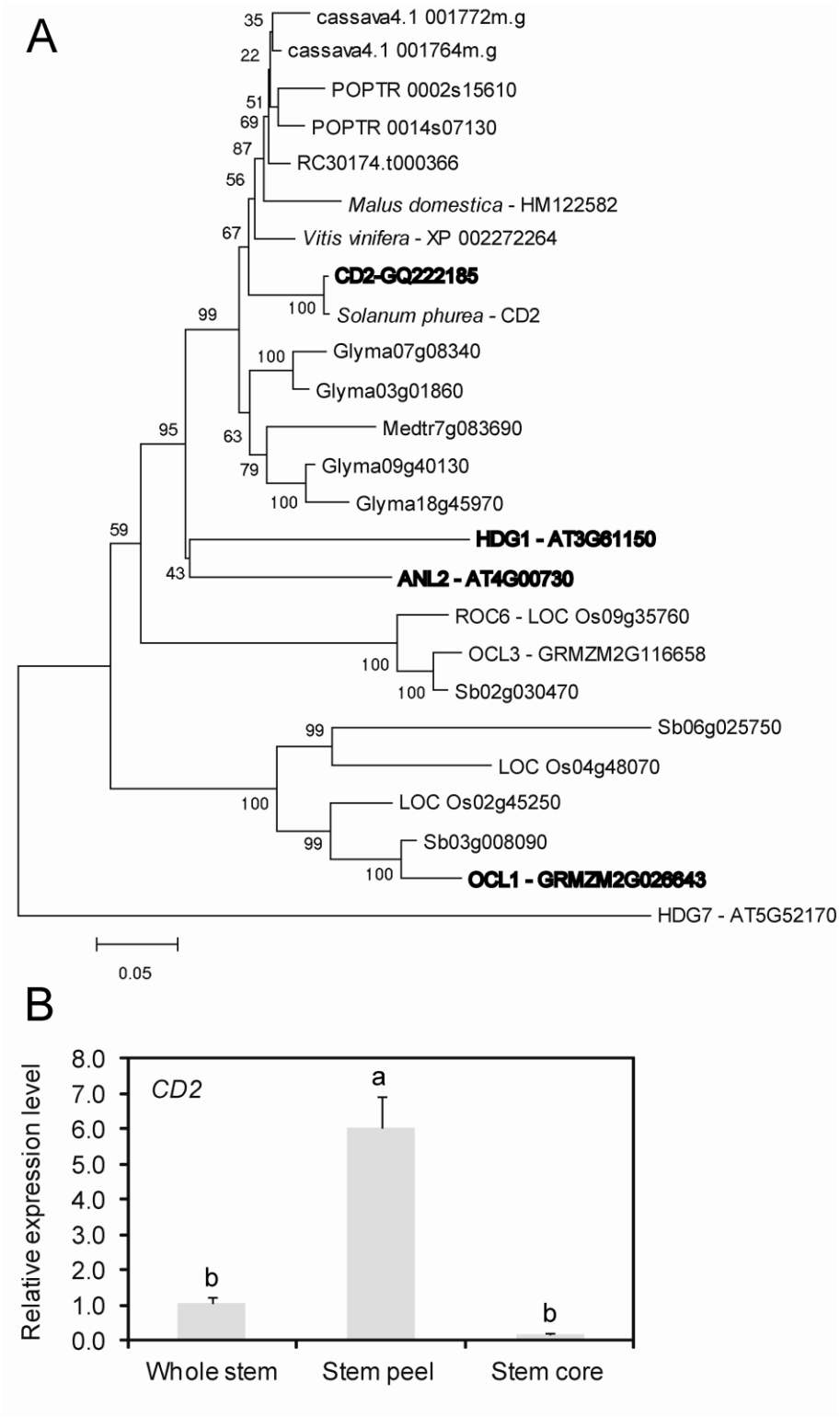

Figure 2.9. Phylogenetic and expression analysis of *CD2*.

Figure 2.9 (cont'd)

A) A neighbor-joining phylogenetic tree derived from a multiple sequence alignment of the deduced full-length amino acid sequences of CD2 homologs constructed using MEGA V5.0 software (Tamura et al., 2011). *HDG7* is included as an out-group. Bootstrap values are from 2,000 replicates, indicated above the nodes. Proteins highlighted in bold have defined functions in cuticle biosynthesis. B) qRT-PCR analysis of *CD2* expression in stem peel of AC relative to stem core and whole stem. Three biological and three technical replications for each sample were analyzed. Data are presented as the mean expression values ±SE relative to that observed in whole stem. Values labeled with different letter are significantly different (LS Means, $p < 0.05$).

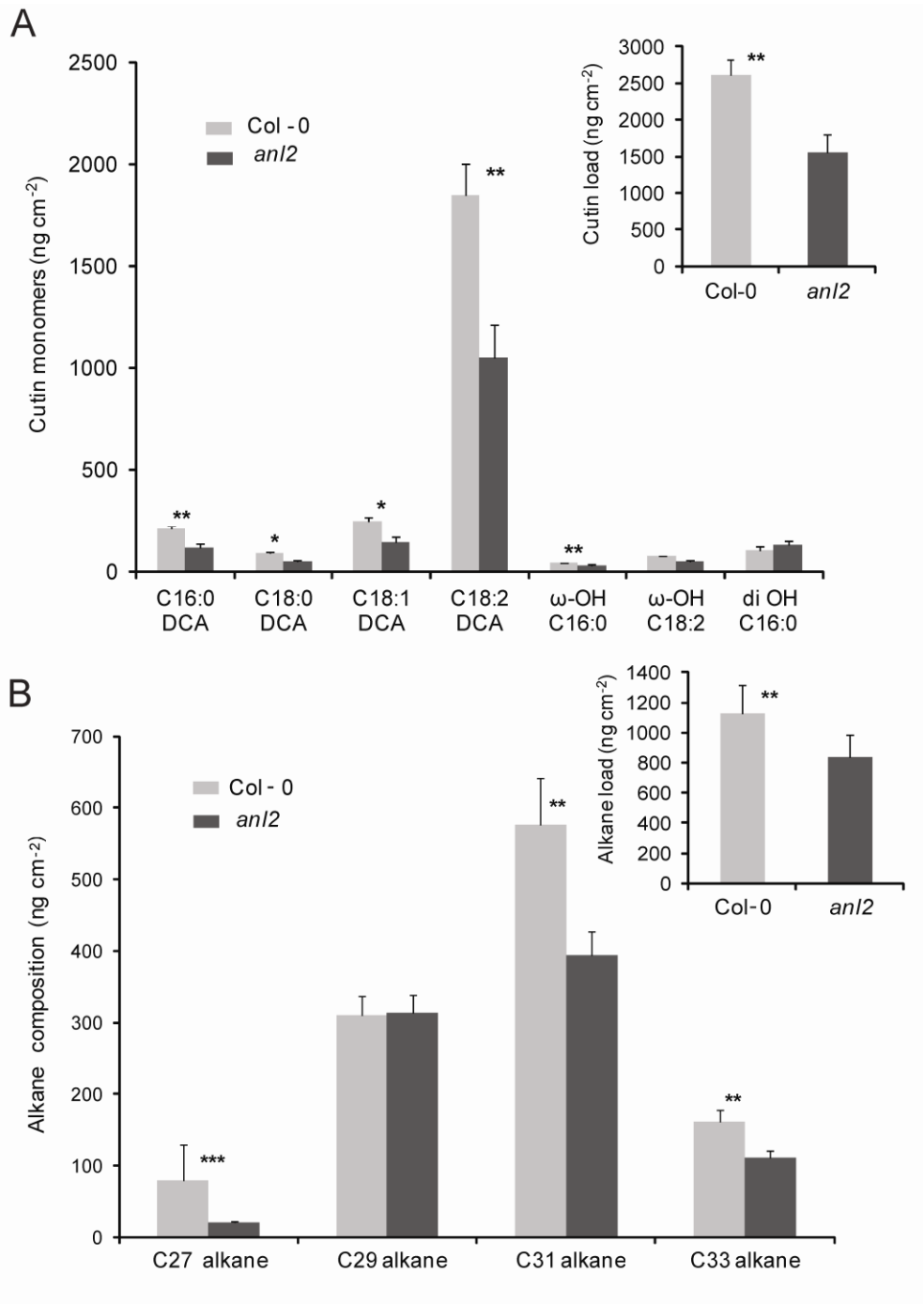

Figure 2.10. Cutin monomer and wax profile of Arabidopsis Col-0 and *anl2* leaves. A) Leaf cutin monomer composition (DCA, α, ω dicarboxylic acid). B) Alkane constituents of leaf wax. Inset graphs indicate total cutin and alkane load. Data represents mean values (n=5) ±SE. Asterisks denote significant differences (*, $p < 0.05$; **, $p < 0.01$; ***, $p < 0.001$) as determined by Student's *t tests*.

Discussion

Characterization of *pe* identifies additional roles for *CD2*

Phenotypic characterization indicates that the *pe* mutant has altered fruit surface chemistry leading to reduced cutin levels and a modified surface wax composition (Figure 2.3, Table 2.3 and Table 2.4). The altered chemical profile leads to a change in the physical properties of the fruit peel including increased glossiness and a higher Young's elastic modulus (Figure 2.3A-C). These phenotypes are identical to those previously described in *cutin deficient* mutants of tomato where cutin deficiency was correlated with altered biomechanical and structural properties together with enhanced susceptibility to microbial infection (Isaacson et al., 2009). A combination of genetic mapping and gene cloning revealed that *pe* represents a new mutant allele of *CD2* that truncates the predicted protein by 160 amino acids and therefore likely represents a null allele (Figure 2.3A).

Previously, the *cd2* phenotype was associated with fruit-specific alteration in cuticle biosynthesis (Isaacson et al., 2009). However, as shown in this study, many additional phenotypes are evident in *pe* including a semi-dwarf stature, reduced anthocyanin accumulation, altered cutin and wax deposition in leaves, increased permeability of the leaf cuticle, and reduced trichome density together with lower volatile terpene production (Figure 2.1, Figure 2.2, Figure 2.5, Figure 2.6 and Table 2.1). These phenotypes were confirmed in the *cd2* allele and VIGS lines targeting *CD2* (Figure 2.8 and Figure 2.11 and Figure 2.12). Together, these data reveal a broad role for *CD2* in plant development, and particularly in relation to metabolism within epidermal and sub-epidermal cells, which is supported by the epidermal enriched expression pattern of *CD2* in stems (Figure 2.9B) and in tomato fruit (Matas et al., 2011).

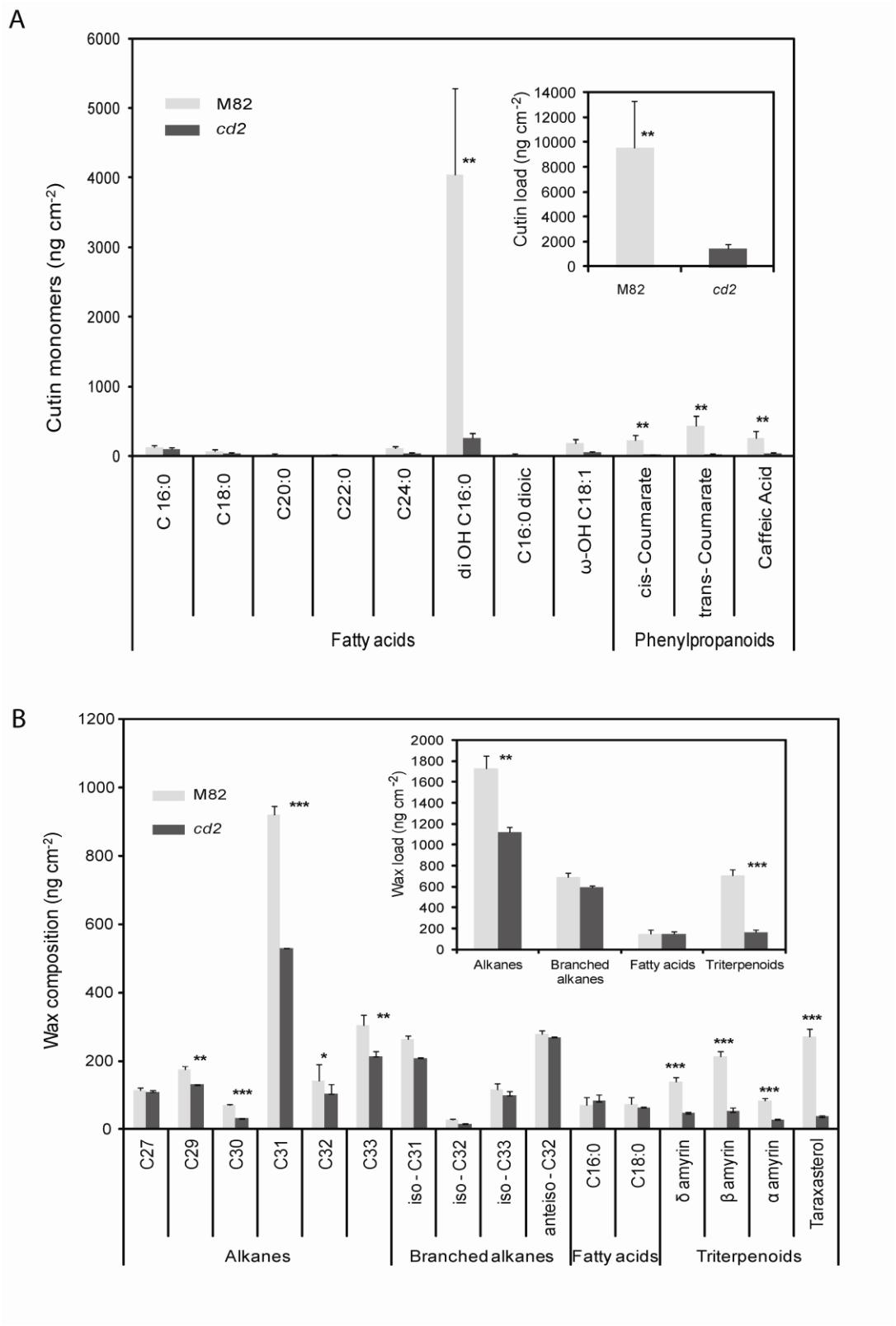

Figure 2.11. Comparison of leaf cutin and wax composition in M82 and *cd2*.

Figure 2.11 (cont'd)

A) Leaf cutin monomers that are identified and quantified. B) Leaf wax constituents were grouped into four classes i) Alkanes ii) Branched chain alkanes iii) Fatty acids iv) Triterpenoids. Inset graphs indicate total cutin and wax loads in M82 and *cd2*. Values represent mean values ($n=5$) ±SE. Asterisks denote significant differences (*, $p < 0.05$; **, $p < 0.01$; ***, $p < 0.001$) as determined by Student's *t tests*.

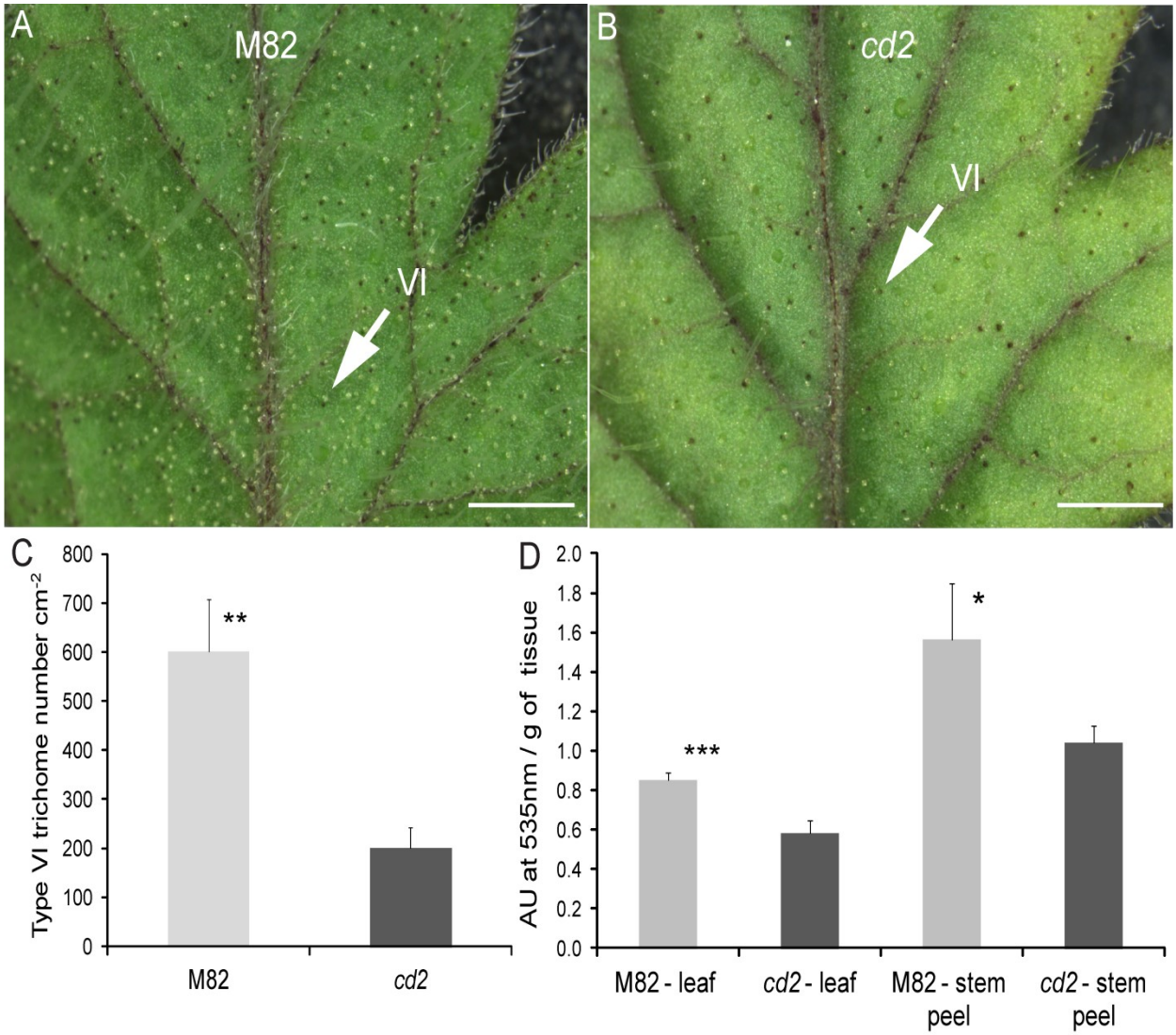

Figure 2.12. Trichome density on leaves and anthocyanin accumulation in leaves and stem peels of A) M82 and B) *cd2*. Scale bars represent 2 mm. C, Density of type VI glandular trichomes on the adaxial leaf surface of M82 and *cd2*. D, Anthocyanin contents (AU 535 nm) of M82 and *cd2* leaves and stem peels. The data shows the mean trichome number (n=5 ±SE). Asterisks denote significant difference (**, $p<0.01$) as determined by student's *t test*.

HD-ZIP IV proteins and cuticle biosynthesis

CD2 belongs to a subgroup of HD-ZIP IV proteins, several of which have defined roles in epidermal cell development and are preferentially expressed within the epidermis (Figure 2.9B) (Javelle et al., 2011). Proteins of this family are characterized by HD-ZIP domain followed by a steroidogenic acute regulatory lipid transfer (START) domain. The fact that HD-ZIP IV proteins are widely distributed in lower plants, gymnosperms and angiosperms but are absent in algae is consistent with a role in the evolution of land plants (Ponting and Aravind, 1999; Mukherjee et al., 2009). Several closely related *CD2* homologs influence cuticle composition and/or regulate genes involved in cuticle biosynthesis. For example, *OUTER CELL LAYER 1* (*OCL1*) of maize is expressed early in embryo development, prior to protoderm formation and is subsequently expressed in the L1 cell layer in the shoot apical meristem (Ingram et al., 1999). Over-expression of *OCL1* in maize altered the wax composition in leaf blade as well as sheath and increased the expression of several genes involved in wax biosynthesis and transport (Javelle et al., 2010). Furthermore, transient assays suggested that activation of the expression of a wax transporter and a non-specific lipid binding protein likely occurs through direct binding of OCL1 to regulatory regions within these genes (Javelle et al., 2010). Similarly, Arabidopsis *HDG1* directly regulates the expression of *BODYGUARD (BDG*) and *FIDDLEHEAD*, two genes involved in cuticle biosynthesis and disruption of *HDG1* function leads to cuticles with increased permeability (Wu et al., 2011). Furthermore, Arabidopsis *ANL2* and *HDG1* are preferentially expressed in epidermal or sub-epidermal cells (Suh et al., 2005; Kubo et al., 2008) (http://efp.ucr.edu/cgi-bin/absolute.cgi) and our analysis indicates that *anl2* has a cutin deficient phenotype (Figure 2.10).

Overall, the characterized members of the *CD2* subclade all possess a common role in the regulation of cuticle biosynthesis, even though the composition of cutin can vary between species and tissues. For example, while tomato cutin is predominantly comprised of hexadecanoic acid-derived monomers, Arabidopsis leaves have a C18:2 dicarboxylic acid-rich cutin (Table 2.3 and Figures. 2.5 and 2.10). These cutins require different sets of biosynthetic genes (Li et al., 2007; Pollard et al., 2008; Li-Beisson et al., 2009) suggesting that while the regulation of cuticle biosynthesis may be generally conserved, these regulatory proteins may target distinct sets of biosynthetic genes in diverse species or tissues contributing to their different cuticle composition. Furthermore, given that several members of the *CD2* subclade influence cuticle biosynthesis (Figure 2.9A), it is possible that the phylogenetically closely-related and as yet uncharacterized genes, may also have a similar role.

A role for *CD2* in reducing leaf water loss

The cuticle regulates non-stomatal water loss and the amount and composition of cuticular wax is associated with cuticle permeability to water. For example, mutants or transgenic lines with reduced levels of very long chain alkanes often display elevated rates of water loss (Vogg et al., 2004; Leide et al., 2007; Qin et al., 2011). Furthermore, enhancing the levels of these wax components can restrict water loss leading to improved drought tolerance (Bourdenx et al., 2011; Seo et al., 2011). Similarly, drought-stressed plants can increase cuticular wax biosynthesis as a defense mechanism to reduce further water loss (Kosma et al., 2009).

The wax composition of leaves and fruits vary in *pe* when compared to AC. For example, hydrocarbons are elevated in *pe* fruits whereas in leaves the straight-chain alkanes are significantly reduced compared to wild-type (Figure 2.5B and Table 2.5). The same trend for cutin and wax is observed in the fruit (Isaacson et al., 2009) and leaves (Figure 2.11) of *cd2*

when compared to the M82 parental line. The basis for the differential *CD2*-mediated control of wax accumulation in leaves and fruits is currently unclear but may occur through altered gene regulation between these tissues or possibly altered fluxes of precursors in mutant tissues. For example, a proportion of the hexadecanoic acid precursor, typically utilized in cutin biosynthesis may be channeled toward alkane biosynthesis when cuticle biosynthesis is limited in *pe* and *cd2* fruits. However, this is unlikely to be a general phenomenon as an increase in alkane accumulation is not observed in *cd1* and *cd3* fruits (Isaacson et al., 2009).

Our data suggest a correlation between cuticular wax composition in *pe* and leaf cuticle permeability. For example, leaf water conductance and chlorophyll leaching are increased in *pe* leaves compared to AC (Figure 2.6). A similar trend was observed in *CD2* silenced lines (Figure 2.8G). In contrast, fruits of the *pe* and *cd2* mutants, which have higher levels of long chain alkanes, do not exhibit enhanced rates of post-harvest water loss (Table 2.5) (Isaacson et al., 2009). Although disruption of individual cutin or wax components can alter permeability, the physical consequences of these changes on the structure of the cutin matrix, is not well understood. Alkanes are proposed to influence cuticle permeability by forming water-impermeable crystalline regions within the cuticle and the packaging of the wax crystals is likely dependent upon the cutin structure (Pollard et al., 2008; Buschhaus and Jetter, 2011). Therefore, while it is not possible to more exactly define the underlying reason for the increased permeability of *pe* leaves, it could be due to one, or a combination of the following factors, including decreased alkane levels, a decreased cutin load, an alteration in the cutin to wax ratio, or an as yet undefined biochemical change. A comparison of wax biosynthesis between wild-type and *pe* leaves and fruit tissues, together with a more in depth understanding of wax

deposition in these genotypes and tissues, may provide insight into how *CD2* influences cuticular permeability.

Leaf water loss is also intricately linked to stomatal structure and physiology and several lines of research have highlighted possible links between cuticle composition and stomatal density and structure. Cutin deficiency in Arabidopsis leads to altered stomatal morphology including a reduction in the cuticular ledges (Li et al., 2007). No structural alterations were observed in stomata of the *pe* mutant suggesting that *CD2* may not influence cuticle biosynthesis in leaf guard cells (Figure 2.6C). Similarly, previous reports have shown that altered cuticular wax composition can positively or negatively influence stomatal density in Arabidopsis (Gray et al., 2000; Chen et al., 2003; Yang et al., 2011). The exact mechanisms through which this process occurs are unknown although it is possible that the altered composition of leaf cuticular waxes in *pe* may exert a compensatory influence leading to the observed reduction in stomatal density (Figure 2.6D).

CD2 and phenylpropanoid biosynthesis

Flux into the phenylpropanoid pathway through the enzyme phenylalanine ammonia lyase represents a branch point between primary and specialized metabolism in plants. The phenylpropanoid pathway synthesizes a wide range of compounds including flavonols, anthocyanins, lignins, suberin and cutin aromatics, and tannins, which have diverse roles in plants as structural polymers, pigments, UV protectants and signaling molecules (Hahlbrock and Scheel, 1989; Vogt, 2010). In agreement with the epidermal enriched expression pattern of *CD2* (Figure 2.9B), the *pe* mutant exhibits reduced accumulation of a subset of phenylpropanoids that typically are synthesized and accumulate in the epidermal and sub-epidermal cells. In addition to the anthocyanins, which are severely reduced in *pe* tissues, coumarates, which comprise between

3 and 5% of the total cutin monomer load in wild type tomato fruits, are also reduced in *pe* (Figure 2.1, Table 2.1 and Table 2.3). The reduction in coumarate is readily ascribed to the reduction of the cutin aliphatic hydroxy fatty acid monomers, to which coumarate is likely esterified. In contrast, the abundance of lignin and suberin ferulates, two biopolymers derived from phenylpropanoid precursors that are not typically associated with epidermal cells, are unaltered in *pe* (Figure 2.7 and Table 2.2). It will be of interest to determine if additional phenylpropanoid-derived metabolites are altered in the epidermal cells of *pe* and to understand the flux through the pathway in these cells in the *pe* mutant. In addition, the role of *CD2/ANL2* in directly regulating anthocyanin biosynthesis, as well as understanding their relationship to known transcriptional regulators of anthocyanin biosynthesis warrants additional investigation.

CD2 as a regulator of epidermal cell function

HD-ZIP IV proteins are master regulators of epidermal cell fate and function in higher plants and have roles in cuticle biosynthesis together with patterning of trichome and stomata (Javelle et al., 2011). Our biochemical characterization of the *pe* mutant of tomato has revealed alterations in multiple pathways associated with epidermal cell function that have evolved to facilitate plant adaptation to stress, including altered cuticle biosynthesis in leaves and fruits, reduced anthocyanin accumulation, and lower trichome and stomatal densities. The subsequent identification of *pe* as an allele of *CD2* extends current knowledge of the role of *CD2* beyond cuticle biosynthesis in tomato fruit to include a spectrum of altered phenotypes associated with epidermal cell function. While mutant alleles of *CD2* influence a broad range of epidermal cell phenotypes, it is difficult to determine whether these alterations constitute primary or secondary effects. For example, altered stomatal and trichome densities can result from perturbation of cuticular wax biosynthesis, including mutations that affect catalytic enzymes, suggesting that

disruption of cuticle structure and / or physiology induces secondary phenotypes (Gray et al., 2000; Chen et al., 2003; Kurata et al., 2003; Aharoni et al., 2004). Establishing cause and effect relationships with respect to the altered stomatal and trichome density phenotypes observed in *pe* will be complex.

Our data suggests that *CD2* is a master regulator of epidermal cell function in tomato. Although the exact role of *CD2* in specifying epidermis-related phenotypes remains to be defined, it is possible that CD2 directly regulates the expression of the biosynthetic genes involved in synthesis of diverse epidermal cell associated molecules. Alternatively, it is equally probable that CD2 acts upstream of these pathways, within a transcriptional network that maintains epidermal cell identity and function. Defining the immediate targets of CD2 will provide insight into these questions and will help identify the regulatory networks that control specialized metabolism within plant epidermal cells.

Materials and Methods

Plant material and growth conditions

Seeds of the *sticky peel* (*pe/pe*) (LA2467), *high pigment-1* (*hp-1/hp-1*) (LA3538), and *entirely anthocyaninless* (*ae*/*ae*) (LA3612) mutants, together with *S. pimpinellifolium* (LA1589) were obtained from the Tomato Genetics Resource Center, UC Davis. The cultivar AC was originally obtained from the Glasshouse Crops Research Institute (Littlehampton, Sussex, UK). As the genetic background of LA2467 was not known, a segregating BC_2F_2 population was generated from an initial cross of LA2467 (*pe/pe*) with AC (*PE/PE*) as the recurrent parent. The mutant plants (*pe/pe*) were selected based on phenotype; short stature, pale green color of the stem and leaves and stickiness of the fruit surface, all of which co-segregated. This population was used for all experiments. Unless otherwise stated, plants were grown in peat-based compost supplemented with fertilizer in greenhouses at Michigan State University under 16 h day (25°C) and 8 h night (20°C). Arabidopsis seeds of *anl2* (SALK_000196) were described previously (Nakamura et al., 2006) and sown in soil (1:1:1 Sure mix: Medium vermiculite: Perlite, Michigan Grower Products Inc., www.suremix.com) and after 3d at 4°C, maintained in a growth chamber under a 16 h photoperiod (145 μmol m^{-2} s^{-1}) at 22°C at a relative humidity of 65%. Tomato fruits were harvested when they reached 35 to 40 mm diameter for green stage or at seven days after the onset of ripening (breaker +7 days) for ripe stage of development. All experiments involving leaves, stems and roots were performed on five-week-old plants unless otherwise stated. Rosette leaves from seven-week-old Arabidopsis plants were used for cutin analysis.

Extraction and analysis of cuticular lipids

Extraction of surface waxes from leaf, root and fruit tissues of tomato or from leaves of Arabidopsis was accomplished through dipping tissue samples in chloroform containing 1% methanol for 2 minutes in the case of fruits and 1 min for other tissues. The surface areas of leaves and fruits were determined prior to wax extraction using a LI-3100C Area Meter (Li-Cor, http://www.licor.com) and Tomato Analyzer version 2.1.0.0., respectively (Brewer et al., 2006). Internal standards of tetracosane, hexadecanol and heptadecanoic acid (5µg/ml each) and ω-pentadecalactone, methyl heptadecanoate (10 µg/ml each) (Sigma-Aldrich, http://www.sigmaaldrich.com) were added to each wax and cutin extract, respectively. Preparation of tri-methyl-silyl derivatives of wax components, followed by delipidation, base-catalyzed trans-methylation and acetyl derivatization of cutin monomers from all the tissues was performed as previously described (Molina et al., 2006). GC (FID) (6890N, Agilent technologies) analysis of the derivatized wax or fatty acid methyl ester products used a DB-5 capillary column. GC temperature was programmed from 140°C to 310°C for cutin and to 330°C for wax, at 5°C min^{-1}. Samples were injected in split mode (330°C injector temperature). Quantification was based on FID ion current using peak areas relative to internal standard peak areas. When necessary, compound identification was performed by GC-MS (EI mode) using an Agilent Technologies 6850 GC, equipped with an HP-5 MS column connected to an Agilent 5975 mass spectrometer. Helium was used as carrier gas at 2 ml min^{-1} and oven temperature was programmed from 120°C to 340°C at 10°C min^{-1}. Split-less injection was used and ions were collected in scan mode (40-800 atomic mass units) with peaks quantified on the basis of their total ion current.

Imaging of cuticular lipids and scanning electron microscopy

Cryosections of fruit pericarp, 8µm thick, were generated using a Microm HM550 cryostat (Thermo scientific, http://www.thermoscientific.com) and stored at -20°C. Sections were stained using Sudan IV, 0.1% w/v in isopropyl alcohol. Bright field images were collected using an Olympus IX81 inverted microscope (Olympus, www.olympus.com) configured with UPlan SApo 20X objective, NA0.75. The images were captured using an Olympus DP72 color camera and analyzed with DP2-BSW software. For imaging of fruit cuticles by scanning electron microscopy, fruits were hand-sectioned and fixed for 30 min in 4% glutaraldehyde followed by 30 min incubation in 0.1 M phosphate buffer (pH 7.4). Further processing of samples and imaging are according to (Li et al., 2007). The same procedures were followed for collecting leaf stomatal images.

Imaging anthocyanin distribution

Images of hand-cut cross sections of stem tissue were collected using an Olympus FluoView FV1000 Confocal Laser Scanning Microscope (Olympus) configured on IX81 inverted microscope with a 10X UPLSAPO objective, NA0.4. An excitation wavelength of 559 nm was generated using solid state laser, while the fluorescence emission was collected using a 570 to 640 nm band pass filter, to eliminate the detection of chlorophyll fluorescence. The DIC transmitted laser light image was collected using the 559 nm laser line and the images presented as overlays of confocal and DIC images.

Determination of stomatal and trichome densities

For stomatal density measurements, leaf surface imprints on abaxial sides of the leaf surface were taken using transparent nail polish and placed onto microscope slides. Imaging was

performed using a Zeiss Axiophot microscope (Carl *Zeiss*, Inc., http://www.zeiss.com) at 20X, image processing was accomplished using Image-pro plus image analysis software (Media Cybernetics, http://www.mediacy.com). Stomatal density was expressed as number of stomata in five different fields of 0.55 mm^2 per leaflet of five individual leaflets. Trichome density was analyzed on three week-old plants of AC, M82, *pe* and *cd2* using plant growth conditions and methods previously described (Kang et al., 2010).

Analysis of volatile terpenes from tomato trichomes

Volatile terpene levels were determined in three-week old plants. Briefly, a leaflet from the second newly emerging leaf was dipped in 1 ml of methyl *tert*-butyl ether containing 5 ng/μl of tetradecane as an internal standard, and allowed to rock for 1 min. GC-MS analysis was performed as previously described (Schilmiller et al., 2009). Terpene identification was based on comparison of mass spectra and retention times with those available in an essential oil library (Adams, 2009).

Determination of fruit glossiness

The glossiness of red-ripe fruits was measured using a custom made gonioreflectometer consisting of a Fire-iTM digital camera (http://www.unibrain.com) and two 60 W incandescent light bulbs located in a light impervious container. Thirty images were taken for each fruit, as it rotated 360°. The average number of saturated blue pixels for all the images was recorded as an index of fruit gloss measured in gloss units (A gloss unit is defined as number of pixels above the saturation threshold which is fixed based on specular reflectance of the sample image) programmed using MATLAB (MathWorks®, www.mathworks.com). The instrument was calibrated using standard glossy and non-glossy green and red spheres prior to data collection.

Mechanical analysis of the fruit cuticle

Young's elastic modulus (Y) of isolated tomato cuticles of 3 cm X 0.5 cm dimension was measured using a dynamic mechanical analyzer (DMA) Q800 (TA Instruments http://www.tainstruments.com) in constant stress ramp mode at room temperature until breakage was observed. Y values were calculated using Universal Analysis 2000 software (TA Instruments).

Determination of anthocyanin and chlorophyll content

Anthocyanins were extracted from leaves according to (Peters et al., 1998). The absorbance (A_{535}) of the aqueous phase was determined spectrophotometrically using a Hitachi U3000 spectrophotometer (Hitachi High Technologies America, Inc, http://www.hitachi-hta.com). Chlorophyll content was sampled from 3 leaf discs. Discs were incubated in darkness for 48 h at 4°C in 100% DMSO. A_{647} and A_{664} were determined spectrophotometrically as described above. Chlorophyll *a* and *b* were calculated according to (Moran, 1982).

Determination of leaf epidermal permeability

Leaf water conductance was measured using Li-Cor 6400 (Li-Cor). Plants were dark acclimated for 3 h prior to measurements being made to eliminate the effect of stomatal conductance. Chlorophyll leaching assays were performed on fully expanded leaves. The amount of chlorophyll extracted into the solution was quantified every 30 minutes as described above and data was expressed as a percentage of the total chlorophyll extracted after 24 h according to (Kosma et al., 2009).

Lignin analysis

Lignin was extracted as previously described (Foster et al., 2010). Results are reported as % acetyl bromide soluble lignin (ABSL) based on the dry weight of the alcohol insoluble residue according to (York et al., 1986; Fukushima et al., 1991; Robinson and Mansfield, 2009). For the calculation of % ABSL content of tomato, the molar extinction coefficient for Arabidopsis (23.35 $g^{-1}l\ cm^{-1}$) was used as an estimate given that no tomato-specific coefficients were available at the time of analysis (Chang et al., 2008).

Genetic mapping

An inter-specific F_2 population of 114 individuals derived from a cross between *S. lycopersicum* (*pe/pe*) (LA2467) and *S. pimpinellifolium* (*PE/PE*) (LA1589), was phenotyped for paleness of the vegetative tissues and stickiness of the fruit peel and simultaneously genotyped with chromosome 1 molecular markers, previously selected to be polymorphic between LA2467 and LA1589 (Table 2.6). Genomic DNA was extracted from expanding leaves as previously described (Barry et al., 2005). Details of genetic maps and molecular markers can be accessed through the Sol Genomics Network (http://solgenomics.net).

Cloning of *CD2* and phylogenetic analysis

Total RNA was extracted from expanding leaves of AC and *pe* using the RNeasy Mini Kit (Qiagen, http://www.qiagen.com). 1µg of RNA was used as a template for oligo dT primed first strand cDNA synthesis using the Transcriptor First Strand cDNA synthesis kit (Roche Applied Science, https://www.roche-applied-science.com). The coding region of *CD2* was amplified from cDNA using *Pfu* Ultra DNA polymerase (Agilent technologies, http://www.home.agilent.com) using the primers CD2-F and CD2-R (Table 2.7). PCR fragments

were purified using the PureLink PCR purification kit (Invitrogen, http://www.invitrogen.com) and cloned into the pCR™4Blunt-TOPO® vector (Invitrogen). Sequencing of inserts was accomplished using vector primers and the gene-specific primers CD1 through CD6 (Table 2.7). Sequences were assembled using Sequencher 4.7 software (Gene Codes Corporation, http://genecodes.com). A neighbor-joining phylogenetic tree was constructed from a multiple sequence alignment of the deduced full-length amino acid sequences of selected *CD2* homologs using MEGA V5.0 software (Table 2.8) (Tamura et al., 2011).

Construct assembly and silencing of *CD2*

Two constructs, CD2V1 and CD2V2, were assembled in the TRV2-LIC vector as previously described (Dong et al., 2007) using the primers CD2V1-F, CD2V1-R, CD2V2-F and CD2V2-R (Table 2.7). VIGS experiments were performed as described by (Velasquez et al., 2009). Tomato cotyledons were infiltrated with *Agrobacterium tumefaciens* strain GV3101 cultures before the appearance of the first true leaves and tissues were harvested four weeks after infiltration. TRV2-LIC empty vector plants were used as controls and *TRV2::PHYTOENE DESATURASE* plants were used to monitor the progression of gene silencing. The VIGS plants were maintained in a growth chamber under a 16 h photoperiod (145 µmol m^{-2} s^{-1}) at a constant temperature of 27°C and a relative humidity of 60%.

qRT-PCR analysis

For *CD2* expression analysis stems were divided into stem peel, stem core (stem devoid of peel) and whole stem. Total RNA was isolated as described above. RNA was treated on column with DNase (Qiagen) and 1µg of RNA was used for reverse transcription using SuperScript™ III First-Strand Synthesis System (Invitrogen). Gene-specific primers for the

analyzed genes were designed by Primer Express 3.0 (ABI); (listed in Table 2.7). The PCR reactions were performed with FAST SYBR Master Mix, 2X (ABI, http://www.appliedbiosystems.com) in a 25 μL volume using an Applied Biosystems StepOnePlus™ Real-Time PCR System (ABI) with the following cycling program: 10 min at 95°C, 15 s at 95°C followed by 40 cycles of 1 min at 60°C, 15 s at 95°C, 1 min at 60°C. The comparative ΔΔCT method was performed according to (Balaji et al., 2008).

Statistical analyses

Statistical analyses were performed using SAS (SAS Institute, www.sas.com). The genotypic constituents were evaluated by Student's *t-test* and LS Means.

Acknowledgements

We thank Carol Flegler, and Drs. Melinda Frame and Alicia Pastor (Centre for Advanced Microscopy, Michigan State University) for assistance with microscopy. We are grateful to Dr. Renfu Lu (Department of Biosystems and Agricultural Engineering, Michigan State University) for help with glossiness measurements; Clifton Foster and the Analytical Cell Wall Facility (Great Lakes Bio-Energy Research Center, Michigan State University) for lignin analysis; Dr. Michael Rich (Composite Materials and Structure Center, College of Engineering, Michigan State University) for guidance with dynamic mechanical analyzer experiments; and Dr. Eliana Gonzales-Vigil (Department of Horticulture, Michigan State University) for help with analysis of trichome chemistry. We also thank Dr. Jocelyn Rose (Cornell University) and Dr. Taku Takahashi (Okayama University) for providing seeds of the *cd2* allele and *anl2* mutant, respectively.

Table 2.6. PCR based genetic markers flanking the *pe* locus

Marker		Primers	Restriction enzyme
C2_At5g13700	For	5'-TCATTCTTCATGATTTTGAAATGGC- 3'	*Hha*I
	Rev	5'- AGTCGACTGTCCATAATTTTACCCTC-3'	
C2_At4g00090	For	5'- AGATATTGGCCACCACTCATGGTTC-3'	*Rsa*I
	Rev	5'- AGGCGACCATGCCATGTCCG-3'	
cTOA-13-J3	For	5'- AGTGATGTCGAGGGTCCTCTGAAAAC -3'	*Rsa*I
	Rev	5'- GTACAAATAGGCCTATCAACAACA -3'	
U151020	For	5'- GTAATGAAGAATCTGGCTCTGCAA -3'	*Dde*I
	Rev	5'-GTCCAATTTAATTTCACTCGATGA -3'	
C2_At2g38730	For	5'- AGCGGACCAAACACTAATGGATG-3'	*Alu*I
	Rev	5'- AGCCACATTCTCAATCTTCCTGAC-3'	
C2_At1g56345	For	5'- TCGGTGGCAACCACAGATTACCCAG-3'	*Msp*I
	Rev	5'- ATCGAGTCTATTAGCTAAATGAAGCTC-3'	
C2_At5g49880	For	5'-TCGGCTCCGTTGCCGGAATC-3'	*Rsa*I
	Rev	5'- ACTGCTTAAGGCATCAAAAAACTC-3'	

Restriction enzyme used to resolve polymorphisms between *S. lycopersicum* LA2467 (*pe/pe*) and *S. pimpinellifolium* LA1589 (*PE/PE*).

Table 2.7. Oligonucleotide primers used in the study

Gene	Primer	Sequence	Use
CD2	CD2-F	5'-GATACAGTGAATCTGTCAAATATAC-3	C&S
#GQ222185	CD2-R	5'-TTAGCTTTCGCATTGAAGTGCAGCT-3	C&S
	CD2-SEQ1	5'-GATCGAGTTTGTGCACTTGCTGGC -3	C&S
	CD2-SEQ2	5'-ATCAAGTGGTATGGGTGGAACCA-3	C&S
	CD2-SEQ3	5'-TGGTGCACCAGAAGTTTCACGGA-3	C&S
	CD2-SEQ4	5'- GCCAGTGTGAGTGTCTTGCAATTC-3	C&S
	CD2-SEQ5	5'-TGTTGTTGGTACATTACTCATACC-3	C&S
	CD2-SEQ6	5'-GCAAATCCAAGAACTTGAATCTC-3	C&S
	CD2-SEQ7	5'-GTTGAAGCACAAACACCAGCACA-3	C&S
	CD2V1-F	5'-CGACGACAAGACCCTGCAAGAGAATGATAAGCTTCGTGC-3	VIGS
	CD2V1-R	5'-GAGGAGAAGAGCCCTGCAGCCAAAGCAAGTTCAAGATAC-3	VIGS
	CD2V2-F	5'-CGACGACAAGACCCTGTCATCCACCGTGTCTGCCAGGGA -3	VIGS
	CD2V2-R	5'-GAGGAGAAGAGCCCTGGAATATCAACTGGCGCGTATACA-3	VIGS
	CD2Q-F	5'-TGGGTGGAACCAGAAATGGT-3	qRT-PCR
	CD2Q-R	5'-TGGTGAAAGCACTTGGAGTTCA-3	qRT-PCR
GAPDH	GAPDHQ-F	5'-ATGCTCCCATGTTTGTTGTGGGTG-3	qRT-PCR
#U97257	GAPDHQ-R	5'-TTAGCCAAAGGTGCAAGGCAGTTC-3	qRT-PCR
(Balaji et al., 2008)			

Cloning & Sequencing – C&S; VIGS constructs – VIGS

Balaji, V., Mayrose, M., Sherf, O., Jacob-Hirsch, J., Eichenlaub, R., Iraki, N., Manulis-Sasson, S., Rechavi, G., Barash, I. and Sessa, G. (2008) Tomato transcriptional changes in response to *Clavibacter michiganensis subsp. michiganensis* reveal a role for ethylene in disease development. *Plant Physiol.*, 146, 1797-1809.

Table 2.8. Homologs of CD2 utilized in phylogenetic analysis

Species name	Protein	Gene Identifier #	Source
Arabidopsis thaliana	HDG7	AT5G52170	http://www.arabidopsis.org/
	HDG1	AT3G61150	
	ANL2	AT4G00730	
Solanum lycopersicum	CD2	GQ222185	http://solgenomics.net/
Solanum phureja	CD2		
Oryza sativa	ROC6	LOC Os09g35760	http://rice.plantbiology.msu.edu/
		LOC Os04g48070	
		LOC Os02g45250	
Zea mays	OCL1	GRMZM2G026643	http://www.gramene.org/
	OCL3	GRMZM2G116658	
Sorghum bicolor		Sb03g008090 Sb06g025750	http://www.gramene.org/
		Sb02g030470	
Glycine max		Glyma07g08340	http://www.phytozome.net/
		Glyma03g01860	
		Glyma09g40130	
		Glyma18g45970	
Medicago truncatula		Medtr7g083690	http://www.phytozome.net/
Vitis vinifera		XP002272264	http://www.phytozome.net/
Populus trichocarpa		POPTR 0002s15610	http://www.phytozome.net/
		POPTR 0014s07130	
Ricinus communis		RC30174.t000366	http://www.phytozome.net/
Manihot esculenta		cassava4.1 001772m.g	http://www.phytozome.net/
		cassava4.1 001764m.g	
Malus domestica		HM122582	http://www.ncbi.nlm.nih.gov/

REFERENCES

REFERENCES

Abe M, Katsumata H, Komeda Y, Takahashi T (2003) Regulation of shoot epidermal cell differentiation by a pair of homeodomain proteins in Arabidopsis. Development **130:** 635-643

Adams RP (2009) Identification of Essential Oil Components by Gas Chromatography/Mass Spectrometry, Ed 4th. Allured books, Carik Stream

Aharoni A, Dixit S, Jetter R, Thoenes E, van Arkel G, Pereira A (2004) The SHINE clade of AP2 domain transcription factors activates wax biosynthesis, alters cuticle properties, and confers drought tolerance when overexpressed in Arabidopsis. Plant Cell **16:** 2463-2480

Balaji V, Mayrose M, Sherf O, Jacob-Hirsch J, Eichenlaub R, Iraki N, Manulis-Sasson S, Rechavi G, Barash I, Sessa G (2008) Tomato transcriptional changes in response to *Clavibacter michiganensis* subsp. *michiganensis* reveal a role for ethylene in disease development. Plant Physiol. **146:** 1797-1809

Bargel H, Koch K, Cerman Z, Neinhuis C (2006) Structure-function relationships of the plant cuticle and cuticular waxes - a smart material? Funct. Plant Biol. **33:** 893-910

Bargel H, Neinhuis C (2005) Tomato (*Lycopersicon esculentum* Mill.) fruit growth and ripening as related to the biomechanical properties of fruit skin and isolated cuticle. J. Exp. Bot. **56:** 1049-1060

Barry CS, McQuinn RP, Thompson AJ, Seymour GB, Grierson D, Giovannoni JJ (2005) Ethylene insensitivity conferred by the *Green-ripe* and *Never-ripe 2* ripening mutants of tomato. Plant Physiol. **138:** 267-275

Beggs CJ, Kuhn K, Bocker R, Wellmann E (1987) Phytochrome-induced flavonoid biosynthesis in mustard (*Sinapis alba L.*) cotyledons. Enzymic control and differential regulation of anthocyanin and quercetin formation. Planta **172:** 121-126

Bourdenx B, Bernard A, Domergue F, Pascal S, Leger A, Roby D, Pervent M, Vile D, Haslam RP, Napier JA, Lessire R, Joubes J (2011) Overexpression of Arabidopsis *ECERIFERUM1* promotes wax very-long-chain alkane biosynthesis and influences plant response to biotic and abiotic stresses. Plant Physiol. **156:** 29-45

Brewer MT, Lang LX, Fujimura K, Dujmovic N, Gray S, van der Knaap E (2006) Development of a controlled vocabulary and software application to analyze fruit shape variation in tomato and other plant species. Plant Physiol. **141:** 15-25

Brown DE, Rashotte AM, Murphy AS, Normanly J, Tague BW, Peer WA, Taiz L, Muday GK (2001) Flavonoids act as negative regulators of auxin transport in vivo in Arabidopsis. Plant Physiol. **126:** 524-535

Buschhaus C, Jetter R (2011) Composition differences between epicuticular and intracuticular wax substructures: How do plants seal their epidermal surfaces? J. Exp. Bot. **62:** 841-853

Butler L (1952) *Sticky peel (pe)* a new character in the seventh linkage group. Rep Tomato Genet Coop **2:** 2

Chang XF, Chandra R, Berleth T, Beatson RP (2008) Rapid, microscale, acetyl bromide-based method for high-throughput determination of lignin content in *Arabidopsis thaliana*. J. Agric. Food Chem. **56:** 6825-6834

Chen XB, Goodwin SM, Boroff VL, Liu XL, Jenks MA (2003) Cloning and characterization of the *WAX2* gene of Arabidopsis involved in cuticle membrane and wax production. Plant Cell **15:** 1170-1185

Christie PJ, Alfenito MR, Walbot V (1994) Impact of low-temperature stress on general phenylpropanoid and anthocyanin pathways: Enhancement of transcript abundance and anthocyanin pigmentation in maize seedlings. Planta **194:** 541-549

Cooper-Driver GA (2001) Biological roles for phenolic compounds in the evolution of early land plants. *In* PG Gensel, Edwards, D., ed, Plants Invade the Land: Evolution and Environmental Perspectives. Columbia Univ. Press, New York, pp 159–172

Darby L, Ritchie D, Taylor I (1978) Isogenic lines of the tomato "Ailsa Craig". *In* Annual Report Glasshouse Crops Research Institute, 1977, Littlehampton, UK, pp 168-184

Dong Y, Burch-Smith TM, Liu Y, Mamillapalli P, Dinesh-Kumar SP (2007) A ligation-independent cloning tobacco rattle virus vector for high-throughput virus-induced gene silencing identifies roles for *NbMADS4-1* and *-2* in floral development. Plant Physiol. **145:** 1161-1170

Edwards D, Abbott GD, Raven JA (1996) Cuticles of early land plants: a palaeoecophysiological evaluation. *In* G Kerstiens, ed, Plant cuticles: an integrated functional approach. Oxford: Bios Scientific Publishers, pp 1-32

Emmons CLW, Scott JW (1997) Environmental and physiological effects on cuticle cracking in tomato. J. Am. Soc. Hortic. Sci. **122:** 797-801

Emmons CLW, Scott JW (1998) Ultrastructural and anatomical factors associated with resistance to cuticle cracking in tomato (*Lycopersicon esculentum* Mill.). Int. J. Plant Sci. **159:** 14-22

Foster CE, Martin TM, Pauly M (2010) Comprehensive compositional analysis of plant cell walls (lignocellulosic biomass) part I: Lignin. J Vis Exp**:** e1745

Fuglevand G, Jackson JA, Jenkins GI (1996) UV-B, UV-A, and blue light signal transduction pathways interact synergistically to regulate chalcone synthase gene expression in Arabidopsis. Plant Cell **8:** 2347-2357

Fukushima RS, Dehority BA, Loerch SC (1991) Modification of a colorimetric analysis for lignin and its use in studying the inhibitory effects of lignin on forage digestion by ruminal microorganisms. J. Anim Sci. **69:** 295-304

Gallego-Giraldo L, Escamilla-Trevino L, Jackson LA, Dixon RA (2011) Salicylic acid mediates the reduced growth of lignin down-regulated plants. Proc. Natl. Acad. Sci. U. S. A. **108:** 20814-20819

Glover BJ (2000) Differentiation in plant epidermal cells. J. Exp. Bot. **51:** 497-505

Gray JE, Holroyd GH, van der Lee FM, Bahrami AR, Sijmons PC, Woodward FI, Schuch W, Heterington AM (2000) The HIC signalling pathway links CO2 perception to stomatal development. Nature **408:** 713-716

Grncarevic M, Radler F (1967) The effect of wax components on cuticular transpiration-model experiments. Planta **75:** 23-27

Hahlbrock K, Scheel D (1989) Physiology and molecular biology of phenylpropanoid metabolism. Annu. Rev. Plant Physiol. Plant Mol. Biol. **40:** 347-369

Hichri I, Barrieu F, Bogs J, Kappel C, Delrot S, Lauvergeat V (2011) Recent advances in the transcriptional regulation of the flavonoid biosynthetic pathway. J. Exp. Bot. **62:** 2465-2483

Hovav R, Chehanovsky N, Moy M, Jetter R, Schaffer AA (2007) The identification of a gene (*Cwp1*), silenced during *Solanum* evolution, which causes cuticle microfissuring and dehydration when expressed in tomato fruit. Plant J. **52:** 627-639

Ingram G (2008) Epidermal signalling and the control of plant shoot growth
In L Bogre, G Beemster, eds, Plant growth signaling, Vol 10. Springer Berlin / Heidelberg, pp 127-153

Ingram GC, Boisnard-Lorig C, Dumas C, Rogowsky PM (2000) Expression patterns of genes encoding HD-ZipIV homeo domain proteins define specific domains in maize embryos and meristems. Plant J. **22:** 401-414

Ingram GC, Magnard JL, Vergne P, Dumas C, Rogowsky PM (1999) *ZmOCL1*, an *HDGL2* family homeobox gene, is expressed in the outer cell layer throughout maize development. Plant Mol. Biol. **40:** 343-354

Isaacson T, Kosma DK, Matas AJ, Buda GJ, He YH, Yu BW, Pravitasari A, Batteas JD, Stark RE, Jenks MA, Rose JKC (2009) Cutin deficiency in the tomato fruit cuticle consistently affects resistance to microbial infection and biomechanical properties, but not transpirational water loss. Plant J. **60:** 363-377

Javelle M, Klein-Cosson C, Vernoud V, Boltz V, Maher C, Timmermans M, Depege-Fargeix N, Rogowsky PM (2011) Genome-wide characterization of the HD-ZIP IV transcription factor family in maize: preferential expression in the epidermis. Plant Physiol. **157:** 790-803

Javelle M, Vernoud V, Depege-Fargeix N, Arnould C, Oursel D, Domergue F, Sarda X, Rogowsky PM (2010) Overexpression of the epidermis-specific homeodomain-leucine zipper IV transcription factor OUTER CELL LAYER1 in maize identifies target genes involved in lipid metabolism and cuticle biosynthesis. Plant Physiol. **154:** 273-286

Javelle M, Vernoud V, Rogowsky PM, Ingram GC (2011) Epidermis: the formation and functions of a fundamental plant tissue. New Phytol. **189:** 17-39

Kang JH, Shi F, Jones AD, Marks MD, Howe GA (2010) Distortion of trichome morphology by the hairless mutation of tomato affects leaf surface chemistry. J. Exp. Bot. **61:** 1053-1064

Kolattukudy PE (1980) Bio-polyester membranes of plants - cutin and suberin. Science **208:** 990-1000

Kosma DK, Bourdenx B, Bernard A, Parsons EP, Lu S, Joubes J, Jenks MA (2009) The impact of water deficiency on leaf cuticle lipids of Arabidopsis. Plant Physiol. **151:** 1918-1929

Kubo H, Kishi M, Goto K (2008) Expression analysis of *ANTHOCYANINLESS2* gene in Arabidopsis. Plant Science **175:** 853-857

Kubo H, Peeters A, Aarts M, Pereira A, Koornneef M (1999) *ANTHOCYANINLESS2*, a homeobox gene affecting anthocyanin distribution and root development in Arabidopsis. Plant Cell **11:** 1217 - 1226

Kurata T, Kawabata-Awai C, Sakuradani E, Shimizu S, Okada K, Wada T (2003) The YORE-YORE gene regulates multiple aspects of epidermal cell differentiation in Arabidopsis. Plant J. **36:** 55-66

Landry LG, Chapple CC, Last RL (1995) Arabidopsis mutants lacking phenolic sunscreens exhibit enhanced ultraviolet-B injury and oxidative damage. Plant Physiol **109:** 1159-1166

Leide J, Hildebrandt U, Reussing K, Riederer M, Vogg G (2007) The developmental pattern of tomato fruit wax accumulation and its impact on cuticular transpiration barrier properties: Effects of a deficiency in a *beta-ketoacyl-coenzyme A synthase (LeCER6)*. Plant Physiol. **144:** 1667-1679

Li-Beisson Y, Pollard M, Sauveplane V, Pinot F, Ohlrogge J, Beisson F (2009) Nanoridges that characterize the surface morphology of flowers require the synthesis of cutin polyester. Proc. Natl. Acad. Sci. U. S. A. **106:** 22008-22013

Li-Beisson Y, Shorrosh B, Beisson F, Andersson MX, Arondel V, Bates PD, Baud Sb, Bird D, DeBono A, Durrett TP, Franke RB, Graham IA, Katayama K, Kelly A, Larson T, Markham JE, Miquel M, Molina I, Nishida I, Rowland O, Samuels L, Schmid KM, Wada H, Welti R, Xu C, Zallot R, Ohlrogge J (2010) Acyl-lipid metabolism. *In* R Last, MD Rockville, eds, The Arabidopsis Book, Vol 8. The American Society of Plant Biologists, pp 1-65

Li H, Pinot F, Sauveplane V, Werck-Reichhart D, Diehl P, Schreiber L, Franke R, Zhang P, Chen L, Gao YW, Liang WQ, Zhang DB (2010) Cytochrome P450 family member *CYP704B2* catalyzes the omega-hydroxylation of fatty acids and is required for anther cutin biosynthesis and pollen exine formation in rice. Plant Cell **22:** 173-190

Li JY, Oulee TM, Raba R, Amundson RG, Last RL (1993) Arabidopsis flavonoid mutants are hypersensitive to UV-B irradiations. Plant Cell **5:** 171-179

Li X, Bonawitz ND, Weng J-K, Chapple C (2010) The growth reduction associated with repressed lignin biosynthesis in *Arabidopsis thaliana* is independent of flavonoids. Plant Cell **22:** 1620-1632

Li YH, Beisson F, Koo AJK, Molina I, Pollard M, Ohlrogge J (2007) Identification of acyltransferases required for cutin biosynthesis and production of cutin with suberin-like monomers. Proc. Natl. Acad. Sci. U. S. A. **104:** 18339-18344

Lu P, Porat R, Nadeau JA, O'Neill SD (1996) Identification of a meristem L1 layer-specific gene in Arabidopsis that is expressed during embryonic pattern formation and defines a new class of homeobox genes. Plant Cell **8:** 2155-2168

Martin C, Gerats T (1993) Control of pigment biosynthesis genes during petal development. Plant Cell **5:** 1253-1264

Matas AJ, Cobb ED, Bartsch JA, Paolillo DJ, Niklas KJ (2004) Biomechanics and anatomy of *Lycopersicon esculentum* fruit peels and enzyme-treated samples. Am. J. Bot. **91:** 352-360

Matas AJ, Yeats TH, Buda GJ, Zheng Y, Chatterjee S, Tohge T, Ponnala L, Adato A, Aharoni A, Stark R, Fernie AR, Fei Z, Giovannoni JJ, Rose JKC (2011) Tissue- and cell-type specific transcriptome profiling of expanding tomato fruit provides insights into metabolic and regulatory specialization and cuticle formation. Plant Cell **23:** 3893 - 3910

McFarlane HE, Shin JJH, Bird DA, Samuels AL (2010) Arabidopsis ABCG transporters, which are required for export of diverse cuticular lipids, dimerize in different combinations. Plant Cell **22:** 3066-3075

Mintz-Oron S, Mandel T, Rogachev I, Feldberg L, Lotan O, Yativ M, Wang Z, Jetter R, Venger I, Adato A, Aharoni A (2008) Gene expression and metabolism in tomato fruit surface tissues. Plant Physiol. **147:** 823-851

Molina I, Bonaventure G, Ohlrogge J, Pollard M (2006) The lipid polyester composition of *Arabidopsis thaliana* and *Brassica napus* seeds. Phytochemistry **67:** 2597-2610

Moran R (1982) Formulas for determination of chlorophyllous pigments extracted with *N, N*-Dimethylformamide. Plant Physiol. **69:** 1376-1381

Mukherjee K, Brocchieri L, Burglin TR (2009) A comprehensive classification and evolutionary analysis of plant homeobox genes. Mol. Biol. Evol. **26:** 2775-2794

Mutschler MA, Tanksley SD, Rick CM (1987) Linkage maps of the tomato. Rep Tomato Genet Coop **37:** 5-28

Nakamura M, Katsumata H, Abe M, Yabe N, Komeda Y, Yamamoto KT, Takahashi T (2006) Characterization of the class IV homeodomain-leucine zipper gene family in Arabidopsis. Plant Physiol. **141:** 1363-1375

Panikashvili D, Savaldi-Goldstein S, Mandel T, Yifhar T, Franke RB, Hofer R, Schreiber L, Chory J, Aharoni A (2007) The Arabidopsis *DESPERADO/AtWBC11* transporter is required for cutin and wax secretion. Plant Physiol. **145:** 1345-1360

Panikashvili D, Shi JX, Schreiber L, Aharoni A (2009) The Arabidopsis *DCR* encoding a soluble BAHD acyltransferase is required for cutin polyester formation and seed hydration properties. Plant Physiol. **151:** 1773-1789

Peters JL, Szell M, Kendrick RE (1998) The expression of light-regulated genes in the high-pigment-1 mutant of tomato. Plant Physiol. **117:** 797-807

Pollard M, Beisson F, Li YH, Ohlrogge JB (2008) Building lipid barriers: biosynthesis of cutin and suberin. Trends Plant Sci. **13:** 236-246

Ponting CP, Aravind L (1999) START: a lipid binding domain in StAR, HD-ZIP and signalling proteins. Trends Biochem. Sci. **24:** 130-132

Qin B-X, Tang D, Huang J, Li M, Wu X-R, Lu L-L, Wang K-J, Yu H-X, Chen J-M, Gu M-H, Cheng Z-K (2011) Rice *OsGL1-1* is involved in leaf cuticular wax and cuticle membrane. Mol. Plant. **6:** 985 - 995

Riederer M, Schreiber L (2001) Protecting against water loss: analysis of the barrier properties of plant cuticles. J. Exp. Bot. **52:** 2023-2032

Robinson AR, Mansfield SD (2009) Rapid analysis of poplar lignin monomer composition by a streamlined thioacidolysis procedure and near-infrared reflectance-based prediction modeling. Plant J. **58:** 706-714

Samuels L, Kunst L, Jetter R (2008) Sealing plant surfaces: Cuticular wax formation by epidermal cells. Annu. Rev. Plant Biol. **59:** 683-707

Schilmiller AL, Last RL, Pichersky E (2008) Harnessing plant trichome biochemistry for the production of useful compounds. Plant J. **54:** 702-711

Schilmiller AL, Schauvinhold I, Larson M, Xu R, Charbonneau AL, Schmidt A, Wilkerson C, Last RL, Pichersky E (2009) Monoterpenes in the glandular trichomes of tomato are synthesized from a neryl diphosphate precursor rather than geranyl diphosphate. Proc. Natl. Acad. Sci. U. S. A. **106:** 10865-10870

Schreiber L (2010) Transport barriers made of cutin, suberin and associated waxes. Trends Plant Sci. **15:** 546-553

Seo PJ, Lee SB, Suh MC, Park MJ, Go YS, Park CM (2011) The MYB96 transcription factor regulates cuticular wax biosynthesis under drought conditions in Arabidopsis. Plant Cell **23:** 1138-1152

Sieber P, Schorderet M, Ryser U, Buchala A, Kolattukudy P, Metraux J-P, Nawrath C (2000) Transgenic Arabidopsis plants expressing a fungal cutinase show alterations in the structure and properties of the cuticle and postgenital organ fusions. Plant Cell **12:** 721-737

Steyn WJ, Wand SJE, Holcroft DM, Jacobs G (2002) Anthocyanins in vegetative tissues: a proposed unified function in photoprotection. New Phytol. **155:** 349-361

Suh MC, Samuels AL, Jetter R, Kunst L, Pollard M, Ohlrogge J, Beisson F (2005) Cuticular lipid composition, surface structure, and gene expression in Arabidopsis stem epidermis. Plant Physiol. **139:** 1649-1665

Tamura K, Peterson D, Peterson N, Stecher G, Nei M, Kumar S (2011) MEGA5: Molecular evolutionary genetics analysis using maximum likelihood, evolutionary distance, and maximum parsimony methods. Mol. Biol. Evol. **28:** 2731-2739

Velasquez AC, Chakravarthy S, Martin GB (2009) Virus-induced gene silencing (VIGS) in *Nicotiana benthamiana* and tomato. J Vis Exp **10:** pii:1292

Vogg G, Fischer S, Leide J, Emmanuel E, Jetter R, Levy AA, Riederer M (2004) Tomato fruit cuticular waxes and their effects on transpiration barrier properties: functional characterization of a mutant deficient in a very-long-chain fatty acid beta-ketoacyl-CoA synthase. J. Exp. Bot. **55:** 1401-1410

Vogt T (2010) Phenylpropanoid biosynthesis. Mol. Plant. **3:** 2-20

Wang ZY, Xiong LM, Li WB, Zhu JK, Zhu JH (2011) The plant cuticle is required for osmotic stress regulation of abscisic acid biosynthesis and osmotic stress tolerance in Arabidopsis. Plant Cell **23:** 1971-1984

Wu R, Li S, He S, Waaymann F, Yu C, Qin G, Schreiber L, Qu L-J, Gu H (2011) CFL1, a WW domain protein, regulates cuticle development by modulating the function of *HDG1*, a Class IV Homeodomain transcription factor, in rice and Arabidopsis. Plant Cell **23:** 3392-3411

Yang J, Ordiz MI, Jaworski JG, Beachy RN (2011) Induced accumulation of cuticular waxes enhances drought tolerance in Arabidopsis by changes in development of stomata. Plant Physiology and Biochemistry **49:** 1448-1455

Yeats TH, Howe KJ, Matas AJ, Buda GJ, Thannhauser TW, Rose JKC (2010) Mining the surface proteome of tomato (*Solanum lycopersicum*) fruit for proteins associated with cuticle biogenesis. J. Exp. Bot. **61:** 3759-3771

York WS, Darvill AG, McNeil M, Stevenson TT, Albersheim P, Arthur Weissbach HW (1986) Isolation and characterization of plant cell walls and cell wall components. *In* Methods Enzymol., Vol 118. Academic Press, pp 3-40

CHAPTER III

KNOX genes influence a gradient of fruit chloroplast development through regulation of *GOLDEN2-LIKE* expression in tomato

Satya Swathi Nadakuduti, William L. Holdsworth[1], Chelsey L. Klein and Cornelius S. Barry[2]

(The Plant Journal *in press*)

Abstract

The chlorophyll content of unripe fleshy fruits positively correlates to nutrient content and flavor of ripe fruit. In tomato (*Solanum lycopersicum*) fruit, the *uniform ripening (u)* locus, which encodes a *GOLDEN 2-LIKE* transcription factor (*SlGLK2*), influences a gradient of chloroplast development that extends from the calyx end to the base of the fruit. With the exception of the *u* locus, the factors that influence the formation of this developmental gradient are unknown. In this study, characterization and positional cloning of the *uniform gray-green* (*ug*) locus of tomato reveals a hereto unknown role for the class I *KNOTTED1-LIKE HOMEOBOX* (*KNOX*) gene, *TKN4,* in specifying formation of this chloroplast gradient. The involvement of KNOX in fruit chloroplast development was confirmed through characterization of the *Curl* (*Cu*) mutant, a dominant gain-of-function mutation of *TKN2*, which displays ectopic fruit chloroplast development that resembles *SlGLK2* over-expression. *TKN2* and *TKN4* act upstream of *SlGLK2* and the related gene *ARABIDOPSIS PSEUDO RESPONSE REGULATOR 2-LIKE* (*SlAPRR2-LIKE*) to establish their latitudinal gradient of expression across developing fruit that leads to a gradient of chloroplast development. Class I *KNOX* genes typically influence plant morphology through maintenance of meristem activity but this study identifies a role for *TKN2* and *TKN4* in specifically influencing chloroplast development in fruit but not leaves, suggesting that this fundamental process is differentially regulated in these two organs.

Introduction

In plants, many biochemical pathways, including those associated with photosynthesis and synthesis of primary and specialized metabolites are located within the chloroplast. Leaves are typically the primary source of photosynthate although it is estimated that photosynthesis by fleshy fruits contributes up to 20% of the total fruit carbohydrate (Blanke and Lenz, 1989; Hetherington et al., 1998). Enhanced chloroplast development and chlorophyll content of unripe fruits increases their photosynthetic capacity leading to greater starch accumulation (Dinar and Stevens, 1981; Powell et al., 2012; Sagar et al., 2013). Furthermore, the starch content of unripe fruit is positively correlated with the sugar content in ripe fruit, which directly contributes to fruit quality by influencing nutritive value and taste (Davies and Hobson, 1981). Thus, chloroplast development and the carbohydrate status of unripe fruits impact the composition and quality of ripe fruit.

In tomato, several loci influence fruit chloroplast development and the subsequent quality of ripe fruit. Mutations at the *high-pigment 1* and *2* (*hp-1* and *hp-2*) loci, which encode negative regulators of photomorphogenesis, possess increased chloroplast number and plastid compartment size, leading to fruits with higher levels of chlorophyll and carotenoids (Mustilli et al., 1999; Cookson et al., 2003; Liu et al., 2004; Kolotilin et al., 2007; Rohrmann et al., 2011). Alteration of phytohormone biosynthesis and responses, including those associated with auxin, ABA, cytokinins and brassinosteroids (BRs), can also positively impact chloroplast development to influence ripe fruit quality (Martineau et al., 1994; Galpaz et al., 2008; Sagar et al., 2013; Liu et al., 2014). In contrast, mutation at the *uniform ripening* (*u*) locus negatively impacts fruit chloroplast development, due to loss of the green shoulder that surrounds the calyx end of developing fruit, leading to ripe fruits with reduced sugar content (Powell et al., 2012). Positional

cloning of *u* revealed a mutation in a tomato homolog of the *GOLDEN 2-LIKE* (GLK) transcription factor of maize, designated *SlGLK2* (Powell et al., 2012). *GLKs* are required for chloroplast development (Fitter et al., 2002; Waters et al., 2008) and *SlGLK2* is preferentially expressed in the shoulder of the fruit, where in *U/U* genotypes, it is involved in enhancing chloroplast development while ectopic expression of *SlGLK2* results in homogeneously dark-green fruit (Powell et al., 2012). Similarly, over-expression of *ARABIDOPSIS PSEUDO RESPONSE REGULATOR 2-LIKE* (*SlAPRR2-LIKE*) in tomato, which is related to *SlGLK2*, causes enhanced fruit chloroplast development (Pan et al., 2013). How these loci interact to jointly influence fruit chloroplast development is not fully understood although recent evidence suggests a role for both auxin and BRs in regulating *GLK* expression (Sagar et al., 2013; Liu et al., 2014). Furthermore, except for the involvement of *SlGLK2*, the factors that establish the latitudinal gradient of gene expression and chloroplast development in tomato fruit remain undefined.

Fruits of the *uniform gray-green* (*ug*) mutant of tomato are similar to *u* and lack the green shoulder surrounding the calyx (Bohn and Scott, 1945). In this study, positional cloning revealed that *UG* encodes *TKN4*, a class I KNOTTED1-LIKE HOMEOBOX (KNOX) transcription factor. *KNOX* genes typically influence plant morphology, and particularly leaf shape, through maintenance of stem cell populations within apical meristems (Hay and Tsiantis, 2010). However, this research identifies a previously undefined role for these homeobox proteins in fleshy fruit development, and in particular in the establishment of a gradient of chloroplast development through regulation of *SlGLK2* expression.

Results

Positional cloning of *ug* defines a role for *KNOX* in fruit chloroplast development

The *ug* mutant lacks the green shoulder surrounding the calyx end of developing fruit (Figure 3.1A). Chlorophyll levels are reduced in *ug* fruit pericarp (Figure 3.1B-E). Individual chloroplast development in *ug* fruit is also impaired with a reduction in size and thylakoids per granum (Figure 3.1F-K). The phenotypes of *ug* are similar to fruits with the *u* mutant allele (Powell et al., 2012) (Figure 3.1A-D, G and J). Genetic mapping assigned the *ug* locus to the long arm of chromosome 1, with tight linkage to the marker C2_At1g56345. Fine mapping refined the *ug* locus to a 14.6 kb interval between the markers *Solyc01g100500* and *Solyc01g100520* that spans nucleotides SL2.40chr1: 82268632-82283258 and contains the single gene, *Solyc01g100510*, which encodes the KNOX transcription factor, TKN4. Sequencing of *TKN4* from flower cDNA of *UG/UG* and *ug/ug* genotypes revealed a single T > A nucleotide change within exon 2 of *TKN4* corresponding to a phenylalanine to leucine substitution at residue 137 (Figure 3.2A). Phenylalanine 137 represents an invariant amino acid within the KNOX2 domain of diverse class I KNOX proteins (Figure 3.2B). The KNOX2 domain mediates protein-protein interactions between homeodomain proteins (Bellaoui et al., 2001; Smith et al., 2002). Genotyping of the SNP associated with the *ug* phenotype from LA4025 and Purple Prince, which lack the green shoulder and are purported to carry the *ug* mutation implied that the F137L substitution co-segregates with the mutant phenotype, indicating that the SNP is conserved in *ug/ug* genotypes (Figure 3.2C and Figure 3.3).

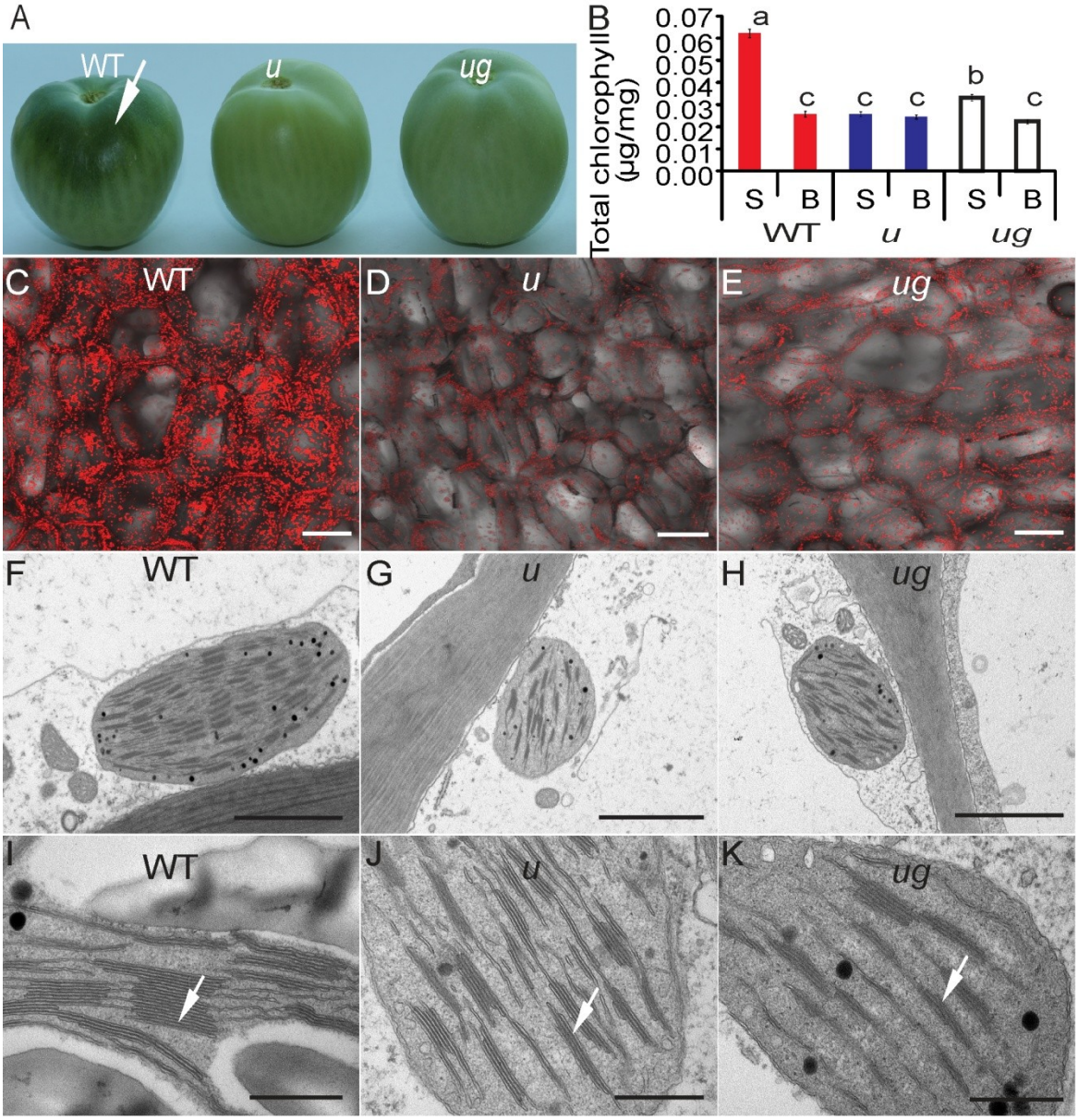

Figure 3.1. Fruit phenotype and chloroplast development in *ug*. A) Phenotypes of the *u* and *ug* mutants compared to Ailsa Craig wild type (WT). The arrow highlights the presence of the green shoulder in WT fruit. B) Chlorophyll content in the pericarp isolated from the shoulder (S) and base (B) of WT, *u,* and *ug* fruit at 28 days post-anthesis (dpa). Data are presented as the mean ± SEM of *n*=5 and means with different letters are significantly different (*LS Means, p < 0.05*). C-E) Confocal laser scanning microscopy images of WT, *u*, and *ug* fruit shoulder pericarp showing chlorophyll autofluorescence (Scale bar = 10 µm). F-K) TEM of 28 dpa fruit chloroplasts of WT, *u*, and *ug* (Scale bar for F-H = 2µm; I-K = 0.5µm).

Attempts failed to genotype the *ug* mutant allele in the LA0021 accession, which lacks a green shoulder but is reported to be a *ug* mutant (Figure 3.3). Similarly, amplification of *TKN4* from LA0021 flower cDNA was unsuccessful (Figure 3.2D). Subsequent amplification and sequencing of *TKN4* genomic fragments from LA0021 revealed the existence of a second mutant allele that contains a 2.4kb internal deletion spanning nucleotides SL2.40chr1: 82280365-82282785 of the tomato genome reference assembly (Figure 3.2E). Although mutations in Class I *KNOX* genes typically cause phenotypes associated with altered morphology, and particularly leaf shape (Parnis et al., 1997; Venglat et al., 2002; Hay and Tsiantis, 2010), the effect of *ug* is subtle and plants carrying the *ug* mutant allele are indistinguishable from wild-type (WT) except for the lack of the green shoulder in developing fruit.

No impact was observed on leaf shape or leaf chlorophyll in *ug* (Figure 3.4A-C). *TKN4* is expressed in flower pistils and mature green fruits but expression is low in leaves supporting the lack of an altered phenotype in leaves of the *ug* mutant (The Tomato Genome Consortium, 2012) (Figure 3.4D and E). As the *ug* and *u* fruit phenotypes are virtually identical (Figure 3.1A), germplasm lacking a green shoulder was also genotyped for the *u* mutant allele. While LA4025 is homozygous for both *u* and *ug* mutant alleles, LA3539, LA0021 and the Purple Prince cultivar possess the WT (*U/U*) allele (Figure 3.2C and Figure 3.3). These data indicate that the lack of a green shoulder in these accessions is the result of mutations in *TKN4* and not mutations at the *u* locus.

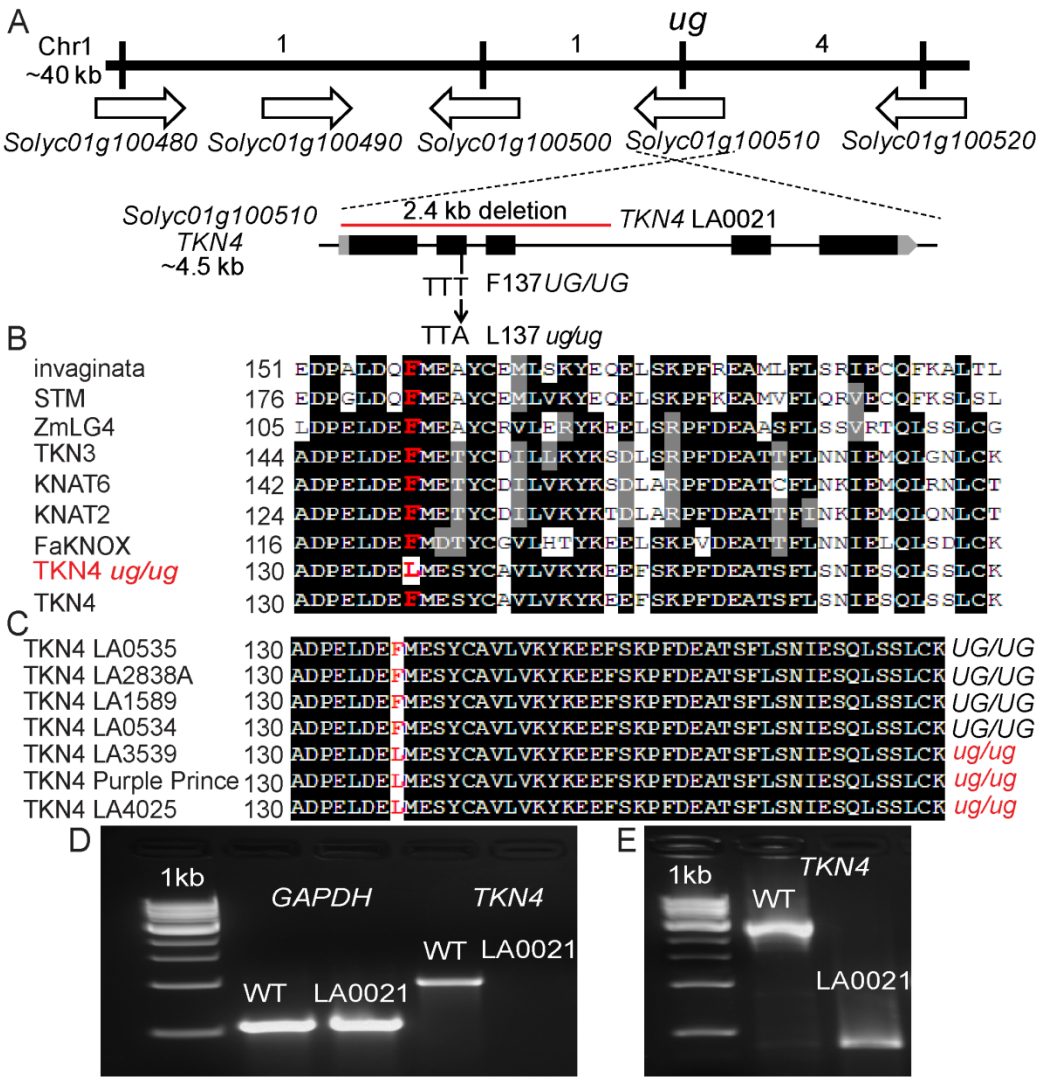

Figure 3.2. Genetic mapping of the *ug* locus. A) Genetic and physical map of the *ug* locus identifying a single candidate gene, *Solyc01g100510*, which encodes *TKN4*. Numbers of recombinant individuals between genetic markers are provided. Sequencing of *TKN4* from wild type (WT) (*UG/UG*) and mutant (*ug/ug*) plants identified a single nucleotide polymorphism that converts phenylalanine 137 to leucine. B) Alignment of the KNOX2 domain of phylogenetically distinct KNOX proteins. The invariant phenylalanine residue within this domain and its substitution to leucine in *ug/ug* are shown in red. C) Correlation of L137 with the *ug/ug* phenotype in selected accessions of tomato. D) RT-PCR amplification of *TKN4* from Ailsa Craig (WT) and LA0021 flower cDNA. E) *TKN4* amplification from WT and LA0021 genomic DNA highlighting 2.4kb deletion in LA0021. This deletion spans the first three exons of location of *TKN4* and is highlighted by the red bar in A).

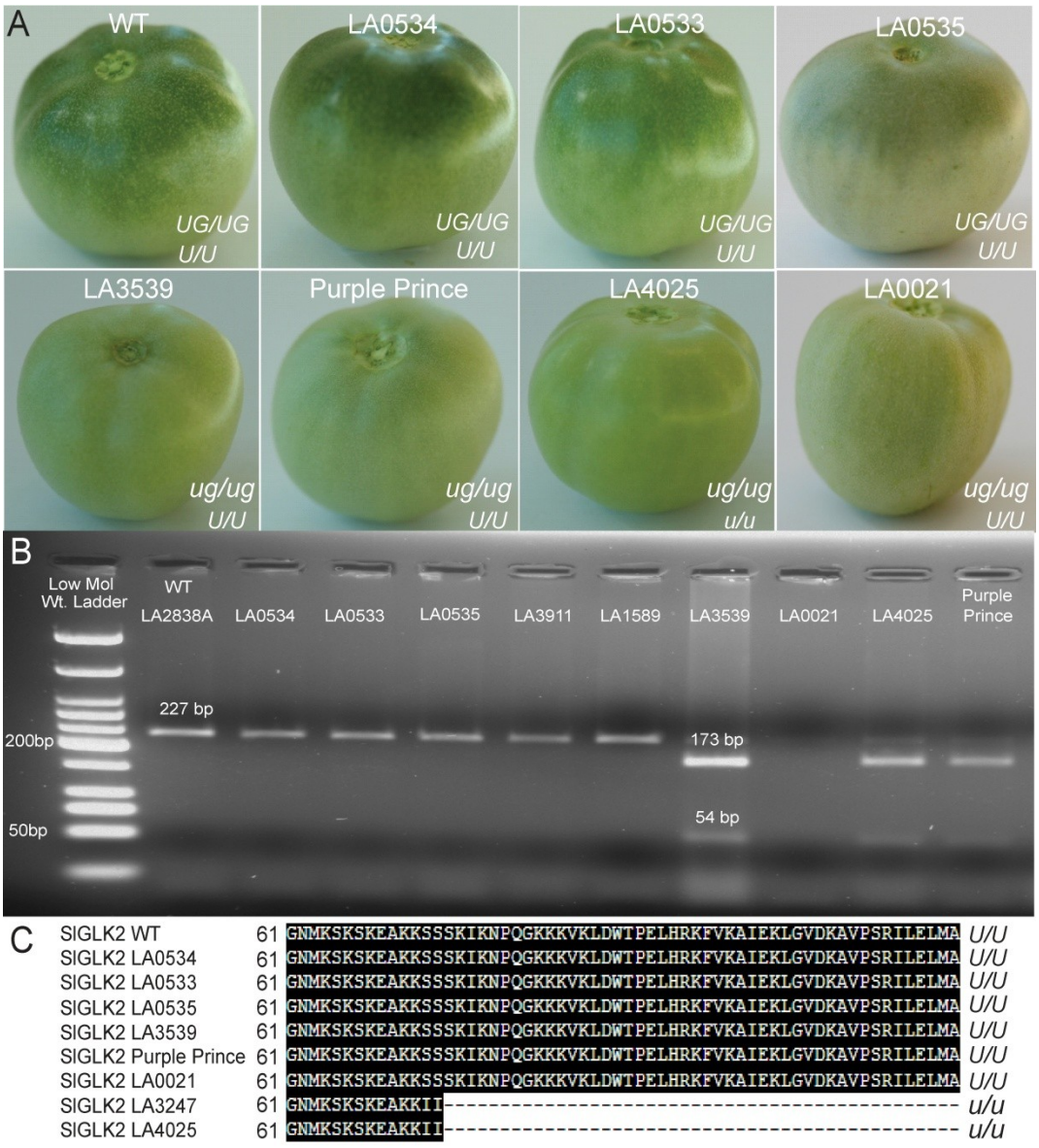

Figure 3.3. Genotyping of *TKN4* and *SlGLK2* in various tomato accessions. A) Fruit phenotypes of the tomato accessions compared to Ailsa Craig wild type (WT). Note the association of fruit shoulder with WT alleles of *UG* and *U*. Genotypes defined as *UG/UG* and *U/U* contain the wild type alleles and possess a dark green shoulder whereas genotypes defined as either *ug/ug* or *u/u* lack the shoulder. B) Genotyping tomato accessions using a cleaved amplified polymorphic sequence marker digested by *Mse*I. Genotypes defined as *UG/UG* show a single 227 bp band whereas *ug/ug* genotypes show two bands corresponding to 173 bp and 54 bp. No amplification was observed from accession LA0021. C) Single base insertion causes frameshift and a pre-mature stop codon, which results in truncation of SlGLK2 in *u/u* accessions.

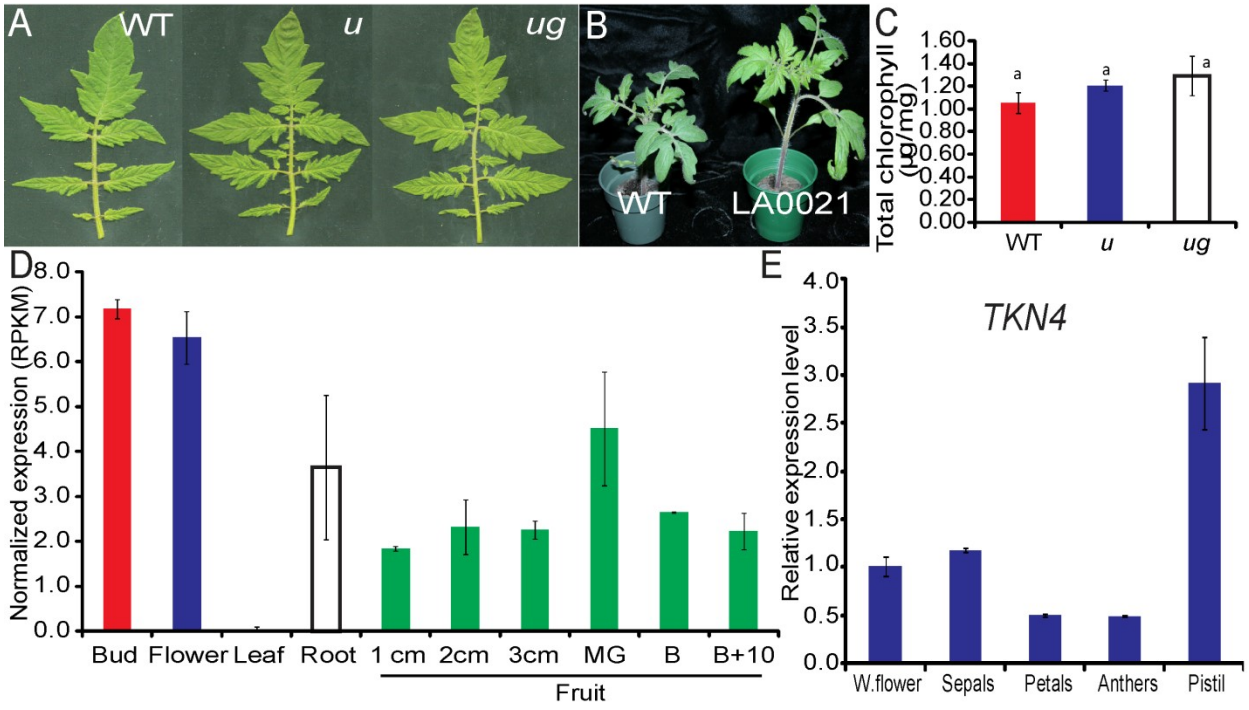

Figure 3.4. Leaf phenotypes and relative expression of *TKN4*. A) Leaf phenotypes of wild type (WT), *u,* and *ug*. B) Leaf phenotype of WT and LA0021 in four-week-old plants. C) Chlorophyll content in the leaf of WT, *u,* and *ug* ($n = 5$). D) Relative expression of *TKN4* in different plant organs (The Tomato Genome Consortium, 2012). E) Relative expression of *TKN4* in different organs of WT flowers. Means ± SEM with different letters are significantly different (*LS Means,* $p < 0.05$).

KNOX over-expression alters fruit development and positively impacts chlorophyll accumulation

Additional support for a role for *KNOX* genes in regulating fruit chloroplast development is evident from characterization of the *Curl* (*Cu*) mutant. *Cu* represents a dominant gain-of-function mutation resulting from ectopic expression of *TKN2*, leading to altered plant morphology (Parnis et al., 1997). Developing fruit of *Cu* possess elevated chlorophyll levels that extend across the entire surface of the fruit (Figure 3.5A-E). In addition to increased chloroplast number and higher chlorophyll content in *Cu* fruit, the size of the chloroplasts is larger than in WT and there is a general increase in the number of thylakoids per granum (Figure 3.5F-I). The phenotypes of *Cu* fruit are reminiscent of *SlGLK2* and *SlAPRR2-LIKE* over-expression lines (Powell et al., 2012; Pan et al., 2013). To assess the potential relationship between *Cu* and the *SlGLKs* and *SlAPRR2-LIKE*, the expression of these genes was examined in WT and *Cu* fruit pericarp. The expression of *TKN2*, *SlGLKs* and *SlAPRR2-LIKE* is elevated in *Cu* fruit (Figure 3.5J-M). However, *SlGLK1* expression, which is typically lower than *SlGLK2* expression in tomato fruit (Powell et al., 2012), was not statistically different between WT and *Cu.* These data suggest that *SlGLK2* and *SlAPRR2-LIKE* act downstream of KNOX activity to regulate fruit chloroplast development.

In support of this hypothesis, fruit of a double mutant constructed from a cross between *Cu* and *u* partially suppresses the *Cu* mutant phenotype (Figure 3.5N and O). *Cu* fruit are smaller in size (WT=37.61g ± 2.53g; *Cu*=17.24g ± 1.69g, *n*=8) with a thinner pericarp and smaller cell size that results in an increased density of cells per unit area (Figure 3.5D, 3P and Q). Congruent with the phenotype of the *ug* allele (Figure 3.4A-C), the *Cu* allele does not impact leaf chlorophyll content (Figure 3.6A) and while the expression of the *SlGLK*s remains unchanged, the expression of *SlAPRR2-LIKE* is slightly elevated in *Cu* leaves (Figure 3.6B-E).

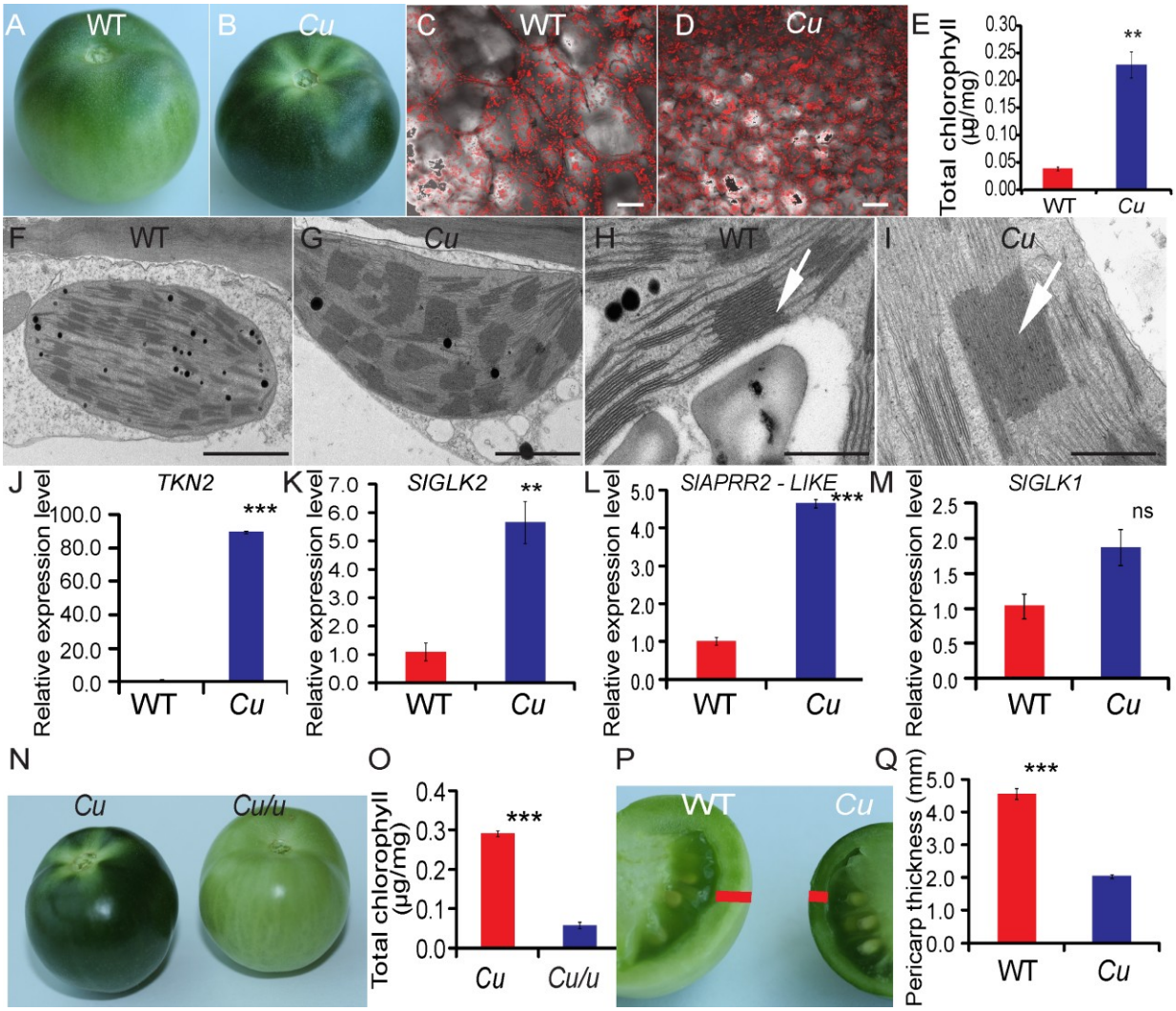

Figure 3.5. Enhanced chloroplast development in *Cu* fruit. A and B) Variation in fruit phenotype between Ailsa Craig wild type (WT) and *Cu* at 16 days post-anthesis (dpa). C and D) Confocal laser scanning microscopy images of WT and *Cu* fruit shoulder pericarp showing chlorophyll autofluorescence. (Scale bar = 10 µm). E) Chlorophyll content of WT and *Cu* fruit pericarp (*n*=5). F-I) TEM of 28 dpa fruit chloroplasts of WT and *Cu* (Scale bar for F and G = 2µm; H and I = 0.5µm). J-M) qRT-PCR analysis of gene expression in WT and *Cu* fruit pericarp. N) Fruit phenotype of *Cu* and *Cu*/*u*. O) Chlorophyll content of *Cu* and *Cu*/*u* fruit pericarp (*n=3*). (P and Q) Pericarp thickness of WT and *Cu* fruit (*n=6*). Data are presented as the mean ± SEM. Asterisks denote significant differences (***, $p < 0.001$; **, $p < 0.01$) as determined by Student's *t tests*. ns = not significant.

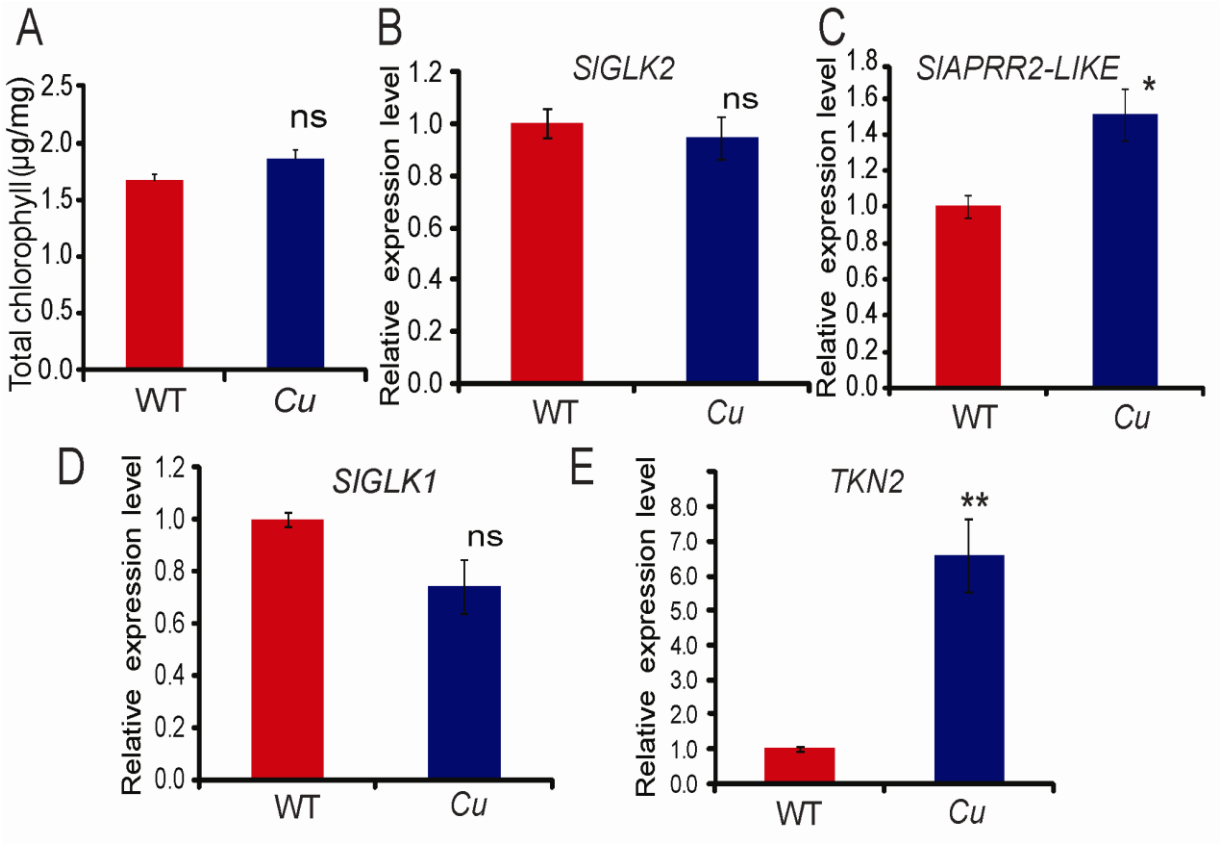

Figure 3.6. Chlorophyll and relative expression of genes in *Cu* leaf. A) Chlorophyll content of Ailsa Craig wild type (WT) and *Cu* leaves (*n=5*). B-E) Relative expression level of *SlGLK2*, *SlAPRR2-LIKE*, *SlGLK1* and *TKN2* in WT and *Cu* leaves (*n=3*). Data are presented as the mean ± SEM. Asterisks denote significant differences (**, $p < 0.01$; *, $p < 0.05$) as determined by Student's *t-tests*. ns = not significant.

KNOX loci establish gradients of *SlGLK2* expression that impact fruit chlorophyll accumulation

The presence of a green shoulder in immature tomato fruit highlights the existence of a latitudinal gradient of chloroplast development that correlates with the increased expression of *SlGLK2* at the calyx end of the fruit relative to the stylar end (Powell et al., 2012). To assess the role of *KNOX* genes in regulating the formation of this gene expression gradient and its associated differential pattern of chlorophyll accumulation, fruit pericarp was divided into whole, shoulder, middle and base, and the expression of *SlGLK2*, *SlAPRR2-LIKE*, *TKN2* and *TKN4* investigated (Figure 3.7A).

In WT fruit, chlorophyll levels are higher in the fruit shoulder when compared to the middle and the base of the fruit (Figure 3.7B), and the expression of each gene matches the gradient in chlorophyll accumulation with higher transcript levels observed in the shoulder compared to the middle and the base, although this pattern is more pronounced for *SlGLK2*, *TKN2* and *TKN4* (Figure 3.7C-F and Figure 3.8). The *Cu* and *ug* mutations disrupt both the chlorophyll gradient (Figure 3.7B) and expression gradient that is present in WT fruit. For example, the expression level of *SlGLK2* is positively impacted by *Cu* and negatively by *ug*, and the typical gradient of expression is disrupted (Figure 3.7C). In contrast, the *ug* locus does not impact the expression of *SlAPRR2-LIKE* and while the expression of this gene is elevated in *Cu*, the expression gradient is not disrupted (Figure 3.7D). Together, these data not only support the role of *KNOX* genes in regulating both chloroplast development and gene expression gradients but also highlights that while *SlGLK2* and *SlAPRR2-LIKE* both positively impact fruit chloroplast development (Powell et al., 2012; Pan et al., 2013), they are regulated by overlapping, yet distinct mechanisms.

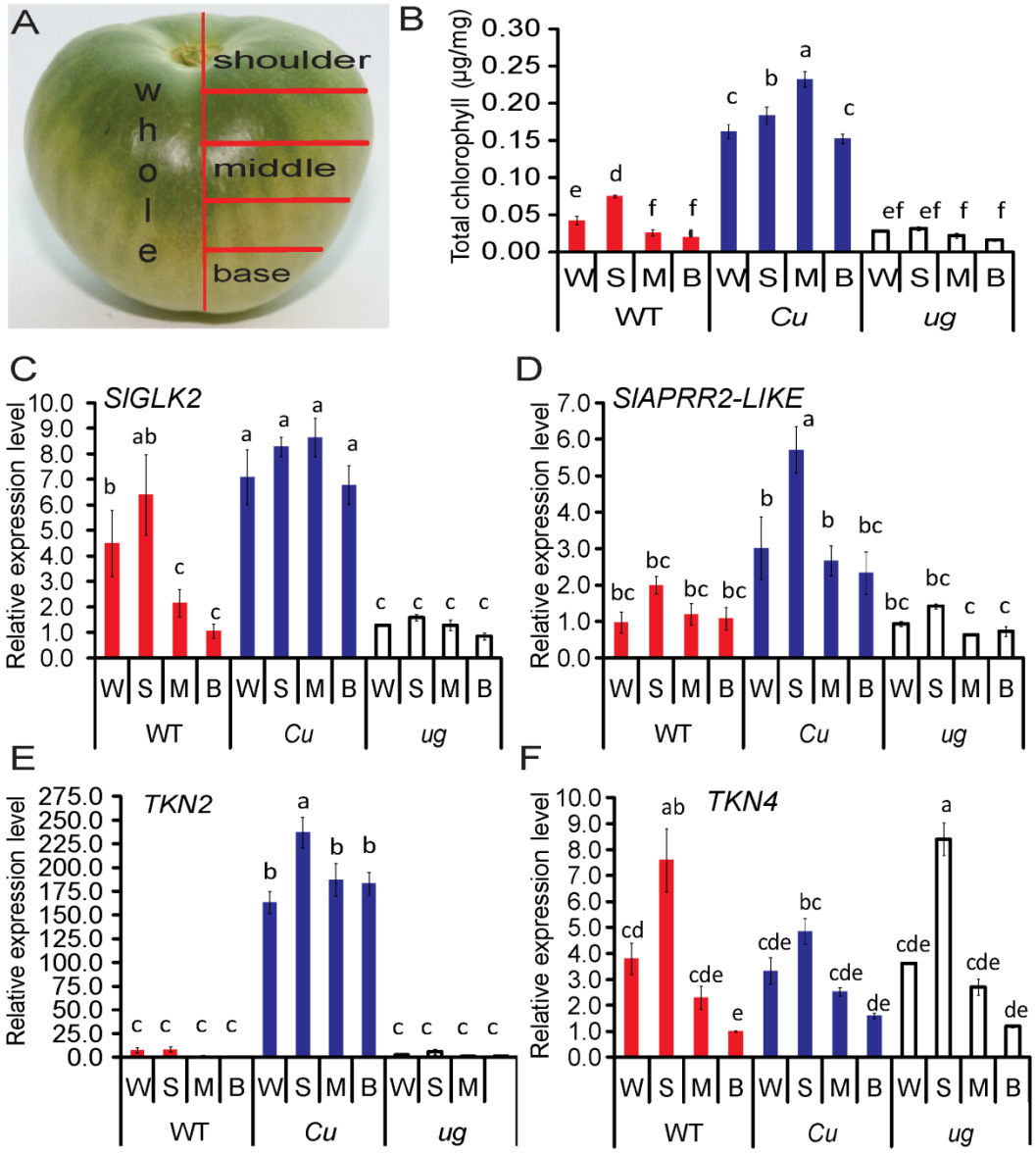

Figure 3.7. Mutations at *knox* loci disrupt the gradient of *SlGLK2* expression to impact fruit chloroplast development. A) Depiction of the sampling strategy. B) Chlorophyll content in the pericarp isolated from the whole (W), shoulder (S), middle (M) and base (B) of Ailsa Craig wild-type (WT), *Cu*, and *ug* mutant fruit at 28 days post-anthesis (*n=5*). C-F) qRT-PCR analysis of expression of *SlGLK2*, *SlAPRR2-LIKE*, *TKN2* and *TKN4* in the same tissue samples as described in B) relative to the expression level in base of WT fruits (*n=3*). Data are presented as the mean ± SEM and means with different letters are significantly different (*LS Means, p < 0.05*).

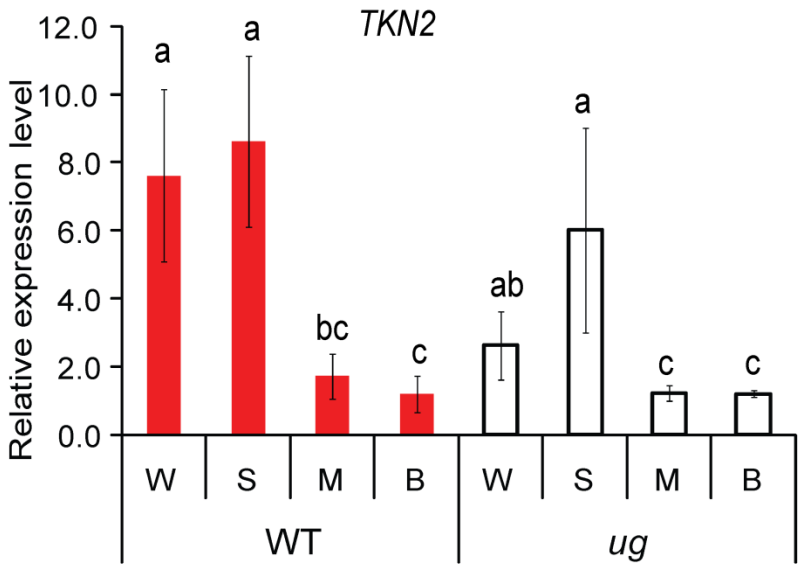

Figure 3.8. Relative expression gradient of *TKN2* within the fruit. qRT-PCR analysis of expression of *TKN2* in the pericarp isolated from the whole (W), shoulder (S), middle (M) and base (B) of Ailsa Craig wild-type (WT), and *ug* mutant fruit at 28 days post-anthesis (*n=3*). Data are presented as the mean ± SEM and means with different letters are significantly different (*LS Means, $p < 0.05$*). This represents an alternative depiction of the data presented in Figure 3.7 to highlight the gradient dependent expression of *TKN2* in WT and *ug* fruit pericarp that are masked by the elevated expression of *TKN2* in the *Cu* mutant background.

Several studies implicate phytohormones in mediating fruit chloroplast development in tomato, and in the case of auxin and BRs, enhanced fruit chloroplast development is positively correlated with increased *SlGLK* expression (Martineau et al., 1994; Galpaz et al., 2008; Sagar et al., 2013; Liu et al., 2014). In addition, auxin gradients are involved in several developmental processes and disruption of auxin signaling in the *arf6/arf8* double mutant results in ectopic *KNOX* expression and altered floral morphology (Benkova et al., 2003; Petersson et al., 2009; Tabata et al., 2010). The potential role of auxin in regulating the *KNOX*-mediated fruit chloroplast gradient in tomato fruit was investigated utilizing *SlARF4*-silenced lines, which possess increased starch content, enhanced chloroplast development and elevated *SlGLK1* expression (Sagar et al., 2013). The *SlARF4*-silenced lines were developed in the Micro-Tom background (Kobayashi et al., 2014), which is homozygous for the *u* mutation and lacks a functional *SlGLK2*. Unexpectedly, and unlike the *u* mutant allele in the Ailsa Craig background (Figure 3.1A and B), a decreasing gradient of chlorophyll content from the shoulder to the base of the fruit was observed in both Micro-Tom and an *SlARF4*-silenced line, with the latter displaying the expected elevated chlorophyll content (Figure 3.9A). The expression of *SlGLK2* and *SlAPRR2-LIKE* are elevated in the *SlARF4*-silenced line, particularly in the shoulder, and whereas the expression of *TKN2* and *TKN4* was also enriched in the fruit shoulder, the difference in expression levels between Micro-Tom and the *SlARF4*-silenced line are minor (Figure 3.9B-E). These data highlight the existence of a gradient of chlorophyll accumulation in Micro-Tom that occurs independently of *SlGLK2* and suggests that *SlARF4* negatively regulates *SlGLK2* and *SlAPRR2-LIKE* expression.

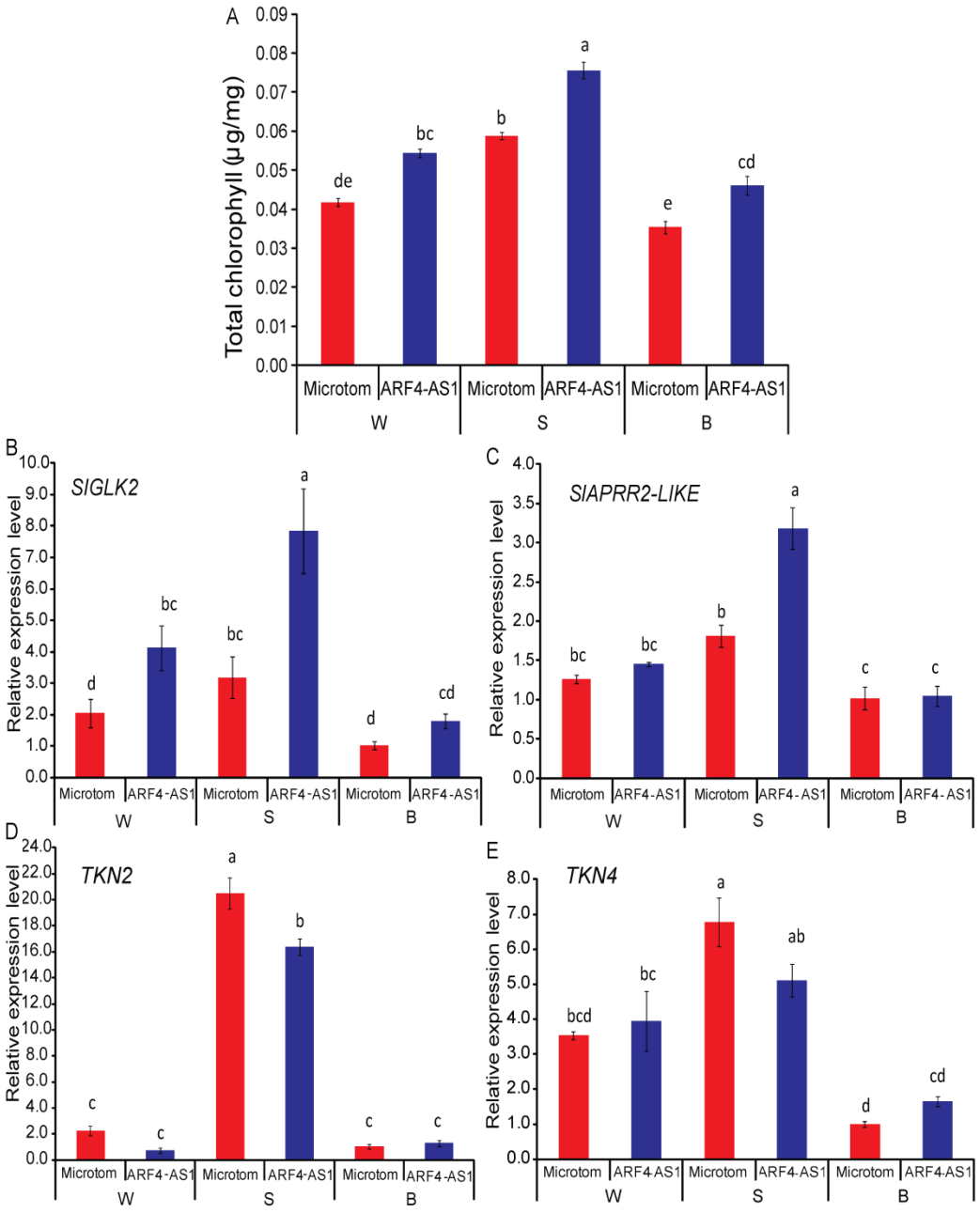

Figure 3.9. Silencing of *SlARF4* impacts fruit chlorophyll and expression of *SlGLK2* and *SlAPRR2-LIKE*. A) Chlorophyll content in whole (W), shoulder (S) and base (B) pericarp of Micro-Tom and *SlARF4* antisense lines at 21 days post-anthesis (*n=5*). B-E) Relative expression level of *SlGLK2*, *SlAPRR2-LIKE*, *TKN2* and *TKN4* in same samples as described in A). Data are presented relative to the expression level in base of Microtom fruits (*n=3*). Means ± SEM with different letters are significantly different (*LS Means, $p < 0.05$*).

The fruit phenotype of *hp-1* is partially suppressed by *u* and *ug*

Fruits of the *hp-1* mutant have increased chloroplast number, increased plastid compartment size and a higher chlorophyll content (Cookson et al., 2003). The contribution of *KNOX* and *SlGLK2* to the *hp-1* phenotype was assessed using a combination of single and double mutants in both WT and the *hp-1* background. Both *u* and *ug* partially suppress the *hp-1* phenotype although suppression by *u* is greater than that achieved by *ug* and a slightly additive phenotype is apparent when *u* and *ug* are combined (Figure 3.10A and B). Congruent with the elevated levels of chlorophyll, the expression of *SlGLK2*, *SlAPRR2-LIKE*, *TKN2* and *TKN4* are higher in *hp-1* compared to WT (Figure 3.10C-F). Together, these data indicate that both *SlGLK2* and *TKN4* contribute to the *hp-1* mutant phenotype and are also suggestive of a role for *SlAPRR2-LIKE* in determining the elevated chlorophyll content of *hp-1* fruit, possibly via regulation by *TKN2*. The reduced suppression of *hp-1* by *ug* compared to *u* may be due to the residual expression of *SlGLK2* observed in the *ug* mutant (Figure 3.7C), which may indicate that the *ug* allele (accession LA3416), which carries the F137L substitution, is not a complete null or that additional unknown factors regulate *SlGLK2* expression. Furthermore, evidence for the involvement of *SlAPRR2-LIKE* or additional TFs in determining the elevated chlorophyll content of *hp-1* fruit is supported by the observation that while chlorophyll levels of the *hp1/u* mutant are reduced compared with those observed in WT fruit, they are not reduced to the levels observed in the *u* mutant (Figure 3.10B).

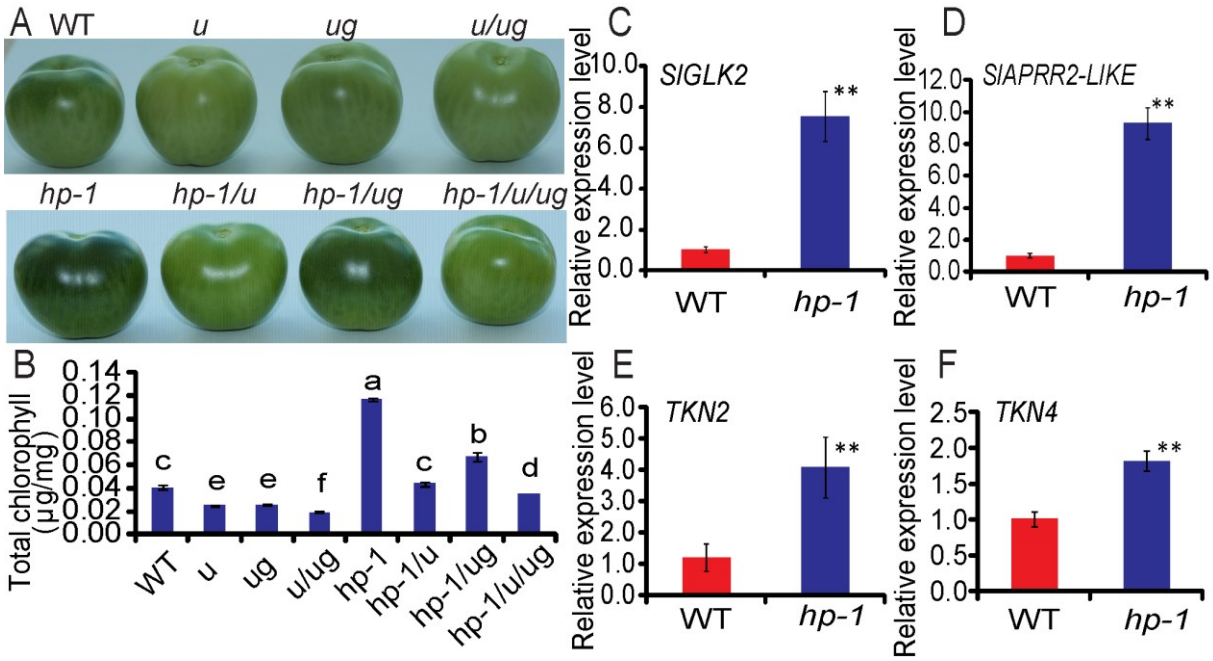

Figure 3.10. The *u* and *ug* loci partially suppress *hp-1*. A) Variation in fruit phenotype between single, double and triple mutant combinations of *hp-1*, *u* and *ug* at 21 days post-anthesis (dpa). B) Chlorophyll content in the pericarp of genotypes in A) (n=5). C-F) Relative expression level of *SlGLK2*, *SlAPRR2-LIKE*, *TKN2*, and *TKN4* in wild type (WT) and *hp-1* pericarp at 21 dpa. Data are presented as the mean ± SEM. Means with different letters are significantly different (*LS Means,* $p < 0.05$) and asterisks denote significant differences (**, $p < 0.01$) as determined by Student's *t-test*.

Discussion

A role for *KNOX* genes in fleshy fruit development

KNOX genes influence multiple aspects of plant morphology and are typically expressed within apical meristems where they maintain pluripotent cell populations required for organ initiation (Jackson et al., 1994; Long et al., 1996; Byrne et al., 2002; Belles-Boix et al., 2006; Hay and Tsiantis, 2010). Loss of KNOX activity can lead to inhibition of shoot formation, whereas ectopic *KNOX* expression results in pleiotropic phenotypes including increased lobe formation in simple leaves and increased complexity of compound leaves (Lincoln et al., 1994; Hareven et al., 1996; Long et al., 1996). In addition to roles in shoot apical meristem formation and leaf development, *KNOX* genes influence plant height, disrupt apical dominance and alter patterns of cell division and elongation (Douglas et al., 2002; Venglat et al., 2002). The Arabidopsis *KNOX* genes, *SHOOT MERISTEMLESS* (*STM*), *BREVIPEDICELLUS* (*BP*), *KNAT2* and *KNAT6* also influence inflorescence and carpel development together with architecture of abscission zones (Ragni et al., 2008; Shi et al., 2011). The role of individual *KNOX* genes in tomato remains obscure, but the identification of the underlying basis of the *ug* mutant has revealed an atypical role for *TKN4* in influencing fruit chloroplast development and specifically the formation of the green shoulder (Figure 3.1). This role is supported through characterization of the fruit phenotypes of *Cu* that result from ectopic expression of *TKN2* (Figure 3.5).

TKN2 is closely related to the *STM* gene of Arabidopsis, which is required for both vegetative and reproductive meristem development (Long et al., 1996; Scofield et al., 2007; Hay and Tsiantis, 2010). As observed by *TKN2* over-expression in the *Cu* mutant, ectopic expression of *STM* also leads aberrant meristem activity and altered plant morphology (Parnis et al., 1997; Gallois et al., 2002; Scofield et al., 2013). Within the shoot apical meristem, both *TKN2* and *STM*

function in part through modulation of hormone activity, and particularly through influencing the levels of cytokinins and gibberellins (Hay et al., 2002; Jasinski et al., 2005; Yanai et al., 2005; Hay and Tsiantis, 2010; Shani et al., 2010). At present the role of these hormones in contributing to the altered phenotypes observed in the fruit of the *Cu* mutant (Figure 3.5), remain to be defined. *TKN4* does not possess an apparent ortholog in Arabidopsis, although previous phylogenetic analysis suggested that it is closely related to *FaKNOX1* from strawberry and *NTH1* of tobacco (Chatterjee et al., 2011). Manipulation of *FaKNOX1* expression in transgenic strawberry and Arabidopsis alters plant morphology, including leaf, flower and meristem architecture (Chatterjee et al., 2011). However, altered expression of additional *KNOX* family members was also apparent in *FaKNOX1*-silenced lines, raising the possibility that the observed phenotypes could, in part, be due to altered expression of other strawberry *KNOX* genes (Chatterjee et al., 2011). Similarly, over-expression of *NTH1* in tobacco altered plant morphology, manifest through crinkling of the leaves and altered phyllotaxy, phenotypes that are typical of *KNOX* over-expression (Tamaoki et al., 1999). Interestingly, the *ug* mutant does not display any obvious phenotypes related to organ morphology (Figure 3.4), which may be the result of partial redundancy, a phenomenon often observed between *KNOX* genes (Byrne et al., 2002; Belles-Boix et al., 2006) that is supported by the overlapping expression patterns of the four tomato Class I *KNOX* genes *TKN1-4* in different tissues and organs (The Tomato Genome Consortium, 2012). However, functional specificity also exists between the tomato *KNOX* genes, as although *TKN2* and *TKN4* display increased expression in the shoulder of the fruit (Figure 3.7 and Figure 3.8), *TKN2* does not substitute for reduced TKN4 activity in the *ug* mutant. Furthermore, characterization of *Cu* revealed a broader role for *KNOX* genes in fleshy fruit development as *TKN2* over-expression not only promoted chloroplast development but also

impacted fruit size, pericarp thickness and pericarp cell density (Figure 3.5). Identification of a loss-of-function allele of *TKN2* or fruit-specific gene silencing of this gene will facilitate improved understanding of its role in both fruit development, including chloroplast development.

Differential regulation of chloroplast development in leaves and fruits of tomato

Both *u* and *ug* impact the gradient of chloroplast development in tomato fruit although neither locus influences chloroplast development in leaves (Figure 3.1 and 3.4A-C). In the case of the *u* locus, a lack of impact on leaf chloroplast development is likely due to redundancy and the overlapping expression of *SlGLK1* and *SlGLK2* in tomato leaf (Powell et al., 2012) whereas the lack of impact of *ug* on leaf chlorophyll content may be due to the absence of *TKN4* expression in leaves (The Tomato Genome Consortium, 2012). However, over-expression of *TKN2* in the *Cu* mutant does not increase chlorophyll content in leaves but impacts chloroplast development and chlorophyll accumulation in fruit (Figure 3.5 and Figure 3.6). These data suggest differential regulation of chloroplast development in fruits and leaves of tomato, a hypothesis supported by data indicating that over-expression of *GLKs*, and *SlAPRR2-LIKE*, together with suppression of *SlARF4*, positively impacts fruit, but not leaf, chloroplast development (Powell et al., 2012; Pan et al., 2013; Sagar et al., 2013). The underlying basis for this differential regulation of chloroplast development in tomato is unknown but may be due to saturation of chloroplast development in tomato leaves, as these contain approximately 20-fold higher levels of chlorophyll than fruit (Figure 3.1B and Figure 3.4C) and therefore maybe less amenable to further enrichment. In addition to the apparent differential regulation of chloroplast development in leaves and fruits of tomato, parallel pathways regulate fruit chloroplast development. For example, the impact of *SlAPRR2-LIKE* over-expression on fruit chloroplast development is independent of *SlGLK2*, as experiments were performed in Micro-Tom, which is

homozygous for the *u* mutant allele (Pan et al., 2013; Kobayashi et al., 2014). Similarly, although *u* and *ug* suppress the *hp-1* mutant phenotype, they do not restore chlorophyll to levels detected in the single mutants in the absence of the *hp-1* (Figure 3.10A and B). This discrepancy may be due in part to the elevated expression of *SlAPRR2-LIKE* in the *hp-1* background (Figure 3.10D). Availability of *SlAPRR2-LIKE* mutant alleles or silencing of *SlAPRR2-LIKE* in WT and mutant backgrounds will facilitate greater understanding of the role of this gene in chloroplast development, together with its relationship to *KNOX* genes and *SlGLK2*.

TKN4 **influences the gradient of chloroplast development in tomato fruit through regulation of** ***SlGLK2***

Transcription factor gradients play important roles in the development of multicellular organisms but remain poorly understood in plants (Stathopoulos and Levine, 2002; Sozzani et al., 2010; Chen et al., 2012). In grasses, leaf differentiation proceeds basipetally and is accompanied by a gradient of differential gene expression, chloroplast development and photosynthetic competency (Leech et al., 1973; Li et al., 2010). Similarly, this study has investigated a tissue-level macro-gradient of chloroplast formation that occurs during tomato fruit development that leads to the formation of a green shoulder. The physiological role of this chloroplast gradient is unknown but its formation is increased under shade conditions, and the shoulder possesses higher photosynthetic capacity than the remaining pericarp tissues, suggesting that this may be an adaptive trait that contributes to fruit photosynthesis (Smillie et al., 1999). Manipulation of KNOX activity, either through mutation in *TKN4* in *ug* or over-expression of *TKN2* in *Cu*, disrupts the gradient of chloroplast development in tomato fruit by altering the spatial expression of *SlGLK2* and *SlAPRR2-LIKE* (Figure 3.7).

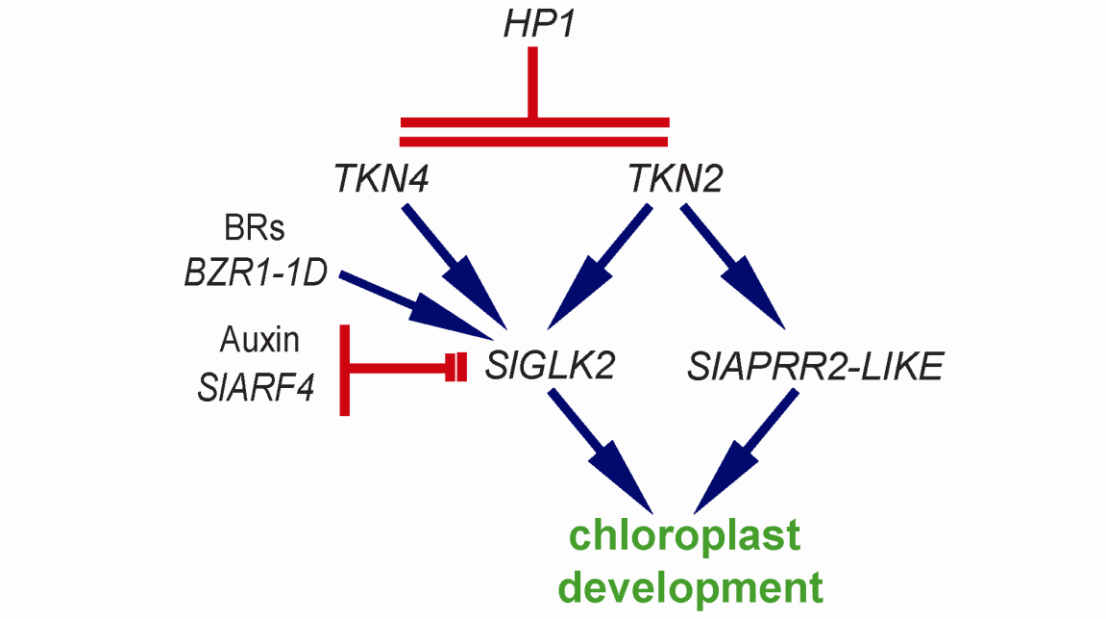

Figure 3.11. A proposed model for KNOX activity in developing tomato fruit. The *KNOX* genes *TKN2* and *TKN4* positively influence *SlGLK2* and *SlAPRR2-LIKE* expression to promote fruit chloroplast development. Auxin, via *SlARF4*, represses the expression of *SlGLK2* and *SlAPRR2-LIKE* and brassinosteroids (BRs), via *SlBZR1,* promote *SlGLK2* expression (Liu et al., 2014). Data indicate that *TKN2* influences the expression of both *SlGLK2* and *SlAPRR2-LIKE* whereas *TKN4* only influences the expression of *SlGLK2*. *HP-1* acts upstream of these genes to repress their expression.

However, *TKN2* and *TKN4* possess overlapping and distinct activities and while over-expression of *TKN2* influences the expression of both *SlGLK2* and *SlAPRR2-LIKE*, reduced *TKN4* activity only disrupts *SlGLK2* expression (Figure 3.7 and 6). These data promote a model (Figure 3.11) suggesting the existence of distinct regulatory modules that influence chloroplast development in tomato fruit and it will be of interest to determine whether TKN2 and TKN4 directly bind to regulatory regions of *SlGLK2* and *SlAPRR2-LIKE*. Similarly, while suppression of *SlARF4* did not dramatically alter the expression of *TKN2* and *TKN4*, both *SlGLK2* and *SlAPRR2-LIKE* expression was elevated (Figure 3.9). These data suggest multiple regulatory inputs that influence the expression of *SlGLK2* and *SlAPRR2-LIKE*, a hypothesis supported by the recent report indicating that activation of BR responses leads to elevated expression of *SlGLK2* and enhanced chloroplast development (Liu et al., 2014). Although *TKN4* influences the latitudinal gradient of *SlGLK2* expression in tomato fruit, *TKN2* and *TKN4* also display a gradient-dependent expression pattern in developing fruit, suggesting that *KNOX* genes themselves do not establish the gene expression gradient that exists in this tissue and that as yet unidentified signaling pathways are required. Furthermore, KNOX proteins and their mRNAs are also trafficked through plasmodesmata (Lucas et al., 1995), raising the possibility that the fruit chloroplast gradient may, at least in part, also be regulated through cell-cell movement of these proteins as well as their gradient-dependent transcript accumulation. The impact of gene expression gradients in plants are not fully understood but this study has identified a role for *KNOX* genes, whereby they regulate the gradient-dependent expression pattern of transcription factors required for fruit chloroplast development.

Materials and Methods

Plant material, growth conditions and chlorophyll extraction

Seeds of tomato (*Solanum lycopersicum*) cultivars, mutants, and mutant combinations at the *uniform ripening* (*u*), *uniform gray-green* (*ug*), *Curl* (*Cu*), and *high-pigment 1*(*hp-1*) loci (Table 3.1), together with *Solanum pimpinellifolium* accession LA1589, were obtained from the Tomato Genetics Resource Center, UC Davis or commercial vendors. Plants were grown in peat-based compost supplemented with fertilizer in greenhouses at Michigan State University, East Lansing, MI under 16 h day (25°C) and 8 h night (20°C). Micro-Tom and the *SlARF4*-silenced line (Sagar et al., 2013) were grown in a growth room under similar conditions. Flowers were tagged at anthesis and fruits subsequently harvested at defined ages based on days post-anthesis. Chlorophyll content was sampled from fruit pericarp and the terminal leaflet of expanding leaves of 4 week-old plants as previously described (Nadakuduti et al., 2012).

Genetic mapping of the *ug* locus and genotyping

An inter-specific F_2 population segregating for the *ug* locus was generated from a cross between *S. lycopersicum* (*ug/ug)* (LA3539) and *S. pimpinellifolium* (*UG/UG*) (LA1589). Fruit of 60 F_2 individuals were phenotyped for the presence or absence of a green shoulder and plants were genotyped with genetic markers spanning the tomato genome. Subsequent fine mapping was performed on further 1600 F_2 individuals using chromosome 1 genetic markers (Table 3.2). Genomic DNA was extracted as previously described (Barry et al., 2005) and details of genetic and physical maps together with associated molecular markers are available through the Sol Genomics Network. Genotyping tomato accessions (Table 3.1) for the *ug* mutant allele was achieved using a cleaved amplified polymorphic sequence marker (Table 3.3) that was resolved

by digestion with *Mse*I. Genotyping for the *u* mutant allele was achieved through sequencing of PCR fragments, amplified using primers (Table 3.3) that span the single nucleotide insertion site (Powell et al., 2012).

Molecular cloning and sequence analysis

Full-length cDNA clones of *TKN4* were amplified and cloned from flower cDNA of wild type and the *ug* mutant as previously described (Nadakuduti et al., 2012). Five independent clones from each genotype were selected for sequencing. The entire *TKN4* gene was sequenced from LA0021 genomic DNA. Sequences from the region with unexpected band size containing the deletion were cloned and four independent clones were sequenced and assembled using SequencherTM version 4.7. Amino acid alignments were generated using MUSCLE (Edgar, 2004). Primers are listed in (Table 3.3) and additional sequences utilized in multiple sequence alignments are provided in (Table 3.4).

qRT-PCR analysis

Expression analysis was performed according to (Nadakuduti et al., 2012) with the exception that 10µL PCR reactions were assembled using a Biomek 3000 liquid handler and amplified using an Applied Biosystems ABI Prism 7900HT Real-Time PCR System with the following program: 2 min at 50°C and 10 min at 95°C, followed by 40 cycles of 15 s at 95°C and 1 min at 60°C. Primers are listed in (Table 3.3).

Microscopy

Chloroplast imaging using confocal laser-scanning microscopy (CLSM) and transmission electron microscopy (TEM) was performed as previously described (Barry et al., 2012) with minor modifications. CLSM images were captured using an objective with numerical aperture of

0.5 and maximum intensity projection images were generated from a confocal z-series acquired through an average thickness of 170 µm in 10 µm increments. Samples for TEM imaging were embedded in Spurr resin.

Statistical analyses

Statistical analyses were performed using SAS. The genotypic constituents were evaluated by Student's *t-test* and LS Means.

Acknowledgements

This research was supported by a Discretionary Funding Initiative award from Michigan State University (MSU), a Strategic Partnership Grant from the MSU Foundation and by USDA National Institute of Food and Agriculture, hatch project number MICL02265. W.L.H. was supported by the MSU College of Agriculture and Natural Resources Undergraduate Research Program, the Larry D. Fowler Endowment Undergraduate Research Stipend and an Undergraduate Research Support Program Grant from MSU College of Natural Sciences. We thank Prof. Mondher Bouzayen, University of Toulouse for providing seeds of the *SlARF4* antisense line, Drs. Alicia Pastor and Melinda Frame of the Center for Advanced Microscopy at MSU for their assistance and Dr. Rebecca Grumet for comments on the manuscript.

Table 3.1. Tomato accessions used in the study

Accession #	Genetic background	Green shoulder	Genotype	Source of material
LA2838A	Ailsa Craig	yes	*U/U* & *UG/UG*	www.tgrc.ucdavis.edu
LA0533	Codine Red	yes	*U/U* & *UG/UG*	www.tgrc.ucdavis.edu
LA0534	Lukullus	yes	*U/U* & *UG/UG*	www.tgrc.ucdavis.edu
LA0535	Rheinlands Rhum	yes	*U/U* & *UG/UG*	www.tgrc.ucdavis.edu
LA1589	*S.pimpinellifolium*	yes	*U/U* & *UG/UG*	www.tgrc.ucdavis.edu
LA0021	Uniform Globe	NO	*U/U* & *ug/ug*	www.tgrc.ucdavis.edu
LA3539	Ailsa Craig	NO	*U/U* & *ug/ug*	www.tgrc.ucdavis.edu
LA4025	Florida 7547	NO	*u/u* & *ug/ug*	www.tgrc.ucdavis.edu
	Purple Prince	NO	*U/U* & *ug/ug*	Gary Ibsen's
LA3911	Micro-Tom	NO	*u/u* & *UG/UG*	www.tgrc.ucdavis.edu
LA3247	*u* (Ailsa Craig)	NO		www.tgrc.ucdavis.edu
LA3740	*Cu* (Ailsa Craig)			www.tgrc.ucdavis.edu
LA 3538	*hp1* (Ailsa Craig)			www.tgrc.ucdavis.edu
LA3542	*u/ug* (Ailsa Craig)			www.tgrc.ucdavis.edu
LA3371	*hp1/u* (Ailsa Craig)			www.tgrc.ucdavis.edu
LA3416	*hp1/ug* (Ailsa Craig)			www.tgrc.ucdavis.edu
LA3593	*hp1/u/ug* (Ailsa Craig)			www.tgrc.ucdavis.edu
	ARF4-AS1			(Sagar et al., 2013)

Sagar, M., Chervin, C., Mila, I., Hao, Y., Roustan, J.-P., Benichou, M., Gibon, Y., Biais, B.t., Maury, P., Latche, A., Pech, J.-C., Bouzayen, M. and Zouine, M. (2013) SI-ARF4, an auxin response factor involved in the control of sugar metabolism during tomato fruit development. *Plant Physiol.*, **161**, 1362-1374.

Table 3.2. PCR based genetic markers flanking the *ug* locus

Gene / Marker		Oligonucleotide Primer Sequence	
C2_At1g56345	Forward	5′-TCGGTGGCAACCACAGATTACCCAG-3′	*Msp*I
	Reverse	5′- ATCGAGTCTATTAGCTAAATGAAGCTC-3′	
TG197	Forward	5′- GTACTACGAGAATTAAGGCATGGT-3′	SNP Marker C → T
	Reverse	5′- GTGTAAGTTTCAAGGCATTCACGA-3′	
	Sequence	5′- GGTCTCATCTTGTTTCCTGTGGC-3′	
Solyc1g100480	Forward	5′- GTCTAGTAGTTATGAAGCTCCTGC -3′	*Hpy*CH4IV
	Reverse	5′-GGATGAAAAGCAAGTTAGAATCT-3′	
Solyc1g100500	Forward	5′-GCCATTATCGAGCGAGTTTATTCC-3′	*Hpy*CH4V
	Reverse	5′-TCTGAACCCAATGATATGATCTCC-3′	
Solyc1g100520	Forward	5′-GGCTAAAGTAACTTTCTTTGTCC-3′	Amplicon based indel
	Reverse	5′-GGCATATGCATTTATGTATGCCTC-3′	
Solyc1g100530	Forward	5′-GTGAAATTATGTGAATATGCAGC-3′	*Dra*I
	Reverse	5′-TCAACAACCATGTCTAATAGGCTA -3′	
Solyc1g100580	Forward	5′-TGCACTGGTTCAAGAAATGGAGCA-3′	*Eco*NI
	Reverse	5′-TAGCAACATGGCAAATGTAGAGC-3′	
C2_At3g05810	Forward	5′- GCCGCAGTTGTTTGAATTACAACC-3′	*Nhe*I
	Reverse	5′- GCCCTTCACTTATGCATAGCACC-3′	
C2_At5g02270	Forward	5′- GGAGGAGGGAAGTTGCGTTTGC-3′	*Rsa*I
	Reverse	5′- AACCTTAATTAGTTCGTCTCGTC-3′	
HBa57A01T7	Forward	5′-GTTAGATGATCAATATGGTAGTTTC-3′	*Rsa*I
	Reverse	5′- GGTTTATTGAGGGATATATGCCGCC-3′	
SGN-U316057	Forward	5′-GAGATGAATGAAATTGCTACTGC-3′	Amplicon based indel
	Reverse	5′-GGCGACTAGTGTGCCATATTATAGT-3′	
T0276	Forward	5′-CTCGAGGAAGACGAGAACTTTGTC-3′	*Afe*I

Sequences of the oligonucleotide primers utilized to amplify chromosome 1 genetic markers, together with the appropriate restriction enzyme to resolve the marker between *Solanum lycopersicum* accession LA3539 (*ug/ug*) and *Solanum pimpinellifolium* accession LA1589 (*UG/UG*). The TG197 marker is a SNP based marker resolved through direct sequencing of the amplicons and Solyc1g100520 and SGN-U316057 are indel markers that were directly resolved through gel electrophoresis of the amplicon.

Table 3.3. Oligonucleotide primers used in the study

Gene	Primer	Sequence	Use	Ref
TKN4	UG CAPS-F	5 -TCCAGCTCACGTCACAGTAGTGA-3	Genotyping	
(Solyc01g100510)	UG CAPS-R	5 -GTTTCTTGAGTAACATAGAGTCA-3	Genotyping	
	TKN4-qF	5 -TATCGATGGCCTTATCCCACGGAA-3	qRT-PCR	(1)
	TKN4-qR	5 -TCGATCCAGCACTTACACCTTCCA-3	qRT-PCR	
	UG inter-6F3	5'- CATGTGGGTCCGCCCTGTGATTC-3'	PCR	
	LA0021 deln-R2	5'- CATGCGCAGGCGTGCTTGTCAGC-3'	PCR	
	UG inter-6F1	5'-GACTTGGAACCAGTGGCGGATC-3'	Cloning	
	UG inter-9R	5'-GCCATCGATAGTGATTCTTCCACC-3'	Cloning	
	TKN4 ORF-F	5'-ATGATGGATGAATTGAGCAAAC -3'	RT-PCR	
	TKN4 ORF-STOPR	5'-GGAGGTACTGGAAATATTGGCACTTGA-3'	RT-PCR	
SlGLK2	SlGLK2-F	5 -ATGCTTGCTCTATCTTCATCATTGA-3	Genotyping	(2)
(Solyc10g008160)	SlGLK2-R	5 -TTGAAGATGACTAGCAATGTTATGTCT-3	Genotyping	
	SlGLK2-qF	5 -CCTTACATGTTTGGGGGCATCCAC -3	qRT-PCR	(2)
	SlGLK2-qR	5 -GGGGTGCAAATCAGAGGC -3	qRT-PCR	
GAPDH	GAPDHQ-F	5 - ATGCTCCCATGTTTGTTGTGGGTG-3	qRT-PCR	(3)
(Solyc05g014470)	GAPDHQ-R	5 -TTAGCCAAAGGTGCAAGGCAGTTC-3	qRT-PCR	
	GAPDH-F	5'- GACAAGGCTGCTGCTCACTT-3'	RT-PCR	
	GAPDH-R	5'- GCTTGACCTGCTGTCACCAAC-3'	RT-PCR	
TKN2	TKN2-qF	5 -CCATATCCATCGGAATCTCAG-3	qRT-PCR	(4)
(*Solyc02g081120*)	TKN2-qR	5 -TGGTTTCCAATGCCTCTTTC-3	qRT-PCR	
SlGLK1	SlGLK1-qF	5 -CCGTAAGCAGTGGTGATGAGTCTG-3	qRT-PCR	(2)
(*Solyc07g053630)*	SlGLK1-qR	5 -AACCCGAACCTACATCCGAAGC-3	qRT-PCR	
SlAPRR2-LIKE	Solyc08g077230-qF2	5'-GCAACTCTGCTGCTGAGATGAA-3'	qRT-PCR	
(*Solyc08g077230*)	Solyc08g077230-qR2	5'-CGTTGCAGAACGAGTAGACTATGTAGT-3'	qRT-PCR	

1. **Balaji, V., Mayrose, M., Sherf, O., Jacob-Hirsch, J., Eichenlaub, R., Iraki, N., Manulis-Sasson, S., Rechavi, G., Barash, I. and Sessa, G.** (2008) Tomato transcriptional changes in response to *Clavibacter michiganensis* subsp. *michiganensis* reveal a role for ethylene in disease development. *Plant Physiol.*, **146**, 1797-1809.
2. **Meir, S., Philosoph-Hadas, S., Sundaresan, S., Selvaraj, K.S.V., Burd, S., Ophir, R., Kochanek, B., Reid, M.S., Jiang, C.Z. and Lers, A.** (2010) Microarray analysis of the abscission-related transcriptome in the tomato flower abscission zone in response to auxin depletion. *Plant Physiol.*, **154**, 1929-1956.
3. **Powell, A.L.T., Nguyen, C.V., Hill, T., Cheng, K.L., Figueroa-Balderas, R., Aktas, H., Ashrafi, H., Pons, C., Fernandez-Munoz, R., Vicente, A., Lopez-Baltazar, J., Barry, C.S., Liu, Y.S., Chetelat, R., Granell, A., Van Deynze, A., Giovannoni, J.J. and Bennett, A.B.** (2012) *Uniform ripening* encodes a *Golden 2-like* transcription factor regulating tomato fruit chloroplast development. *Science*, **336**, 1711-1715.
4. **Shani, E., Burko, Y., Ben-Yaakov, L., Berger, Y., Amsellem, Z., Goldshmidt, A., Sharon, E. and Ori, N.** (2009) Stage-specific regulation of *Solanum lycopersicum* leaf maturation by class 1 KNOTTED1-LIKE HOMEOBOX proteins. *Plant Cell*, **21**, 3078-3092.

Table 3.4. KNOX genes used for amino acid alignments

Species	Name	Gene identifier#	Source
Solanum lycopersicum	*TKN4*	*Solyc01g100510*	http://solgenomics.net/
Solanum lycopersicum	*TKN3*	*Solyc05g005090*	http://solgenomics.net/
Arabidopsis thaliana	*STM*	*AT1G62360.1*	http://www.arabidopsis.org/
Arabidopsis thaliana	*KNAT2*	*AT1G70510.1*	http://www.arabidopsis.org/
Arabidopsis thaliana	*KNAT6*	*AT1G23380.2*	http://www.arabidopsis.org/
Antirrhinum majus	*invaginata*	*AY072736*	http://www.uniprot.org
Fragaria vesca	*FaKNOX*	*GU339211*	https://www.ncbi.nlm.nih.gov/
Zea mays	*ZmLG4*	*AF457121*	https://www.ncbi.nlm.nih.gov/

REFERENCES

REFERENCES

Barry CS, Aldridge GM, Herzog G, Ma Q, McQuinn RP, Hirschberg J, Giovannoni JJ (2012) Altered chloroplast development and delayed fruit ripening caused by mutations in a zinc metalloprotease at the *lutescent2* locus of tomato. Plant Physiol. **159:** 1086-1098

Barry CS, McQuinn RP, Thompson AJ, Seymour GB, Grierson D, Giovannoni JJ (2005) Ethylene insensitivity conferred by the *Green-ripe* and *Never-ripe 2* ripening mutants of tomato. Plant Physiol. **138:** 267-275

Bellaoui M, Pidkowich MS, Samach A, Kushalappa K, Kohalmi SE, Modrusan Z, Crosby WL, Haughn GW (2001) The Arabidopsis BELL1 and KNOX TALE homeodomain proteins interact through a domain conserved between plants and animals. Plant Cell **13:** 2455-2470

Belles-Boix E, Hamant O, Witiak SM, Morin H, Traas J, Pautot V (2006) *KNAT6*: an Arabidopsis homeobox gene involved in meristem activity and organ separation. Plant Cell **18:** 1900-1907

Benkova E, Michniewicz M, Sauer M, Teichmann T, Seifertova D, Jurgens G, Friml J (2003) Local, efflux-dependent auxin gradients as a common module for plant organ formation. Cell **115:** 591-602

Blanke MM, Lenz F (1989) Fruit photosynthesis. Plant Cell Environ. **12:** 31-46

Bohn GW, Scott DH (1945) A 2nd gene for uniform unripe fruit color in the tomato. J. Hered. **36:** 169-172

Byrne ME, Simorowski J, Martienssen RA (2002) *ASYMMETRIC LEAVES1* reveals *knox* gene redundancy in Arabidopsis. Development **129:** 1957-1965

Chatterjee M, Bermudez-Lozano CL, Clancy MA, Davis TM, Folta KM (2011) A strawberry *KNOX* gene regulates leaf, flower and meristem architecture. PLOS ONE **6:** e24752

Chen HT, Xu Z, Mei C, Yu DY, Small S (2012) A system of repressor gradients spatially organizes the boundaries of bicoid-dependent target genes. Cell **149:** 618-629

Cookson PJ, Kiano JW, Shipton CA, Fraser PD, Romer S, Schuch W, Bramley PM, Pyke KA (2003) Increases in cell elongation, plastid compartment size and phytoene synthase

activity underlie the phenotype of the *high pigment-1* mutant of tomato. Planta **217:** 896-903

Davies JN, Hobson GE (1981) The constituents of tomato fruit - the influence of environment, nutrition, and genotype. Crit. Rev. Food Sci. Nutr. **15:** 205-280

Dinar M, Stevens MA (1981) The relationship between starch accumulation and soluble solids content of tomato fruits. J. Am. Soc. Hortic. Sci. **106:** 415-418

Douglas SJ, Chuck G, Dengler RE, Pelecanda L, Riggs CD (2002) KNAT1 and ERECTA regulate inflorescence architecture in Arabidopsis. Plant Cell **14:** 547-558

Edgar RC (2004) MUSCLE: multiple sequence alignment with high accuracy and high throughput. Nucleic Acids Res. **32:** 1792-1797

Fitter DW, Martin DJ, Copley MJ, Scotland RW, Langdale JA (2002) *GLK* gene pairs regulate chloroplast development in diverse plant species. Plant J. **31:** 713-727

Gallois JL, Woodward C, Reddy GV, Sablowski R (2002) Combined SHOOT MERISTEMLESS and WUSCHEL trigger ectopic organogenesis in *Arabidopsis*. Development **129:** 3207-3217

Galpaz N, Wang Q, Menda N, Zamir D, Hirschberg J (2008) Abscisic acid deficiency in the tomato mutant *high-pigment 3* leading to increased plastid number and higher fruit lycopene content. Plant J. **53:** 717-730

Hareven D, Gutfinger T, Parnis A, Eshed Y, Lifschitz E (1996) The making of a compound leaf: genetic manipulation of leaf architecture in tomato. Cell **84:** 735-744

Hay A, Kaur H, Phillips A, Hedden P, Hake S, Tsiantis M (2002) The gibberellin pathway mediates KNOTTED1-type homeobox function in plants with different body plans. Curr. Biol. **12:** 1557-1565

Hay A, Tsiantis M (2010) *KNOX* genes: versatile regulators of plant development and diversity. Development **137:** 3153-3165

Hetherington SE, Smillie RM, Davies WJ (1998) Photosynthetic activities of vegetative and fruiting tissues of tomato. J. Exp. Bot. **49:** 1173-1181

Jackson D, Veit B, Hake S (1994) Expression of maize *KNOTTED1* related homeobox genes in the shoot apical meristem predicts patterns of morphogenesis in the vegetative shoot. Development **120:** 405-413

Jasinski S, Piazza P, Craft J, Hay A, Woolley L, Rieu I, Phillips A, Hedden P, Tsiantis M (2005) KNOX action in *Arabidopsis* is mediated by coordinate regulation of cytokinin and gibberellin activities. Curr. Biol. **15:** 1560-1565

Kobayashi M, Nagasaki H, Garcia V, Just D, Bres C, Mauxion J-P, Le Paslier M-C, Brunel D, Suda K, Minakuchi Y, Toyoda A, Fujiyama A, Toyoshima H, Suzuki T, Igarashi K, Rothan C, Kaminuma E, Nakamura Y, Yano K, Aoki K (2014) Genome-wide analysis of intraspecific DNA polymorphism in 'Micro-Tom', a model cultivar of tomato (*Solanum lycopersicum*). Plant Cell Physiol. **55:** 445-454

Kolotilin I, Koltai H, Tadmor Y, Bar-Or C, Reuveni M, Meir A, Nahon S, Shlomo H, Chen L, Levin I (2007) Transcriptional profiling of *high pigment-2*(*dg*) tomato mutant links early fruit plastid biogenesis with its overproduction of phytonutrients. Plant Physiol. **145:** 389-401

Leech RM, Rumsby MG, Thomson WW (1973) Plastid differentiation, acyl lipid, and fatty acid changes in developing green maize leaves. Plant Physiol. **52:** 240-245

Li PH, Ponnala L, Gandotra N, Wang L, Si YQ, Tausta SL, Kebrom TH, Provart N, Patel R, Myers CR, Reidel EJ, Turgeon R, Liu P, Sun Q, Nelson T, Brutnell TP (2010) The developmental dynamics of the maize leaf transcriptome. Nat. Genet. **42:** 1060-1067

Lincoln C, Long J, Yamaguchi J, Serikawa K, Hake S (1994) A *knotted1*-like homeobox gene in Arabidopsis is expressed in the vegetative meristem and dramatically alters leaf morphology when overexpressed in transgenic plants. Plant Cell **6:** 1859-1876

Liu LH, Jia CG, Zhang M, Chen DL, Chen SX, Guo RF, Guo DP, Wang QM (2014) Ectopic expression of a BZR1-1D transcription factor in brassinosteroid signalling enhances carotenoid accumulation and fruit quality attributes in tomato. Plant Biotechnol. J. **12:** 105-115

Liu YS, Roof S, Ye ZB, Barry C, van Tuinen A, Vrebalov J, Bowler C, Giovannoni J (2004) Manipulation of light signal transduction as a means of modifying fruit nutritional quality in tomato. Proc. Natl. Acad. Sci. U. S. A. **101:** 9897-9902

Long JA, Moan EI, Medford JI, Barton MK (1996) A member of the KNOTTED class of homeodomain proteins encoded by the *STM* gene of Arabidopsis. Nature **379:** 66-69

Lucas WJ, Bouche-Pillon S, Jackson DP, Nguyen L, Baker L, Ding B, Hake S (1995) Selective trafficking of KNOTTED1 homeodomain protein and its mRNA through plasmodesmata. Science **270:** 1980-1983

Martineau B, Houck CM, Sheehy RE, Hiatt WR (1994) Fruit-specific expression of the *A. tumefaciens* isopentenyl transferase gene in tomato: effects on fruit ripening and defense-related gene expression in leaves. Plant J. **5:** 11-19

Mustilli AC, Fenzi F, Ciliento R, Alfano F, Bowler C (1999) Phenotype of the tomato *high pigment-2* mutant is caused by a mutation in the tomato homolog of *DEETIOLATED1*. Plant Cell **11:** 145-157

Nadakuduti SS, Pollard M, Kosma DK, Allen C, Ohlrogge JB, Barry CS (2012) Pleiotropic phenotypes of the *sticky peel* mutant provide new insight into the role of *CUTIN DEFICIENT2* in epidermal cell function in tomato. Plant Physiol. **159:** 945-960

Pan Y, Bradley G, Pyke K, Ball G, Lu CG, Fray R, Marshall A, Jayasuta S, Baxter C, van Wijk R, Boyden L, Cade R, Chapman NH, Fraser PD, Hodgman C, Seymour GB (2013) Network inference analysis identifies an *APRR2-Like* gene linked to pigment accumulation in tomato and pepper fruits. Plant Physiol. **161:** 1476-1485

Parnis A, Cohen O, Gutfinger T, Hareven D, Zamir D, Lifschitz E (1997) The dominant developmental mutants of tomato, *Mouse-ear* and *Curl*, are associated with distinct modes of abnormal transcriptional regulation of a knotted gene. Plant Cell **9:** 2143-2158

Petersson SV, Johansson AI, Kowalczyk M, Makoveychuk A, Wang JY, Moritz T, Grebe M, Benfey PN, Sandberg G, Ljung K (2009) An auxin gradient and maximum in the Arabidopsis root apex shown by high-resolution cell-specific analysis of IAA distribution and synthesis. Plant Cell **21:** 1659-1668

Powell ALT, Nguyen CV, Hill T, Cheng KL, Figueroa-Balderas R, Aktas H, Ashrafi H, Pons C, Fernandez-Munoz R, Vicente A, Lopez-Baltazar J, Barry CS, Liu YS, Chetelat R, Granell A, Van Deynze A, Giovannoni JJ, Bennett AB (2012) *Uniform ripening* encodes a *Golden 2-like* transcription factor regulating tomato fruit chloroplast development. Science **336:** 1711-1715

Ragni L, Belles-Boix E, Gunl M, Pautot V (2008) Interaction of KNAT6 and KNAT2 with BREVIPEDICELLUS and PENNYWISE in Arabidopsis inflorescences. Plant Cell **20:** 888-900

Rohrmann J, Tohge T, Alba R, Osorio S, Caldana C, McQuinn R, Arvidsson S, van der Merwe MJ, Riano-Pachon DM, Mueller-Roeber B, Fei Z, Nesi AN, Giovannoni JJ, Fernie AR (2011) Combined transcription factor profiling, microarray analysis and metabolite profiling reveals the transcriptional control of metabolic shifts occurring during tomato fruit development. Plant J. **68:** 999-1013

Sagar M, Chervin C, Mila I, Hao Y, Roustan J-P, Benichou M, Gibon Y, Biais Bt, Maury P, Latche A, Pech J-C, Bouzayen M, Zouine M (2013) Sl-ARF4, an auxin response

factor involved in the control of sugar metabolism during tomato fruit development. Plant Physiol. **161:** 1362-1374

Scofield S, Dewitte W, Murray JAH (2007) The *KNOX* gene *SHOOT MERISTEMLESS* is required for the development of reproductive meristematic tissues in Arabidopsis. Plant J. **50:** 767-781

Scofield S, Dewitte W, Nieuwland J, Murray JA (2013) The Arabidopsis homeobox gene *SHOOT MERISTEMLESS* has cellular and meristem-organisational roles with differential requirements for cytokinin and CYCD3 activity. Plant J. **75:** 53-66

Shani E, Ben-Gera H, Shleizer-Burko S, Burko Y, Weiss D, Ori N (2010) Cytokinin regulates compound leaf development in tomato. Plant Cell **22:** 3206-3217

Shi CL, Stenvik GE, Vie AK, Bones AM, Pautot V, Proveniers M, Aalen RB, Butenko MA (2011) Arabidopsis Class I KNOTTED-Like homeobox proteins act downstream in the IDA-HAE/HSL2 floral abscission signaling pathway. Plant Cell **23:** 2553-2567

Smillie RM, Hetherington SE, Davies WJ (1999) Photosynthetic activity of the calyx, green shoulder, pericarp, and locular parenchyma of tomato fruit. J. Exp. Bot. **50:** 707-718

Smith HMS, Boschke I, Hake S (2002) Selective interaction of plant homeodomain proteins mediates high DNA-binding affinity. Proc. Natl. Acad. Sci. U. S. A. **99:** 9579-9584

Sozzani R, Cui H, Moreno-Risueno MA, Busch W, Van Norman JM, Vernoux T, Brady SM, Dewitte W, Murray JAH, Benfey PN (2010) Spatiotemporal regulation of cell-cycle genes by SHORTROOT links patterning and growth. Nature **466:** 128-132

Stathopoulos A, Levine M (2002) Dorsal gradient networks in the *Drosophila* embryo. Dev. Biol. **246:** 57-67

Tabata R, Ikezaki M, Fujibe T, Aida M, Tian C, Ueno Y, Yamamoto KT, Machida Y, Nakamura K, Ishiguro S (2010) Arabidopsis AUXIN RESPONSE FACTOR6 and 8 regulate jasmonic acid biosynthesis and floral organ development via repression of class 1 *KNOX* Genes. Plant Cell Physiol. **51:** 164-175

Tamaoki M, Nishimura A, Aida M, Tasaka M, Matsuoka M (1999) Transgenic tobacco over-expressing a homeobox gene shows a developmental interaction between leaf morphogenesis and phyllotaxy. Plant Cell Physiol. **40:** 657-667

The Tomato Genome Consortium (2012) The tomato genome sequence provides insights into fleshy fruit evolution. Nature **485:** 635-641

Venglat SP, Dumonceaux T, Rozwadowski K, Parnell L, Babic V, Keller W, Martienssen R, Selvaraj G, Datla R (2002) The homeobox gene *BREVIPEDICELLUS* is a key regulator of inflorescence architecture in Arabidopsis. Proc. Natl. Acad. Sci. U. S. A. **99:** 4730-4735

Waters MT, Moylan EC, Langdale JA (2008) GLK transcription factors regulate chloroplast development in a cell-autonomous manner. Plant J. **56:** 432-444

Yanai O, Shani E, Dolezal K, Tarkowski P, Sablowski R, Sandberg G, Samach A, Ori N (2005) Arabidopsis KNOXI proteins activate cytokinin biosynthesis. Curr. Biol. **15:** 1566-1571

CHAPTER IV

Genetic mapping and morphological characterization of the tomato fruit developmental mutants *easy peel* (*ep*) and *peach* (*p*)

Abstract

Tomato (*Solanum lycopersicum*) has long served as a model crop species to study fleshy fruit development and tomato fruit mutants have significantly contributed to understanding the molecular basis of fruit development and ripening. In this study, two monogenic tomato fruit surface related mutants, *peach* (*p*) and *easy peel* (*ep*) were characterized and the mutant loci mapped. Fruit of the *p* mutant is characterized by a dull epidermis with an uneven surface and abundance of trichomes. Scanning electron microscopy (SEM) of the surface of *p* mutant fruit revealed that the fruit surface contains ridges and the epidermal cells are small and conical, unlike the wild type (WT) cells that possess an essentially smooth fruit surface. Analysis of cuticle chemistry revealed increased epidermal wax abundance in *p* fruit cuticles compared to WT. Genetic mapping positioned the *p* locus to within a 965 kbp region of chromosome 2. Fruit of the *ep* mutant are identical to those of WT except that ripe fruits can be easily peeled incurring less damage to the underlying sub-dermal cells. Anatomical characterization by SEM revealed that the *ep* phenotype is probably due to modifications in cell layers just beneath the epidermis rather than specific defects in the cuticle and epidermis. The *ep* locus was placed on chromosome 8 to within a 20 Mbp interval. Future identification of these mutant loci will facilitate greater understanding of the underlying biological mechanisms that contribute to the morphology of the fruit exocarp.

Introduction

Fruit ripening is a complex biological phenomenon that is extensively studied using tomato (*Solanum lycopersicum*) as a model crop species. Several biochemical modifications occur as a part of the fruit ripening process, including sugar accumulation, reduction in organic acids, alteration in pigments responsible for development of color, production of volatiles responsible for aroma profile, modifications to the ultra-structure and composition of cell wall such as dissolution of the cell wall and middle lamella and water accumulation in the fruit, leading to changes in texture and firmness (Brady, 1987; Liu et al., 2004; Saladie et al., 2007). All these changes require extensive transcriptional and epigenetic reprogramming at the onset of ripening (Alba et al., 2005; Osorio et al., 2011; Rohrmann et al., 2011; Zhong et al., 2013).

Water content in ripe fruit of tomato accounts for more than 90% of the total weight (Ho et al., 1987) increasing the internal pressure, which is ultimately transmitted to the outer skin. Therefore, the mechanical performance of the fruit skin is of considerable importance so that the fruit can retain water and maintain physical integrity while undergoing these modifications. The fruit skin is a protective layer comprised of the cuticle, epidermis and a variable number of underlying sub-dermal cells, which together affect fruit appearance, postharvest handling and storage (Bargel and Neinhuis, 2005; Lara et al., 2014). The mechanical properties of the fruit skin are mainly attributed to the cuticle (Bargel and Neinhuis, 2005). Tomato fruit have a prominent continuous cuticle that is approximately 10 µm thick and that lacks stomata (Vogg et al., 2004). The tomato fruit cuticle is deposited on the exterior surface of the epidermal cells but also surrounds their radial and tangential walls and can even extend beyond to the hypodermis (Bargel and Neinhuis, 2005). The tomato fruit cuticle undergoes various changes in chemical composition, thickness, elasticity and extensibility from anthesis to ripening (Baker et al., 1982;

Matas et al., 2004; Dominguez et al., 2011). The cuticle affects surface phenomena in fruits such as the color, sheen, texture and uniformity. The surface of tomato fruits also contains epidermal hairs known as trichomes. Type I and type VI glandular trichomes are predominantly present in immature fruits and their density decreases as the fruits expand and the majority abscise prior to maturity and ripening (Li et al., 2004; Mintz-Oron et al., 2008). Glandular trichomes synthesize and secrete a variety of specialized metabolites, including terpenes, acylsugars and flavonoids that are toxic or repellent to herbivores (Kennedy, 2003; Sallaud et al., 2009; Schilmiller et al., 2009; McDowell et al., 2011; Weinhold and Baldwin, 2011). Recently, progress in fruit surface biology, and especially the identification of enzymes and regulators involved in cuticle biosynthesis, has been achieved through the characterization of mutants with altered cuticle properties (Hovav et al., 2007; Leide et al., 2007; Isaacson et al., 2009; Nadakuduti et al., 2012; Yeats et al., 2012; Shi et al., 2013; Yeats et al., 2014).

In this study, the phenotypes and map positions of the tomato fruit surface mutants easy peel (*ep*) and peach (*p*) were investigated (Price and Drinkard, 1908; Lindstrom, 1925; Verkerk and Contant, 1969). Fruits of the *p* mutant are dull and are covered by dense and unusual persistence of trichomes even in ripe fruits. Phenotypic characterization of the fruit cuticles using scanning electron microscopy (SEM) and biochemical analysis through Gas chromatography – mass spectrometry (GC-MS) reveals that *p* has altered epidermal cell structure and cuticular composition. Fruits of the *ep* mutant look identical to those of wild type Ailsa Craig (AC) plants except that the ripe fruits can be peeled easily without much damage to underlying pericarp cells. Inter-specific crosses of *p* and *ep* mutants generated with *S. pimpinellifolium* were performed to produce F_2 mapping populations that were screened with polymorphic markers to assign the mutant loci to chromosomes 2 and 8, respectively. The aim of this research is to ultimately

isolate these mutant loci by positional cloning and perform functional analysis of each gene. As the fruit surface is an important determinant of fruit quality the combined genetic and phenotypic analyses will provide valuable insight into fruit surface biology.

Results

Phenotypic characterization of the *peach* mutant

At all stages of development, fruit of the *peach* (*p*) mutant are characterized by a dull colored epidermis with an uneven surface that contains an abundance of trichomes (Lindstrom, 1925) (Figure 4.1A). Two morphologically distinct trichome types are typically evident on the surface of tomato fruit, type I glandular trichomes, which have a long multicellular stalk with a single celled gland at the tip and type VI trichomes which are shorter but are topped with a four celled glandular head. The prevalence of both trichome types is increased in *p* mutant fruit. In addition, the surface of *p* mutant fruits is uneven, the epidermal cells appear smaller in size, are cone shaped and covered by an abundance of ridges, in contrast to WT fruits which possess a fairly smooth fruit surface. Variation in the extracellular deposits on the ridged surface of *p* fruit was also evident (Figure 4.1D-E). Although the fruits have an altered surface, cuticle thickness appears normal except that the cuticle does not penetrate beyond the epidermal cell layer, as is typically the case in WT fruit (Figure 4.1F-G). Furthermore, as a general observation, *p* mutant fruit have a rubbery texture, and ripe fruits seldom crack, even when left to over-ripen on the vine.

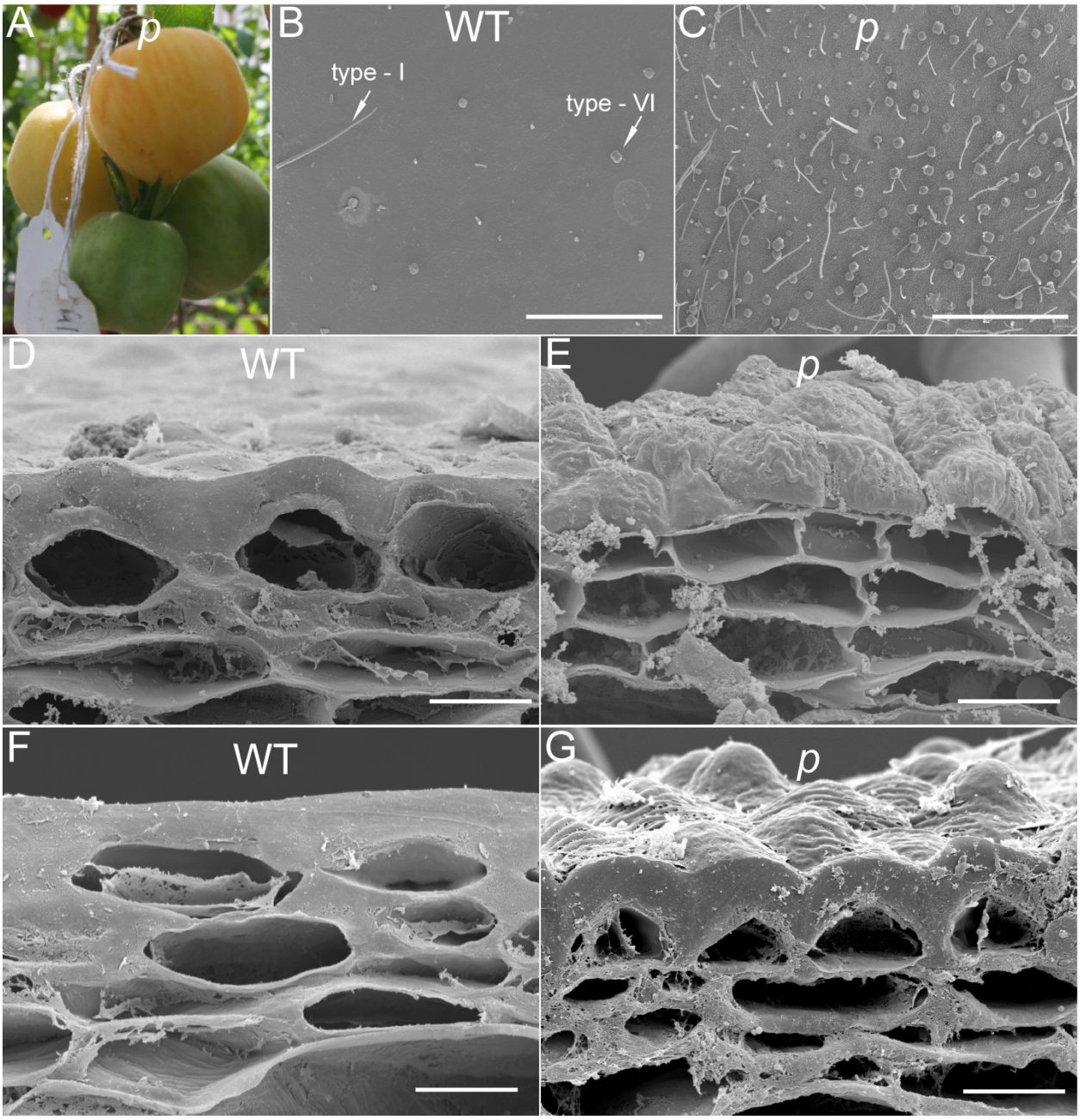

Figure 4.1. Fruit phenotype of *peach* (*p*) LA2357. A) Dull appearance of fruits of *p*. B-C) SEM micrograph of mature green (MG) *p* fruit surface showing increased trichome density in *p*. D-E) SEM micrograph of MG fruit cross sections of WT and *p* showing variation in the surface morphology of epidermis. F-G) SEM micrograph of ripe fruit cross section of WT and *p* showing extracellular cuticle (Scale bar in B-C = 1 mm, D-G= 20µm). Note the ridged appearance of the epidermal surface in *p* fruit visible in G.

The genetic background of the *peach* mutant

At the initiation of this research, the genetic background of the *p* mutant was unknown, which creates problems in making accurate phenotypic comparisons and drawing conclusions from these comparisons. Therefore, a backcross strategy was initiated to introgress the *p* mutation into the Ailsa Craig (AC) genetic background, a cultivar previously selected for introgression of varied morphological mutants of tomato (Darby *et al.*, 1978). The mutants were selected for dullness and hairiness during the backcrossing and a BC_2F_2 population that contains approximately 87.5% of the AC genetic background was derived. The BC_2F_2 *p* fruits are dull throughout their development (Figure 4.2A-B) and have increased trichome abundance compared to the WT (Figure 4.2C-D). They also retain the ridged and rough nature of their fruit epidermal surface whereas the surface of WT fruit is smooth (Figure 4.2E-F). These morphological differences in the fruit surface persist as the fruit ripens. Generally, as WT fruit develops and ripens, trichomes desiccate and abscise but more trichomes are retained in ripe fruit of the *p* mutant (Figure 4.3A-B). However, the uneven fruit surface observed in *p* mutant fruit may, in part, be caused by the remnants of structures retained after the trichomes abscise, particularly the base cells (Figure 4.3C-D). A prominent cuticle is also deposited on the surface of ripe fruit of the *p* mutant, which is comparable to WT (Figure 4.3E-F).

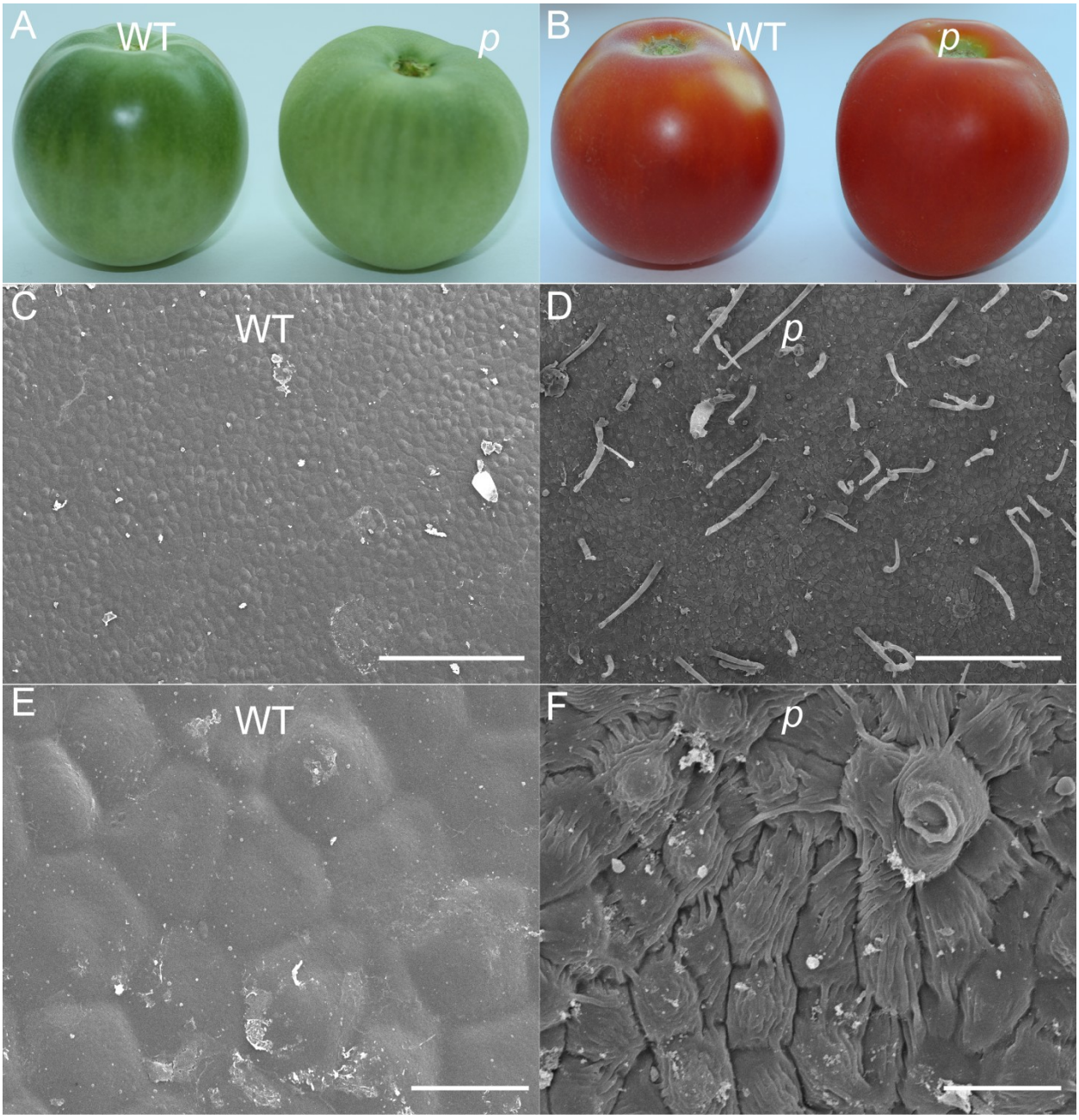

Figure 4.2. *peach* (*p*) fruit has altered fruit surface. A-B) Mature green fruit and ripe fruit of wild type (WT) and *p* from BC_2F_2 population respectively. Note the association of dullness in both stages of fruit development. C-D) SEM micrograph of 16 days post anthesis (dpa) WT fruit cross section and the same aged fruit of *p* showing many trichomes on the fruit surface respectively. E-F) SEM micrograph of 16dpa fruit surface of WT fruit having a smooth surface compared to ridged fruit surface in case of *p* fruit. (Scale bar in C-D = 100 µm, E-F= 10µm).

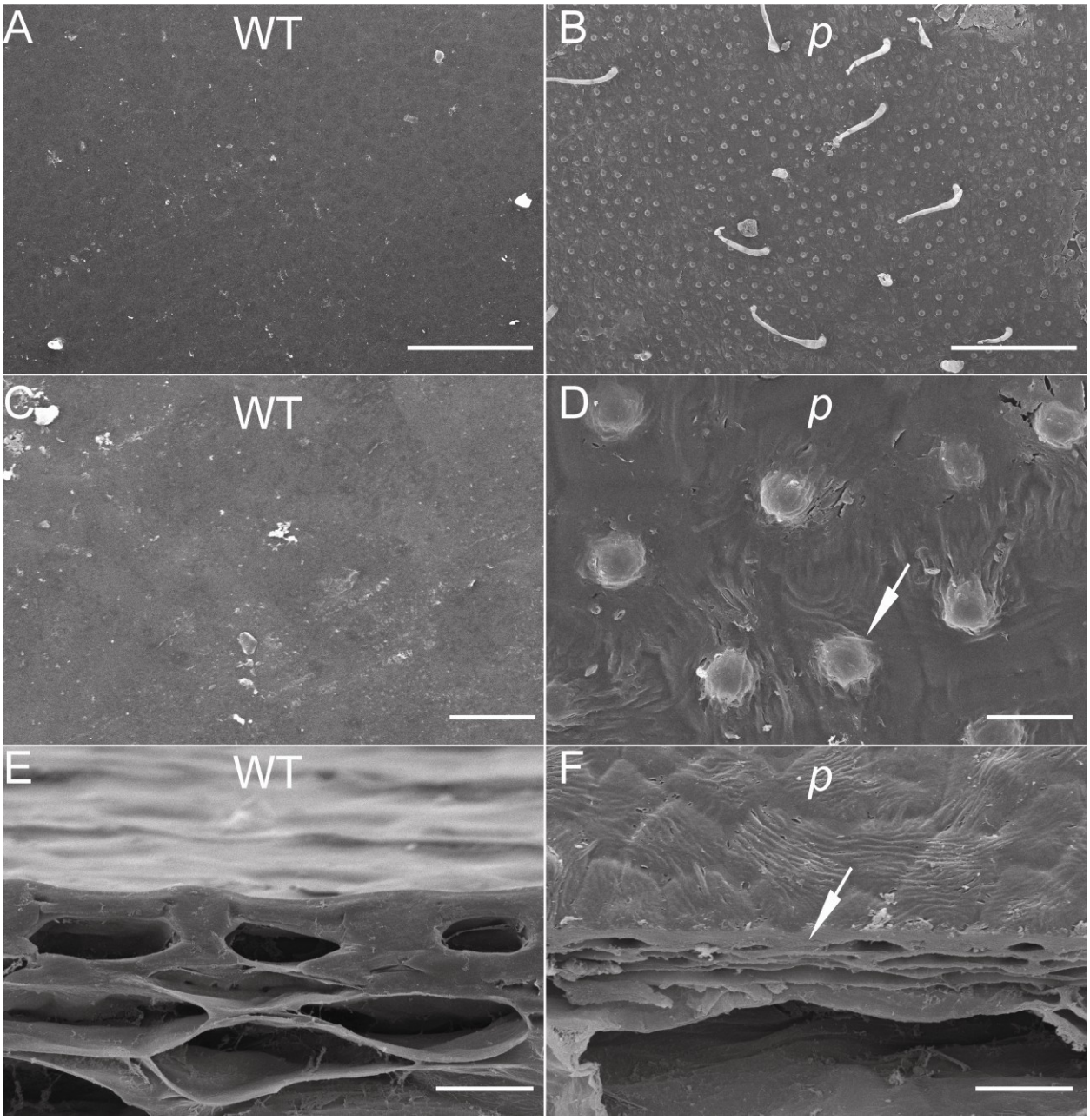

Figure 4.3. Variations in *peach* (*p*) ripe fruit surface. A-B) Ripe fruit surface of wild type (WT) and *p* from BC_2F_2 population respectively. Note the retention of trichomes in *p*. C-D) SEM micrographs of WT fruit surface compared to *p* respectively. Arrow highlights the bumpy fruit surface in *p*. E-F) SEM micrograph of ripe fruit cross section of WT fruit having a smooth surface compared to ridged appearance in case of *p* fruit. Arrow highlights the cuticle deposition in *p* fruit. (Scale bar in A-B = 100µm, C-D = 10µm and E-F= 20µm).

Fruit of the *peach* mutant have altered cuticular wax composition

Based on the morphology of the *p* mutant, it is evident that it possesses several altered phenotypes associated with the fruit surface (Figure 4.1 – 4.4). To investigate whether these altered phenotypes are associated with differences in cuticular composition, wax and cutin load of fruit cuticles of the BC_2F_2 lines of *p* and WT were analyzed at two developmental stages, mature green stage (MG) and ripe stage (breaker + 10days).

Typically, tomato fruit wax consists of hydrocarbons, triterpenoids, fatty acids, alcohols, sterols and coumarates (Baker et al., 1982; Vogg et al., 2004) and overall, the *p* fruit showed considerably enhanced wax abundance compared to WT at both stages of fruit development. This increase was manifest both through quantitative changes in components typically observed in WT together with the appearance of a few minor components in *p* fruit that were not detected in WT (Figure 4.4 and Table 4.1). The increased wax content in *p* is predominantly due to elevated levels of alkanes and triterpenoids, the two major constituents of wax that together contribute greater than 80% of the total wax load (Figure 4.4A-B, Table 4.1). Hydrocarbons comprising of straight chain alkanes, branched chain alkanes and alkenes are major components of wax which in MG fruit of *p* were 3.6 times and ripe fruit were 2.7 times higher than WT (Table 4.1). Among the alkanes, nonacosane (C29) and hentriacontane (C31) are the major alkanes at both stages of fruit development and these increased the most in *p* fruit. Dotriacontane (C32) alkane, although not as abundant in WT, showed a proportionally greater increase than C29 and C31 alkanes in *p* (Figure 4.4A). Triterpenoids, dominated by α, β and δ amyrins increased nearly two-fold in both MG and ripe stages in *p* fruit (Figure 4.4B, Table 4.1). Alkanes are generally associated with the epicuticular waxes and triterpenoids with intracuticular waxes

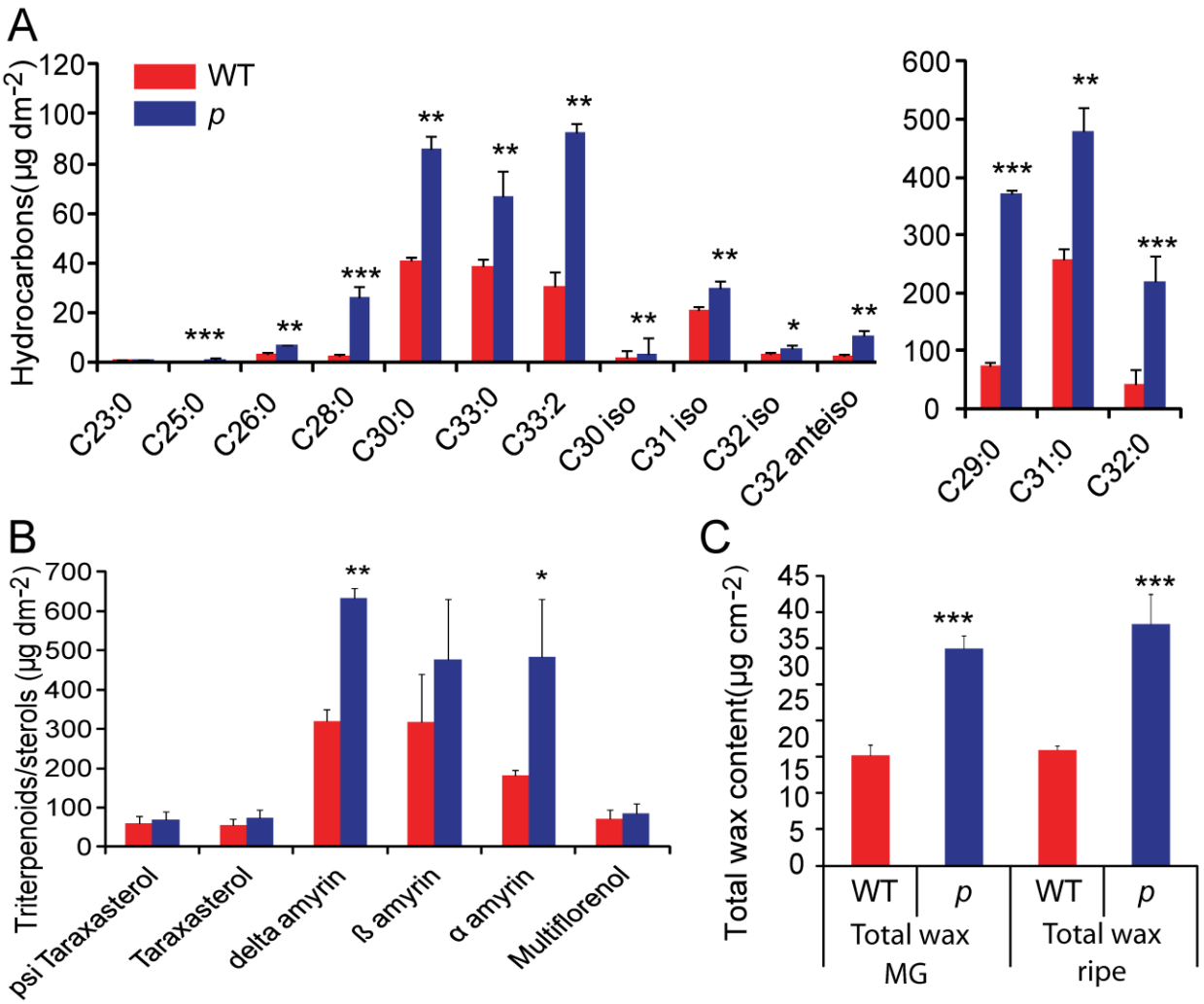

Figure 4.4. Cuticular wax constituents of fruits of WT and *p*. A) Hydrocarbon constituents of fruit wax include straight chain alkanes, branched chain alkanes and alkene. B) Triterpenoid and sterol constituents of fruit wax of WT and *p*. C) Total wax content at mature green (MG) and ripe stages of fruit development in WT and *p*. Data represents mean values (n=5) ±SE. Asterisks denote significant differences (*, $p < 0.05$; **, $p < 0.01$; ***, $p < 0.001$) as determined by Student's *t* tests.

Table 4.1. Fruit wax composition of AC and *p* in µg dm^{-2}

Wax class	C chain length/compound	Green fruit		Ripe fruit	
		AC	*p*	AC	*p*
Alkanes	C23:0	-	0.70 ± 0.001***	0.75 ± 0.07	0.97 ± 0.05
	C25:0	-	1.29 ± 0.2***	-	1.07 ± 0.09***
	C26:0	-	5.97 ± 0.01***	3.26 ± 0.9	6.87 ± 3.0**
	C28:0	2.24 ± 0.2	28.04 ± 5.7***	2.63 ± 0.5	26.35 ± 4.5***
	C29:0	65.21 ± 5.4	325.94 ± 38.8***	74.31 ± 4.9	371.30 ± 52.4***
	C30:0	28.59 ± 1.4	51.40 ± 4.0***	40.52 ± 2.1	86.23 ± 8.7**
	C31:0	136.97 ± 15.0	346.57 ± 33.3***	257.10 ± 9.9	480.66 ± 60.2**
	C32:0	10.54 ± 2.7	135.56 ± 53.2***	40.82 ± 2.6	221.10 ± 43.0***
	C33:0	6.76 ± 0.8	43.71 ± 8.6**	38.66 ± 2.7	66.90 ± 10.2**
Iso alkanes	C30:0	-	2.78 ± 0.5***	1.39 ± 0.3	3.51 ± 0.6**
	C31:0	14.42 ± 5.6	30.12 ± 2.3	21.06 ± 1.1	29.62 ± 2.8**
	C32:0	1.70 ± 0.2	1.85 ± 0.1	3.34± 0.2	5.21 ± 1.5
Anteiso alkanes	C32:0	1.41 ± 0.1	5.44 ± 0.7***	2.25 ± 0.0	10.44 ± 2.2**
Alkenes	C33:2	1.95 ± 0.2	8.33 ± 2.6**	30.72 ± 5.5	92.27 ± 4.27**
Alkanols	C20:0	-	1.86 ± 0.02***	2.56 ± 0.7	1.83 ± 0.5
	C22:0	1.57 ± 0.3	3.39 ± 0.5	4.79 ± 0.7	3.73 ± 0.3
	C23:0	0.52 ± 0.2	0.98 ± 0.01	2.20 ± 0.5	3.82 ± 0.7
	C24:0	0.85 ± 0.1	3.10 ± 0.7*	2.23 ± 0.7	2.50 ± 0.7
	C26:0	-	2.03 ± 0.3***	-	1.74 ± 0.4***
	C27:0	-	4.37 ± 0.9***	-	5.64 ± 2.4***
	C29:0	3.23 ± 1.6	5.67 ± 0.6	4.65 ± 0.5	14.25 ± 5.6*
	C32:0	-	11.54 ± 3.1***	5.41 ± 1.1	14.84 ± 5.3*
Alkenols	C22:2	1.80 ± 0.8	1.36 ± 0.5	4.28 ± 0.5	4.40 ± 1.8
	C24:2	21.76 ± 1.3	10.52 ± 3.1*	8.25 ± 3.1	5.50 ± 2.5
Fatty acids	C16:0	10.73 ± 2.4	22.88 ± 9.8*	13.09 ± 2.4	18.76 ± 4.3*
	C18:0	17.66 ± 3.4	10.24 ± 4.6*	4.75 ± 1.7	7.91 ± 1.8
	C 20:0	0.73 ± 0.2	2.48 ± 0.9**	0.93 ± 0.5	1.50 ± 0.3
	C22:0	-	-	-	0.87 ± 0.1***
	C24:0	-	0.55 ± 0.04***	-	2.60 ± 0.3***
Triterpenoids/	trans - Coumarate	33.35 ± 6.9	26.72 ± 3.2	20.39 ± 2.9	24.14 ± 5.1
Sterols/	ψ Taraxasterol	70.41 ± 3.3	61.02 ± 9.0	59.19 ± 1.9	67.85 ± 12.2
Coumarate	Taraxasterol	37.29 ± 7.1	64.95 ± 10.1	54.13 ± 7.1	72.94 ± 22.0
	delta amyrin	438.61. ± 50.8	830.88 ± 15.6**	321.00 ± 63.4	634.42 ± 36.3**
	ß amyrin	242.43 ± 30.4	405.76 ± 69.4*	317.44 ± 47.6	476.47 ± 53.3
	α amyrin	276.22 ± 53.6	452.22 ± 70.4**	180.90 ± 48.2	482.31 ± 47.5*
	Multiflorenol	88.07 ± 8.8	79.14 ± 11.3	71.01 ± 8.8	84.85 ± 14.3

Data are shown as means ± SE (n = 5). Asterisks denote significant differences between genotypes of the same developmental stage (*, $p < 0.05$; **, $p < 0.01$; ***, $p < 0.001$) as determined by Student's *t*-tests.

(Vogg et al., 2004), illustrating a general increase in both types of waxes in *p* (Table 4.1). Two other minor classes of wax components are fatty acids and fatty alcohols. There was an overall increase in fatty acids but no major differences in fatty alcohols were evident between the two genotypes (Table 4.1). Overall, the total amount of wax was doubled in both MG fruit (WT:*p* is 15.2:29.9 µg cm^{-2}) and ripe fruit (WT:*p* is 15.9: 33.4 µg cm^{-2}) in *p* compared to WT (Figure 4.4C).

In tomato fruits, cutin comprises 80% of the total cuticle weight, waxes account for approximately 3% and the remainder is attributed to polysaccharides (Baker et al., 1982). Tomato cutin is comprised of both C16 and C18 fatty acids, their oxygenated derivatives and *cis* and *trans* coumaric acids, although nearly 70 - 75% of the total cutin is composed of 10, 16 di hydroxy hexadecanoic acid (Table 4.2). Fruits of *p* at both MG and ripe developmental stages exhibited a pattern of cutin deposition similar to WT, with the majority of the cutin distributed at the MG stage. Limited variation in cutin composition is present between WT and *p* fruits and these occurred in minor components. For example, 9-OH, 16-oxo hexadecanoic acid showed a ripening-related increase from MG to ripe fruit in WT, whereas in *p* fruit it remained the same. 9, 18-diOH octadecanoic acid and C16:1 hexadecenoic acid levels were higher in *p* compared to WT although these represent minor cutin monomers out of the total cutin load and their contribution to the fruit phenotype is unclear. Overall, whereas the cutin fraction of the cuticle is not dramatically altered in *p* compared to WT, the wax component is increased considerably, translating to a reduced cutin monomer to wax ratio, of approximately 73:1 (961.5 : 13.25 µg cm^{-2}) in ripe fruits of WT to 22:1 (835.6 : 38.60 µg cm^{-2}) in *p*.

Table 4.2. Cutin monomer composition of WT and *p* in µg cm^{-2} (%)

	Green fruit		Ripe fruit	
Cutin monomer	AC	*p*	AC	*p*
cis - Coumarate	3.5 ± 0.3 (0.5)	4.8 ± 0.6 (0.6)	3.6 ± 0.3 (0.4)	5.2 ± 0.3 (0.6)**
trans - Coumarate	7.8 ± 0.7 (1.0)	10.9 ± 1.3 (1.7)	10.9 ± 1.0 (1.1)	12.1 ± 0.8 (1.5)
Hexadecanoic acid	0.8 ± 0.1 (0.1)	0.9 ± 0.1 (0.1)	1.1 ± 0.0 (0.1)	0.8 ± 0.1 (0.1)
Hexadecane 1,16 - dioic acid	6.0 ± 0.5 (0.8)	5.5 ± 0.5 (0.6)	8.3 ± 0.4 (0.9)	5.8 ± 0.5(0.7)*
C16:1 Hexadecenoic acid	1.6 ± 0.3 (0.2)	3.9 ± 0.4 (0.5)**	4.6 ± 0.2 (0.5)	3.2 ± 0.4 (0.4)*
16-OH Hexadecanoic acid	22.6 ± 2.2 (3.0)	21.7 ± 1.6 (2.4)	26.2 ± 1.5 (2.7)	21.9 ± 2.2 (2.6)
9-OH, 16-oxo Hexadecanoic acid	7.2 ± 1.0 (0.9)	12.4 ± 1.5 (1.4)***	21.5 ± 1.3 (2.2)	11.2 ± 1.9 (1.3)**
Octadecane 1,16 - dioic acid	1.7 ± 0.2 (0.2)	2.9 ± 0.2 (0.3)*	2.9 ± 0.2 (0.3)	2.9 ± 0.3 (0.3)
8-OH Hexadecane 1,16 - dioic acid	17.2 ± 2.1 (2.3)	20.7 ± 1.8 (2.4)	24.5 ± 1.2 (2.5)	22.3 ± 2.0(2.7)
18-OH Octadecanoic acid	2.9 ± 0.3 (0.4)	4.2 ± 0.2 (0.5) *	3.5 ± 0.2 (0.4)	3.5 ± 0.3 (0.4)
9, 18-diOH Octadecanoic acid	10.9 ± 1.5 (1.4)	20.7 ± 1.0 (2.3)***	14.4 ± 0.9 (1.5)	17.8 ± 1.6 (2.1)
10, 16-diOH Hexadecanoic acid	568.4 ± 64.9 (75.1)	625.0 ± 35.9 (71.7)	684.6 ± 31.7 (71.2)	576.8 ± 58.3 (68.7)
Not identified	111.8 ± 18.3 (14.5)	138.8 ± 11.9 (15.9)	160.1 ± 9.6 (16.7)	157.7 ± 14.1 (19.2)
Total	759.0 ± 91.1	871.6 ± 53.6	961.5 ± 41.9	835.6 ± 72.6

Data are shown as means ± SE (n = 5). Asterisks denote significant differences between genotypes of the same developmental stage (*, $p < 0.05$; **, $p < 0.01$; ***, $p < 0.001$) as determined by Student's t-tests

.

Genetic mapping of the *peach* locus

To initiate genetic mapping of the *p* locus, an inter-specific F_2 mapping population comprised of 128 individuals was developed from a cross between *S.lycopersicum* (*p/p*) (LA2357) and *S.pimpinellifolium* (*P/P*). *S. pimpinellifolium* (LA1589) was chosen as the mapping parent because of its close phylogenetic relationship with cultivated tomato, fertility of the F_2 individuals, which is essential for phenotyping a fruit-related trait, and availability of polymorphic markers. As described above, *p* mutant fruits of accession LA2357 had a dull surface, from mature green (MG) to ripe and denser persistent pubescence of fruit epidermis. Dullness and hairiness segregated in the F_2 population, where some dull fruits were not hairy and some hairy fruits were not dull. The basis for this segregation remains unknown, but the dull fruit phenotype was more consistent than the trichome phenotype and was therefore used for phenotyping of the F_2 mapping population. Previously, the *p* locus was assigned to chromosome 2 of the classical linkage map of tomato (Rick and Butler, 1956) and using a combination of available (http://solgenomics.net/) and custom designed chromosome 2 genetic markers this location was confirmed and the *p* locus was positioned between the LEOH113 (~85.0cM) and LEOH174 (~120.0cM) markers on chromosome 2 (Figure 4.5). Additional markers within the region were utilized to refine the *p* locus to an interval flanked by C2_At2g04700 (~97.0cM) (SL2.40ch02:44259745..44264878) and T1480 (~100.6cM) (SL2.40ch02:45223579..45224990) which, based on the tomato genome assembly (The Tomato Genome Consortium, 2012), represents a 965 kilobase physical gap containing 139 predicted genes. The marker information for this region is provided in Table 4.3.

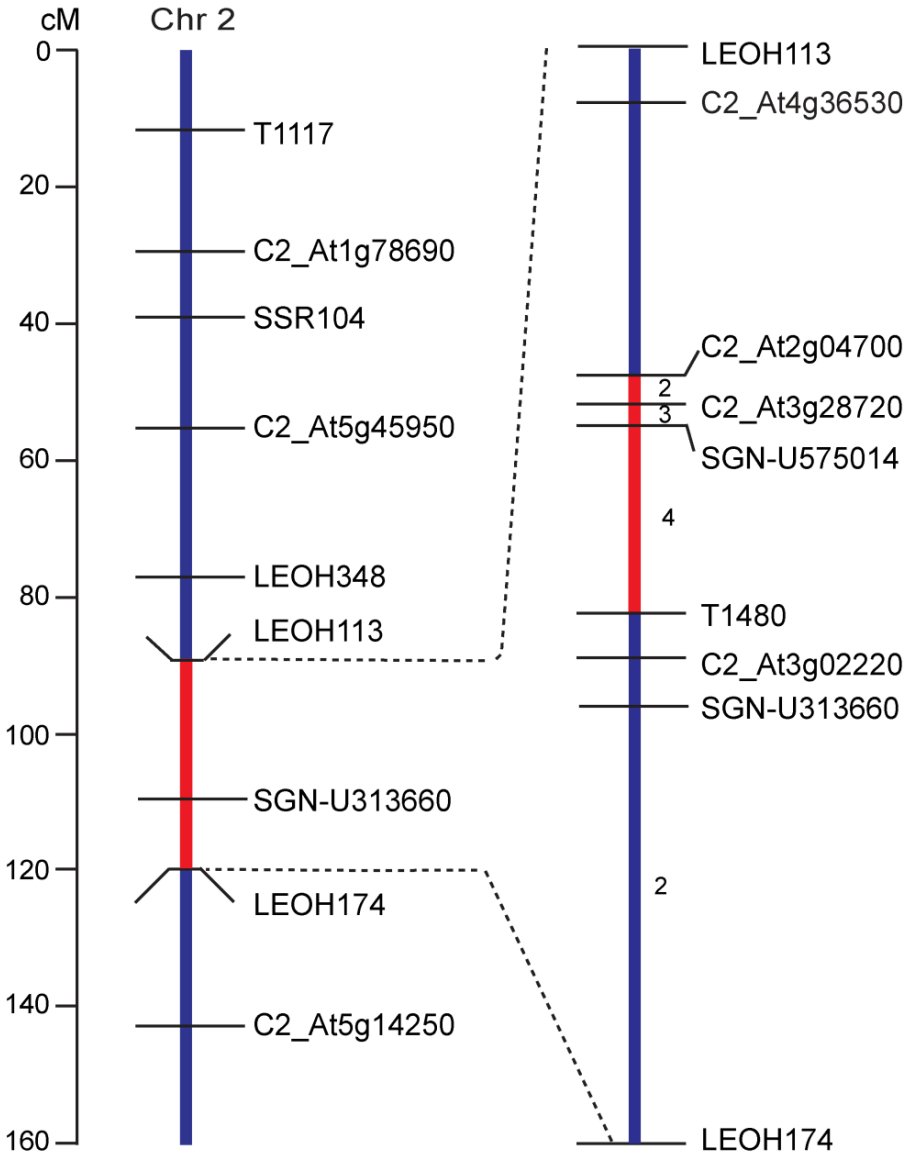

Figure 4.5. Genetic linkage map of chromosome 2. Blue bar represents chromosome 2 with genetic markers used in the study along with their centimorgan intervals on the left are shown. The Red bar represents the region to which the locus is initially narrowed down. The numbers in between adjacent markers represent the informative recombinant individuals from a total of 128 F_2 plants. Further populating the region with markers led to narrow down the interval further, highlighted by red bar.

Table 4.3. PCR based genetic markers used for mapping *p* locus

Gene / Marker	Oligonucleotide Primer Sequence	Restriction enzyme
T1117	Forward 5'-CAACTCCGTC TTTGTCAGCC-3'	*Bgl*II
	Reverse 5'-TGCTTTGTCG TCTGCACCCT-3'	
C2_At1g78690	Forward 5'-TCCAGAAGGGAAGGTCTGTCAAGAAG-3'	*Alu*I
	Reverse 5'-AGTCATGTACAGACATTTTTGTGCTGC-3'	
LEOH 23.3	Forward 5'-CTATGCGTTTGTCGGTCGT-3'	*Tsp*509I
	Reverse 5'-CAAGGTAGTTGAAGGTATGACCA-3'	
C2_At5g45950	Forward 5'-GCATCATTCTGGAAGCTGTCCA-3'	*Rsa*I
	Reverse 5'-AGCTTTAAGAGCTTCATTAGCCA-3'	
SSR104	Forward 5'-TTCCATTTGAATTCCAACCC-3'	indel
	Reverse 5'-CCCACTGCACATCAACTGAC-3'	
LEOH348	Forward 5'-TGTTTCCCTTCATTCATGCT-3'	*Hpy*CH4IV
	Reverse 5'-CCAATTGGATAAATTGGTGGT-3'	
LEOH 113	Forward 5'-AAACAGAGGTGCCGAAGAAA-3'	*Nla*III
	Reverse 5'-GAGCTACAAGCAGCAAACCA-3'	
C2_At4g36530	Forward 5'-AGATTTGCTAGGCTTTGGTTGGAG-3'	*Hpy*188III
	Reverse 5'-AGTGAATCCCCAAACTGTCCTGC-3'	
C2_At2g04700	Forward 5'-ATGAGAACTCTTCAAGCTTCCACCTC-3'	*Hpy*CH4IV
	Reverse 5'-TGACCACAGAAGTAACACCTTTGTCC-3'	
cLED-19-B24	Forward 5'-GGCACCATCAGAACTTCATGCAGA-3'	*Msp*I
	Reverse 5'-GTACCATTATGATAATGAGGTGTTA-3'	
T1480	Forward 5'-ACCACCTTGGATGAATACCG-3'	*Alu*I
	Reverse 5'-TGCAACAGCTTTTCCCTCTC-3'	
C2_At3g02220	Forward 5'-TGTAGAGATCAAATTGATTGGAAGCG-3'	*Hin*fI
	Reverse 5'-TATCCCGTTCTCGAGCATTCTTG-3'	
SGN-U313660	Forward 5'-GTCCTAAGTCCATTTTCACATCAC-3'	*Taq*I
	Reverse 5'-GTCAAACAGAACATATCATCAAAGC-3'	
LEOH174	Forward 5'-CGAGTCCGAGGAAGACTGAT-3'	indel
	Reverse 5'-TCAAGACAGACACGGATTGC-3'	
C2_At5g14250	Forward 5'-ATCTCATTCCCAGTTGCAAAGGAGC-3'	*Bam*HI
	Reverse 5'-AGTCAGCATTGGAGCCACACCACG-3'	
C2_At1g65720	Forward 5'-CCTCGATTCCGTGCTTTCTTCGT-3'	*Hin*fI
	Reverse 5'-GTCACGGATTGAGCTCGTCACCGA-3'	
C2_At3g28720	Forward 5'-ATCCATCCCCTGCTTTCACCAAG-3'	*Tfi*I
	Reverse 5'-ACCATATCCTTAAAGGCCACAGACTG-3'	
SGN-U575014	Forward 5'-GAATCTCCTCCAAGTTCCAGAGA-3'	*Hin*fI
	Reverse 5'-GGCTTCATTATTTCTCCATCCAC-3'	

Sequences of the oligonucleotide primers utilized to amplify chromosome 2 genetic markers, together with the appropriate restriction enzyme to resolve the marker between *Solanum lycopersicum* accession LA2357 (*p/p*) and *Solanum pimpinellifolium* accession LA1589 (*P/P*). SSR104 and LEOH174 are indel markers that were directly resolved through gel electrophoresis of the amplicon.

Phenotypic characterization of the *easy peel* mutant

Fruits of the *easy peel* (*ep*) mutant are indistinguishable from those of wild-type until the onset of ripening. Then, as ripening proceeds, the skin of mutant fruits can be more easily removed from the pericarp compared to that of wild-type and congruent with this easy-peel phenotype, less of the underlying sub-dermal cells adhere to the skin (Figure 4.6). In addition, a general observation made while growing this mutant is that the fruits are prone to cracking as they ripen, which ultimately promotes opportunistic fungal infections. Although the cuticle is often associated with fruit cracking (Chu and Thompson, 1972; Emmons and Scott, 1997; Emmons and Scott, 1998; Matas et al., 2004; Bargel and Neinhuis, 2005; Dominguez et al., 2011), there was no difference in fruit cuticle deposition in *ep* suggesting that the mutant phenotype is due to an alteration in the properties of the epidermal or sub-dermal cells (Figure 4.6B-C). In support of this hypothesis, integrity of the fruit peel failed at the level of the sub-dermal cell layers of ripe *ep* fruit during preparation for SEM analysis (Figure 4.6D-E).

Genetic mapping of the *easy peel* locus

The *ep* mutant was originally recovered as a recessive allele in the progeny of thermal neutron irradiated seeds of the cultivar Money Maker (Verkerk and Contant, 1969). To initiate genetic mapping, an inter-specific F_2 mapping population of 205 F_2 individuals was developed from a cross between *S.lycopersicum* (*ep/ep*) (LA3616) and *S.pimpinellifolium* (LA1589) (*EP/EP*). Fruits of the F_2 population were phenotyped for easy removal of fruit peel and clean fruit peel. As the *ep* mutant was not assigned to a chromosome, a collection of markers that are evenly spaced across the entire twelve chromosomes were used to genotype a subset of the F_2 population that displayed the *ep* mutant phenotype at high confidence.

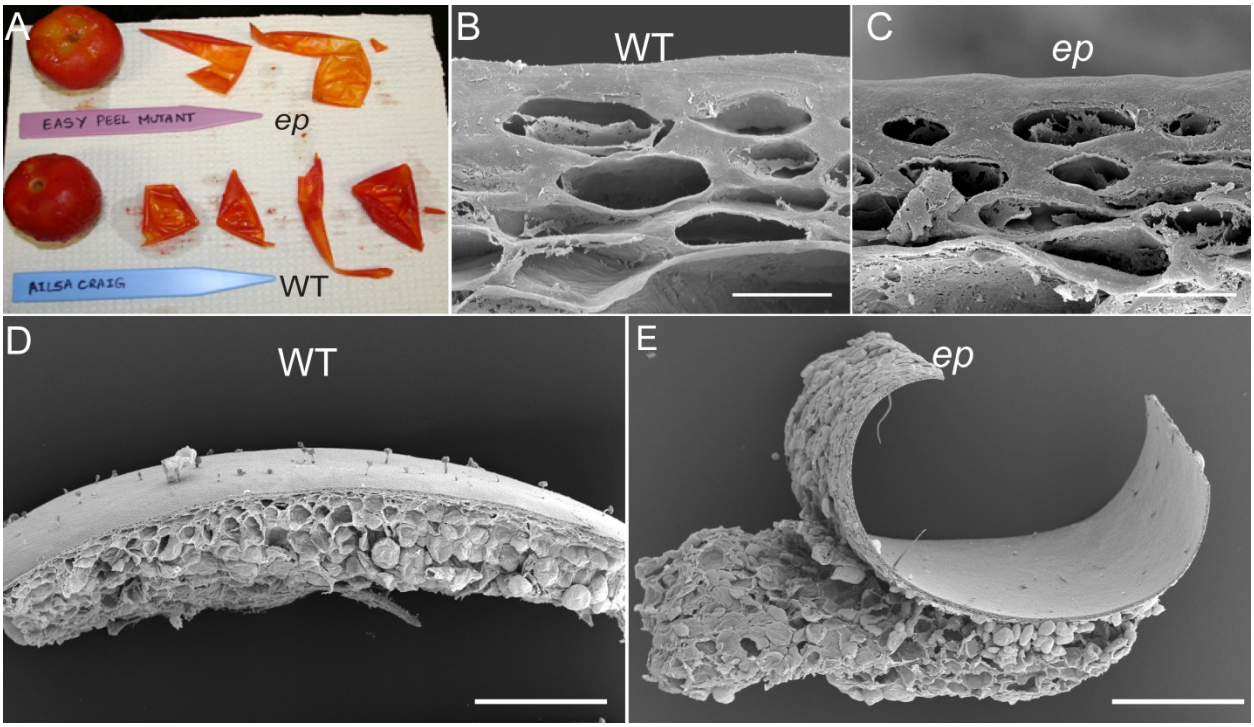

Figure 4.6. Fruit phenotypes of *easy peel* (*ep*). A) The *ep* mutant is readily peeled from the underlying pericarp cells whereas pericarp cells adhere to the cuticle of wild type (WT) Ailsa Craig (AC) fruit. B-C) Scanning electron micrographs (SEM) of ripe fruit cross sections of WT and *ep* respectively. D-E) SEM micrographs showing the peel coming off of the ripe fruit cross section of *ep* easily as compared to AC. Note the attachment of 2-3 layers of cells beneath the cuticle as it peel off. (Scale bar in B-C = 2 mm, D-E= 20μm).

Linkage was observed between these high confidence mutant individuals and the C2_At5g27390 marker, which is located on chromosome 8 (Figure 4.7). Following assignment of the *ep* locus to chromosome 8, additional markers (Table 4.4) were mapped within the entire population, ultimately placing the locus between C2_At5g27390 (20.5cM) (SL2.40ch08:30094098..30099462) and cLER-5-P17 (51.75cM) (SL2.40ch08:51752314..51754989) which represents a large physical distance of 21.66 megabases but only contains 465 predicted genes (The Tomato Genome Consortium, 2012).

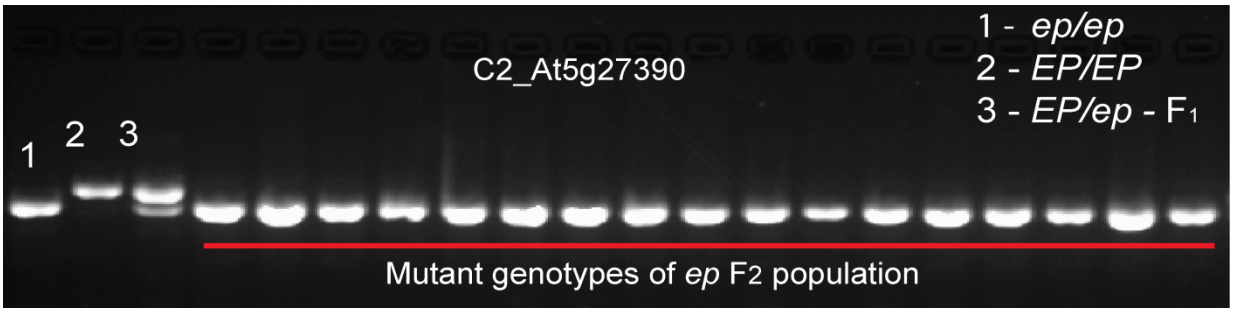

Figure 4.7. Association of C2_At5g27390 marker to *ep* phenotype. Screening the mutant phenotypes of F_2 mapping population from a cross between *S.lycopersicum* (e*p/ep*) (LA3616) with *S.pimpinellifolium* (*P/P*) with the maker C2_At5g27390 located on chromosome 8 shows a strong correlation between the genotype and the phenotype, thus placing the *EP* locus on chromosome 8. The 17 genotypes used are high confidence mutants from the F_2 mapping population.

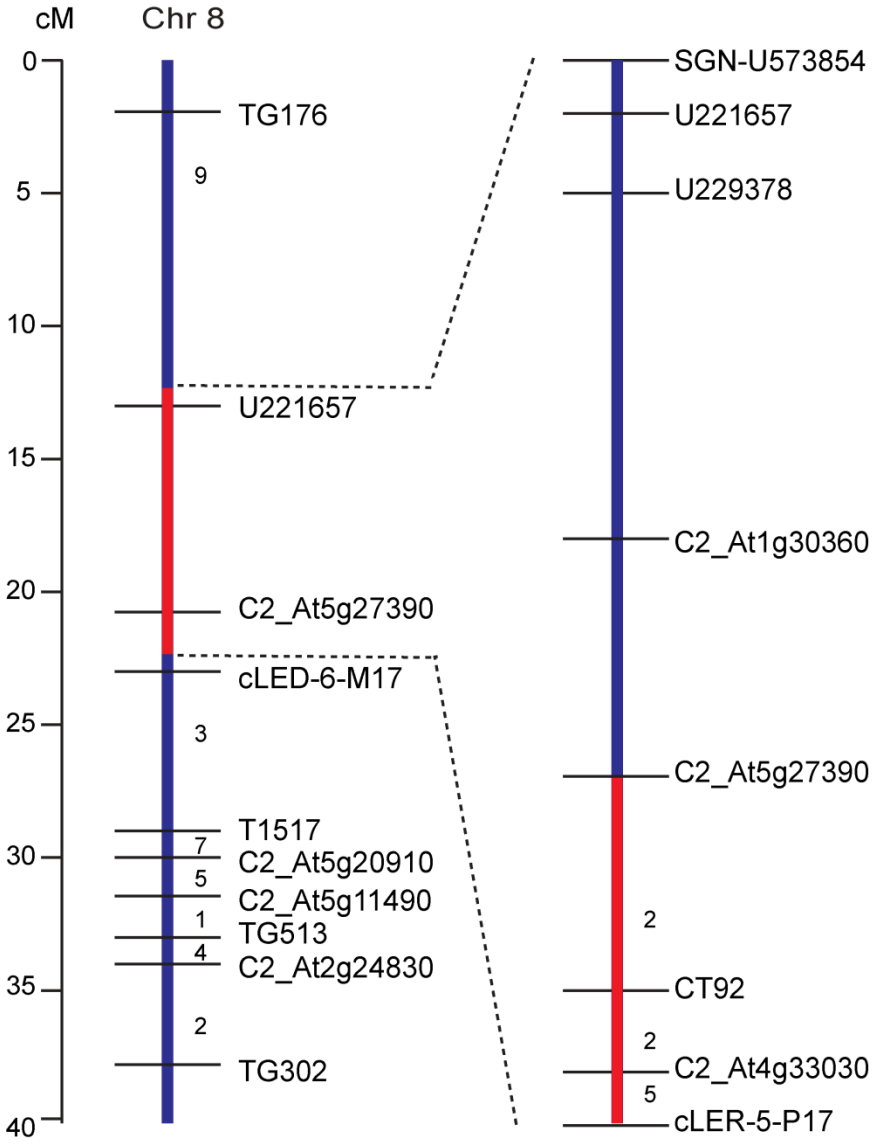

Figure 4.8. Genetic linkage map of chromosome 8 showing the region of interest. Blue bar represents chromosome 8 with genetic markers used in the study along with their centimorgan intervals on the left are shown. The Red bar represents the region to which the locus is initially narrowed down based on the informative recombinant individuals, represented by the numbers in between adjacent markers from a total of 205 F_2 plants. Further populating the region with markers led to narrow down the interval further, highlighted by red bar.

Table 4.4. PCR based genetic markers used for mapping *ep* locus

Gene / Marker	Oligonucleotide Primer Sequence	Restriction enzyme
TG176	Forward 5'-AGTAATAGCACTGCCCCACA-3'	*Dra*I
	Forward 5'-TTCGGCAAGTTTAGCCAAATA-3'	
SGN-U573854	Forward 5'-TCCACAAATGTTGAAATTCATGCA-3'	*Rsa*I
	Reverse 5'-GAGAATCGGACGCAGATCTGAGATC-3'	
SGN-U221657	Forward 5'-AGGTTTCAATGGTGGAGCAC-3'	*Msp*I
	Reverse 5'-ACAGCTGCTCGTTTCAGACC-3'	
SGN-U229378	Forward 5'-AGGCAGTGGTTGATATACCTTTTGC-3'	*Nru*I
	Reverse 5'-TGTTCCCATATTCATACGGTTTCC-3'	
C2_At1g30360	Forward 5'-GCTCTGTACGCGTAGTTTGTGTG-3'	*Hpy*CH4V
	Reverse 5'-AGGTGGTAGCCTGGTAGGTGAGG-3'	
C2_At5g27390	Forward 5'-ATGGCCATGTCCACGCTCCTC-3'	*Rsa*I
	Reverse 5'-TGGGCTTAGCCTTATCTCCATATAG-3'	
CT92	Forward 5'-GCCCTCTTACTATCTGTTGTTTG-3'	*Msp*I
	Reverse 5'-GACAAGTTGCTATACCAGGACCT-3'	
C2_At4g33030	Forward 5'-CTCGGGACCATGGGGGAATATGG-3'	*Nsi*I
	Reverse 5'-AGTGGATGTCCAACAGCAGCCTG-3'	
cLER-5-P17	Forward 5'-CCACATCCAGACTGAGTCACCAC-3'	*Taq*I
	Reverse 5'-CTCTTGGGCTTCGCTGAGTTGCT-3'	
cLED-6-M17	Forward 5'-GTTGCTCGTTTACGAGTACATGG-3'	*Nru*I
	Reverse 5'-CCTGTCACTAGCTCCAATAGCAC-3'	
T1517	Forward 5'-CGGTAGTCCATACCTAAATAGCA-3'	*sml*I
	Reverse 5'-GCAAGGGCATTATTGTCTTAACG-3'	
C2_At5g20910	Forward 5'-GGCATATATTCCAGTCCTCAACC-3'	*Ase*1
	Reverse 5'-CCTTCTGCTTCACCATCTCTTCG-3'	
C2_At5g11450	Forward 5'-CCACTCTTGGCAAGCAATGGGAA-3'	*Rsa*I
	Reverse 5'-GCCCTTGCCCAGAGCATATTGGG-3'	
C2_At5g11490	Forward 5'-CAGTCCCGATCCTTCCACTGAAA-3'	*Rsa*I
	Reverse 5'-CCTCCCATGCAAAACCGTCTTAC-3'	
TG513	Forward 5'-CCTGGCTGGTTAGCTGGTCTGAT-3'	*Eco*RI
	Reverse 5'-CCGGATGGACTCGAGGATCCAAG-3'	
C2_At2g24830	Forward 5'-CGTGGCATAGCTTCCAAGATGAT-3'	*Hin*fI
	Reverse 5'-CATGCACTGCAAGCTGAGTATTG-3'	
TG302	Forward 5'-CTCTCCGGGTGGCTATTACA-3'	*Alu*I
	Reverse 5'-TCTTGGGACTCCTCCTTTTCT-3'	

Sequences of the oligonucleotide primers utilized to amplify chromosome 8 genetic markers, together with the appropriate restriction enzyme to resolve the marker between *Solanum lycopersicum* accession LA3616 (*ep/ep*) and *Solanum pimpinellifolium* accession LA1589 (*EP/EP*).

Discussion

A range of altered fruit surface properties contributes to the *p* mutant phenotype

Fruit of the *p* mutant display pleiotropic phenotypes pertaining to the fruit surface. For example, there is an increase in the number of trichomes, altered cuticular wax composition and a ridged fruit surface with smaller and conical shaped epidermal cells (Figure 4.1 - 4.4). Analysis of the cuticle composition of the *p* mutant revealed that although cutin load did not change, cuticular wax load increased. A recent analysis of ethyl methane sulfonate (EMS) generated brightness mutants in tomato showed that all mutants that were recovered with a dull fruit surface, displayed an increase in wax load compared to WT and interestingly had characteristic morphological alterations in epidermal cells along with a rugged fruit surface, although no correlation between cutin load and dullness was observed. The epidermal cells in these dull mutants were smaller in size, less elongated and more conical shaped with higher cell density than WT, which is equivalent to *p* fruit phenotypes (Petit et al., 2013). Noting that *p* fruit have an abundance of trichomes, which are themselves surrounded by a cuticle layer (Mahlberg and Kim, 1991), there is a possibility that these could contribute to the increased wax phenotype. The cutin load was not increased in the *p* mutant when compared to WT and it is possible that this may be the result of the exhaustive delipidation phase employed during the cutin extraction process, which may remove the trichomes. Light reflection from an object determines whether its surface appears glossy/shiny or dull. In relation to the *p* mutant, surface wax as well as epidermal trichomes are known to alter light reflection properties (Bargel et al., 2006). The difference in the shape of the epidermal cells could also alter the light reflecting pattern of the fruit surface. With a smooth surface, there is increased specular reflectance of incident light, just like reflection

from mirror, whereas light becomes diffused if the surface is bumpy and ridged, which could make the fruit appear dull (Petit et al., 2013).

Previously characterized tomato fruit wax mutant, *lecer6*, defective in a β-ketoacyl-coenzyme A synthase that is involved in wax biosynthesis and cultivar Delayed Fruit Deterioration (DFD) demonstrated the importance of cuticular waxes, especially long chain alkanes in the permeability of tomato fruit cuticles. The presence of higher amounts of alkanes generally reduces cuticle permeability and limits the transpiration loss from fruit surfaces (Hovav et al., 2007; Leide et al., 2007; Saladie et al., 2007). Interestingly, although the *p* mutant fruits have high amounts of alkanes as well as total wax, the surface has more shriveled appearance and the fruit texture is rubbery and not as juicy when ripe. Identifying the gene underlying the mutant could possibly address questions pertaining to the relationship between epidermal cell morphology and dull appearance of fruit together with the regulation of water relations in fruit.

An anatomical perspective of the *easy peel* phenotype

The *ep* fruits can be peeled without causing much damage to the underlying pericarp cells. Based on the anatomy of the fruit pericarp cells, a study comparing *ep* genotypes with *dark green* (*dg*) genotypes that are hard to peel, suggested anatomical differences between the varieties. The fruits of *ep* genotypes have a steep cell size gradient near the outer surface and enlarged intercellular spaces resulting in a noticeable separation layer along with thinning of parenchyma cell walls in the outer pericarp (Chu and Thompson, 1972; Mohr, 1990) (Mohr, 1990).

Typically primary cell walls are composed of cellulose, hemicellulose and a glycan polymer network of pectin, which is abundant in fruit cell walls (Brummell, 2006; Cosgrove and Jarvis, 2012). Textural modification during fruit ripening mainly involves cell wall disassembly

of parenchyma cells, the major cell type in fruits, along with degradation of middle lamella that cements adjoining cells. This is achieved by solubilization of cell wall components by cell wall modifying enzymes including, polygalacturonase, pectin methyl esterase, pectate lyase and expansins (Eliel and Rose, 2013). These alter the firmness, cell-cell adhesion and textural properties of fruits as they ripen. In the *ep* mutant, the dissociation of peel could be due to a lack of cell-cell adhesion, specifically in the outermost cell layers of the fruit pericarp. Identification of the gene underlying *ep* mutant and its functional analysis will shed light on the regulation of cellular processes in the outer fruit pericarp.

Noting that *ep* fruits almost always cracked when ripe suggests possible relationship between cracking and easy peeling. The role of the cuticle in imparting resistance to fruit cracking is well documented. The extent of cuticle deposition, high stiffness of the peel could play a role in crack resistance (Chu and Thompson, 1972; Emmons and Scott, 1997; Emmons and Scott, 1998; Matas et al., 2004; Bargel and Neinhuis, 2005; Dominguez et al., 2011). However, anatomical analysis of the cuticle of *ep* fruit does not support its role as the underlying basis of the mutant phenotype and instead suggests that disruption of the subdermal cells may lead to the observed structural defects (Figure 4.6B-C).

Advancing genetic mapping strategies to identify the genes associated with *ep* and *p* loci

The genetic mapping experiments presented in this study were performed before the release of the tomato genome sequence assembly. Although, both polymorphic markers and some scaffold regions were available, there were regions, particularly those associated with the *ep* locus, which could not be populated with molecular markers. The availability of the tomato genome sequence should facilitate positional cloning efforts for these loci. In addition, next generation sequencing, either in the form of genome re-sequencing or transcriptome sequencing

may be utilized, together with the current, or slightly refined, map positions to identify the underlying genes. In particular, as the *ep* mutant was recovered following irradiation with thermal neutrons, it is expected to be a deletion mutant. Furthermore, as the mutant phenotype is only manifest during the ripening process, it is possible that candidate genes may be identified by mining the mapping interval for genes whose expression changes during ripening or are specifically expressed in fruit. Alternatively, comparative transcriptome sequencing of WT and *ep* ripe fruit pericarp may identify chromosome 8 genes that are not expressed in the mutant due to a possible deletion at the *ep* locus.

Problems associated with phenotyping of the F_2 mapping populations were also encountered during this study. In the case of the *p* locus, the F_1 heterozygous plants from a cross between *S. lycopersicum* (*p/p)* and *S. pimpinellifolium* (*P/P*) (LA1589) showed normal colored fruits and the F_2 showed a Mendelian phenotypic segregation of normal to dull fruits indicating that dullness is completely recessive. However, the presence of trichomes did not co-segregate with dullness, which initially made phenotyping a problem. This suggests a possibility of more than one gene being associated with the *p* locus or perhaps the existence of genetic interactions with loci derived from the *S. pimpinellifolium* mapping parent. For mapping the *ep* locus, the segregating F_2 plants from cross between *S. lycopersicum* (*ep/ep)* (LA3616) and *S. pimpinellifolium* (*EP/EP*) (LA1589) showed variation in the degree of peeling that ranged from easy to difficult. This suggests the possible existence of an intermediate phenotype between the two homozygous parental phenotypes, which may occur if the *ep* allele is only partially recessive to the WT allele or if the *S. pimpinellifolium* mapping parent alters fruit morphology of individuals from within the F_2 mapping population. In support of the latter hypothesis, continuous variation in fruit phenotypes, which range from those observed in the *S. lycopersicum*

to those of the *S. pimpinellifolium* parents, are evident. Now that chromosomal regions pertaining to the *ep* and *p* loci are identified, it may be possible to overcome ambiguous phenotypes associated with interspecific F_2 populations by developing new F_2 mapping populations with the appropriate *S. pennellii* introgression line (Eshed and Zamir, 1995). These lines carry overlapping, marker defined chromosomal segments of *S. pennellii* that span the entire genome, within a *S. lycopersicum* background. Thus, while polymorphisms and phenotypic variation can be captured from the introgression of interest, utilizing these lines will create less phenotypic variability within derived F_2 populations.

Materials and Methods

Plant material and growth conditions

Seeds of the *peach* (*p/p*) (LA2357) and *easy peel* (e*p/ep*) (LA3616) mutants together with *Solanum pimpinellifolium* (LA1589) were obtained from the Tomato Genetics Resource Center (http://tgrc.ucdavis.edu/). Seeds of the wild-type Ailsa Craig cultivar were originally obtained from the Glasshouse Crops Research Institute (Littlehampton, Sussex, UK). Plants were grown in peat-based compost supplemented with fertilizer in greenhouses at Michigan State University, East Lansing, MI under 16 h day (25°C) and 8 h night (20°C). Flowers were tagged at anthesis and fruits subsequently harvested at defined ages based on days post-anthesis.

Genetic Mapping

Two inter-specific F_2 populations segregating for the *p* and *ep* loci were generated from crosses between *S. lycopersicum* (*p/p)* (LA2357) and *S. pimpinellifolium* (*P/P*) (LA1589) and *S. lycopersicum* (*ep/ep)* (LA3616) and *S. pimpinellifolium* (*EP/EP*) (LA1589), respectively. Fruit of 128 and 205 F_2 individuals were phenotyped for dull fruits and easy peeling, respectively and in the case of the *ep* F_2 population, plants were genotyped with genetic markers spanning the tomato genome whereas genotyping was restricted to chromosome 2 genetic markers in the case of the *p* F_2 population. Genomic DNA was extracted from expanding leaves as previously described (Barry et al., 2005). Details of genetic maps and molecular markers can be accessed through the Sol Genomics Network (http://solgenomics.net). A combination of previously defined cleaved amplified polymorphic sequence markers and custom markers with experimentally determined polymorphisms between the *S.pimpinellifolium* and *S. lycopersicum* parents of the F_2 mapping populations were utilized for genetic mapping.

Extraction and Analysis of Cuticular Lipids

Extraction of tomato fruit surface waxes was accomplished through dipping fruit in chloroform containing 1% methanol for 1 min. Internal standards of tetracosane, hexadecanol and heptadecanoic acid (5 µg/mL each; Sigma-Aldrich, http://www.sigmaaldrich.com) were added to these chloroform extracts and were then dried under nitrogen gas and derivatized using BSTFA (*N, O*- bis-(trimethlysilyl) trifluoroacetamide) and pyridine at 110ºC for 10 min to prepare trimethyl-silyl derivatives of wax components. After cooling, the wax derivatives were dissolved in 1:1 heptane: toluene (1:1 v/v).

Compound identification was performed by GC-mass spectrometry (MS; EI mode) using an Agilent Technologies 6850 GC, equipped with an HP-5 MS column connected to an Agilent 5975 mass spectrometer. Helium was used as carrier gas at 2 mL min^{-1} and oven temperature was programmed from 120°C to 340°C at 10°C min^{-1}. Splitless injection was used and ions were collected in scan mode (40–800 atomic mass units) with peaks quantified on the basis of their total ion current. The surface area of fruits was determined prior to wax extraction. The diameter of the fruits were measured at three principal axes and fruit areas are calculated using formula for an ellipsoid $S= 4\pi ((ab)^{1.6} + (ac)^{1.6} + (bc)^{1.6} / 3)^{1/1.6}$ (Igathinathane and Chattopadhyay, 1998). The fruit surface area measurements were validated in other experiments and were very comparable with fruit areas measured using Tomato Analyzer version 2.1.0.0., (Brewer et al., 2006).

Following the chloroform dip, fruits were air dried and peeled. The fruit peel was scraped to remove the underlying pericarp cells to obtain a clean cuticle. The fruit cuticles were delipidated using chloroform: methanol (2:1 v/v) at room temperature for approximately 8-10 hrs. They were re-extracted with chloroform: methanol (1:2 v/v) overnight and finally with 100% methanol for an hour. All the above extractions were performed by shaking and exchanging fresh

solvent periodically. Following exhaustive delipidation, the cuticles were air dried and once completely dried, dry weight was recorded. The dried cuticles were ground to a fine powder using liquid nitrogen and stored at -20°C until required.

Cutin composition was determined as previously described (Molina et al., 2006) using 50 mg of the finely ground delipidated cuticle powder. Methyl heptadecanoate and ω-pentadecalactone (10 µg/mL each; Sigma-Aldrich, http://www.sigmaaldrich.com) were added as internal standards. Base catalyzed depolymerization was carried out in methanol containing 15% (v/v) methyl acetate and 6% (w/v) sodium methoxide by heat suspension at 60°C with periodic vortexing for two hours. Glacial acetic acid, was added to adjust to pH 4.6, diluted brine solution (0.5M sodium chloride) was used to wash the organic phase and then extracted with dichloromethane. The organic phase was washed three times with brine and dried over sodium sulfate. The product was dried under nitrogen gas and derivatized using acetic anhydride and pyridine to corresponding acetyl derivatives. Cutin monomer identification was performed by GC-MS as described above. Both cutin and wax compounds were quantified by gas chromatography (GC)-flame ionization detector (6890N, Agilent Technologies) analysis of the derivatized wax or fatty acid methyl ester products used a DB-5 capillary column. GC temperature was programmed from 140°C to 310°C for cutin and to 330°C for wax, at 5°C min^{-1}. Samples were injected in split mode (330°C injector temperature). Quantification was based on flame ionization detector ion current using peak areas relative to internal standard peak areas. Both cutin and wax amounts were expressed on a per unit fruit surface area basis.

Scanning electron microscopy

To image fruit cuticles by scanning electron microscopy, fruits were hand-sectioned and fixed for 30 min in 4% glutaraldehyde followed by 30 min incubation in 0.1 M phosphate buffer (pH 7.4). The samples were dehydrated through a graded ethanol series and further processed using a critical point dryer. Following desiccation, the samples were mounted onto aluminium stubs and sputter coated with 30nm gold particles using a SC-500 sputter coater (Emscope Laboratories, Ashford, U.K). The micrographs were captured using a 6400V scanning electron microscope (JEOL, Tokyo, Japan).

Statistical analyses

Statistical analyses were performed using SAS (SAS Institute, www.sas.com). The genotypic constituents were evaluated by either Student's *t*-tests or Least Squares Means analysis.

REFERENCES

REFERENCES

Alba R, Payton P, Fei ZJ, McQuinn R, Debbie P, Martin GB, Tanksley SD, Giovannoni JJ (2005) Transcriptome and selected metabolite analyses reveal multiple points of ethylene control during tomato fruit development. Plant Cell **17:** 2954-2965

Baker EA, Bukovac MJ, Hunt GM (1982) Composition of tomato fruit cuticle as related to fruit growth and development. *In* The Plant Cuticle Academic Press, London, UK

Bargel H, Koch K, Cerman Z, Neinhuis C (2006) Structure-function relationships of the plant cuticle and cuticular waxes - a smart material? Funct. Plant Biol. **33:** 893-910

Bargel H, Neinhuis C (2005) Tomato (*Lycopersicon esculentum* Mill.) fruit growth and ripening as related to the biomechanical properties of fruit skin and isolated cuticle. Journal of Experimental Botany **56:** 1049-1060

Barry CS, McQuinn RP, Thompson AJ, Seymour GB, Grierson D, Giovannoni JJ (2005) Ethylene insensitivity conferred by the *Green-ripe* and *Never-ripe 2* ripening mutants of tomato. Plant Physiol. **138:** 267-275

Brady CJ (1987) Fruit ripening. Annu. Rev. Plant Physiol. Plant Mol. Biol. **38:** 155-178

Brewer MT, Lang LX, Fujimura K, Dujmovic N, Gray S, van der Knaap E (2006) Development of a controlled vocabulary and software application to analyze fruit shape variation in tomato and other plant species. Plant Physiol. **141:** 15-25

Brummell DA (2006) Cell wall disassembly in ripening fruit. Funct. Plant Biol. **33:** 103-119

Chu MCY, Thompson AE (1972) Comparative anatomy of pericarps of four tomato mutants. J. Am. Soc. Hort. Sci. **97:** 478-481

Cosgrove DJ, Jarvis MC (2012) Comparative structure and biomechanics of plant primary and secondary cell walls. Front. Plant Sci. **3:** 204

Darby L, Ritchie D, Taylor I (1978) Isogenic lines of the tomato "Ailsa Craig". *In* Annual Report Glasshouse Crops Research Institute, 1977. Littlehampton, UK, pp 168-184

Dominguez E, Cuartero J, Heredia A (2011) An overview on plant cuticle biomechanics. Plant Sci. **181:** 77-84

Eliel RM, Rose JKC (2013) Cell wall architecture and metabolism in ripening fruit and the complex relationship with softening. *In* The molecular biology and biochemistry of fruit ripening. Wiley-Blackwell, pp 163-187

Emmons CLW, Scott JW (1997) Environmental and physiological effects on cuticle cracking in tomato. J. Am. Soc. Hortic. Sci. **122:** 797-801

Emmons CLW, Scott JW (1998) Ultrastructural and anatomical factors associated with resistance to cuticle cracking in tomato (*Lycopersicon esculentum Mill.*). Int. J. Plant Sci. **159:** 14-22

Eshed Y, Zamir D (1995) An introgression line population of *Lycopersicon pennellii* in the cultivated tomato enables the identification and fine mapping of yield-associated Qtl. Genetics **141:** 1147-1162

Giovannoni JJ (2004) Genetic regulation of fruit development and ripening. Plant Cell **16:** S170-S180

Ho LC, Grange RI, Picken AJ (1987) An analysis of the accumulation of water and dry-matter in tomato fruit. Plant Cell Environ. **10:** 157-162

Hovav R, Chehanovsky N, Moy M, Jetter R, Schaffer AA (2007) The identification of a gene (*Cwp1*), silenced during *Solanum* evolution, which causes cuticle microfissuring and dehydration when expressed in tomato fruit. Plant J. **52:** 627-639

Igathinathane C, Chattopadhyay PK (1998) Numerical techniques for estimating the surface areas of ellipsoids representing food materials. J. Agr. Eng. Res **70:** 313-322

Isaacson T, Kosma DK, Matas AJ, Buda GJ, He YH, Yu BW, Pravitasari A, Batteas JD, Stark RE, Jenks MA, Rose JKC (2009) Cutin deficiency in the tomato fruit cuticle consistently affects resistance to microbial infection and biomechanical properties, but not transpirational water loss. Plant J. **60:** 363-377

Kennedy GG (2003) Tomato, pests, parasitoids, and predators: tritrophic interactions involving the genus *Lycopersicon*. Annu. Rev. Entomol. **48:** 51-72

Lara I, Belge B, Goulao LF (2014) The fruit cuticle as a modulator of postharvest quality. Postharvest Biol. Technol. **87:** 103-112

Leide J, Hildebrandt U, Reussing K, Riederer M, Vogg G (2007) The developmental pattern of tomato fruit wax accumulation and its impact on cuticular transpiration barrier properties: Effects of a deficiency in a *beta-ketoacyl-coenzyme A synthase (LeCER6)*. Plant Physiol. **144:** 1667-1679

Li L, Zhao YF, McCaig BC, Wingerd BA, Wang JH, Whalon ME, Pichersky E, Howe GA (2004) The tomato homolog of CORONATINE-INSENSITIVE1 is required for the maternal control of seed maturation, jasmonate-signaled defense responses, and glandular trichome development. Plant Cell **16:** 126-143

Lindstrom E (1925) Inheritance in tomato. Genetics **10:** 305 - 317

Mahlberg PG, Kim ES (1991) Cuticle development on glandular trichomes of *Cannabis sativa* (Cannabaceae). Am. J. Bot. **78:** 1113-1122

Matas AJ, Cobb ED, Bartsch JA, Paolillo DJ, Niklas KJ (2004) Biomechanics and anatomy of *Lycopersicon esculentum* fruit peels and enzyme-treated samples. Am. J. Bot. **91:** 352-360

McDowell ET, Kapteyn J, Schmidt A, Li C, Kang JH, Descour A, Shi F, Larson M, Schilmiller A, An LL, Jones AD, Pichersky E, Soderlund CA, Gang DR (2011) Comparative functional genomic analysis of *Solanum* glandular trichome types. Plant Physiol. **155:** 524-539

Mintz-Oron S, Mandel T, Rogachev I, Feldberg L, Lotan O, Yativ M, Wang Z, Jetter R, Venger I, Adato A, Aharoni A (2008) Gene expression and metabolism in tomato fruit surface tissues. Plant Physiol. **147:** 823-851

Mohr WP (1990) The influence of fruit anatomy on ease of peeling of tomatoes for canning. Int. J. Food Sci. Tech. **25:** 449-457

Molina I, Bonaventure G, Ohlrogge J, Pollard M (2006) The lipid polyester composition of *Arabidopsis thaliana* and *Brassica napus* seeds. Phytochemistry **67:** 2597-2610

Nadakuduti SS, Pollard M, Kosma DK, Allen C, Ohlrogge JB, Barry CS (2012) Pleiotropic phenotypes of the *sticky peel* mutant provide new insight into the role of *CUTIN DEFICIENT2* in epidermal cell function in tomato. Plant Physiol. **159:** 945-960

Osorio S, Alba R, Damasceno CMB, Lopez-Casado G, Lohse M, Zanor MI, Tohge T, Usadel B, Rose JKC, Fei ZJ, Giovannoni JJ, Fernie AR (2011) Systems biology of tomato fruit development: Combined transcript, protein, and metabolite analysis of tomato transcription factor (*nor*, *rin*) and ethylene receptor (*Nr*) mutants reveals novel regulatory interactions. Plant Physiol. **157:** 405-425

Petit J, Bres C, Just D, Garcia V, Mauxion J-P, Marion D, Bakan B, Joubes J, Domergue F, Rothan C (2013) Analyses of tomato fruit brightness mutants uncover both cutin-deficient and cutin-abundant mutants and a new hypomorphic allele of GDSL Lipase. Plant Physiol. **164:** 888-906

Price HL, Drinkard AWJ (1908) Inheritance in tomato hybrids. Virginia Agr. Expt. Sta. Bull. **177:** 1-53

Rick CM, Butler L (1956) Cytogenetics of the tomato. Adv. Genet. **8** 267–382

Rohrmann J, Tohge T, Alba R, Osorio S, Caldana C, McQuinn R, Arvidsson S, van der Merwe MJ, Riano-Pachon DM, Mueller-Roeber B, Fei Z, Nesi AN, Giovannoni JJ, Fernie AR (2011) Combined transcription factor profiling, microarray analysis and metabolite profiling reveals the transcriptional control of metabolic shifts occurring during tomato fruit development. Plant J. **68:** 999-1013

Saladie M, Matas AJ, Isaacson T, Jenks MA, Goodwin SM, Niklas KJ, Ren XL, Labavitch JM, Shackel KA, Fernie AR, Lytovchenko A, O'Neill MA, Watkins CB, Rose JKC (2007) A reevaluation of the key factors that influence tomato fruit softening and integrity. Plant Physiol. **144:** 1012-1028

Sallaud C, Rontein D, Onillon S, Jabes F, Duffe P, Giacalone C, Thoraval S, Escoffier C, Herbette G, Leonhardt N, Causse M, Tissier A (2009) A novel pathway for sesquiterpene biosynthesis from *Z,Z*-Farnesyl pyrophosphate in the wild tomato *Solanum habrochaites*. Plant Cell **21:** 301-317

Schilmiller AL, Schauvinhold I, Larson M, Xu R, Charbonneau AL, Schmidt A, Wilkerson C, Last RL, Pichersky E (2009) Monoterpenes in the glandular trichomes of tomato are synthesized from a neryl diphosphate precursor rather than geranyl diphosphate. Proc. Natl. Acad. Sci. USA **106:** 10865-10870

Shi JX, Adato A, Alkan N, He YH, Lashbrooke J, Matas AJ, Meir S, Malitsky S, Isaacson T, Prusky D, Leshkowitz D, Schreiber L, Granell AR, Widemann E, Grausem B, Pinot F, Rose JKC, Rogachev I, Rothan C, Aharoni A (2013) The tomato SlSHINE3 transcription factor regulates fruit cuticle formation and epidermal patterning. New Phytol. **197:** 468-480

The Tomato Genome Consortium (2012) The tomato genome sequence provides insights into fleshy fruit evolution. Nature **485:** 635-641

Verkerk K, Contant RB (1969) Radiation induced easy peeling and oblong fruit mutants of the tomato. Neth. J. Agri. Sci. **17:** 221-228

Vogg G, Fischer S, Leide J, Emmanuel E, Jetter R, Levy AA, Riederer M (2004) Tomato fruit cuticular waxes and their effects on transpiration barrier properties: functional characterization of a mutant deficient in a very-long-chain fatty acid beta-ketoacyl-CoA synthase. J. Exp. Bot. **55:** 1401-1410

Weinhold A, Baldwin IT (2011) Trichome-derived *O*-acyl sugars are a first meal for caterpillars that tags them for predation. Proc. Natl. Acad. Sci. USA **108:** 7855-7859

Yeats TH, Huang W, Chatterjee S, Viart HMF, Clausen MH, Stark RE, Rose JKC (2014) Tomato *Cutin Deficient 1* (*CD1*) and putative orthologs comprise an ancient family of cutin synthase-like (CUS) proteins that are conserved among land plants. Plant Journal **77:** 667-675

Yeats TH, Martin LBB, Viart HMF, Isaacson T, He YH, Zhao LX, Matas AJ, Buda GJ, Domozych DS, Clausen MH, Rose JKC (2012) The identification of cutin synthase: formation of the plant polyester cutin. Nat. Chem. Biol. **8:** 609-611

Zhong S, Fei Z, Chen Y-R, Zheng Y, Huang M, Vrebalov J, McQuinn R, Gapper N, Liu B, Xiang J, Shao Y, Giovannoni JJ (2013) Single-base resolution methylomes of tomato fruit development reveal epigenome modifications associated with ripening. Nat. Biotechnol. **31:** 154-159

CHAPTER V

Conclusions and perspectives

One of the main challenges facing biology in this post genomic era is to assign molecular functions to the numerous uncharacterized genes discovered as a result of genome sequencing projects. This holds true for the various fruit genomes sequenced, including tomato, where functional analysis of the majority of the encoded genes is lacking. Several approaches to predict or determine unknown gene function can be utilized, for example gene-to-gene co-expression analyses, predictions of sub-cellular localization and large scale determination of protein-protein interactions each provide correlative analysis of potential gene functions. However, in order to understand the function of specific genes, gene knock-out or knock-down approaches are required and in many fleshy fruit bearing species, these approaches remain slow and laborious. Forward genetics-based approaches have the advantage of beginning with a mutant of biological interest but the disadvantage that the underlying gene is unknown. However, in the case of tomato, the combination of high-density genetic maps and a reference genome sequence, facilitates the process of identifying genes associated with mutant phenotypes. The studies presented in this dissertation focus on the characterization of four monogenic mutants of tomato that alter different aspects of fruit development. These mutants were characterized using a combination of physiological, molecular and chemical analyses, they were mapped to the tomato genome and in two cases the underlying genes were identified and characterized.

CD2, a master regulator of epidermal cell function

The *sticky peel* (*pe*) mutant of tomato disrupts several epidermis-related phenotypes, including fruit and leaf cuticle biosynthesis, anthocyanin formation, stomatal density and trichome formation (Nadakuduti et al., 2012). Map based cloning identified *pe* as a new mutant allele of *CUTIN DEFICIENT2*, a class IV homeodomain-leucine zipper (HD-ZIP IV) family

transcription factor (TF). Previously, *CD2* was shown to be required for tomato fruit cuticle formation (Isaacson et al., 2009) but this research revealed a broader role for this TF in plant development. Furthermore, characterization of the *anthocyaninless 2* mutant of Arabidopsis (Kubo et al., 1999), which encodes a CD2 homolog, revealed that this mutant also exhibits a mild perturbation in cuticle biosynthesis and defined a regulatory link between cuticle and flavonoid biosynthetic pathways operating in epidermal cells.

The Class IV homeodomain-Leu zipper (HD-ZIP IV) family of TFs is unique to the plant kingdom and is found from moss to higher plants but is not present in algal genomes suggesting that the presence of these genes pertains to the evolution of terrestrial plants (Mukherjee et al., 2009; Javelle et al., 2011). This hypothesis is supported by the epidermal-specific expression of the majority of the characterized family members and through functional characterization of a limited number of family members that all disrupt epidermal-cell related development and metabolism (Valle et al., 1997; Dong et al., 1999; Ingram et al., 2000; Ito et al., 2002; Swigonova et al., 2004; Nakamura et al., 2006; Guan et al., 2008; Isaacson et al., 2009; Javelle et al., 2011; Chew et al., 2013). No comprehensive analysis of the *HD-ZIP IV* family has thus far been performed in tomato and the only characterized *HD-ZIP IV* genes are *CD2* and *Woolly* (*Wo*), a spontaneous mutation that promotes trichome formation and causes embryo lethality in its homozygous state (Yang et al., 2011). There are 37 predicted *HD-ZIP IV* genes present in the tomato genome, some of which are present as tandem duplications within the genome and functional characterization of these genes would represent a major effort but would provide insight into their role in plant development and epidermal cell function.

In addition, identifying the target genes of CD2 is critical to elucidate the transcriptional regulatory network in which it participates. Genome wide identification of target genes can be

achieved using chromatin immunoprecipitation (ChIP) coupled with deep sequencing (ChIP-seq) using a purified antibody against CD2 or by an epitope-tagged version of CD2. Studies involving genome-wide characterization of the *HD-ZIP IV* family in diverse species revealed that these TFs are associated with epidermis-related expression and/or function (Javelle et al., 2011) and Q-RT-PCR analysis in tomato, performed on stem peel, core and whole stem indicates that *CD2* is preferentially expressed in stem epidermis (Nadakuduti et al., 2012). Therefore to perform the above experiments, the peel tissue could be separated from fruit or stem of WT and *pe* mutant samples to increase specificity. From the ChIP-seq data it should be possible to identify the *in vivo* binding sites of CD2 near the candidate genes and this approach could be coupled with transcriptome sequencing of WT, mutant and *CD2* over-expression lines to reveal direct and indirect targets of CD2. In particular, placing the function of CD2 into context with SlSHINE3 as well as homologs of regulators of cuticle biosynthesis yet to be identified in tomato, including members of other SHN TFs, MYB TFs that are biotic and abiotic stress responsive along with HDG1 in Arabidopsis, and WXP1 identified in *Medicago sativa* (Zhang et al., 2005; Raffaele et al., 2008; Seo et al., 2009; Seo and Park, 2010; Oshima et al., 2013) will facilitate identification of distinct and overlapping regulons that influence epidermal cell function and in particular the biosynthesis of cuticular lipids.

Uncovering the genetic basis of fruit chlorophyll gradients

Many fruits develop as green photosynthetic organs before they begin to ripen and exhibit gradients of chlorophyll accumulation that are visibly obvious. These chlorophyll patterns on fruits are intriguing and specific to each fruit, however limited knowledge exists on the genetic mechanisms that control chloroplast development and chlorophyll accumulation patterns in developing fruits. In tomato, a latitudinal gradient of chloroplast development exists,

forming a green shoulder at the peduncle end of the fruit. Although, there has been a tremendous advancement in regulation of fruit ripening, there is a knowledge gap that is particularly evident for transcription factors acting during the early stages of fruit development. Chloroplast development and fruit photosynthesis are crucial in determining the sugar, nutritional composition and antioxidant capacity of the ripe fruit (Dinar and Stevens, 1981; Powell et al., 2012; Sagar et al., 2013). Hence the fruit shoulder has a positive impact on the ripe fruit nutrient content (Powell et al., 2012). One of the components of the regulatory network for fruit chloroplast development was recently identified as the *GOLDEN 2-LIKE* transcription factor, *SlGLK2* (Powell et al., 2012).

Our research identified the gene that underlies the *uniform gray-green* (*ug*) locus of tomato, which possesses a mutant phenotype that is virtually identical to that of the *u* locus. *UG* encodes a previously uncharacterized class *I KNOTTED-LIKE* homeobox (*KNOX*) gene, *TKN4*, providing the first evidence for involvement of *KNOX* genes in fleshy fruit development and in particular, chloroplast development. The functional relationship between KNOX and fruit chloroplast development was confirmed through characterization of the *Curl* (*Cu*) mutant, a dominant gain-of-function mutation in the *KNOX* gene, *TKN2* (Parnis et al., 1997), which displays ectopic fruit chloroplast development. Furthermore, chlorophyll levels were not influenced in the leaves of the *ug* or *Cu* mutants suggesting that separate pathways influence chloroplast development in leaves and fruit of tomato. This hypothesis is supported by functional characterization of *SlAPRR2-LIKE* and *SlARF4*, which also influenced fruit chloroplast development but not leaf chloroplast development (Pan et al., 2013; Sagar et al., 2013). Gene expression analysis indicates that *TKN2* and *TKN4* act upstream of *SlGLK2* and *SlAPRR2-LIKE* and influences their gradient-dependent expression, whereby transcript abundance is higher in

the calyx end of the fruit and this stimulates shoulder formation. Recently, RNAseq analysis of WT fruits at different stages of development revealed that latitudinal gene expression gradients are robust and extend beyond the TF regulon identified in this study to encompass additional classes of genes (Nguyen et al., 2014). Current understanding of the role of *KNOX* genes in fleshy fruit development, and particularly chloroplast development is in its infancy and there are several different approaches that could be pursued to increase the understanding of these TFs with the ultimate aim of defining the regulatory framework in which they function.

To acquire further insight into establishment of chloroplast gradients and the specific role played by *KNOX* genes in this process, generating transcriptome data from green fruit of *Cu, ug* and WT by RNA-seq from tissue collected from the shoulder, middle and base portions of the fruit could be pursued. We anticipate that the gradient of gene expression that correlates with chloroplast development will be disrupted by *ug* and constitutively activated in *Cu* as a result of reduced and enhanced KNOX activity, respectively. In addition, this dataset may provide insight into potential broader roles of *KNOX* genes in fleshy fruit development and will therefore aid in further expanding the current model of the *KNOX*-mediated regulatory network in tomato fruit development.

SlGLK2 and *SlAPRR2-LIKE* may represent direct targets of KNOX and in the case of *SlAPRR2-LIKE*, there is a repeated TGAC motif within the promoter sequence. Although KNOX binding sites are often degenerate, genes with duplicated TGAC motifs within their regulatory sequences often represent KNOX targets (Bolduc and Hake, 2009; Bolduc et al., 2012; Lin et al., 2013). The ability of KNOX proteins to bind to regulatory regions of *SlGLK2* and *SlAPRR2-LIKE* can therefore be tested using a combination of chromatin immunoprecipitation (ChIP), electrophoretic mobility shift assays (EMSAs) and transient expression assays. It is also possible

that KNOX-mediated regulation of *SlGLK2* and *SlAPRR2-LIKE* expression occurs through an indirect mechanism. For example, ChIP-seq analysis of maize KNOTTED-1 revealed that it targets hundreds of loci (Bolduc et al., 2012). Similarly, a ChIP-seq approach will be useful for characterizing potentially broader roles for both TKN2 and TKN4 in fruit development and may be necessary to gain further insight into this TF regulatory network if their impact on *SlGLK2* and *SlAPRR2-LIKE* expression occurs through an indirect mechanism.

To date, the functional analysis of *KNOX* genes in fleshy fruit development has focused on available mutant lines and has been restricted to reduced function of *TKN4* and a gain of function of *TKN2*. It would also be useful to examine the reciprocal activities. For example, silencing of *TKN2* may provide insight into the broader role of this gene in fruit development and over-expression of *TKN4* would allow the assessment of overlap with *TKN2* and in particular to determine whether over-expression of *TKN4* mimics the *Cu* mutant phenotype. Manipulation of KNOX activity can lead to highly pleiotropic phenotypes associated with altered plant morphology as is observed in the *Cu* mutant. Therefore, fruit-specific manipulation of both *TKN2* and *TKN4* may overcome these pleiotropic phenotypes, while focusing specifically on those related to fruit development. A series of vectors for both fruit-specific silencing and over-expression are available that could facilitate such an analysis (Fernandez et al., 2009). In addition, *KNOX* genes can act redundantly (Jackson et al., 1994; Long et al., 1996; Parnis et al., 1997; Vollbrecht et al., 2000; Byrne et al., 2002; Belles-Boix et al., 2006). To counteract this phenomenon, Shani et al., 2009 fused *TKN2* to the EAR repressor motif of the Arabidopsis SUPERMAN gene (Hiratsu et al., 2003; Shani et al., 2009). The EAR motif acts as dominant repressor by suppressing the expression of target genes even in the presence of redundant transcription factors, thus resulting in a dominant loss of function phenotype. This approach was

utilized for examining early leaf development and shape in tomato (Shani et al., 2009) but could also be modified to encompass fruit-specific promoters and the resulting transgenic fruit evaluated for altered development and potential changes to gene expression gradients.

KNOX proteins function by interacting with BEL1-Like (BELL) homeodomain proteins and form heterodimers to target several genes by directly binding to the promoters of those genes (Bellaoui et al., 2001; Smith et al., 2002; Smith and Hake, 2003). These interactions occur through the MEINOX and SKY/BELL domains of KNOX and BELL proteins, respectively. A single KNOX protein can interact with multiple BELL proteins, potentially providing flexibility and specificity to signal outputs (Bellaoui et al., 2001; Smith et al., 2002; Hackbusch et al., 2005). The role of BELL genes in fleshy fruit development is currently unknown and mining of tomato transcriptome data revealed that 12 *BELL* genes are expressed at different stages of fruit development (The Tomato Genome Consortium, 2012). This obviously creates the potential for genetic redundancy and coupled with the potential complexity of interactions between KNOX and BELL proteins, it will be difficult to determine the individual roles of these proteins in fruit development. In the absence of defined mutants at these loci or the resources to attempt to silence each gene singly, or in combination, it may be possible to also utilize an EAR domain fusion to assess the potential impact of these genes on fruit development and gene expression gradients.

Identification of loci underlying *ep* and *p* mutants will contribute to better understanding of fruit exocarp

The *peach* (*p*) and *easy peel* (*ep*) mutants are the fruit developmental mutants of focus in chapter IV. Fruits of the *p* mutant are dull and covered with dense trichomes, which persisted even in ripe fruits. The shape and size of the epidermal cells are altered in *p* mutant fruits and

they also display altered cuticular composition. This implies that the *p* mutant has pleiotropic phenotypes pertaining to the fruit epidermis. Genetic mapping to isolate both loci is in progress. We encountered problems in phenotyping *p* mutant, as fruit dullness and presence of trichomes were segregating in the interspecific F_2 mapping population. As the map position for this locus is narrowed down to 1 Mbp on chromosome 2, developing new F_2 mapping populations with the appropriate *S. pennellii* introgression line will reduce this ambiguity of phenotyping and allow us to fine map the locus fairly quickly.

Fruits of *ep* mutant can be peeled with limited damage to the underlying pericarp cells. The dissociation of the fruit peel could be due to a lack of cell-cell adhesion, specifically in the outer cell layers of the fruit pericarp. SEM micrographs suggest that the phenotype is beneath the epidermis probably in parenchyma cells as fruit peel includes epidermis and some layers of collenchyma cells. Genetic mapping placed the locus on chromosome 8. For further narrowing down the interval, we have high confidence mutants in the F_2 mapping population which will aid in using the same population. With the availability of the reference genome of tomato and the draft genome of *S. pimpinellifolium*, one of the parents of our F_2 mapping population, it should be possible to design and add more molecular markers to the mapping interval and increase the mapping population to refine the map position. Comparative transcriptome sequencing of WT and *ep* could also be utilized to detect the missing transcript in the mutant, due to a possible deletion at the *ep* locus. The incorporation of laser capture micro dissection into this experimental strategy could facilitate this approach as it would allow the precise isolation of the exocarp tissue along with layers of parenchyma cells where we observe the peel dissociation to occur. This method of sample collection for RNA-seq experiments has already been utilized to obtain cell-specific transcripts in tomato fruit pericarp at an early stage of fruit development

(Matas et al., 2011). However, some optimization may be required to fix and section tissues at a later stage of fruit development when the *ep* phenotype is observed due to increased cell expansion and ripening-induced cell wall disassembly. Identifying both *p* and *ep* loci will enhance understanding of the molecular basis of fruit exocarp development and in the case of *ep* may yield additional insight into the metabolic changes that occur during fruit ripening.

Importance of gene discovery in fruit crops and its impact on science and agriculture

Fruits form an essential component of the human diet as they provide minerals, vitamins, antioxidants, carbohydrates and fiber to enrich the nutrient content along with enhancing our overall enjoyment of food through the sensory pleasures of sweetness, color, flavor and aroma. Tomato is a nutritious fruit commonly used as a vegetable crop that is grown throughout the world. Tomato fruits are specifically rich in vitamins A, C and folic acid and contain a wide array of carotenoids such as lycopene, beta-carotene, gamma-carotene, phytoene as well as several minor carotenoids that possess antioxidant properties (Beecher, 1998). Additionally, tomato serves as an excellent model system for studying fleshy fruit biology due to the availability of an array of genetic and genomic resources. The basic knowledge gained from tomato can often be applied to additional fruit crop species. Therefore, identification of genes and their functional characterization in tomato will generate knowledge that can be utilized to improve the production, yield, quality and nutritional value of additional fruit crops.

The cuticle is a hydrophobic protective layer present on all the aerial surfaces of terrestrial plants. In fruit crops the cuticle provides structural integrity to the fruit along with protection from uncontrolled water loss or uptake, mechanical damage, pathogens, herbivores and thereby influences growth, ripening and post harvest quality, particularly in relation to fruit cracking (Chu and Thompson, 1972; Emmons and Scott, 1997; Emmons and Scott, 1998; Matas

et al., 2004; Saladie et al., 2007; Dominguez et al., 2011). The presence of much thicker cuticle in fruits compared to leaves of tomato (Nadakuduti et al., 2012) suggests its mechanistic role in maintaining fruit integrity and physiological role in regulating post harvest water loss from the astomatous fruit surface. Identifying the regulatory factors and transcriptional mechanisms regulating fruit cuticle formation will lead to improved understanding of the role of cuticle in fruit development and post harvest maintenance. It also provides opportunity for selecting desirable cuticle traits for use in breeding programs targeting improvement of fruit quality.

Fruit color is a horticultural trait with large impact on the nutritional quality of the fruit. Chloroplast development and chlorophyll accumulation in developing fruits are critical for fruit photosynthesis, which contributes to up to 20% of fruit carbohydrates (Hetherington et al., 1998) and is therefore important for determining the sugar, nutritional composition and flavor of the ripe fruit (Powell et al., 2012). Thereby enhancing the photosynthetic competency of the fruit by increasing the efficiency of chloroplast function or by increasing chloroplast number, represent potential strategies for enhancing the nutritional value and flavor of fleshy fruits. The discovery that *KNOX* genes regulate fruit-specific chloroplast development not only advances our scientific knowledge of a basic process unique to plants but also creates the potential to identify novel targets for selection in fruit crops that could be used for improving nutritional quality of fleshy fruits.

In the US, consumption of processed tomatoes outweighs that of the fresh produce (USDA-ARS 2006) and tomatoes are the highest consumed canned vegetable (National Agricultural Statistics Service, 2005). Before processing and canning the fruit peel is generally removed by various processes including steam, hot water, lye or cryogenic methods (Garcia and Barrett, 2006). Removal of the fruit peel represents an essential component of tomato processing

that is important to the final quality of the product. However, this requires extra inputs in the form of energy or chemicals such as lye that creates issues with waste disposal. As such, there might be an advantage of the easy peeling phenotype of the *ep* mutant in the processing and canning industry as fruit can be peeled without any pre-treatment. Once identified it may be possible to introduce the *ep* mutant into commercial canning varieties to exploit the potential of easy peeling during processing. However, the agricultural performance of such a trait would first need to be explored as there is the potential negative impact of increased disease incidence in *ep* fruit. As the *ep* mutant likely carries a deletion allele (Verkerk and Contant, 1969) it likely represents a severe mutant allele but once the gene is identified, it may become possible to isolate additional mutant alleles from EMS mutagenized populations that are less severe than the original *ep* mutant allele. Alternatively, it may be possible to use the existing allele as a heterozygote in F_1 hybrids if an intermediate phenotype is observed. These approaches may allow the fruits to be peeled easily without the associated disease penalty.

The long-term vision of the work described in this dissertation is to develop an improved understanding of the fundamental biological processes that determine fruit development and quality while identifying genes that may be useful for integration into tomato or additional fleshy fruit crop breeding programs.

REFERENCES

REFERENCES

Beecher GR (1998) Nutrient content of tomatoes and tomato products. Exp. Biol. Med. **218:** 98-100

Bellaoui M, Pidkowich MS, Samach A, Kushalappa K, Kohalmi SE, Modrusan Z, Crosby WL, Haughn GW (2001) The Arabidopsis BELL1 and KNOX TALE homeodomain proteins interact through a domain conserved between plants and animals. Plant Cell **13:** 2455-2470

Belles-Boix E, Hamant O, Witiak SM, Morin H, Traas J, Pautot V (2006) *KNAT6*: an Arabidopsis homeobox gene involved in meristem activity and organ separation. Plant Cell **18:** 1900-1907

Bolduc N, Hake S (2009) The maize transcription factor KNOTTED1 directly regulates the gibberellin catabolism gene *ga2ox1*. Plant Cell **21:** 1647-1658

Bolduc N, Yilmaz A, Mejia-Guerra MK, Morohashi K, O'Connor D, Grotewold E, Hake S (2012) Unraveling the KNOTTED1 regulatory network in maize meristems. Genes Dev. **26:** 1685-1690

Byrne ME, Simorowski J, Martienssen RA (2002) *ASYMMETRIC LEAVES1* reveals *knox* gene redundancy in Arabidopsis. Development **129:** 1957-1965

Chew W, Hrmova M, Lopato S (2013) Role of homeodomain leucine zipper (HD-Zip) IV transcription factors in plant development and plant protection from deleterious environmental factors. Int. J. Mol. Sci. **14:** 8122-8147

Chu MCY, Thompson AE (1972) Comparative anatomy of pericarps of four tomato mutants. J. Am. Soc. Hort. Sci. **97:** 478-481

Dinar M, Stevens MA (1981) The relationship between starch accumulation and soluble solids content of tomato fruits. J. Am. Soc. Hort. Sci. **106:** 415-418

Dominguez E, Cuartero J, Heredia A (2011) An overview on plant cuticle biomechanics. Plant Sci. **181:** 77-84

Dong Y-H, Yao J-L, Atkinson RG, Morris BA, Gardner RC (1999) Mdh3 encoding a Phalaenopsis O39-like homeodomain protein expressed in ovules of *Malus domestica*. J. Exp. Bot. **50:** 141-142

Emmons CLW, Scott JW (1997) Environmental and physiological effects on cuticle cracking in tomato. J. Am. Soc. Hortic. Sci. **122:** 797-801

Emmons CLW, Scott JW (1998) Ultrastructural and anatomical factors associated with resistance to cuticle cracking in tomato (*Lycopersicon esculentum Mill.*). Int. J. Plant Sci. **159:** 14-22

Fernandez AI, Viron N, Alhagdow M, Karimi M, Jones M, Amsellem Z, Sicard A, Czerednik A, Angenent G, Grierson D, May S, Seymour G, Eshed Y, Lemaire-Chamley M, Rothan C, Hilson P (2009) Flexible tools for gene expression and silencing in tomato. Plant Physiol. **151:** 1729-1740

Garcia E, Barrett DM (2006) Peelability and yield of processing tomatoes by steam or lye. J. Food Process. Preserv. **30:** 3-14

Guan XY, Li QJ, Shan CM, Wang S, Mao YB, Wang LJ, Chen XY (2008) The HD-Zip IV gene *GaHOX1* from cotton is a functional homologue of the Arabidopsis *GLABRA2*. Physiol. Plant. **134:** 174-182

Hackbusch J, Richter K, Muller J, Salamini F, Uhrig JF (2005) A central role of *Arabidopsis thaliana* ovate family proteins in networking and subcellular localization of 3-aa loop extension homeodomain proteins. Proc. Natl. Acad. Sci. USA **102:** 4908-4912

Hetherington SE, Smillie RM, Davies WJ (1998) Photosynthetic activities of vegetative and fruiting tissues of tomato. J. Exp. Bot. **49:** 1173-1181

Hiratsu K, Matsui K, Koyama T, Ohme-Takagi M (2003) Dominant repression of target genes by chimeric repressors that include the EAR motif, a repression domain, in Arabidopsis. Plant J. **34:** 733-739

Ingram GC, Boisnard-Lorig C, Dumas C, Rogowsky PM (2000) Expression patterns of genes encoding HD-ZipIV homeo domain proteins define specific domains in maize embryos and meristems. Plant J. **22:** 401-414

Isaacson T, Kosma DK, Matas AJ, Buda GJ, He YH, Yu BW, Pravitasari A, Batteas JD, Stark RE, Jenks MA, Rose JKC (2009) Cutin deficiency in the tomato fruit cuticle consistently affects resistance to microbial infection and biomechanical properties, but not transpirational water loss. Plant J. **60:** 363-377

Ito M, Sentoku N, Nishimura A, Hong SK, Sato Y, Matsuoka M (2002) Position dependent expression of GL2-type homeobox gene, *Roc1*: significance for protoderm differentiation and radial pattern formation in early rice embryogenesis. Plant J. **29:** 497-507

Jackson D, Veit B, Hake S (1994) Expression of maize *KNOTTED1* related homeobox genes in the shoot apical meristem predicts patterns of morphogenesis in the vegetative shoot. Development **120:** 405-413

Javelle M, Klein-Cosson C, Vernoud V, Boltz V, Maher C, Timmermans M, Depege-Fargeix N, Rogowsky PM (2011) Genome-wide characterization of the HD-ZIP IV transcription factor family in maize: preferential expression in the epidermis. Plant Physiol. **157:** 790-803

Kubo H, Peeters A, Aarts M, Pereira A, Koornneef M (1999) *ANTHOCYANINLESS2*, a homeobox gene affecting anthocyanin distribution and root development in Arabidopsis. Plant Cell **11:** 1217 - 1226

Lin T, Sharma P, Gonzalez DH, Viola IL, Hannapel DJ (2013) The impact of the long-distance transport of a BEL1-Like messenger RNA on development. Plant Physiol. **161:** 760-772

Long JA, Moan EI, Medford JI, Barton MK (1996) A member of the KNOTTED class of homeodomain proteins encoded by the *STM* gene of Arabidopsis. Nature **379:** 66-69

Matas AJ, Cobb ED, Bartsch JA, Paolillo DJ, Niklas KJ (2004) Biomechanics and anatomy of *Lycopersicon esculentum* fruit peels and enzyme-treated samples. Am. J. Bot. **91:** 352-360

Matas AJ, Yeats TH, Buda GJ, Zheng Y, Chatterjee S, Tohge T, Ponnala L, Adato A, Aharoni A, Stark R, Fernie AR, Fei ZJ, Giovannoni JJ, Rose JKC (2011) Tissue- and

cell-type specific transcriptome profiling of expanding tomato fruit provides insights into metabolic and regulatory specialization and cuticle formation. Plant Cell **23:** 3893-3910

Mukherjee K, Brocchieri L, Burglin TR (2009) A comprehensive classification and evolutionary analysis of plant homeobox genes. Mol. Biol. Evol. **26:** 2775-2794

Nadakuduti SS, Pollard M, Kosma DK, Allen C, Ohlrogge JB, Barry CS (2012) Pleiotropic phenotypes of the *sticky peel* mutant provide new insight into the role of *CUTIN DEFICIENT2* in epidermal cell function in tomato. Plant Physiol. **159:** 945-960

Nakamura M, Katsumata H, Abe M, Yabe N, Komeda Y, Yamamoto KT, Takahashi T (2006) Characterization of the class IV homeodomain-leucine zipper gene family in Arabidopsis. Plant Physiol. **141:** 1363-1375

Nguyen CV, Vrebalov JT, Gapper NE, Zheng Y, Zhong S, Fei Z, Giovannoni JJ (2014) Tomato *GOLDEN2-LIKE* transcription factors reveal molecular gradients that function during fruit development and ripening. Plant Cell **26:** 585-601

Oshima Y, Shikata M, Koyama T, Ohtsubo N, Mitsuda N, Ohme-Takagi M (2013) MIXTA-like transcription factors and WAX INDUCER1/SHINE1 coordinately regulate cuticle development in Arabidopsis and *Torenia fournieri*. Plant Cell **25:** 1609-1624

Pan Y, Bradley G, Pyke K, Ball G, Lu CG, Fray R, Marshall A, Jayasuta S, Baxter C, van Wijk R, Boyden L, Cade R, Chapman NH, Fraser PD, Hodgman C, Seymour GB (2013) Network inference analysis identifies an *APRR2-Like* gene linked to pigment accumulation in tomato and pepper fruits. Plant Physiol. **161:** 1476-1485

Parnis A, Cohen O, Gutfinger T, Hareven D, Zamir D, Lifschitz E (1997) The dominant developmental mutants of tomato, *Mouse-ear* and *Curl*, are associated with distinct modes of abnormal transcriptional regulation of a knotted gene. Plant Cell **9:** 2143-2158

Powell ALT, Nguyen CV, Hill T, Cheng KL, Figueroa-Balderas R, Aktas H, Ashrafi H, Pons C, Fernandez-Munoz R, Vicente A, Lopez-Baltazar J, Barry CS, Liu YS, Chetelat R, Granell A, Van Deynze A, Giovannoni JJ, Bennett AB (2012) *Uniform ripening* encodes a *Golden 2-like* transcription factor regulating tomato fruit chloroplast development. Science **336:** 1711-1715

Raffaele S, Vailleau F, Leger A, Joubes J, Miersch O, Huard C, Blee E, Mongrand S, Domergue F, Roby D (2008) A MYB transcription factor regulates very-long-chain fatty

acid biosynthesis for activation of the hypersensitive cell death response in Arabidopsis. Plant Cell **20:** 752-767

Sagar M, Chervin C, Mila I, Hao Y, Roustan J-P, Benichou M, Gibon Y, Biais Bt, Maury P, Latche A, Pech J-C, Bouzayen M, Zouine M (2013) Sl-ARF4, an auxin response factor involved in the control of sugar metabolism during tomato fruit development. Plant Physiol. **161:** 1362-1374

Saladie M, Matas AJ, Isaacson T, Jenks MA, Goodwin SM, Niklas KJ, Ren XL, Labavitch JM, Shackel KA, Fernie AR, Lytovchenko A, O'Neill MA, Watkins CB, Rose JKC (2007) A reevaluation of the key factors that influence tomato fruit softening and integrity. Plant Physiol. **144:** 1012-1028

Seo PJ, Park CM (2010) MYB96-mediated abscisic acid signals induce pathogen resistance response by promoting salicylic acid biosynthesis in Arabidopsis. New Phytol. **186:** 471-483

Seo PJ, Xiang F, Qiao M, Park JY, Lee YN, Kim SG, Lee YH, Park WJ, Park CM (2009) The MYB96 transcription factor mediates abscisic acid signaling during drought stress response in Arabidopsis. Plant Physiol. **151:** 275-289

Shani E, Burko Y, Ben-Yaakov L, Berger Y, Amsellem Z, Goldshmidt A, Sharon E, Ori N (2009) Stage-specific regulation of *Solanum lycopersicum* leaf maturation by class 1 Knotted1-like homeobox proteins. Plant Cell **21:** 3078-3092

Smith HMS, Boschke I, Hake S (2002) Selective interaction of plant homeodomain proteins mediates high DNA-binding affinity. Proc. Natl. Acad. Sci. USA **99:** 9579-9584

Smith HMS, Hake S (2003) The interaction of two homeobox genes, *BREVIPEDICELLUS* and *PENNYWISE*, regulates internode patterning in the Arabidopsis inflorescence. Plant Cell **15:** 1717-1727

Swigonova Z, Lai J, Ma J, Ramakrishna W, Llaca V, Bennetzen JL, Messing J (2004) Close split of sorghum and maize genome progenitors. Genome Res. **14:** 1916-1923

The Tomato Genome Consortium (2012) The tomato genome sequence provides insights into fleshy fruit evolution. Nature **485:** 635-641

Valle EM, Gonzalez DH, Gago G, Chan RL (1997) Isolation and expression pattern of *hahr1*, a homeobox-containing cDNA from *Helianthus annuus*. Gene **196:** 61-68

Verkerk K, Contant RB (1969) Radiation induced easy peeling and oblong fruit mutants of the tomato. Neth. J. Agri. Sci. **17:** 221-228

Vollbrecht E, Reiser L, Hake S (2000) Shoot meristem size is dependent on inbred background and presence of the maize homeobox gene, *knotted1*. Development **127:** 3161-3172

Yang C, Li H, Zhang J, Luo Z, Gong P, Zhang C, Li J, Wang T, Zhang Y, Lu Y, Ye Z (2011) A regulatory gene induces trichome formation and embryo lethality in tomato. Proc. Natl. Acad. Sci. USA **108:** 11836-11841

Zhang JY, Broeckling CD, Blancaflor EB, Sledge MK, Sumner LW, Wang ZY (2005) Overexpression of *WXP1*, a putative *Medicago truncatula* AP2 domain-containing transcription factor gene, increases cuticular wax accumulation and enhances drought tolerance in transgenic alfalfa (*Medicago sativa*). Plant J. **42:** 689-707